

CHAPTER ONE

INTRODUCTION

1.1 Background of the Study

Composites are materials that comprise strong load bearing material (known as reinforcement) imbedded in weaker material (known as matrix), with the reinforcement providing strength and rigidity, helping to support the structural load, while the matrix or binder, which may be organic or inorganic, maintains the position and orientation of the reinforcement(Taj et al, 2007; Ku et al, 2011).Natural fibers have been used to reinforce materials for over 3500 years, but the emergence of polymers in the beginning of the 19th century ushered a new era of research with a new option of using the natural fibers in more diversified fields. At the same time interest in synthetic fibers, like glass fiber - because of its superior dimensional and other properties - gained popularity and slowly replaced the natural fibers in different applications. However, change in the raw materials and production of synthetic composites required a large quantum of energy and quality of environment suffered because of the pollution generated during the production and recycling of these synthetic materials. This has once again drawn the attention towards natural fibers due to their distinct advantages.

Natural fibers have advantages such as being abundantly available, low cost, low density (about half that of glass fibers), low weight, cheaper, renewable, non-irritation to skin, non-abrasive to equipment, high strength to weight ratio and interesting specific properties, producing composites that are environment friendly to a large extent. They also have some disadvantages such as moisture absorption, quality variations, low thermal stability and poor compatibility with the hydrophobic polymer matrix.

Though the high moisture absorption tendency of natural fibers would lead to composites with weak interface but pretreatments of natural fibers are aimed at improving the adhesion between fibers and matrix. In pretreatments, either hydroxyl groups get activated or new moieties are added that can effectively interlock with the matrix. This has been a subject of major research (Wang, 2004; Taj et al, 2007; Kalia et al, 2009; Ku et al, 2011).

The renewed interest in the natural fibers has resulted in a large number of modifications to bring it at par and even superior to synthetic fibers. Due to such tremendous changes in the quality of natural fibers, they are fast emerging as a reinforcing material in composites, especially for packaging and automotive applications. Global natural fiber composite market has grown from \$1.086 Billion in 2005, to \$2.1 Billion in 2010 and is expected to reach \$3.8 Billion by 2016, with automotive and construction applications having the largest share. The demand in automotive application alone increased by 45% between 2009 and 2012, up to 40kg per car, and it is estimated that automotive application of natural fibers in Europe in 2010 is about 100,000 tons, especially as they show better crash behavior and are thus safer than glass fiber parts (Bledzki and Gassan, 1999; Bledzki et al, 2002; Mueller, 2004; Ceccarini and Angelini, 2010; Timmins et al, 2011; McIntyre, 2012). This is a market for developing nations like Nigeria, where most fibers are seen as agricultural wastes, to harness. Thus the essence of this work is to present optimal conditions for use of selected local natural fibers in automotive applications.

1.2 Statement of the Problem

Although tremendous research results have been published regarding natural fiber mercerization treatment, which is the primary fiber treatment technique, there are still scanty works conducted in dealing with interaction of factors and optimizing the mercerization treatment conditions.

Most parameters considered in mercerization treatment were alkali concentration, fiber soaking temperature and fiber soaking duration. Although similar types of reinforced fiber are used, it could give different values in its final composite mechanical properties due to different parameter setting during a mercerization treatment process. Therefore, there is a significant need to conduct further work focusing on main effect and interaction effect of mercerization parameters setting toward enhancement of natural fiber reinforced composite mechanical properties (Hashim et al, 2012). The case is similar for other chemical treatments which have received less research attention in comparison to mercerization.

In addition, the traditional way of measuring the Modulus of Elasticity of a material is to measure the slope of the Stress-Strain curve in the linear-elastic region of the curve, but this technique produces values that are inaccurate, often by a factor of two or more, because of contributions to the strain from material creep or deflection of the test machine. It has been suggested that accurate values of Modulus of Elasticity are measured dynamically: by exciting the natural vibrations (vibration at natural frequency which is related to stiffness and mass) of a beam or wire or by measuring the velocity of longitudinal or shear sound waves in the material (Ashby and Cebon, 2011). There are hardly works available in open literature that present an approach to improve the accuracy of properties obtained from this traditional method.

Thirdly, homogenous isotropic linear elastic materials have their elastic properties uniquely determined by any two moduli among six elastic moduli: Young's modulus, Poisson ratio, shear modulus, bulk modulus, Lamé's modulus and wave modulus. Given any two, any other of the elastic moduli can be calculated (Bower, 2011). There are scarcely works available in open literature that provide at least two moduli for natural fibers studied, thus posing a challenge in

modeling composite properties from those of the fiber and matrix, making research in the later area also scanty.

The purpose of this study is to proffer solution to these observed short falls in research, with focus on application of natural fiber reinforced composites in automobile applications.

1.3 Aim and Objectives

1.3.1 The aim of this research work is to model the mechanical properties of selected natural fiber (empty plantain bunch fiber, empty palm bunch fiber and rattan palm fiber) reinforced composites for automobile application.

1.3.2 The objectives of the research work are as follows:

- * To determine the chemical compositions of the three selected natural fibers and two polymer matrices used.
- * To study the effects of selected chemical treatments on the fibers and determine the best chemical treatments and treatment conditions for each fiber using Statistical modeling and optimization.
- * To propose a new approach for analysis of data from the traditional way of measuring modulus of elasticity of materials that will give more accurate results.
- * To study the effects of fiber volume fraction and fiber length (aspect ratio) on composite mechanical properties using Statistical modeling and optimization.
- * To obtain compatible micro-mechanics based model for matching of different fiber reinforced polymer composites mechanical properties against fiber and matrix properties.

- * To obtain a neural network model for the composite mechanical properties as a function of fiber aspect ratio and volume fraction.

- * To recommend the best conditions for use of the fibers, possible improvements and future research areas with respect to automobile applications.

1.4 Scope of the Study

This research work studied the optimal conditions for treatment of three selected natural fibers (with concentration of treatment chemical and treatment time as factors), using selected treatment options, and their use in the reinforcement of epoxy and polyester matrices, with a focus on automobile applications. Fiber volume fraction and fiber aspect ratio were the factors of interest in composite study, using a random orientation. Simple equations, based on reasonable assumptions, were presented to extend the analysis of the mechanical properties of the fibers and their composites for use in determination of at least two moduli (Young's modulus and Poisson ratio) and a technique that will improve accuracy in the determination of the Modulus of elasticity was also presented. Micromechanics modeling of composite properties based on the individual properties of the fiber and matrix was studied. Temperature was not considered as a factor during the treatment process, as all treatments were done at room temperature, also fiber orientation, as a factor, is outside the scope of study for the composites, because a random orientation was used.

1.5 Justification of the Study

- * To contribute in advancing the extent of available knowledge in the area of Material Science in general and particularly composite manufacture using natural fibers.
- * To project other natural fibers that can compete favourably with flax, hemp and kenaf which are already in use for automotive body manufacture and present treatment conditions that will give them a competitive edge.
- * To present export opportunity for Nigeria and other developing countries, especially to Europe, by using waste agricultural products in producing fibers that have economic value.
- * To contribute in environmental management and job/wealth creation by presenting alternative uses for non-wood natural fiber sources.

CHAPTER TWO

LITERATURE REVIEW

2.1 Fibers

Fiber is a class of materials that are continuous filaments or are in discrete elongated pieces similar to threads. They can be spun into filaments, strings or ropes used as components of composite materials, or matted into sheets to make products such as paper or felt. The strongest Engineering materials often incorporate fibers, for example, carbon fiber and ultra high molecular weight polyethylene. Fibers can be classified as natural or synthetic. Synthetic fibers, like glass fiber, can often be produced very cheaply and in large amounts compared to natural fibers, but for some applications like clothing, natural fibers give benefits such as comfort over their synthetic counterparts.

2.1.1 Natural Fibers

A natural fiber is any hair like raw material directly obtainable from an animal, vegetable or mineral source and convertible into non-woven fabrics such as felt or after spinning into yarns or woven cloth. It may be further defined as an agglomeration of cells in which the diameter is negligible in comparison with the length (Taj et al, 2007). Plant (vegetable) fibers are of interest in this work.

2.1.2 Classification of Natural Fibers

Fibers for reinforced plastics can be generally classified into two categories based on their aspect ratio: (i) Short Fibers (Discontinuous Fibers): These are fibers with aspect ratio (ratio of length to diameter) between the values of 20 and 60.

(ii) Long Fibers (Continuous Fibers): These are fibers with aspect ratio (ratio of length to diameter) between the values of 200 and 500 (Kalpakjian and Schmid, 2001).

A more frequently used approach for classification of natural fibers is the classification based on their origin, and the plant-based fibers can be further categorized based on part of the plant they are recovered from as seed, bast, leaf and fruit fibers; with the bast and leaf (the hard fibers) types being the most commonly used in composite applications (Williams and Wool, 2000).

A general classification for natural fibers is provided in Figure 2.1.

2.1.2.1 Advantages of natural fibers

In addition to having comparable mechanical properties; low specific weight which results in a higher specific strength and stiffness, plant fibers have the following advantages over synthetic fibers:

- * They provide better thermal and acoustic insulation properties, especially as an automotive interior or construction material part, due to presence of lumen/void in the fiber.
- * They are easy to process in the traditional textile machinery for making reinforcement elements, like yarn, mat or woven fiber.
- * They are not harsh, like synthetic fibers, on the processing machinery like extruder, pelletizer or injection moulding machine.
- * They can be thermally recycled where glass or other synthetic fibers cause problems in combustion furnace.
- * They do not cause any allergies or lung diseases if breathed in or come in contact with.

* In automotive interior parts, they function as better and safer components as they do not show any sharp fractures.

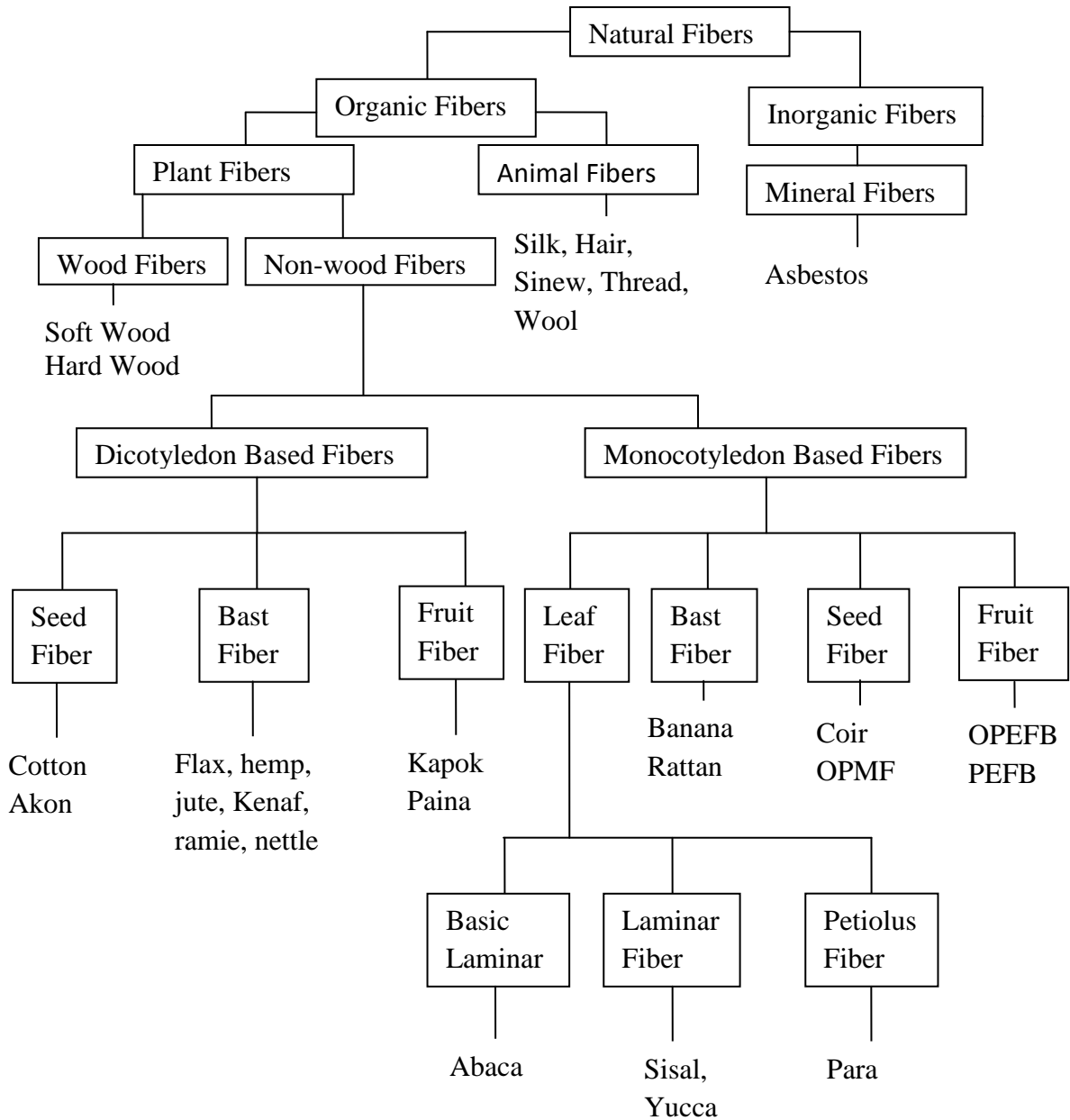


Figure 2.1: Classification of Natural fibers (Adapted from: Ichhaporia(2008))

- * They are light weight compared to synthetic fibers reinforced composites thereby producing better fuel efficiency or the weight saved, in interior and car trim panels, can be used in other car components to improve its performance.
- * They are a renewable resource, a green product (environmentally friendly), fully biodegradable, with the production requiring little energy, CO₂ being used, while oxygen is given back to the environment.
- * They are abundantly available and producible with low investment, at low cost, which makes an interesting product for low income countries. They thus provide an economic incentive and a marketing advantage.

2.1.2.2 Disadvantages of natural fibers

- * The prices of natural fibers can fluctuate by harvest result or agricultural politics.
- * Lower durability (fiber treatment can improve this considerably)
- * Moisture absorption which causes swelling of the fibers (Fiber treatment improves this).
- * Lower strength properties, particularly its impact strength.
- * Poor wettability and Incompatibility with some polymer matrices (Fiber treatment can improve this considerably)(Taj et al, 2007; Ichhaporia, 2008).

2.1.3 Properties of Natural Fibers

Natural plant fibers are composites of cellulose fibers, consisting of helically wound cellulose microfibrils, bound together by an amorphous lignin matrix. Hemicellulose found in the natural fibers is believed to be a compatibilizer between cellulose and lignin. Each fiber has a complex, layered structure consisting of a thin primary wall, which is the first layer deposited during cell

growth, encircling a secondary wall. The secondary wall is made up of three layers and the thick middle layer determines the mechanical properties of the fiber. The middle layer consists of a series of helically wound cellular microfibrils formed from long chain cellulose molecules. The angle between the fiber axis and the microfibrils is called the microfibrillar angle. These microfibrils have typically a diameter of about 10-30 nm and are made up of 30-100 cellulose molecules in extended chain conformation and provide mechanical strength to the fiber (Kalia et al, 2009).

The properties of natural fibers are affected by many factors such as variety, climate, location, weather conditions, soil characteristics, harvest, maturity, retting degree, decortications, disintegration (mechanical, steam explosion treatment), fiber modification, textile and technical processes (spinning and carding). To better understand the properties of natural fiber-reinforced composite materials, it is necessary to know the mechanical, physical and chemical properties of natural fibers (Kalia et al, 2009).

2.1.3.1 Physical and chemical composition of natural fiber

Properties such as density, electrical resistivity, ultimate tensile strength and initial modulus are related to the internal structure and chemical composition of fibers. The chemical composition of natural fibers varies depending upon the type of fibers. The chemical composition (Table 2.1) as well as the structure of the plant fibers is fairly complicated. Plant fibers are composite materials designed by nature. The fibers are basically a rigid, crystalline cellulose microfibril-reinforced amorphous lignin and/or with hemicellulosic matrix. Most plant fibers, except for cotton, are composed of cellulose, hemicellulose, lignin, waxes, and some water-soluble compounds, where cellulose, hemicelluloses, and lignin are the major constituents. The properties

of the constituents contribute to the overall properties of the fiber. Hemicellulose is responsible for the biodegradation, micro-absorption and thermal degradation of the fiber as it shows least resistance, whereas lignin is thermally stable but prone to UV degradation. The percentage composition of each of these components varies for different fibers. Generally, the fiber contains 60-80 % cellulose, 5-20 % lignin and up to 20 % moisture. The cell wall of the fiber undergoes pyrolysis with increasing processing temperature and contributes to char formation. These charred layers help to insulate the lignocelluloses from further thermal degradation (Bledzki and Gassan, 1999; Amar et al, 2005).

2.1.3.2 Mechanical properties of natural fibers

The mechanical properties and physical properties of natural fibers vary considerably depending on the chemical and structural composition, fiber type and growth conditions. Mechanical properties of plant fibers are much lower when compared to those of the most widely used competing reinforcing glass fibers (Table 2.2). However, because of their low density, the specific properties (property-to-density ratio), specific strength, and specific stiffness of plant fibers can be comparable to the values of glass fibers (Wanbua et al, 2003; Amar et al, 2005).

Table 2.1: Chemical composition of some plant fibers (Mohanty et al, 2000; Rowell et al, 2000)

Fiber	Cellulose (%)	Hemi-Cellulose (%)	Lignin (%)	Extra ctives (%)	Ash (%)	Pectin (%)	Wax (%)	Spiral Angle (deg)	Moisture Content (%)
Abaca	56-63	15-17	7-13	-	1-3	1	-	-	5-10
Bagasse	32-48	27-32	19-24	-	1.5-5	0.7-3.5	-	-	-
Bamboo	26-43	15-26	21-31	-	1.7-5	0.7	-	-	-
Banana	63-64	10	5	-	-	-	-	-	10-12
Barley	31-45	24-29	14-15	-	5-7	3-6	-	-	-
Coir	32-43	0.15-0.25	40-45	-	-	3-4	-	41-45	8
Cotton	82.7-90	5.7	-	-	-	0-1	0.6	-	7.85-8.5
Flax	71-78.5	18.6-20.6	2.2	2.3	1.5	2.2-2.3	1.7	5-10	8-12
Hard wood	43-47	25-35	16-24	2-8	0.4	-	-	-	-
Hemp	70.2-74.4	17.9-22.4	3.7-5.7	3.6	2.6	0.9	0.8	6.2	6.2-12
Henequen	77.6	4-8	13.1	-	-	-	-	-	-
Jute (Bast)	61-71.5	13.6-20.4	12-13	-	-	0.2	0.5	8.0	12.5-13.7
Jute (Core)	41-48	18-22	21-24	-	0.8	-	-	-	-
Kenaf-Bast	44-57	22-23	15-19	3.2	2-5	3-5	-	8	-
Kenaf-Core	37-49	18-24	15-21	-	2-4	-	-	-	-
Nettle	86	-	-	-	-	-	-	-	11-17
Oat	31-48	27-38	16-19	-	6-8	4-6.5	-	-	-
Oil-Palm EBF	65	-	19	-	-	-	42	-	-
Oil Palm Mesocarp	60	-	11	-	-	-	46	-	-
Pineapple	70-82	-	5-12.7	-	-	-	-	14	11.8
Ramie	68.6-76.2	13.1-16.7	0.6-0.7	-	-	1.9	0.3	7.5	7.5-17
Rice	24-48	23-38	12-16	-	15-20	9-14	-	-	-
Rye	33-50	27-30	16-19	-	2-5	0.5-4	-	-	-
Sisal	67-68	10-14.2	8-11	-	0.6-1	10	2	10-25	11
Soft wood	40-44	25-29	25-31	5	0.2	-	-	-	-
Wheat	29-51	26-32	16-21	-	4.5-9	3-7	-	-	-

2.1.4 Pretreatments of Natural Fibers

The interest in using natural fibers in composites has increased in recent years due to their lightweight, nonabrasive, combustible, nontoxic, low cost and biodegradable properties. However, lack of good interfacial adhesion, low melting point and poor resistance to moisture absorption, make the use of natural fiber reinforced composites less attractive. Pretreatments of

the fiber can clean the fiber surface, chemically modify the surface, stop the moisture absorption process and increase the surface roughness. As the natural fibers bear hydroxyl groups from cellulose and lignin, therefore, they are amenable to modification. The hydroxyl groups may be involved in the hydrogen bonding within the cellulose molecules thereby reducing the activity towards the matrix. Chemical modifications may activate these groups or can introduce new moieties that can effectively interlock with the matrix (Scandola et al, 2000; Kalia et al, 2009).

Table 2.2: Comparative Properties of Natural fibers and Conventional Man-made fibers

(Adapted from: Mohanty et al, 2000; Suraya and Khalil, 2011)

Fiber	Density (g/cm ³)	Diameter (μm)	Tensile Strength (MPa)	Young's Modulus (GPa)	Elongation at Break (%)
Abaca	1.5	-	400	12	3-10
Alfa	0.89	-	350	22	5.8
Bamboo	0.6-1.1	-	140-230	11-17	-
Banana	1.35	50-250	500-780	12	5.9
Coir	1.15-1.2	100-450	131-175	4-6	15-40
Cotton	1.5-1.6	-	287-800	5.5-12.6	7-8
Curaua	1.4	-	500-1150	11.8	3.7-4.3
Date Palm	1-1.2	-	97-196	2.5-5.4	2-4.5
Flax	1.5	-	345-1100	27.6	2.7-3.2
Hemp	1.48	-	690	70	1.6
Henequen	1.2	-	430-570	10.1-16.3	3.7-5.9
Isora	1.2-1.3	-	500-600	-	5-6
Jute	1.3-1.45	20-200	393-773	13-26.5	1.16-1.8
Kenaf	-	-	930	53	1.6
Nettle	-	-	650	38	1.7
Oil Palm	0.7-1.55	-	248	3.2	25
Piassava	1.4	-	134-143	1.07-4.59	2.9-7.8
Pineapple	0.8-1.6	20-80	400-627	34.5-82.51	1.6
Ramie	1.5	-	400-938	61.4-128	1.2-3.8
Sisal	1.45-1.5	50-200	468-640	9.4-22	2-7
Soft wood	1.5	-	1000	40	-
Viscose	-	-	593	11	11.4
Aramid	1.4	-	3000-3150	63-67	3.3-3.7
Carbon	1.7	-	4000	230-240	1.4-1.8
E-glass	2.5	-	2000-3500	70	15-40
S-glass	2.5	-	4570	86	2.5

2.1.4.1 Surface chemical modifications of natural fibers

Several studies have shown the influence of various types of chemical modification on the performance of natural fiber and fiber-reinforced composites. The different surface chemical modifications of natural fibers such as mercerization, silane treatment, permanganate treatment, peroxide treatment, isocyanate treatment, sodium chlorite treatment, plasma treatment, acetylation, acrylation, etherification, benzylation, graft copolymerization, latex coating and others, have achieved various levels of success in improving fiber mechanical properties and fiber-matrix adhesion in natural fiber composites (Kalia et al, 2009).

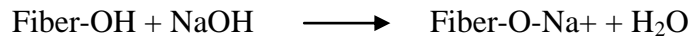
Brief descriptions of some important fiber chemical modifications are summarized in the following sub-sections.

i. Mercerization (alkali treatment) of natural fibers

Alkali treatment of cellulosic fibers, also called mercerization, is the usual method to produce high quality fibers (Ray et al. 2001). The standard definition of mercerization as proposed by ASTM D1965 is: the process of subjecting a vegetable fiber to an interaction with a fairly concentrated aqueous solution of strong base, to produce great swelling with resultant changes in the fine structure, dimension, morphology and mechanical properties (Hashim et al, 2012). Alkali treatment improves the fiber-matrix adhesion due to the removal of natural and artificial impurities (Mishra et al. 2001). It leads to fibrillation, which causes the breaking down of the composite fiber bundle into smaller fibers. In other words, alkali treatment reduces fiber diameter, thereby increasing the aspect ratio (reduction in fiber diameter and subsequent increase in aspect ratio increases the surface area of fiber in contact with the matrix thus enhancing fiber-matrix adhesion). The development of a rough surface topography and enhancement in aspect

ratio offer better fiber-matrix interface adhesion and an increase in mechanical properties (Joseph et al. 2000). Alkali treatment increases surface roughness resulting in better mechanical interlocking and the amount of cellulose exposed on the fiber surface. This increases the number of possible reaction sites and allows better fiber wetting.

The following reaction takes place as a result of alkali treatment:



Mercerization affects the chemical composition of natural fibers, degree of polymerization and molecular orientation of the cellulose crystallites due to cementing substances like lignin and hemicellulose which are removed during the mercerization process. Consequently, mercerization has a lasting effect on the mechanical behavior of natural fibers, especially on fiber strength and stiffness (Gassan and Bledzki, 1999). It also leads to the increase in the amount of amorphous cellulose at the expense of crystalline cellulose and the removal of hydrogen bonding in the network structure (Mishra et al. 2002; Joseph et al. 2000; Sreekala et al. 2000; Wang, 2004; Kalia et al, 2009).

ii. Silane treatment of natural fibers

Coupling agents usually improve the degree of cross-linking in the interface region and offer a perfect bonding. Silane coupling agents have been found to be effective in modifying natural fiber-matrix interface. Efficiency of silane treatment was high for alkaline treated fiber, than untreated, because more reactive sites can be generated for silane reaction. Various silanes were effective in improving the interface properties of wood-polypropylene (Coutinho et al. 1997), fiber-reinforced epoxies (Culler et al. 1986) and phenolics composites (Ghatge and Khisti 1989). Silanes undergo hydrolysis, condensation and bond formation stage, alkoxy silanes are able to

form bonds with hydroxyl groups and Silanols can form polysiloxane structures by reaction with hydroxyl group of the fibers. In the presence of moisture, hydrolysable alkoxygroup leads to the formation of silanols, which then react with hydroxyl group of fiber, forming stable covalent bonds to cell wall that are chemisorbed onto the fiber surface.

González et al. (1997) investigated the effect of silane coupling agent on the interfaceperformance of henequen fiber-reinforced high-density polyethylene composites. The fiber-surface silanization resulted in better interfacial load transfer efficiency but did not improve the wetting of the fiber. Hydrogen and covalent bonding mechanisms could be found in the natural fiber-silane system. Silane treatment of cellulosic fibers can increase the interfacial strength and therefore the mechanical properties of the composite (George et al. 1998; Bataille et al. 1989; Joseph et al. 2000).

iii. Permanganate treatment of natural fibers

This is done using different concentrations of potassium permanganate solution in acetone with soaking duration from 1-3mins, after alkaline pre-treatment. This reduces the hydrophilic tendency of fibers and thus water absorption of fiber-reinforced composite, with marginal increase in the tensile strength values of the composite. Hydrophilic tendency decreased with increase in permanganate concentration, but at higher concentrations of 1.0wt%, degradation of cellulosic fiber occurred, resulting in formation of polar groups between fiber and matrix. To improve the bonding at the fiber-polymer interface, permanganate treatment of natural fibers is the best method (Joseph et al, 2000; Sreekala et al, 2000).

iv. *Peroxide treatment of natural fibers*

Peroxide-induced adhesion in cellulose fiber-reinforced thermoplastic composites has attracted the attention of various researchers due to easy processability and improvement in mechanical properties. Organic peroxide easily decompose to free radicals, which further react with hydrogen group of matrix and cellulose fibers at the interface during the time of curing of composites. Sapieha et al. (1990) indicated that the addition of a small amount of benzoyl peroxide or dicumyl peroxide to cellulose-polymer (LLDPE) systems during processing improved the composite mechanical properties. The improvement of mechanical properties is attributed to the peroxide-induced grafting of polyethylene onto cellulose surfaces. Joseph et al. (2000) investigated benzoyl peroxide treatment on short sisal fiber reinforced polyethylene composites. They reported that peroxide-treated composites showed an enhancement in tensile properties due to the peroxide-induced grafting. Sreekala et al. (2000) also studied benzoyl peroxide treatment on oil palm fiber reinforced phenol formaldehyde composites. Fibers were coated with benzoyl peroxide from acetone solution after alkali pre-treatments. They reported that peroxide-treated fiber composites could withstand the tensile stress to higher strain level.

v. *Acetylation of natural fibers*

Acetylation of natural fibers is a well-known esterification method applied to introduce plasticization to cellulosic fibers. It was originally applied to wood cellulose to stabilize the cell walls against moisture, improving dimensional stability and environmental degradation. Pretreatment of fibers with acetic anhydride substitutes the hydroxyl groups of the cell wall with acetyl groups, modifying the properties of these polymers so that they become hydrophobic. The hydroxyl groups that react with the reagent are those of lignin and hemicelluloses (amorphous

material), whereas the hydroxyl groups of cellulose (crystalline material) are being closely packed with hydrogen bonds, prevent the diffusion of reagent and thus result in very low extents of reaction (Rowell, 1991; Ebrahimzadeh, 1997; Murray, 1998; Rowell, 1998). Acetylation is beneficial in reducing the moisture absorption of natural fibers. Bledzki and Gassan (1999) reported about 50% reduction in moisture uptake for acetylated jute fibers and of up to 65% for acetylated pine fibers.

vi. *Etherification of natural fibers*

Epoxides, like epichlorohydrin, have a strained ring (3, 4-member) containing oxygen that creates electron withdrawal from adjacent carbons. This arrangement makes epoxides relatively reactive with alcohol containing molecules like cellulose. Modification of cellulosic fibers by etherification enhances certain new ranges of properties and makes it more useful and acceptable in diversified applications. Sodium hydroxide plays an important role in forming a charged intermediate species with the fiber, which allows the faster nucleophilic addition of epoxides, alkyl halides, benzyl chloride, acrylonitrile, and formaldehyde. It is reported that wood is pretreated with NaOH concentration greater than 25% at temperatures greater than 90°C to minimize hydrolysis of wood components. Though the modified wood products have shear strength similar to that of unmodified wood, the thermo plasticization of wood by benzyl chloride created a wood derivative that could be pressed or extruded into films or molded products (Kalia et al, 2009).

vii. *Benzoylation of natural fibers*

Inclusion of benzoyl group in natural fiber (mostly using benzoyl chloride) is responsible for the decreased hydrophilic nature of the treated fiber. The fiber was initially pre-treated with 18% NaOH solution for 30mins (followed by filtration and washing with water) to activate the hydroxyl groups of the cellulose and lignin in the fiber; then the treated fiber was suspended in 10% NaOH solution and agitated with 50ml benzoyl chloride solution for 15 min. The isolated fibers were then soaked in ethanol for 1 hour to remove the benzoyl chloride and finally was washed with water and dried in the oven at 80°C for 24 hours (Joseph et al, 2000; Wang, 2004).

viii. *Sodium chlorite treatment of natural fibers*

Sodium chlorite treatment of natural fibers is a bleaching process that removes non-cellulosic compounds from the natural fiber thus improving its mechanical and physical characteristics as well as its behavior during processing and wearing. A novel chemical formulation for bleaching flax fibers (machine tow) in a one-step process was developed based on activation of sodium chlorite by hexamethylenetetramine (HMTA) in the presence of a nonionic wetting agent. The optimum formulation for bleaching the flax fibers consists of: Sodium chlorite = 5g/l, [HMTA] = 0.25 g/l and wetting agent = 1 g/l provided that bleaching is carried-out at 90°C for 3 hours using a material-to-liquor ratio (M/L) of 1:50. It was reported that, when the optimum formulation was used, HMTA activates decomposition of sodium chlorite to liberate nascent oxygen rather than chlorine dioxide (Kalia et al, 2009).

ix. *Isocyanate treatment of natural fibers*

Isocyanate has $-N=C=O$ functional group, which is very susceptible to reaction with the hydroxyl group of cellulose and lignin in the fibers and forms strong covalent bonds, thereby creating better compatibility with the binder resin in the composites. This treatment is known to improve the fiber-matrix interfacial adhesion(Kalia et al, 2009).

x. *Acrylation, maleic anhydride, and titanate treatment of natural fibers*

Acrylation treatment, maleated polypropylene/maleic anhydride treatment and titanate treatment of natural fibers have been reported by many researchers. The treatment of natural fibers with MAPP (maleated polypropylene/maleic anhydride)copolymer provides covalent bonds across the interface, increasing the surface energy of the fibers and thereby providing better wet-ability and high interfacial adhesion. Many other compounds such as chromium complexes and titanates can be used as coupling agents. Sreekala et al. (2000) treated Oil palm fibers with various concentrations of acrylic acid at 50°C for 1 hour after pre-treatment with 10% NaOH for about 30 min. The fibers were then washed with aqueous alcoholic solution and dried. MAPP as coupling agent for the surface modification of jute fibers was used by Mohanty et al. (2004). They reported that 30% fiber loading with 0.5% MAPP concentration in toluene and 5 min impregnation time with 6 mm average fiber length gave best results. It has been reported by Mishra et al. (2000) that maleic anhydride treatment reduced the water absorption to a great extent in hemp, banana and sisal fibers and their composites.

xi. Graft copolymerization of natural fibers

Graft copolymerization is an effective method of surface chemical modification of natural fibers and has been in use since 1943 when the first graft copolymer of vinyl and allyl ethers of cellulose copolymerized with maleic acid ester appeared in the literature. Creation of an active site on the preexisting polymeric backbone is the common feature of most methods for the synthesis of graft copolymers. The active site may be either a free-radical or a chemical group which may get involved in an ionic polymerization or in a condensation process. Polymerization of an appropriate monomer onto this activated back-bone polymer leads to the formation of a graft copolymer. A number of methods can be used for the generation of active sites on the polymeric backbone and can be described as: physical method, chemical method, physico-mechanical method, radiation method and enzymatic grafting. The conventional techniques of grafting of natural fibers require significant time and energy. It has been found that grafting under microwave radiations is the best method in terms of time consumption and cost effectiveness. Grafting of methyl methacrylate onto flax fiber was performed under different reaction conditions such as in air, under pressure and under the influence of micro-wave radiations. Maximum percentage grafting (41.7%) has been observed in case of graft copolymerization performed in air at 55^oC followed by grafting under pressure (36.4%) at 0.8 MPa and under the influence of microwave radiations (24.6%) at 210 W microwave power. Optimum reaction conditions for getting maximum graft yield in case of graft copolymerization are available in literature (Kalia et al, 2009).

xii. Plasma treatment of natural fibers

Plasma treatment is an effective method to modify the surface of natural polymers without changing their bulk properties. The plasma discharge can be generated by either corona treatment or cold plasma treatment. Both methods are considered as a plasma treatment when ionized gas has an equivalent number of positive and negative charged molecules that react with the surface of the present material. The distinguishing feature between the two categories of plasma is the frequency of the electric discharge. High-frequency cold plasma can be produced by microwave energy, whereas a low frequency alternating current discharge at atmospheric pressure produces corona plasma. The type of ionized gas and the length of exposure influenced the modification of the wood and synthetic polymer surfaces (Goring, 1976; Young, 1992). It was observed that air corona treatment caused a reduction in the molecular weight of cellulose and with a change in gas to nitrogen; the corona treatment did not lower the intrinsic viscosity of cellulose, thus demonstrating that the type of gas influences the degree of modification. Water and methanol extractives were increased, indicating that the cellulose and hemicelluloses were changed. However, the ratio of syringyl aldehyde to vanillin (found by alkaline nitrobenzene oxidation) remained unchanged for the corona treatments, which indicated that the non-condensed type of lignin showed no effects for the corona treatment. Pretreatment of wool fabric with low-temperature plasma resulted in improvement in fabric hydrophilicity and wettability and created new active sites along with improved initial dyeing rate, proving the suitability of DC plasma treatment in textile industry for enhancing the wettability of fibers (Kalia et al, 2009).

2.2 Matrices

The role of matrix in a fiber-reinforced composite is to transfer stress between the fibers, to keep the fibers in the desired location and orientation, to provide a barrier against an adverse environment and to protect the surface of the fibers from mechanical abrasion. The matrix plays a major role in the tensile load carrying capacity of a composite structure. The binding agent or matrix in the composite is of critical importance. Four major types of matrices have been reported: Polymeric, metallic, ceramic and carbon. Most of the composites used in the industry today are based on polymer matrices. Polymer resins have been divided broadly into two categories: Thermoplastics and thermosetting (Taj et al, 2007).

2.2.1 Thermoplastic polymers

Thermoplastics are polymers that require heat for their processing and retain their shape after cooling. In addition, these polymers may be reheated and reformed, often without significant changes in their properties. The thermoplastics which have been used as matrix for natural fiber reinforced composites are as follows: High density polyethylene (HDPE); Low density polyethylene (LDPE); Chlorinated polyethylene (CPE); Polypropylene (PP); Normal polystyrene (PS); Poly (Vinyl chloride) (PVC); Mixtures of polymers and recycled thermoplastics. Only those thermoplastics whose processing temperature (temperature at which fiber is incorporated into polymer matrix) does not exceed 230°C may be used for natural fiber reinforced composites. These are, most of all, polyolefines, like polyethylene and polypropylene. Technical thermoplastics, like polyamides, polyesters and polycarbonates require processing temperatures greater than 250°C and therefore cannot be used for such natural fiber composite processing without fiber degradation (Sinha, 2000; Taj et al, 2007).

2.2.2 Thermosetting polymers

Thermosets are a hard and stiff cross-linked material that does not soften or become moldable after it has been heated or cured. Thermosets are stiff and do not stretch the way that elastomers and thermoplastics do. Most commonly used thermoset polymers are epoxy resins and other resins (Unsaturated polyester resins (as in fiberglass) vinyl ester, phenolic epoxy, novolac and polyamide) (Sinha, 2000; Taj et al, 2007).

2.2.2.1 Epoxy resins

Epoxy resins are polyether resins containing more than one epoxy group capable of being converted into the thermoset form. These resins, on curing, do not create volatile products in spite of the presence of a volatile solvent and so have low cure shrinkage. The epoxies may be named as oxides, such as ethylene oxides (epoxy ethane), or 1,2-epoxide. The epoxy group, also known as oxirane, contains an oxygen atom bonded with two carbon atoms, which in their turn are bound by separate bonds. They can be obtained in either liquid or solid states. Epoxy resins are easily and quickly cured at any temperature from 5°C to 150°C, depending on the choice of curing agent. The curing of epoxy resins is an exothermic process, resulting in the production of limited-size molecules; having molecular weights of a few thousands. Epoxy resins shrink on curing, thus both the density and refractive index increase. Applications for epoxy resins are extensive: adhesives, bonding, construction materials (flooring, paving, and aggregates), composites, laminates, coatings, molding, textile finishing, aircraft and spacecraft industries, with the composite industry consuming 27.6% of the epoxy resins produced (Bhatnagar, 1996).

Epoxies generally out-perform most other resin types in terms of mechanical properties and resistance to environmental degradation, which leads to their almost exclusive use in aircraft

components. Epoxies differ from polyester resins in that they are cured by a 'hardener' rather than a catalyst. The hardener, often an amine, is used to cure the epoxy by an 'addition reaction' where both materials take place in the chemical reaction (Singla and Chawla, 2010).

2.2.2.2 Polyester resins

Polyester resins are heterochain macromolecules that possess carboxylate ester groups as an integral component of their polymer backbones. It is a liquid which will cure to a solid when the hardener, often referred to as catalyst, is added. It has been specially formulated to cure at room temperature. The hardener, MEKP (Methyl Ethyl Ketone Peroxide) is added to cure, or harden the resin. Polyester resins have a limited shelf life of one year. Polyester resins can be classified as saturated polyester resin; alkyd resin; vinyl ester resin and unsaturated Polyester resin. Vinyl ester resins are becoming increasingly important in new industrial applications such as coating, printed circuit boards, metal foil laminates, building materials, automotive parts, rigid foams and fiber reinforced composites. They combine the excellent mechanical, chemical and solvent resistance properties of epoxy resins with the properties found in the unsaturated polyester resins. Unsaturated polyesters are cost effective and extremely versatile in properties and applications and have been a popular thermoset used as the polymer matrix in composites. They are widely produced industrially as they possess many advantages compared to other thermosetting resins including room temperature cure capability, good mechanical properties and transparency (Sharifah et al, 2005).

2.3 Composites

Composites are materials that comprise strong load carrying materials (known as reinforcement) imbedded in weaker material (known as matrix). Reinforcement provides strength

and rigidity, helping to support structural load. The matrix or binder (organic or inorganic) maintains the position and orientation of the reinforcement. Significantly, constituents of the composites retain their individual, physical and chemical properties; yet together they produce a combination of qualities which individual constituents would be incapable of producing alone (Hull and Clyne, 1996).

Composites can be grouped into four categories based on the nature of the matrix each type possesses; Polymer Matrix Composites (PMCs); Metal Matrix Composites (MMCs); Ceramic Matrix Composites (CMCs) and Carbon-Carbon Composites (CCCs). The most common advanced composites are polymer matrix composites. These composites consist of a polymer thermoplastic or thermosetting reinforced by fiber. The reason for these being most common is their low cost, high strength and simple manufacturing principles (Amar et al, 2005).

2.3.1 Natural Fiber Reinforced Polymer Composites

These are composites obtained by the reinforcement of polymers with natural fibers (especially non-wood plant fibers, with respect to this study). Natural fiber reinforced composites have received increased attention both by the academic sector and the industry because of the significant advantages of natural fibers over synthetic fibers. Currently, many types of natural fibers have been investigated for use in plastics including flax, hemp, jute straw, wood, rice husk, wheat, barley, oats, rye, cane (sugar and bamboo), grass, reeds, kenaf, ramie, oil palm empty fruit bunch, sisal, coir, water hyacinth, pennywort, kapok, paper mulberry, raphia, banana fiber, pineapple leaf fiber and papyrus (Bledzki and Gassan, 1999).

2.3.2 Processing of Fiber Reinforced Polymer Composites

Polymer composite processing utilizes the same technique as polymer processing which include injection molding, compression molding and extrusion. There are other techniques which are unique only to polymer composite processing. These include filament winding, pultrusion, and hand lay-up.

2.3.2.1 Hand lay-up moulding

Hand lay-up moulding is the method of laying down fabrics made of reinforcement and painting with the matrix resin layer by layer until the desired thickness is obtained. This is the most time and labor consuming composite processing method, but majority of aerospace composite products is made by this method in combination with the autoclave method. Due to the hand assembly involved in the lay-up procedure, one can align long fibers with controlled orientational quality. Another advantage of this method is the ability to accommodate irregular-shaped products. Such advantages are utilized in low performance composites including fiber-glass boat and bath tub manufacturing (Ishida, 1990;Skramstad, 1999).

2.3.2.2 Spray-up moulding

Spray-up moulding is much less labor intensive than the hand lay-up method by utilizing a spray gun and a fiber cutter. However, only short fiber reinforced composites can be made. A continuous fiber is fed into the cutter and chopped. The chopped fiber is sprayed upon a mold with the stream of resin mist and catalyst delivered through separate nozzles. The sprayed mixture of fiber and resin soon cures on the mold at room temperature and the product is produced. Because of the spraying operation, large and complex-shaped objects can be easily made (Ishida, 1990;Skramstad, 1999).

2.3.2.3 Compression moulding, transfer moulding and resin transfer moulding

Compression moulding uses a press to compress either dough of resin and fiber mixture, or the layers placed by a hand lay-up method or mechanical means, typically at an elevated cure temperature. With the compressive force, the void content is lower than the ordinary atmospheric pressure processing method. A matched die mold allows shaping of the composite precursor into reproducible shapes. Although a compression molding machine is used, it is still a labor intensive method as the dough or layed-up materials must be weighed and hand-fed into the mold.

Transfer moulding is the improved version of compression moulding from the material metering point of view as the fiber/resin mixture is transferred from the reservoir into the mold cavity by the press. However, a long-fiber reinforced composite cannot be made. This method is nearly identical to a plunger-type injection moulding operation based on the material flow. The term "transfer moulding" is used for a compression press operation while plungertype injection moulding is obviously carried out in an injection moulding machine.

Resin transfer moulding is the same as the ordinary transfer moulding except that only the resin is transfer moulded into the mould cavity where fabrics are placed beforehand. Preforms of fibers and other reinforcements can be made with short fibers and sometimes continuous fibers. Preforms must be made to withstand the pressure of resin injection in order to avoid compression of the fibers during mold filling which would lead to inhomogeneous fiber distributions in the final part. Curing proceeds after filling at an elevated temperature (Ishida, 1990;Skramstad, 1999).

2.3.2.4 Injection moulding

Injection moulding is probably the most extensively used method for processing short-fiber reinforced thermoplastics. The fiber/resin mixture, whether it is pre-blended or fed as a physical mixture, is fed into the hopper and transferred into the heated barrel. The material softens by the heat transfer from the barrel wall. At the same time, the screw rotates to apply high-shear process to further heat the material and fill the barrel. The molten material is collected in front of the screw by the rotation of the screw, and then injected with a high pressure into the mold cavity through the runner and the gate. The mould is cooled below the solidification temperature of the resin in case of thermoplastics composites. The level of automation of this method is the highest among many processing methods.

Due to the intensive mixing with high-shear and passage through a narrow gate, extensive fiber damage occurs; therefore, injection moulding for composite materials is suitable only with short fiber reinforced or particulate-filled polymers. There is a critical length of fibers below which the fiber length does not degrade. The critical length is determined by the rheological properties of the composite mould, fiber properties and instrument factors. Less fiber damage occurs when a plunger-type injection moulding machine is used rather than a screw-type injection molding machine. Because the plunger-type injection moulding machine does not achieve a high degree of mixing in the machine, the raw materials must be thoroughly mixed prior to feeding (Ishida, 1990;Skramstad, 1999).

2.3.2.5 Reaction injection moulding

Reaction injection moulding (RIM) is one of the newest processing methods. Instead of using already polymerized materials as matrices, highly reactive monomeric or oligomeric ingredients

are placed in two tanks which are then quickly mixed by impingement, and injected into the mould cavity. As soon as the two materials are mixed, chemical reaction begins to form a polymeric matrix, which completes typically within 5-30 seconds. Thus, the major portion of the RIM machine is a high pressure pump and a metering system. Again, with high intensive shear, only short fibers and fillers can be used as reinforcements. However, RIM utilizes low viscosity chemicals and this allows the pre-placement of continuous fiber-woven fabrics in the mold in the same manner as resin transfer moulding. Distinction is made between these two methods based on the preparation of the resin precursor. When the resin formulation is already made, the method is called resin transfer moulding while if the resin is prepared in-situ by an impingement or static mixer, the method is termed RIM (Ishida, 1990;Skramstad, 1999).

2.3.2.6 Pultrusion

Pultrusion is used only for polymer composite processing. A bundle of fiber rovings is passed through a wet resin bath, squeezed into a desired shape, passed through a heated die, and cured into a final composite. The solidified composite, typically reinforced unidirectionally with continuous fibers or sometimes bidirectionally, is pulled by a puller to continuously feed the uncured portion of the wet fibers into the hot die, thus the name, "pultrusion".

This is one of very few continuous processing methods for continuous fiber reinforced composites. Only constant cross-sectional products can be made; the shape of the cross-section does not necessarily have to be the same, however (Ishida, 1990;Skramstad, 1999).

2.3.2.6 Filament winding

Filament winding is also a unique processing method for polymer composite processing with a continuous reinforcing fiber. Resin-wet rovings are wound with a certain pattern around a

mandrel. The wound mandrel is then placed into an oven and cured to a solid composite. Due to the controlled tension, squeezing action and controlled winding pattern, the fiber content can be very high to produce composites with one of the highest mechanical properties. The winding process is time consuming and is the cause of low productivity.

However, due to its very high mechanical properties with automated operation, it is actively evaluated by aerospace industries (Ishida, 1990).

2.3.3 Automotive Application of Natural Fiber Reinforced Composites

The use of plant fiber based automotive parts such as various panels, shelves, trim parts and brake shoes is attractive for automotive industries worldwide because of its reduction in weight of about 10%, energy production of 80% and cost reduction of 5%. The major car manufacturers like Volkswagen, BMW, Mercedes, Ford and Opel now use natural fiber composites in applications such as those listed in Table 2.3 and parts shown in Figure 2.2. Also, new plant fiber based composite materials are being increasingly used.

BMW has been using natural materials since the early 1990's in the 3, 5 and 7 series models with up to 24 kg of renewable materials being utilized. In 2001, BMW used 4000 tons of natural fibers in the 3 series alone. The combination used is 80% flax with 20% sisal blend for increased strength and impact resistance. The main application is in the interior door linings and paneling. The present level of car production in Western Europe is about 16 million vehicles per year, which equates to a current usage of 80 000 to 160 000 tons of natural fibers per year (Akova, 2013).

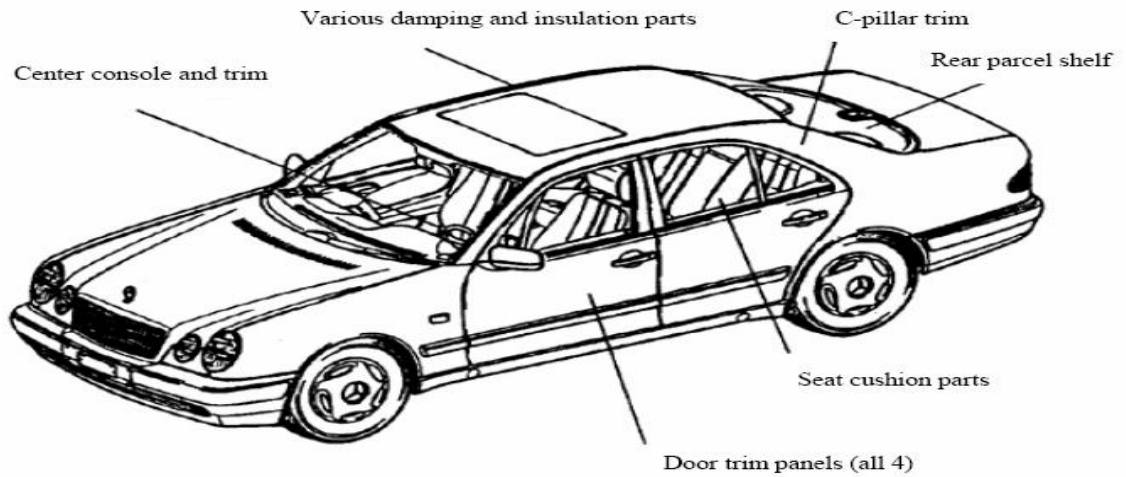


Figure 2.2 Plant fiber applications in the current Mercedes-Benz R-class (Doan, 2006)

Table 2.3: Current well-established applications of natural fibers in automotive industry (Suddel, 2009)

Automotive Manufacturer	Model Applications
AUDI	A2, A3, A4, A6, A8, Roadster, Coupe (Seat backs, side and back door panels, boot lining, hat rack and spare tyre lining).
BMW	3, 5, 7 series (Door panels, headliner panel, boot lining, seat backs, noise insulation panels)
CITROEN	C5 (Interior door paneling)
FIAT	Punto, Brava, Marea, Alfa Romeo 146, 156
FORD	Mondeo CD 162, Focus
LOTUS	Eco Elise (Body panels, Spoiler, Seats, Interior carpets)
PEUGEOT	406 (Seat backs, parcel shelf)
RENAULT	Clio, Twingo (Rear parcel shelf)
ROVER	2000 and others (Insulation, rear storage shelf/panel)
SEAT	Door panels, seat backs
TOYOTA	Brevis, Harrier, Celsior, Raum (Door panels, seat backs, spare tyre cover)
VOLKSWAGEN	Golf, Passat, Bora (Door panel, seat back, boot lid finish panel, boot liner)
VOLVO	C70, V70 (Seat padding, natural foams, cargo floor tray)

2.4 Definitions of Some Properties of Fibers and Composites

Different materials possess different properties in varying degrees and therefore behave in different ways under given conditions. These properties include mechanical properties, electrical properties, thermal properties, chemical properties, magnetic properties and physical properties. A design engineer is interested in the behaviour of materials under load which is mechanical in nature. Mechanical properties are those characteristics of materials which describe their behaviour under external loads. Tensile strength, yield strength, elongation, reduction of area, hardness, impact strength, and bend ability are examples of mechanical properties.

i. Density: Mass per unit volume of the solid matter of which a fiber is composed, measured under specified conditions.

ii. Aspect Ratio: In an essentially two-dimensional rectangular structure, the ratio of the long dimension to the short dimension. Also, in fiber micro-mechanics, it is referred to as the ratio of length to diameter of a fiber.

iii. Strength: It is the resistance offered by a material when subjected to external loading. Depending upon the type of load applied the strength can be tensile, compressive, shear or torsional. The maximum stress that any material will withstand before destruction is called its ultimate strength.

iv. Tensile strength or stress: This is the maximum tensile load per unit area of original cross section, within the gauge boundaries, sustained by the specimen during a tension test. Tensile load is interpreted to mean the maximum tensile load sustained by the specimen during the test, whether or not this coincides with the tensile load at the moment of rupture.

v. *Flexural strength*: This is the resistance of a material to being broken by bending stresses; the strength of a material in bending, expressed as the tensile stress of the outermost fibers of a bent test sample at the instant of failure.

vi. *Yield strength*: This is the stress at which a material exhibits a specified limiting deviation from the proportionality of stress to strain; the lowest stress at which a material undergoes plastic deformation. Below this stress, the material is elastic; above it, viscous. (The deviation is expressed in terms of strain such as 0.2 percent for the Offset Method or 0.5 percent for the Total Extension under Load Method).

vii. *Compressive strength*: This is a material's ability to resist a force that tends to crush or buckle; maximum compressive load a specimen sustains divided by the specimen's original cross-sectional area.

viii. *Elasticity*: Elasticity of a material is its power of coming back to its original position after deformation when the stress or load is removed. Elasticity is a tensile property of its material. The greatest stress that a material can endure without taking up some permanent set is called elastic limit.

ix. *Stiffness (Rigidity)*: The resistance of a material to deflection is called stiffness or rigidity. Steel is stiffer or more rigid than aluminium. Stiffness is measured by Young's modulus, E. The higher the value of the Young's modulus, the stiffer is the material.

x. *Modulus of elasticity (Young's modulus)*: This is the ratio of the stress or load applied to the strain or deformation produced in a material that is elastically deformed.

xi. Modulus of rigidity (Shear modulus or Torsional modulus): This is the ratio of stress to strain below the proportional limit for shear or torsional stress.

xii. Poisson's ratio: This is the absolute value of the ratio of transverse strain to the corresponding axial strain resulting from uniformly distributed axial stress below the proportional limit of the material.

xiii. Ductility: Ductility of a material is the property that enables it to draw out into thin wire on application of the load. Ductility decreases with increase of temperature. The percent elongation and the reduction in area in tension are often used as empirical measures of ductility.

xiv. Elongation at break: This is the elongation recorded at the moment of rupture of the specimen, often expressed as a percentage of the original length.

xv. Reduction of area: This is the difference between the original cross sectional area of a tension test specimen and the area of its smallest cross section, usually expressed as a percentage of the original area.

xvi. Brittleness: The brittleness of a material is the property of breaking without much permanent distortion. There are many materials, which break or fail before much deformation takes place. Such materials are brittle e.g., glass, cast iron. Therefore, a non-ductile material is said to be a brittle material. Usually the tensile strength of brittle materials is only a fraction of their compressive strength. A brittle material should not be considered as lacking in strength. It only shows the lack of plasticity. On stress-strain diagram, these materials don't have yield point and value of Young's modulus is small.

xvii. *Toughness*:The toughness of a material is its ability to withstand both plastic and elastic deformations. It is a highly desirable quality for structural and machine parts to withstand shock and vibration. Toughness is a measure of the amount of energy a material can absorb before actual fracture or failure takes place. “The work or energy a material absorbs is called modulus of toughness”. Toughness can be measured from the area under the stress-strain curve from the origin to the breaking point.

xviii. *Hardness*:Hardness is closely related to strength. It is the ability of a material to resist scratching, abrasion, indentation, or penetration. It is directly proportional to tensile strength and is measured on special hardness testing machines by measuring the resistance of the material against penetration of an indenter of special shape and material under a given load. The different scales of hardness are Brinell hardness, Rockwell hardness, Vicker’s hardness, etc.

xix. *Impact strength*:This can be defined as the resistance of the material to fracture under impact loading, i.e., under quickly applied dynamic loads. Two standard tests are normally used to determine this property; IZOD impact test and CHARPY test (Milauskas, 2013).

2.5 Response Surface Methodology (RSM)

Response Surface Methodology (RSM) is a collection of mathematical and statistical techniques useful for the modeling and analysis of problems in which a response (output variable), y , of interest is influenced by several independent variables (input variables), x_1, x_2, \dots, x_k , and the objective is to optimize this response (Montgomery, 2005). In general, such a relationship is unknown but can be approximated by a low-degree polynomial model of the form in eq. (2.1), for a case of two independent variables:

$$y = f(x_1, x_2) + \varepsilon \tag{2.1}$$

Where ϵ is the experimental error term. It represents any measurement error on the response, as well as other type of variations not counted in f . It is a statistical error that is assumed to distribute normally with zero mean and variance. The surface represented by $f(x_1, x_2)$ is called a response surface. The response can be represented graphically, either in the three-dimensional space or as contour plots that help visualize the shape of the response surface. Contours are curves of constant response drawn in the x_i, x_j plane keeping all other variables fixed. Each contour corresponds to a particular height of the response surface.

The purpose of considering a model is threefold:

1. To establish a relationship, albeit approximate, between y and x_1, x_2, \dots, x_k that can be used to predict response values for given values of the independent variables.
2. To determine, through hypothesis testing, significance of the factors (independent variables) whose levels are represented by x_1, x_2, \dots, x_k .
3. To determine the optimum values of x_1, x_2, \dots, x_k that result in the maximum (or minimum) response over a certain region of interest.

In order to achieve the above three objectives, a series of n experiments should first be carried out, in each of which the response y is measured (or observed) for specified values of the independent variables (Khuri and Mukhopadhyay, 2010).

2.5.1 Design of Experiments

Design of experiments (DoE) is an important aspect of RSM originally developed for the model fitting of physical experiments, but can also be applied to numerical experiments. The objective of DoE is the selection of the points where the response should be evaluated. Most of the criteria

for optimal design of experiments are associated with the mathematical model of the process. Generally, these mathematical models are polynomials with an unknown structure, so the corresponding experiments are designed only for every particular problem. The choice of the design of experiments can have a large influence on the accuracy of the approximation and the cost of constructing the response surface (Box and Draper, 1987).

The first-degree model and second-degree model are the most-frequently used approximating polynomial models in classical RSM. Designs for fitting first-degree models are called first-order designs and those for fitting second-degree models are referred to as second-order designs.

First-Order Designs include: The 2^k Factorial Design, The Plackett-Burman Design and The Simplex design. The Second-Order Designs include: The 3^k factorial Design, The Central Composite Design and the Box-Behnken Design. Other designs include D-optimal Designs and Taguchi Robust Designs.

2.5.1.1 The 3^k factorial design

A factorial experiment is an experimental strategy in which design variables are varied together, instead of one at a time. The 3^k factorial design is a Second-Order Design. Second-Order Designs are useful in approximating a portion of the true response surface with parabolic curvature; they are flexible, because they can take a variety of functional forms and approximate the response surface locally, thereby giving a good estimation of the true response surface (Bradley, 2007).

The 3^k factorial design consists of all the combinations of the levels of the k control variables which have three levels each. If the levels are equally spaced, then they can be coded so that they correspond to -1 , 0 , and 1 . The number of experimental runs for this design is 3^k , which can be

very large for a large k . Fractions of a 3^k design can be considered to reduce the cost of running such an experiment (Khuri and Mukhopadhyay, 2010). Table 2.4 below shows the experimental runs in coded values for a 3^k factorial design with two control variables or factors ($k = 2$).

Table 2.4: Coded values for 3^k factorial design with two factors

Experimental runs	1	2	3	4	5	6	7	8	9
X_1 (First factor or variable)	1	1	1	0	0	0	-1	-1	-1
X_2 (Second factor or variable)	1	0	-1	1	0	-1	1	0	-1

2.5.1.2 Central composite designs

Central composite designs (CCD) combine two-level full or fractional factorial designs with additional axial or star points and at least one point at the center of the experimental region being investigated. It allows the determination of both linear and quadratic models. The CCD is a better alternative to the full factorial three-level design when many factors are being considered, since it demands a smaller number of experiments while providing comparable results. In general, a CCD for k factors, coded as (x_1, \dots, x_k) , consists of three parts:

- (1) A factorial (or cubic) design, containing a total of n_{fact} points with coordinates $x_i = -1$ or $x_i = +1$, for $i = 1, \dots, k$;
- (2) An axial (or star) part, formed by $n_{\text{ax}} = 2k$ points with all their coordinates null except for one that is set equal to a certain value α (or $-\alpha$);
- (3) A total of n_c runs performed at the center point, where, of course, $x_1 = \dots = x_k = 0$.

To build a central composite design, we need to specify each of these three parts. We have to decide how many cubic points to use and where they will be, what will be the value of α , and

how many replicate runs should be conducted at the center point. The design is such that values for α usually range from 1 to \sqrt{k} . When $\alpha = \sqrt{k}$, the cubic and axial points are located on the (hyper) surface of a (hyper) sphere, and the design is called spherical.

An example for two factors as given in Table 2.5 has the first four runs (2^2 factorial design) making up the cubic part, the star design are the last four (with $\alpha = \sqrt{2}$) and there are three replicate runs at the center point (Ferreira et al, 2007).

Table 2.5: Coded factor levels for central composite design with two factor systems

Experimental runs	1	2	3	4	5	6	7	8	9	10	11
X ₁ (First factor or variable)	-1	1	-1	1	0	0	0	-1.414	1.414	0	0
X ₂ (Second factor or variable)	-1	-1	1	1	0	0	0	0	0	-1.414	1.414

2.5.1.3 Box-Behnken design

Box–Behnken designs constitute an alternative to central composite designs. They are a class of rotatable or nearly rotatable second-order designs based on three-level incomplete factorial designs. Table 2.6 shows coded values for the Box–Behnken design for three factors. It is easy to see that this design consists of three parts of four runs. Within each part, two factors are arranged in a full two-level design, while the level of the third factor is set at zero. The points lie on the surface of a sphere centered at the origin of the coordinate system and tangential to the midpoint of each edge of the cube. Compared to the central composite design, this design has some advantages. The three-factor Box–Behnken design requires only 12 runs plus the replicates at the center point, whereas its central composite counterpart has 14 non-center points. In general the number of experimental points is given by $2k(k-1) + C_0$. Also, each factor is studied at only three levels, which is an important feature in some experimental situations. On the other hand, using

$\alpha=1$ in a central composite design also results in three levels for each factor. In most real applications these differences are probably not decisive in determining which design to use, at least for this number of factors. However, since Box–Behnken designs do not contain combinations where all the factors are at their higher or lower levels, they may be useful in avoiding experiments under extreme conditions, for which unsatisfactory results might occur. Conversely, they are not indicated for situations in which we would like to know the responses at the extremes, that is, at the vertices of the cube (Ferreira et al, 2007).

Table 2.6: Coded factor levels for Box-behnken design with three factor systems

Experimental runs	1	2	3	4	5	6	7	8	9	10	11	12	13	14	15	16
X_1 (First factor)	-1	1	-1	1	-1	1	-1	1	0	0	0	0	0	0	0	0
X_2 (Second factor)	-1	-1	1	1	0	0	0	0	-1	1	-1	1	0	0	0	0
X_3 (Third factor)	0	0	0	0	-1	-1	1	1	-1	-1	1	1	0	0	0	0

2.6 Micromechanics Modelling

The elastic properties of a composite can be predicted by micromechanics models based on the properties of the individual constituent materials of the composite and their geometrical characteristics. Better prediction of the mechanical properties of natural fiber composites will help our understanding of the effect of the constituents on the final properties of the material. Using micromechanics models, the composite properties can be optimized for a given application by varying the composition of the composite.

2.6.1. Models for Composite Modulus Prediction

2.6.1.1 Models for modulus of Long fiber (Continuous fiber) reinforced composites

The simplest micromechanical model used to predict the composite elastic modulus parallel to the principal axis is Rule of Mixture (RoM_P). It is a parallel spring model based on the assumption that the fibers and matrix will experience equal strain during loading in fiber direction. The RoM_P equation for the modulus of a continuous unidirectional fiber composite in the fiber direction can be generally represented as shown below (Virk, 2010);

$$E_1 = kE_f V_f + E_m V_m \quad (2.2)$$

Where E_1 is composite modulus in fiber direction, E_f and E_m are fiber and matrix modulus respectively and V_f and V_m are fiber and matrix volume fraction, while k is the fiber efficiency factor and has values as follows; for complete alignment and when stress is parallel to fibers ($k = 1$); for fibers laid in two directions at right angles (bi-directional or cross-laid fibers) and stress is in one of these directions ($k = 1/2$); for fibers in random and uniform distribution within a specific plane, and stress is in any direction in the plane of the fibers ($k = 3/8$) and for fibers in random and uniform distribution within three dimensions in space, and stress is in any direction ($k = 1/5$). RoM_P provides the upper bound for the composite modulus when;

$$\nu_m = \nu_f \quad (2.3)$$

Where ν_m and ν_f are the matrix and fiber axial Poisson's ratios respectively. The composite modulus in the direction transverse to the fiber direction is given by RoM_S. This series spring model assumes that the fibers and matrix experience the same stress when the composite is loaded in the direction transverse to the fibers (Virk, 2010).

The RoM_S equation is;

$$E_2 = \frac{E_f E_m}{E_f V_m + E_m V_f} \quad (2.4)$$

Where, E_2 is the composite modulus, in a direction transverse to the fibers. R_oM_s gives the lower bound for the composite modulus (Jones, 1998; Hyer and Waas, 2000; Kachy, 2008; Virk, 2010).

Modified models for composite modulus, in a direction transverse to the fibers, are also presented by Voyiadjis and Kaltan (2005):

$$E_2 = \frac{V_f + \eta V_m}{\frac{V_f}{E_{f2}} + \frac{\eta V_m}{E_m}} \quad (2.5)$$

Where, E_{f2} is fiber modulus in the transverse direction and η is the stress-partitioning factor. The stress-partitioning factor satisfies the condition $0 < \eta < 1$, but usually taken between 0.4 and 0.6. Alternatively, we also have;

$$E_2 = \frac{E_{f2} E_m}{E_m \eta_f V_f + E_{f2} \eta_m V_m} \quad (2.6)$$

Where, η_f and η_m are stress-partitioning factors for the fiber and matrix respectively.

Halpin and Tsai (1969) developed a semi-empirical method to predict the composite properties. Halpin-Tsai method tries to make a sensible interpolation between upper and lower bounds of composite properties. Halpin-Tsai equation is;

$$E^* = E_m \left(\frac{1 + \xi \eta V_f}{1 - \eta V_f} \right) \quad (2.7)$$

Where

$$\eta = \frac{E_f - E_m}{E_f + \xi E_m} \quad (2.8)$$

E^* is composite modulus, E_f and E_m are fiber and matrix modulus respectively, V_f is fiber volume fraction and ξ is reinforcing efficiency (which depends on fiber geometry, packing arrangement

and loading condition). A variety of empirical equations for ξ are available in literature and they depend on the shape of the particle and the modulus that is being predicted. For circular or rectangular fiber, assuming tensile modulus on the principal fiber direction is desired;

$$\xi = 2 \left(\frac{L}{T} \right) \text{ or } 2 \left(\frac{L}{D} \right) \quad (2.9)$$

Where L is the length of the fiber in the one direction and T or D is thickness or diameter respectively. In some cases, for the reinforcing efficiency a constant value $\xi = 2$ has been used (Katchy, 2008).

The reinforcing efficiency ξ can be calculated from experimental test result, where composite modulus, E^* and fiber volume fraction, V_f are known and V_m is matrix volume fraction which is equal to $1 - V_f$ assuming a zero void fraction, using the equation below;

$$\xi = \frac{E_f(E^* - E_m) - V_f E^*(E_f - E_m)}{E_m \{(E_f - E^*) - V_m(E_f - E_m)\}} \quad (2.10)$$

Values of reinforcement efficiency, ξ , can vary from 0 to ∞ . When $\xi = \infty$, Halpin-Tsai equation becomes RoM_p and for $\xi = 0$, Halpin-Tsai equation is reduced to RoM_s. The higher reinforcing efficiency signifies that fibers are contributing to the composite stiffness. Halpin-Tsai method offers the advantage of being simple (easy to use in design process) and offers more exact prediction but normally requires empirical data to determine the reinforcing efficiency, ξ .

Though Halpin-Tsai equation is basically used for modulus in the transverse direction, it has been modified for randomly oriented fiber reinforced composites by using the relation below;

$$E = \frac{3}{8} E_1 + \frac{5}{8} E_2 \quad (2.11)$$

Where E_1 and E_2 (composite modulus in fiber direction and in transverse direction respectively) are obtained from Halpin-Tsai equation by using $\xi = 2(l_f/d_f)$ and $\xi = 0.5$ respectively (l_f and d_f are fiber length and diameter respectively) (Jones, 1998; Daniel and Ishai, 2005; Ku et al, 2011).

Similar to the Halpin-Tsai equation is the Bintrup equation for composite modulus in transverse direction is given as;

$$E_2 = \frac{(E'_m E_f)}{[E_f V_m + V_f E'_m]} \quad (2.12)$$

Where $E'_m = E_m / (1 - \nu_m^2)$ and ν_m is the Poisson ratio of the matrix.

2.6.1.2 Models for modulus of short fiber (discontinuous fiber) reinforced composites

The modulus for discontinuous fiber composite can be estimated using Cox Shear-Lag model. The RoM_p is modified by including a length factor, which is a function of fiber length, fiber and matrix properties, fiber geometry and placement. The modified RoM_p equation is;

$$E = \eta_l E_f V_f + E_m V_m \quad (2.13)$$

$$\eta_l = 1 - \frac{\tanh(\beta_{cox} l/2)}{\beta_{cox} l/2} \quad (2.14)$$

$$\beta_{cox} = \sqrt{\left(\frac{2\pi G_m}{E_f A_f \ln\left(\frac{R}{r_0}\right)} \right)} \quad (2.15)$$

Where β_{cox} is the shear-lag parameter, η_l is fiber length distribution factor, l is fiber length, G_m is matrix shear modulus, A_f is fiber cross sectional area, r_0 and R are the fiber radius and half of inter-

fiber spacing respectively. For square and hexagonal fiber arrangement and fiber of circular cross section the fiber volume fraction is given by Equation 2.16 and 2.17 respectively.

$$V_f = \frac{\pi r_0^2}{4R^2} \quad (2.16)$$

$$V_f = \frac{2\pi r_0^2}{\sqrt{3}R^2} \quad (2.17)$$

This model assumes that the interface between fiber and matrix is perfect, fiber and matrix response is elastic and no axial force is transmitted through the fiber ends (Cox, 1952; Piggot, 1980; Folkes, 1982; Virk, 2010).

Facca et al (2006) also presented modified equations for the shear-lag parameter;

$$\beta_{cox} = \frac{1}{r} \sqrt{\left(\frac{2E_m}{E_f(1+\nu_m) \ln\left(\frac{P_f}{V_f}\right)} \right)} \quad (2.18)$$

Where ν_m , P_f and r are poisson ratio of matrix, packing factor of fibers (π for square packing and $2\pi/\sqrt{3}$ for hexagonal packing) and radius of fiber respectively.

For axisymmetric cases, the shear lag parameter below gives more accurate results:

$$\beta_{cox} = \left[\frac{2}{r^2 E_f E_m} \left[\frac{E_f V_f + E_m V_m}{\frac{V_m}{4G_f} + \frac{1}{2G_m} \left[\frac{1}{V_m} \ln\left(\frac{1}{V_f}\right) - 1 - \frac{V_m}{2} \right]} \right] \right]^{1/2} \quad (2.19)$$

Where G_f and G_m are shear modulus of fiber and matrix respectively. A generalized form of eqn. 2.19 is given below:

$$\beta_{cox} = \left[\frac{2}{r^2 E_f E_m} \left[\frac{E_f V_f + E_m V_m}{\frac{V_m}{4G_f} + \frac{1}{2G_m} \left[\frac{1}{V_m} \ln \left(\frac{1}{\chi + V_f} \right) - 1 - \frac{V_m}{2} \right] + \frac{1}{r D_s}} \right] \right]^{1/2} \quad (2.20)$$

The parameter χ is generally taken as 0.009, while D_s is an interface parameter. A value of $D_s = \infty$ indicates perfect adhesion. The above equation can therefore be used to characterize improvement in interfacial adhesion.

The modulus of partially oriented composite can be estimated by including the fiber orientation distribution factor by Krenchel (1964) in the RoM_p equation. The resulting equation is;

$$E = \eta_0 E_f V_f + E_m V_m \quad (2.21)$$

$$\eta_0 = \sum_n a_n \cos^4 \theta_n \quad (2.22)$$

Where η_0 is fiber orientation distribution factor, a_n is the proportion of the fiber making θ_n angle to the applied load.

The modulus (stiffness) of discontinuous fiber composite with partially orientated fibers can be predicted by combining Equation (2.13) and (2.21).

$$E = \eta_l \eta_0 E_f V_f + E_m V_m \quad (2.23)$$

However, if η_l is unity (for long fibers) this returns the same results as Krenchel (Equation (2.21)).

The modulus of natural fibers has been reported to decrease with increasing fiber diameter (Lamy and Baley, 2000; Bodros and Baley, 2008). The modulus of composite reinforced with natural fiber can be estimated by equation proposed by Summerscales et al (2010). The

RoM_p equation is extended to include a fiber “diameter” distribution factor, η_d as in Equation 2.24:

$$E = \eta_d \eta_l \eta_o E_f V_f + E_m V_m \quad (2.24)$$

When the fibers used in the composite are well characterized η_d can be taken as 1 i.e. the modulus of the batch of fiber used has been measured independently.

These modifications are because the rule of mixtures cannot be directly applied to short fiber composites because the assumption of uniform strain does not hold. The critical fiber length (fiber length at which the maximum stress in fiber equals the tensile strength of the fiber (l_c)) or critical fiber aspect ratio (λ_{crit}) is the basis for further model modification. There are three special cases (Katchy, 2008):

1. Fiber length is less than critical length ($l < l_c$)

$$E_c = (\tau_i l / d) E_f V_f + E_m V_m \quad (2.25)$$

2. Fiber length is equal to critical length ($l = l_c$)

$$E_c = (\tau_i l_c / d) E_f V_f + E_m V_m \quad (2.26)$$

3. Fiber length is greater than critical length ($l > l_c$)

$$E_c = (1 - l_c / 2l) E_f V_f + E_m V_m \quad (2.27)$$

E_c and τ_i are the composite moduli and mean shear stress at the fiber/matrix interface respectively.

2.6.2. Models for Composite Strength Prediction

2.6.2.1 Models for strength of long fiber (continuous fiber) reinforced composites

Strength of the unidirectional (continuous fiber) composite can be predicted by assuming all the reinforcing fibers have identical strength and the strain in the fibers and the matrix is equal during loading. If the fiber failure strain is less than the matrix failure strain then the composite longitudinal tensile strength (parallel to the fibers) can be estimated using Kelly-Tyson Equation (2.28) (Kelly and Tyson, 1965);

$$\sigma_c = \sigma_f V_f + (\sigma_m)_{\epsilon_f} (1 - V_f) \quad (2.28)$$

Where σ_c is unidirectional composite tensile strength, σ_f is fiber tensile strength and $(\sigma_m)_{\epsilon_f}$ is matrix stress at the strain equal to failure strain in the fibers. Equation (2.28) is not true for low fiber volume fraction (2% or less - which is below the critical value for effective load transfer between fiber and matrix), therefore for low fiber volume fraction the composite strength is approximated by;

$$\sigma_c \cong \sigma_{m_{max}} (1 - V_f) \quad (2.29)$$

Where $\sigma_{m_{max}}$ is the maximum matrix tensile strength.

The composite strength is given by the higher of the two values calculated using Equation (2.28) and (2.29).

The tensile strength of quasi-unidirectional composite loaded slightly off axis to the fiber direction is given by Potter (1994);

$$\sigma_{cu} = \sigma_c \sec^2 \theta \quad (2.30)$$

Where σ_{cu} is ultimate composite strength, σ_c is unidirectional composite tensile strength and θ is angle between the fiber axes and the composite loading axes.

Katchy (2008) presented some equations for the case when the fiber failure strain is greater than the matrix failure strain, but this case is hardly ever seen in practical applications.

2.6.2.2 Models for strength of short fiber (discontinuous fiber) reinforced composites

Katchy (2008) presented three model equations for application in strength of short fiber reinforced composites, based on the critical fiber length, as follows:

1. Fiber length is less than critical length ($l < l_c$)

$$\sigma_c = (\tau_i l / d) V_f + \sigma_m V_m \quad (2.31)$$

2. Fiber length is equal to critical length ($l = l_c$)

$$\sigma_c = (\tau_i l_c / d) V_f + \sigma_m V_m \quad (2.32)$$

3. Fiber length is greater than critical length ($l > l_c$)

$$\sigma_c = \left(1 - \frac{l_c}{2l}\right) \sigma_{f,max} V_f + \sigma_m V_m \quad (2.33)$$

σ_c and $\sigma_{f,max}$ are the composite tensile strength and maximum fiber tensile strength respectively.

Facca et al (2007) used a micromechanical model which was a semi-empirical modification of the rule of mixture to model composite behavior for several natural fibers and E-glass, with good prediction:

$$\sigma_c = \left(1 - \frac{l_c}{2l}\right) \sigma_{f,max} V_f + \sigma_m^* (1 - V_f) (l \geq l_c) \quad (2.34)$$

Modified equation for cylindrical fibers, ($l \leq l_c$)

$$\sigma_c = \alpha \left(\frac{\tau_i l}{d} \right) V_f + \sigma_m^* (1 - V_f) \quad (2.35)$$

Modified equation for rectangular fibers, ($l \leq l_c$)

$$\sigma_c = \alpha \left(\frac{\tau_i l}{2} \right) V_f \left(\frac{W+T}{WT} \right) + \sigma_m^* (1 - V_f) \quad (2.36)$$

Where α , σ_m^* , d , W and T are the clustering parameter, matrix stress evaluated at the peak composite strength, cylindrical fiber diameter, rectangular fiber width and rectangular fiber thickness respectively.

The mechanical properties predicted by the appropriate micromechanics model were compared to the experimental results to assess the error in the prediction. Knowing that the micromechanics models have inbuilt limitations and assumptions (i.e. they often assume perfect bond between fibers and matrix, fibers are homogenous, linear elastic and regularly spaced in the composite and the matrix is also homogenous, linear elastic and void free), the micromechanics model which most closely predicts the experimental data will be deemed more appropriate for natural fiber composites.

2.7 Water Absorption Kinetics

Natural fibers and their composites are prone to moisture sorption due to their cellulose (Hemicellulose) content. This moisture absorption increases with increase in cellulose content (fiber volume fraction) and is significant at elevated temperatures; causing swelling, degradation and reduction in strength of natural fibers and their composites. However, studies have shown that

fiber treatment and chemical modification significantly reduces rate of water uptake (Dhakal et al, 2006; Srubar et al, 2012).

The moisture transport behavior in polymer systems can be classified into three cases, based on the relation below:

$$\frac{M_t}{M_\infty} = kt^n \quad (2.37)$$

Where M_t is percentage moisture content at any time, M_∞ is the percentage equilibrium moisture content, k is the water sorption rate constant, n is the water sorption index

The moisture sorption behaviour is fickian diffusion controlled if $n = 0.5$, it is polymer relaxation diffusion controlled if $n = 1$ and anomalous (non-fickian) diffusion controlled for $0.5 < n < 1$.

Becker (1960) developed a relation for diffusion in solids of arbitrary shape using Fick's law of molecular diffusion. The relation can be presented in the form below:

$$M_t - M_o = \alpha_b t^{1/2} + M_p \quad (2.38)$$

$$\alpha_b = (2/\sqrt{\pi})(M_\infty - M_o)(s/v)\sqrt{D} \quad (2.39)$$

Where M_t is moisture content at any time, M_∞ is the equilibrium moisture content, α_b is the water sorption rate, M_o is the initial moisture content, M_p is the initial moisture gain due to fast capillary action, t is time, (s/v) is the surface-to-volume ratio of the test sample and D is the diffusion coefficient.

A plot of $(M_t - M_o)$ versus $t^{1/2}$ gives a straight line with α_b as slope. If the plot passes through the origin, intra-particle diffusion is the rate controlling step. The term $(M_\infty - M_o)$ is considered constant for each test sample.

The diffusion coefficient can often be related to absolute temperature as in the relation below:

$$D = D_0 \exp\left(-\frac{E_a}{RT}\right) \quad (2.40)$$

Where D_0 is the permeability index, E_a is activation energy, R is the universal gas constant and T is absolute temperature (Singh and Kulshrestha, 1986; Addo and Bart-Plange, 2009; Srubar et al, 2012).

Dhakal et al (2006) solved the diffusion equation and obtained a relationship for percentage moisture content of hemp reinforced polyester composite as:

$$M = \frac{4M_\infty}{h} \left(\frac{t}{\pi}\right)^{0.5} D_x^{0.5} \quad (2.41)$$

$$D = \frac{d^2}{\pi^2 t_{70}} \quad (2.42)$$

$$D = \pi \left(\frac{kh}{4M_\infty}\right)^2 \quad (2.43)$$

Where M is percentage moisture content at any time, M_∞ is the percentage equilibrium moisture content, h is thickness of specimen, d is sample thickness in mm, t_{70} is time taken to reach 70% saturation in seconds and k is the initial slope of a plot of $M(t)$ versus $t^{1/2}$.

Singh and Kulshrestha (1986) presented an empirical model, in three forms, for cases that are not diffusion controlled, based on the moisture sorption by soybean and pigeon pea, as follows:

$$\frac{M_\infty - M}{M_\infty - M_0} = \frac{1}{kt + 1} \quad (2.44)$$

$$\frac{M - M_0}{M_\infty - M_0} = \frac{kt}{kt + 1} \quad (2.45)$$

$$\frac{1}{M-M_0} = \frac{1}{k(M_\infty-M_0)t} + \frac{1}{M_\infty-M_0} \quad (2.46)$$

The sorption rate constant and equilibrium moisture content are presented as functions of temperature as given in the equations below:

$$k = k_0 \exp\left(-\frac{E_a}{RT}\right) \quad (2.47)$$

$$M_\infty = A \exp\left(\frac{B}{T}\right) \quad (2.48)$$

Where A and B model constants and k_0 is a type of frequency factor.

Yang et al (2012) studied moisture sorption and release of Akund fiber and presented the model:

$$M = a + b \exp(-ct) \quad (2.49)$$

The work is based on percentage moisture content and a , b and c are model constants.

Peleg (1988) presented a model that can predict kinetics of sorption till equilibrium using short-term data using chickpea.

$$M - M_0 = \frac{t}{k_1 + k_2 t} \quad (2.50)$$

With the above equation the equilibrium moisture content can be predicted as:

$$M_\infty = M_0 + \frac{1}{k_2} \quad (2.51)$$

Where M is percentage moisture content at any time, M_∞ is the percentage equilibrium moisture content, M_0 is the percentage initial moisture content, k_1 is Peleg rate constant and relates to sorption rate at the very beginning, while k_2 is Peleg capacity constant which relates maximum attainable moisture content (Turhan et al, 2002).

Hamdaoui et al (2014) presented a Parallel Exponential Kinetic (PEK) model for water sorption of cotton fabric to model the rapid and slow moisture sorption phases:

$$M = M_{1\infty}(1 - \exp(-k_1t)) + M_{2\infty}(1 - \exp(-k_2t)) \quad (2.52)$$

Where M is mass of water absorbed, $M_{1\infty}$ and $M_{2\infty}$ is masses on water absorbed at infinite time associated respectively with the fast and slow processes and k_1 and k_2 are sorption rates for the fast and slow processes.

2.8 Neural Networks (Artificial Neural Networks)

Neural networks are composed of simple elements operating in parallel. These elements are inspired by biological nervous systems. As in nature, the network function is determined largely by the connections between elements. You can train a neural network to perform a particular function by adjusting the values of the connections (weights) between elements. Commonly neural networks are adjusted, or trained, so that a particular input leads to a specific target output. Figure 2.3 shows a schematic diagram of a neural network showing input, output, weight (w^*), biases (b), hidden layer and output layer. The network is adjusted, based on a comparison of the output and the target, until the network output matches the target. Typically many such input/target pairs are needed to train a network. Neural networks have been trained to perform complex functions in various fields, including pattern recognition, identification, classification, speech, vision, and control systems (Ball and Tissot, 2006).

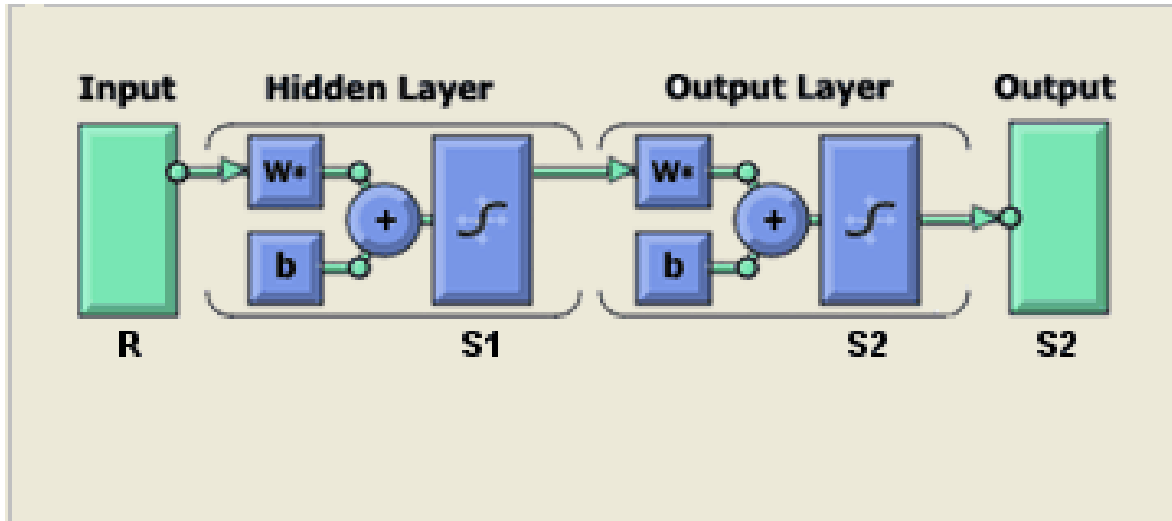


Figure 2.3: Schematic diagram of a neural network architecture

2.9 Review of Some Previous Works

Gassan and Bledzki(1999) reported that treating jute fiberwith 25wt% NaOH for 20 minutes at20°C improves the tensile strength and modulus of the fiber by 120% and 150% respectively and mechanical properties of unidirectional jute/epoxy composite up to 60% compared to untreated fiber composite, at a fiber content of 40 vol. %.

Mohanty et al (2000) studied the influence of different surface modifications of jute on the performance of the bio-composites. More than a 40% improvement in the tensile strength occurred as a result of reinforcement with alkali treated jute. Jute fiber content also affected the bio-composite performance and about 30% by weight of jute showed optimum properties of the bio-composites.

Sreekala et al. (2000) studied Oil Palm fiber and indicated that a 10-30% sodium hydroxide solution produced the best effects on natural fiber properties, for a treatment time of 30minutes.

Ray et al (2001) studied Jute fibers treated with 5% alkali solution for 2, 4, 6, and 8 hours at 30°C and observed loss in weight of the alkali treated fibers within 2 hours of treatment and the optimum improvement in mechanical properties occurred for composites prepared with samples treated for 4 hours.

Mwaikambo and Ansell (2002) treated hemp, jute, sisal and kapok fibers with various concentrations of NaOH and found 6% to be the optimized concentration in terms of cleaning the fiber bundle surfaces, yet retaining a high index of crystallinity.

Mishra et al (2003) studied pineapple leaf fibers and sisal fibers treated with 5% and 10% NaOH for 1 hour at 30°C and observed that at 10% NaOH, excess delignification occurred, making the fiber weaker.

Wang (2004) studied flax fibers by soaking into 2.5-30% NaOH solutions for 30 mins and found that 5, 18 or 10% of sodium hydroxide solution were the appropriate concentrations for mercerization before silane, benzylation or peroxide treatment, respectively.

Edeerozey et al (2007) studied kenaf fiber treated with 3%, 6% and 9% NaOH for 3 hours at room temperature and 95°C for 6% NaOH and observed that 9% NaOH was too strong and might damage fibers, thus resulting in lower Tensile Strength.

Lina Herrera-Estrada et al (2008) established and optimized a process for the production of banana fiber reinforced composite materials with a thermoset, suitable for automotive and transportation industry applications and treatments were studied along with processing conditions for epoxy and eco-polyester banana fiber composites. Flexural tests show that banana fiber/ eco polyester composites have a higher flexural strength and modulus, due to improved fiber/matrix interaction. Environmental tests were conducted and the compressive properties of the composites were evaluated before and after moisture absorption. The resulting banana

fiber/epoxy composites were found to yield a flexural strength of 34.99 MPa and compressive strength of 122.11 MPa when alkaline pretreated, with improved environmental exposure resistance. While the non alkaline pretreated banana fiber/polyester composites were found to yield a flexural strength of 40.16 MPa and compressive strength of 123.28 MPa, with higher hygrothermal resistance than pretreated fiber composites with the same matrix.

Panigrahi et al (2008) studied the reinforcement of polyethylene with flax after pretreatment with NaOH and acrylic acid, to determine appropriate temperature and pressure for injection moulding, and observed that the treatment improved fiber-matrix bonding.

Paul et al (2008) studied banana fiber reinforced polypropylene, after treating the fiber with 2% and 10% NaOH for One hour respectively, and observed that samples produced using fiber treated with 10% NaOH showed better thermophysical properties.

Ratna Prasad et al (2008) studied the mechanical properties of banana empty fruit bunch fiber reinforced polyester composites. The light weight composite material was prepared using banana empty fruit bunch fiber as reinforcement in polyester resin matrix, and its mechanical properties studied. The composites are formulated up to a maximum fiber volume fraction of about 0.37, resulting in a mean tensile strength of 43MPa and tensile modulus of 1.06 GPa which are 36% and 68% higher than those of the plain polyester respectively. The flexural strength of banana empty fruit bunch composites is decreased, whereas flexural modulus of the composite has shown mixed trend compared to that of plain polyester. The specific flexural modulus of the composite is 1.42 times to that of polyester resin and the work of fracture in impact is found to be 141.7J/m.

John et al (2008) studied Sisal and Oil palm fibers treated with 0.5, 1, 2 and 4% NaOH for 1 hour at ambient temperature and reported better tensile properties for NaOH treated fibers over Silane treated fibers.

Myrtha et al (2008) studied incorporation of oil palm empty fruit bunch and glass fiber reinforced polyester composites and observed that oil palm empty fruit bunch fiber incorporated in polyester around 40-70% volume fraction had similar flexural strength with glass fiber reinforced polyester (increasing flexural strength by 350%) but with lower density. They reported that long fibers gave higher flexural strength, 36.8MPa, compared to short fibers, 33.9MPa, both at 18% volume fraction.

Gu (2009) studied coir fiber treated with 2,4,6,8 and 10wt% NaOH for 4 weeks at room temperature and observed that denser NaOH is detrimental to fiber strength due to greater lignin, pectin, fatty acid and cellulose leach out.

Hai et al (2009) studied jute and coir fibers treated with 2-8% NaOH for 24hours and inferred that mechanical properties indicated good adhesion between natural fibers and PP. Jute fibers when treated with 2% NaOH for 24hours showed best improvement in Tensile Strength by 40% and modulus by 9%, while coir fibers treated with 6% NaOH for 24hours showed best improvement in Tensile Strength by 62% and modulus by 17% respectively.

Li et al (2009) studied flax fiber reinforced LLDPE and HDPE. The composites contained 10wt% fiber and was processed by extrusion and injection moulding. Alkali, silane, potassium permanganate, acrylic acid and sodium chlorite treatments were applied and all improved composite strength, with acrylic acid giving best results.

Yu et al (2010) studied Ramie fibers treated with 5% w/v NaOH for 3 hours at room temperature and reported better tensile properties for NaOH treated fibers over Silane treated fibers.

Anyakora and Abubakre (2011) studied Oil Palm Empty Fruit Bunch reinforced polyester composites after mercerization (2wt% for 3 hours) and silane treatment (2% for 30mins) and observed that 10% loading gave the best Impact strength, and the treated fibers at this loading increased the Impact Strength by 221% over untreated fiber.

Sawpan et al (2011) studied Hemp fibers treated with 5% NaOH for 30mins at ambient temperature and reported improvement in Tensile Strength and Young's Modulus.

Chimekwene et.al (2012), conducted studies on plantain empty fruit bunch fiber reinforced epoxy composite laminates. The hand-lay method of fabrication was employed in preparing the composites. Tensile, flexural and hardness properties were investigated as a function of fiber volume fraction and fiber modification (treatments) for the different fiber orientations. It was observed that the mechanical properties of the fibers were enhanced through the fiber treatments as the treated fibers showered better strength compared with the untreated fibers. From the mechanical test results, an optimal tensile strength of 243N/mm^2 was obtained from the woven roving treated fiber orientation at a fiber volume fraction of 40% and flexural strength of 9.4N/mm^2 at 50% volume fraction. It was also discovered that the percentage elongation reduced with increased fiber loadings. This indicates that increased fiber volume fraction in the composite tends to make the material more brittle. An optimal percentage elongation value of 4.9% was obtained at 10% fiber volume fraction of treated woven roving fiber reinforced composite. The least value percentage elongation of 1.33% was recorded at 50% fiber volume fraction of the treated long strand fiber reinforced composite.

Ihueze et.al (2012) focused on the use of control factors (volume fraction of fibers, aspect ratio of fiber and fiber orientation) to determine optimum tensile strength of plantain fiber reinforced polyester resin and plantain pseudo stem fiber reinforced polyester respectively using

Archimedes principle in each case to determine the fiber volume fraction. The fibers were treated with 5% NaOH for 4 hours before use in composite production. The empty fruit bunch fiber reinforced polyester matrix has the optimum tensile strength of 40.82MPa (at 50% volume fraction, 10mm/mm aspect ratio and 90^o orientation), while the pseudo stem plantain fiber matrix composite has the optimum tensile strength of 38.51MPa (at 50% volume fraction, 25mm/mm aspect ratio and 90^o orientation). The properties studied depend greatly on the reinforcement combinations of control factors and the composites of empty fruit bunch are stronger in tension than that of pseudo stem.

Wlodek et al (2012) treated jute fiber with 1-15% NaOH and KOH for 0.5-6hours. The fabric treated with 1-5%-long-time and 15%-short-time NaOH and KOH water solutions showed the best results.

Velumani and Navaneethakrishnan (2012) presented a systematic approach to evaluate and study the effect of process parameters on tensile, flexural and impact strength of untreated short sisal fiber reinforced vinyl ester polymer based composites and predicted the optimum properties of random natural fiber reinforced composites. The natural fiber of sisal at lengths of 10,30 and 50 mm and vinyl ester resin at loadings of 15,30 and 45 (wt.%) were prepared. The composite panel then fabricated using hand lay method in cold process in the size of 180 × 160 mm. Samples were then cut from the panel and subjected to mechanical properties testing such as tensile, flexural and impact strengths. The tensile strength ranged between 27.1 and 43.9 MPa. The flexural strength ranged between 26.9 and 49.5 MPa and the impact strength ranged between 16 and 93 J/m. The strength values were optimized using factorial design and Genetic Algorithm (GA) method.

Ihueze et al (2013) studied the effect of fiber volume fraction, aspect ratio and orientation on hardness strength of plantain fiber reinforced polyester composites. The fibers were treated with 5% NaOH for 4 hours before use in composite production. The empty fruit bunch fiber reinforced polyester matrix and pseudo stem plantain fiber matrix composite had the optimum hardness strength of 19.062MPa and 18.655MPa respectively at 50% volume fraction, 25mm/mm aspect ratio and 90^o orientation.

Ihueze and Okafor (2014a) studied the impact strength of plantain fiber reinforced polyester composites with notch tip radius and notch depth as controlling factors. The fibers were treated with 5% NaOH for 4 hours and optimum impact strength of 167.851KJ/m² (a mean value of 107.9383KJ/m²) was observed at 50% volume fraction

Ihueze and Okafor (2014b) studied the effect of fiber volume fraction, aspect ratio and orientation on flexural strength of plantain fiber reinforced polyester composites. The fibers were treated with 5% NaOH for 4 hours before use in composite production. The empty fruit bunch fiber reinforced polyester matrix has the optimum flexural strength of 42.40MPa (at 50% volume fraction, 10mm/mm aspect ratio and 45^o orientation), while the pseudo stem plantain fiber matrix composite has the optimum flexural strength of 41.16MPa (at 50% volume fraction, 15mm/mm aspect ratio and 30^o orientation).

Okafor and Godwin (2014) studied compressive and energy absorption of plantain empty fruit bunch and pseudo stem fiber reinforced polyester matrix. The fiber source, volume fraction and curing time of composite had most significant effect on the compressive strength. Treated plantain empty fruit bunch gave the optimum compressive strength of 109.17MPa at 50% volume fraction, curing time of 36hours, post curing temperature of 80^oC.

2.10 Summary of Literature Review

Generally, most researches were conducted at specified NaOH concentration and time or to determine the optimum NaOH solution concentration during the mercerization process at specific soaking duration and/or soaking temperature. However, there are limited works reported regarding attempts to determine the main effect and the interaction between these factors, its effect on the natural fiber and its final composite mechanical properties performance (Hashim et al, 2012). This work will determine the main effect and the interaction between NaOH concentration and time, optimum treatment conditions, its effect on the natural fiber and final composite mechanical properties performance.

CHAPTER THREE

MATERIALS AND METHODS

3.1 Chemical Composition Determination

The test materials; empty palm bunch, plantain bunch, and rattan palm were all sourced locally. Palm bunch and plantain bunch were obtained from the horticulture farm garden of National Root Crops Research Institute (NRCRI) while the rattan palm was gotten from the Umuahia central market in its cleaned form as cane. The characterization of the fibers was done at the NRCRI laboratory Umudike.

3.1.1 Equipment and Instruments Used

Equipment and instrument used in the experiment include:

1. Santorius digital weighing balance model number BL3002 (max.=300g).
2. Carbolite electric oven (Serial number 4/95/1113, max. temp 300⁰C, 2700watt, 50-60HZ, 15amps, 220-240volts) England.
3. Arthur Thomas Laboratory mill (Model number Ed-5, USA).
4. General Laboratory glassware and consumables.

3.1.2 Chemicals and Reagents

The Chemicals and reagent used in the proper work were of analytical standard and include:

1. Sodium chloride (1%)
2. Ammonium oxalate solution (0.5%)

3. Hydrochloric acid(2M)

4. Ethanol

3.1.3 Sample Preparation

Each of the test samples was first cut into small strands and dried in the oven at 60⁰C for 12hrs. The dried samples were ground into powdered form in a laboratory mill (Arthur Thomas Mill Ed-5 USA) in which the ground material was sieved through 1mm test sieve. The resulting powdered material was used for the work.

3.1.4 Method of Analysis

The systematic precipitation gravimetric method (Harborne, 1973; Harborne, 2003) was employed. The separation of different polysaccharides from the test plant sample involved series of extractions in which the water soluble polysaccharides were first removed and subsequently repeated extractions were performed on the residue. The composition of the different fibers was obtained and separated from one another by precipitation.

3.1.4.1 Pectin

20grams of each test sample was boiled in 200ml of absolute ethanol and then removed by filtration. To remove the neutral water soluble polysaccharides, the residue was boiled in 1% NaCl solution for 15mins and filtered; the pectin was extracted from the residue by treating it with 0.5%(w/v) ammonium oxalate solution. After filtration, pectin was precipitated by acidifying the filtrate with 2M HCl and subsequently pouring the acidified solution into equal volume of ethanol. The resulting pectin precipitate was recovered by filtration using weighed (Whitman number 42) filter paper. The recovered pectin was dried in the carbolite electric oven

at 80⁰C for 3hrs and weighed after cooling in a desiccator. The weight of pectin precipitate was obtained by difference and expressed as a percentage of the sample weight.

3.1.4.2 Lignin

The residue after removal of pectin was filtered and treated with 1% NaCl solution. The mixture was kept in a water bath at 70⁰C for an hour. The precipitated lignin was recovered by filtration using a weighed filter paper. After drying and cooling, its weight was obtained and expressed as a percentage of the sample weight.

3.1.4.3 Hemicellulose and Cellulose

After the extraction of the lignin, the residue was then soaked with 9% NaOH solution and allowed to stand overnight. The filtrate was acidified by treating with concentrated glacial acetic acid until it tested neutral to litmus paper. The hemicellulose was precipitated with ethanol and removed with weighed filter paper as done earlier. Meanwhile the residue left was washed with several portions of distilled water, dried and then weighed as the cellulose fraction.

The relation below was used to calculate the fiber concentration of each stage.

$$\% \text{ Concentration} = \frac{W_2 - W_1}{W} \times 100 \quad (3.1)$$

W_1 is the weight of empty filter paper, W_2 is the weight of filter paper + dried fiber fraction and W is the weight of sample used in the analysis

3.2 Chemical Treatment and Tensile Property Determination

3.2.1 Equipment and Instruments Used

Equipment and instrument used in the practical include the under listed:

1. Monsanto tensometer machine
2. Pneumatic grips
3. General Laboratory glassware and consumables

3.2.2 Chemicals and Reagents

The chemicals and reagent used in the proper work were of analytical standard and include:

1. Sodium hydroxide
2. Water
3. Acetic acid
4. Alcohol
5. Vinyl triethoxy silane

3.2.3 Sample Preparation and Treatment

The fibers used in this work were prepared at Center for Composite Research & Development (CCRD), JuNeng Nigeria Limited, Nsukka, Nigeria. Extraction of the Empty Plantain bunch and Palm bunch fiber was done through water retting, while Rattan Cane fibers were extracted mechanically from the body of Rattan Cane. The fibers were washed and conditioned at ambient conditions (Temperature of 28 °C and a relative humidity of 50%) until constant mass. The dried fibers were chopped into 100mm lengths and used for the determination of tensile property characterization and chemical treatment of fibers.

3.2.3.1 Fiber treatment

Alkali Treatment (mercerization)

The chopped fibers were each soaked in a transparent plastic vessel containing sodium hydroxide at different concentrations (2wt % NaOH, 4wt % NaOH, 6wt % NaOH, 8wt % NaOH and 10wt % NaOH) and each for different soaking times (30mins, 60mins, 90mins, 120mins and 150mins). The fibers were then washed thoroughly with water to remove the excess of NaOH on the fibers. Final washing was done with water containing little acetic acid. Fibers were dried in an air oven at 70 °C for 3hours.

Silane Treatment

Fibres treated at optimum conditions obtained during mercerization (alkali treatment) were dipped into alcohol/water mixture (60:40) containing 0.25%, 0.75% and 1.25% vinyl triethoxy silane coupling agent for 20mins, 60mins and 100mins respectively. The pH of the solution was maintained between 3.5 and 4. Fibres were washed in distilled water and dried.

3.2.3.2 Tensile test for fibers(ASTM D3822)

Single fibers were carefully separated from the bundles manually and both fiber ends were glued on the pieces of paper for handling purposes. A masking tape was used. During mounting, the specimen was handled only by paper tabs and the working zone of the fiber was not touched. The tests were carried out on a Monsanto tensometer machine at the Civil engineering laboratory, University of Nigeria, Nsukka. The load was measured by the 5N standard load cells and displacement was registered by a drum unit of the tensile stage. During the experiment, the data were plotted on graph sheets. Pneumatic grips were used to clamp the fiber. The distance

between the grips was fixed to 10, 15 or 20 mm, depending on fiber length. The upper end of the fiber was clamped first (right below the paper tab). In order to allow the fiber to self-align, under the weight of lower paper tab, approximately 1–2 min pause was made before the lower end of the fiber was clamped. Lower end of the fiber was clamped just above the lower paper tab. Clamping pads of the grips were covered with masking tape in order to prevent fiber damage in the clamping area. During the clamping, pressure in the grips is reduced to minimal level and after both grips were closed, pressure was raised to the working level (20–30% lower than maximum allowed for these particular grips). All tests were displacement controlled with the loading rate of 0.5 mm/min.

3.3 Water Absorption Test (ASTM D3171)

One gram each of dry untreated empty plantain bunch fiber, empty palm bunch fiber and rattan palm fiber were immersed in deionized water and placed in a constant temperature water bath. Samples were taken out after 5mins, 10mins, 15mins, 20mins and 25mins respectively, wiped dry with a clean and dry cloth and weighed using an electronic weighing balance to determine the amount of water absorbed. This process was done at 30 °C, 40 °C, 50 °C, 60 °C and 70°C respectively. The same process was repeated for all the fibers treated at their optimum conditions (4wt% NaOH for 120mins, for empty plantain bunch fiber and rattan palm fiber, and 6wt% NaOH for 90mins for empty palm bunch fiber) at the same temperatures as above, with samples taken out after 10mins, 20mins, 30mins, 40mins and 50mins respectively, wiped dry and weighed to determine water absorbed.

3.4 Scanning Electron Microscope (SEM) Analysis

Untreated samples of empty plantain bunch fiber, empty palm bunch fiber and rattan palm fiber were platinum coated and studied at different magnifications using a scanning electron microscope. The same procedure was repeated for all the fibers treated at their optimum conditions (4wt% NaOH for 120mins, for empty plantain bunch fiber and rattan palm fiber, and 6wt% NaOH for 90mins for empty palm bunch fiber). This procedure (platinum coating) makes it impossible to do SEM analysis on the same fiber samples before and after treatment, which would have given more accurate results. The SEM diagrams are presented later in this work.

3.5 Composite Formation and Mechanical Properties Determination

3.5.1 Chemicals and Reagents

General Purpose-grade unsaturated polyester resin (HSR 8113M), commercial grade Epoxy Resin 103, amine hardener 301 (polyamine), methyl ethyl ketone peroxide (MEKP) and cobalt naphthenate were supplied by Nycil Industrial Chemicals, Ota, Ogun State, Nigeria.

3.5.2 Composite Formation

Randomly oriented fiber composites containing fibers of varying lengths (10mm, 30mm and 50mm) and fiber volume fractions (10%, 30% and 50%) were prepared by hand lay-up method using a stainless steel sheet female mould with a marble tile male mould having dimensions $300 \times 300 \times 3 \text{mm}^3$ [Figure 3.1]. Calculation of fiber volume fraction of the fibers was done following derivation from rule of mixtures and implementation of Archimedes principle that an object (fiber) displaces is volume of liquid (water) in which it is immersed. The fibers used were

treated using the optimum NaOH concentration and time for mercerization. Prior to the composite preparation, the mould surface was polished well and a mould-releasing agent (mirror-glaze) was applied on the surface of the mould. General unsaturated polyester resin was mixed well with 1 wt. % cobalt naphthenate accelerator and 1wt. % by MEKP catalyst, while the epoxy resin was mixed with amine hardener in a ratio of 2:1. The fiber mat was placed in the mould and the resin mixture was poured evenly on it. Using a metallic roller, the air bubbles were carefully removed and the mat was allowed to wet completely. The mould was closed and the excess resin was allowed to flow out as 'flash' by pressing in a hydraulic press. The pressure was held constant during the curing process at room temperature for 24 hours. The composite sheet was post cured at 80°C for 4 hours. Test specimens, according to ASTM standards, were cut from the sheet.



Fig. 3.1: Mould set-up for fiber-reinforced composites, CCRD, Nsukka

3.5.3 Mechanical Properties Determination

The standard mechanical properties are determined by the procedures found in ASTM standards for plastics.

3.5.3.1 Tensile properties

The tensile properties were determined at the Civil Engineering Laboratory, University of Nigeria, Nsukka(UNN), using a Hounsfield Monsanto Universal Tensometer Machine at a constant rate of traverse of the moving grip of $5\text{mm}\cdot\text{min}^{-1}$ for randomly oriented fiber composites (ASTM D 638-99). The test specimens were rectangular in shape with dimensions $160 \times 19 \times 3 \text{mm}^3$ for randomly oriented fiber composites.

The sides of test specimens were polished using emery paper prior to testing. One grip is attached to a fixed and the other to a movable (power-driven) member so that they will move freely into alignment as soon as any load is applied. The test specimen was held tight by the two grips, the lower grip being fixed. Load was applied by gradually increasing the distance between the clamps until failure occurred. The force was then recorded and the area of cross-section of test sample obtained from which the tensile strength was calculated. The output data in the form of stress-strain graph was used to obtain the modulus, elongation and energy absorbed (toughness).



Fig. 3.2: Hounsfield Monsanto Universal Tensometer

3.5.3.2 Flexural properties

The flexural properties were determined at the Civil Engineering Laboratory, university of Nigeria, Nsukka(UNN), on a Hounsfield Monsanto Universal Tensometer Machine (ASTM D 790-99) at a constant rate of traverse of the moving grip of 5 mm/min[Figure 3.2] for randomly oriented fiber composites. The test specimens were rectangular in shape with dimensions 100 x 19 x 3 mm³ for randomly oriented fiber composites. The specimens were polished using emery paper prior to testing. The depth and width of the specimen were measured nearest to 0.01 mm. The support span was 16 times the depth of the specimen. The specimen was centred on the supports with the long axis of the specimen perpendicular to the loading nose and supports. The load was applied to the specimen and flexural strength and modulus were recorded. The load-deflection curve was also obtained. It was calculated at any point on the stress strain curve by the following equation:

$$S = \frac{3PL}{2bd^2} \quad (3.2)$$

Where S = stress in the outer fibers at midpoint (MPa), P = Load at any point on the load-elongation curve (N), L = support span (mm), b = width of specimen tested (mm), d = depth of specimen (mm).

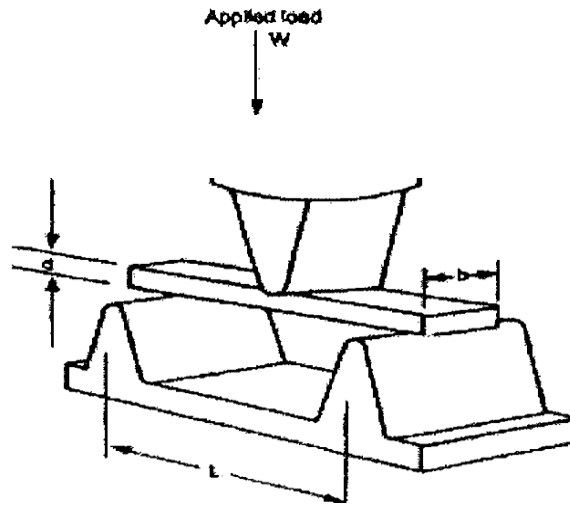


Fig. 3.3: Three-point bending

3.5.3.3 Impact Strength

Charpy impact testing specimens were prepared in accordance with ASTM D 6110-02M to measure the impact strength. The impact testing machine in the mechanical engineering laboratory at University of Nigeria, Nsukka was used for this test. The sharp file with included angle of 45° was drawn across the center of the same cut at 90° to the sample axis to obtain a consistent starter crack. The samples were fractured in a plastic impact testing machine and the net breaking energy and impact resistances were calculated.

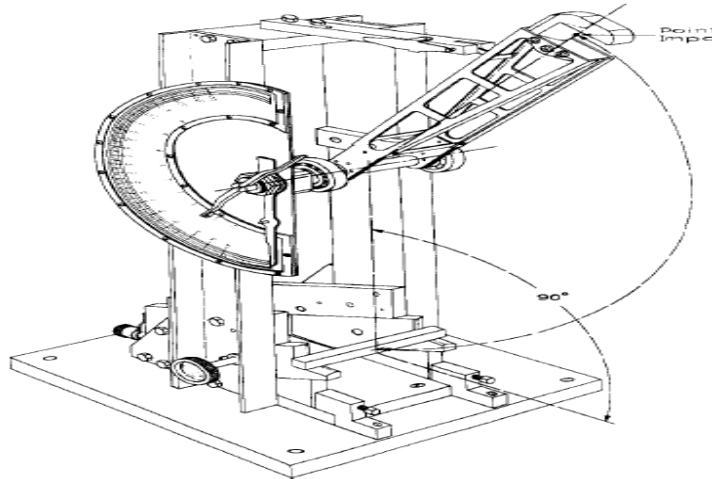


Fig. 3.4: Simple beam (Charpy Type) impact machine

3.6 Mathematical Methods

3.6.1 Design Matrices

The traditional approach was used in analysis of tensile test data, using MATLAB 7.9 software and the procedure described below for each mechanical property.

The tensile strength (ultimate tensile strength) was obtained as the highest point on the stress-strain curve; this often corresponds to the highest value of stress recorded on the stress versus strain table from which the stress-strain curve was plotted.

The modulus of elasticity (Young's modulus or tensile modulus) was obtained by determining the slope of a straight line drawn as tangent to the linear-elastic region of the stress-strain curve. The linear-elastic region of the stress-strain plot can be determined by observation, in addition to ensuring that the linear region chosen gives a good fit ($R^2 \geq 0.99$) to a straight line.

The yield strength (yield point) was obtained as the stress at which a line, drawn at 0.2% offset of the strain and with the modulus of elasticity as its slope, meets the stress-strain curve.

The toughness (energy at break) was obtained as the area under the stress-strain curve. The analysis GUI (Graphic User Interface) of the curve-fitting toolbox of MATLAB 7.9 was used to obtain this, after fitting a non-parametric fit (shape preserving interpolant) on the stress-strain data.

The ductility of the test material was determined from the percentage elongation (%El) also called “elongation at break”, using data which was directly measured by the tensometer, and the percentage reduction in area (%RA). A relationship for obtaining the percentage reduction in area as a function of percentage elongation is presented later in this section.

The Poisson ratio was determined from the percentage elongation using a relationship that was developed later in this section.

The shear modulus (modulus of rigidity) was computed using a relation for homogenous isotropic linear elastic materials:

$$G = \frac{E}{2(1+\nu)} \quad (3.3)$$

where G is the shear modulus, E is the modulus of elasticity and ν the Poisson ratio.

3.6.2 Development of Model for Percentage Reduction in Area (%RA)

Tensile test experiments involve slowly applying an axial load to a standard specimen by means of a suitable testing machine (tensometer) and measurement of the elongation in the direction of the axial load. The experimental results from the tensometer are in the form of plots of load versus elongation, from which the stress-strain curve is developed. This elongation is magnified for ease of measuring and reading of the data. The contraction (reduction in diameter or area) in the lateral direction of the material, due to this elongation, is usually much smaller and poses a

challenge to measure (unless methods like optical microscopy is used), more so for fibers which are characterized by high aspect ratios (length-to-diameter ratio), thus the need to develop an equation to obtain the lateral contraction as a function of elongation in the axial direction (Virk, 2010).

Assumptions:

* The test material may be elastic (elasticity is defined here as the ability of a material to recover to its initial shape and dimensions when the applied stress is removed (Katchy, 2008)) or plastic in behavior, but does not undergo any change in state or significant change in volume during the testing process.

* The cross-sectional area of the test material is approximately constant all through the length of the sample before and after testing.

Let l_o and l be the length of test material before and after the experiment, respectively, a_o and a be the cross-sectional area of the test material before and after the experiment, respectively.

Let V_o and V be the volume of the test material before and after the experiment, respectively.

Based on the assumptions: $V_o = V$ (3.4)

But Volume = Length \times Cross-sectional Area

Thus $a_o l_o = a l$ (3.5)

Percentage elongation: $\%El = \frac{l-l_o}{l_o} = \frac{l}{l_o} - 1$ (3.6)

Percentage reduction in Area: $\%RA = \frac{a_o - a}{a_o} = 1 - \frac{a}{a_o}$ (3.7)

From equation 3.5:
$$\frac{a}{a_o} = \frac{l_o}{l} \quad (3.8)$$

Substituting eqn. 3.8 into eqn. 3.7:
$$\%RA = 1 - \frac{l_o}{l} \quad (3.9)$$

From equation 3.6:
$$\%El + 1 = \frac{l}{l_o} \quad (3.10)$$

Thus
$$\%RA = 1 - \frac{1}{1 + \%El} \quad (3.11)$$

$$\%RA = \frac{\%El}{1 + \%El} \quad (3.12)$$

Homogenous isotropic linear elastic materials have their elastic properties uniquely determined by any two moduli among six elastic moduli: Young's modulus, Poisson ratio, shear modulus, bulk modulus, lame's modulus and wave modulus. Given any two, any other of the elastic moduli can be calculated. Young's modulus and Poisson ratio are the two most common of these moduli used to characterize the elastic property of solids (Bower, 2011).

3.6.3 Development of Model for Poisson Ratio

Elongation of a sample of length l_o is accompanied by contraction in the transverse direction. The ratio of this lateral strain (contraction), ε_T , to the longitudinal strain (extension), ε , is known as the Poisson ratio, ν .

$$\nu = -\frac{\varepsilon_T}{\varepsilon} \quad (3.13)$$

If the test sample is circular in cross-section, with d_o as original diameter and d as instantaneous diameter,

$$\varepsilon_T = (d_o - d)/d_o = 1 - \frac{d}{d_o} \quad (\text{Katchy, 2008}) \quad (3.14)$$

Recall that
$$\%RA = 1 - \frac{a}{a_o} = 1 - \frac{d^2}{d_o^2} \quad (3.15)$$

Thus
$$\%RA = \left(1 - \frac{d}{d_o}\right) \left(1 + \frac{d}{d_o}\right) \quad (3.16)$$

$$\%RA = \varepsilon_T (2 - \varepsilon_T) \quad (3.17)$$

$$\varepsilon_T^2 - 2\varepsilon_T + \%RA = 0 \quad (3.18)$$

Applying quadratic equation formula and retaining only the positive solution, we have;

$$\varepsilon_T = 1 - \sqrt{1 - \%RA} \quad (3.19)$$

In terms of %El:

$$\varepsilon_T = 1 - \sqrt{1 - \left(\frac{\%El}{1 + \%El}\right)} \quad (3.20)$$

$$\nu = \frac{\varepsilon_T}{\varepsilon} = \frac{\varepsilon_T}{\%El} \quad (3.21)$$

Thus

$$\nu = \frac{1 - \sqrt{1 - \left(\frac{\%El}{1 + \%El}\right)}}{\%El} = \frac{1 - \sqrt{\frac{1 + \%El - \%El}{1 + \%El}}}{\%El} \quad (3.22)$$

$$\nu = \frac{1 - \sqrt{\frac{1}{1 + \%El}}}{\%El} \quad (3.23)$$

If the test sample is non-circular in cross-section, the lateral strain can be represented with respect to the area as:

$$\varepsilon_T = (a_o - a)/a_o = 1 - \frac{a}{a_o} \quad (3.24)$$

This is equivalent to the relationship for percentage reduction in area, %RA. The lateral strain in one direction will be half of the above. Applying the previously established relationship between %El and %RA and on the basis of lateral strain in one direction:

$$\nu = \frac{0.5 \varepsilon_T}{\varepsilon} = \frac{0.5 \%RA}{\%El} \quad (3.25)$$

$$\nu = \frac{0.5 \frac{\%El}{1+\%El}}{\%El} \quad (3.26)$$

$$\nu = \frac{0.5}{1+\%El} \quad (3.27)$$

The above will be most accurate for square cross-sections and other similar shapes which have equal dimension on all sides.

3.6.3.1 Validation of Poisson Ratio Equation

The model equations will be validated based on their limiting values for %El → 0 and %El → ∞.

For the Poisson ratio of samples with circular cross-sections as %El → 0, we have:

$$\lim_{\%El \rightarrow 0} \nu = \frac{1 - \sqrt{\frac{1}{1+\%El}}}{\%El} \quad (3.28)$$

Applying l'hopitals rule (differentiating numerator and denominator independently), we have:

$$\lim_{\%El \rightarrow 0} \nu = \frac{0.5}{(1+\%El)^{3/2}} \quad (3.29)$$

Substituting %El → 0 into the above equation gives the limiting value as ν = 0.5.

For the Poisson ratio of samples with circular cross-sections as %El → ∞, we have:

$$\lim_{\%El \rightarrow \infty} \nu = \frac{0.5}{(1+\%El)^{3/2}} \quad (3.30)$$

In a similar way, substituting $\%El \rightarrow \infty$ into the above equation gives the limiting value as $\nu = 0$.

For the Poisson ratio of samples with noncircular cross-sections as $\%El \rightarrow 0$, we have:

$$\lim_{\%El \rightarrow 0} \nu = \frac{0.5}{1+\%El} \quad (3.31)$$

Substituting $\%El \rightarrow 0$ into the above equation gives the limiting value as $\nu = 0.5$.

For the Poisson ratio of samples with noncircular cross-sections as $\%El \rightarrow \infty$, we have:

$$\lim_{\%El \rightarrow \infty} \nu = \frac{0.5}{1+\%El} \quad (3.32)$$

In a similar way, substituting $\%El \rightarrow \infty$ into the above equation gives the limiting value as $\nu = 0$.

It can be observed that the limiting values of the two equations relating the Poisson ratio to Percentage elongation for circular and noncircular cross-sectional samples, for $\%El \rightarrow 0$ and $\%El \rightarrow \infty$ are $\nu = 0.5$ and $\nu = 0$ respectively. These two values are the bound for the Poisson ratio of most common materials, except compressible materials, which is beyond the scope of this study, thus validating the expressions (Greaves et al, 2011).

3.6.4 A New Approach for Analysis of Tensile Test Data

The traditional way of measuring the modulus of elasticity of a material is to measure the slope of the stress-strain curve in the linear-elastic region of the curve, but this technique produces values that are inaccurate, often by a factor of two or more, because of contributions to the strain from material creep or deflection of the test machine. It has been suggested that accurate values of modulus of elasticity are measured dynamically: by exciting the natural vibrations of a beam

or wire or by measuring the velocity of longitudinal or shear sound waves in the material (Ashby and Cebon, 2011).

The above statement implies that modulus of elasticity obtained as slope of linear-elastic region of stress-strain curves are inaccurate and often underestimate the actual modulus, thus making the values of some other mechanical properties, like the yield strength, inaccurate. In addition, since the analyst is left to judge which region of the stress-strain curve is within the linear-elastic region, the results may vary.

A new approach is proposed in this work:

1. An empirical model will be fit to the stress-strain curves. Since these fits use linear and non-linear least square techniques, they reduce the effects of random errors, like deflection of the test machine, on the calculated values of the modulus of elasticity.
2. The slope will be found at the point where the strain is practically zero. This will not only ensure that the curve is within the elastic region, but will remove the effects of contributions to the strain from material creep (change in strain with time) on calculated values of the modulus of elasticity.

Two empirical models were observed to fit the various profiles of stress-strain curves, the models are the Linear-Linear Rational model and the Linear-Quadratic Rational model.

3.6.4.1 Linear-Linear rational model

$$\text{Model Equation: } \sigma = \frac{p_1 \varepsilon + p_2}{\varepsilon + q_1} \quad (3.33)$$

Where σ is the Tensile Stress, ε is the Tensile Strain, p_1 , p_2 and q_1 are model constants.

Equation (3.33) has the following advantages:

* The model is simple and has few model constants and thus a higher degree of freedom and can fit to three data points or more.

* The maximum stress (tensile strength) for the model is equal to its limiting value as the strain tends to infinity, which is equal to p_1 and is thus easy to obtain.

$$\lim_{\varepsilon \rightarrow \infty} \sigma = \frac{p_1 \varepsilon + p_2}{\varepsilon + q_1} \quad (3.34)$$

$$\lim_{\varepsilon \rightarrow \infty} \sigma = \frac{p_1 + p_2/\varepsilon}{1 + q_1/\varepsilon} \quad (3.35)$$

$$\lim_{\varepsilon \rightarrow \infty} \sigma = p_1 \quad (3.36)$$

Equation (3.33) has the following disadvantages:

*The model can only predict the ultimate tensile strength, not the failed strength, because it has a limiting value and not a maximum, making it suitable only for brittle materials.

* The predicted value of Ultimate Tensile Strength is often not very close to the tabulated value.

*It is not possible to find the equation of the slope, thus the model does not enable us find Modulus of Elasticity.

3.6.4.2 Linear-Quadraticrational model

$$\text{Model Equation: } \sigma = \frac{p_1 \varepsilon + p_2}{\varepsilon^2 + q_1 \varepsilon + q_2} \quad (3.37)$$

where σ is the Tensile Stress, ε is the Tensile Strain, p_1, p_2, q_1 and q_2 are model constants.

Advantages:

*The model can predict both the Ultimate Tensile strength and the Failed Strength, thus making it suitable for a wide variety of materials.

*The predicted value of the Ultimate Tensile Strength is often close to the tabulated value. This value is obtained at the point where; $d\sigma/d\varepsilon = 0$.

$$\frac{-p_1\varepsilon^2 - 2p_2\varepsilon + (p_1q_2 - p_2q_1)}{(\varepsilon^2 + q_1\varepsilon + q_2)^2} = 0 \quad (3.38)$$

Solving the above quadratic equation using quadratic equation formula, we have:

$$\varepsilon_u = p_2 - \sqrt{(p_2^2 + p_1(p_1q_2 - p_2q_1))}/-p_1 \quad (3.39)$$

Substituting the above into the linear-Quadratic model, we obtain the Stress at this Strain value as:

$$\sigma_u = \frac{p_1^2}{2\sqrt{(p_2^2 + p_1(p_1q_2 - p_2q_1))} + p_1q_1 - 2p_2} \quad (3.40)$$

Where σ_u and ε_u are the Ultimate Tensile Strength and the corresponding Strain at this Stress respectively.

*The nature of the model enables us to obtain the equation of the slope and thus calculate the Modulus of Elasticity as:

$$E = \lim_{\varepsilon \rightarrow 0} d\sigma/d\varepsilon \quad (3.41)$$

$$E = \lim_{\varepsilon \rightarrow 0} \frac{-p_1\varepsilon^2 - 2p_2\varepsilon + (p_1q_2 - p_2q_1)}{(\varepsilon^2 + q_1\varepsilon + q_2)^2} \quad (3.42)$$

$$E = \frac{(p_1 q_2 - p_2 q_1)}{q_2^2} \quad (3.43)$$

Disadvantages:

*It is more complex (having more constants) than the Linear-Linear Rational model, with a lower degree of freedom and can fit to four data points or more.

3.6.4.3 Further analysis for linear-quadratic rational model

i. Yield strength: This is equivalent to the Stress at which the Stress-Strain curve meets a straight line, drawn from an offset of 0.2% of the Strain with the Modulus of Elasticity as its slope. Thus the point in question must satisfy the equation below:

$$E(\varepsilon - 0.002) = \frac{p_1 \varepsilon + p_2}{\varepsilon^2 + q_1 \varepsilon + q_2} \quad (3.44)$$

Rearranging the above gives the third order polynomial presented below:

$$E \varepsilon^3 + E(q_1 - 0.002) \varepsilon^2 + (E q_2 - 0.002 E q_1 - p_1) \varepsilon - (0.002 E q_2 + p_2) = 0 \quad (3.45)$$

The positive solution to the above third order equation gives the value of the Strain at Yield Strength (ε_y). The Yield Strength (S_y) can therefore be obtained by substituting the value of ε_y into the straight line equation.

$$S_y = E(\varepsilon_y - 0.002) \quad (3.46)$$

ii. Toughness (Energy at break): This is equivalent to the area under the Stress-Strain curve and can be obtained by integrating the linear-quadratic rational model from zero to the maximum Strain (Strain at break), ε_b .

$$\int_0^{\varepsilon_b} \frac{p_1 \varepsilon + p_2}{\varepsilon^2 + q_1 \varepsilon + q_2} d\varepsilon \quad (3.47)$$

On rearrangement, the above integral becomes:

$$\frac{p_1}{2} \int_0^{\varepsilon_b} \frac{2\varepsilon + q_1}{\varepsilon^2 + q_1 \varepsilon + q_2} d\varepsilon + \frac{p_1}{2} \left[\frac{2p_2}{p_1} - q_1 \right] \int_0^{\varepsilon_b} \frac{1}{\left(\varepsilon + \frac{q_1}{2}\right)^2 + \left(\frac{\sqrt{4q_2 - q_1^2}}{2}\right)^2} d\varepsilon \quad (3.48)$$

Integrating the above equation gives:

$$\frac{p_1}{2} \ln[\varepsilon^2 + q_1 \varepsilon + q_2] + \frac{2p_2 - p_1 q_1}{\sqrt{4q_2 - q_1^2}} \left(\arctan \left(\frac{2\left(\varepsilon + \frac{q_1}{2}\right)}{\sqrt{4q_2 - q_1^2}} \right) \right) \quad (3.49)$$

Substituting the specified upper and lower limits of integration gives Toughness (T_s) as:

$$T_s = \frac{p_1}{2} \ln \left[\frac{\varepsilon_b^2 + q_1 \varepsilon_b + q_2}{q_2} \right] + \frac{2p_2 - p_1 q_1}{\sqrt{4q_2 - q_1^2}} \left(\arctan \left(\frac{2\left(\varepsilon_b + \frac{q_1}{2}\right)}{\sqrt{4q_2 - q_1^2}} \right) - \arctan \left(\frac{q_1}{\sqrt{4q_2 - q_1^2}} \right) \right) \quad (3.50)$$

The above equation will give real values for Toughness only if $4q_2 > q_1^2$, but for conditions when $4q_2 \leq q_1^2$, other solutions must be proffered as the above will give complex results.

Firstly, for the case of $4q_2 < q_1^2$ the linear-quadratic rational model can be rearranged into its partial fractions based on the factors of the denominator, thus;

$$\int_0^{\varepsilon_b} \frac{p_1 \varepsilon + p_2}{\varepsilon^2 + q_1 \varepsilon + q_2} d\varepsilon = \int_0^{\varepsilon_b} \frac{\frac{p_1(q_1 + \sqrt{q_1^2 - 4q_2}) - 2p_2}{2\sqrt{q_1^2 - 4q_2}}}{\frac{q_1 + \sqrt{q_1^2 - 4q_2}}{\varepsilon + \frac{q_1 + \sqrt{q_1^2 - 4q_2}}{2}}} d\varepsilon + \int_0^{\varepsilon_b} \frac{\frac{2p_2 - p_1(q_1 + \sqrt{q_1^2 - 4q_2})}{2\sqrt{q_1^2 - 4q_2}}}{\frac{q_1 - \sqrt{q_1^2 - 4q_2}}{\varepsilon + \frac{q_1 - \sqrt{q_1^2 - 4q_2}}{2}}} d\varepsilon \quad (3.51)$$

On integration of the above equation, based on the partial fractions we have;

$$\frac{p_1(q_1 + \sqrt{q_1^2 - 4q_2}) - 2p_2}{2\sqrt{q_1^2 - 4q_2}} \ln \left(\varepsilon + \frac{q_1 + \sqrt{q_1^2 - 4q_2}}{2} \right) + \frac{2p_2 - p_1(q_1 + \sqrt{q_1^2 - 4q_2})}{2\sqrt{q_1^2 - 4q_2}} \ln \left(\varepsilon + \frac{q_1 - \sqrt{q_1^2 - 4q_2}}{2} \right) \quad (3.52)$$

Substituting the specified upper and lower limits of integration gives Toughness (T_S) as:

$$T_S = \frac{p_1(q_1 + \sqrt{q_1^2 - 4q_2}) - 2p_2}{2\sqrt{q_1^2 - 4q_2}} \ln \left(\frac{2\varepsilon_b + q_1 + \sqrt{q_1^2 - 4q_2}}{q_1 + \sqrt{q_1^2 - 4q_2}} \right) + \frac{2p_2 - p_1(q_1 + \sqrt{q_1^2 - 4q_2})}{2\sqrt{q_1^2 - 4q_2}} \ln \left(\frac{2\varepsilon_b + q_1 - \sqrt{q_1^2 - 4q_2}}{q_1 - \sqrt{q_1^2 - 4q_2}} \right) \quad (3.53)$$

Finally, the case when $4q_2 = q_1^2$ is considered, though this may scarcely ever happen due to computer approximation errors. For this the denominator of the linear-quadratic rational model will have two equal roots. The form of the model and its partial fractions are presented below;

$$\int_0^{\varepsilon_b} \frac{p_1 \varepsilon + p_2}{\varepsilon^2 + q_1 \varepsilon + q_2} d\varepsilon = \int_0^{\varepsilon_b} \frac{p_1 \varepsilon + p_2}{(\varepsilon + \frac{q_1}{2})^2} d\varepsilon = \int_0^{\varepsilon_b} \frac{p_1}{\varepsilon + \frac{q_1}{2}} d\varepsilon + \int_0^{\varepsilon_b} \frac{\frac{2p_2 - p_1 q_1}{2}}{(\varepsilon + \frac{q_1}{2})^2} d\varepsilon \quad (3.54)$$

On integration of the above equation, based on the partial fractions we have;

$$p_1 \ln \left(\varepsilon + \frac{q_1}{2} \right) - \frac{\frac{2p_2 - p_1 q_1}{2}}{\varepsilon + \frac{q_1}{2}} \quad (3.55)$$

Substituting the specified upper and lower limits of integration gives Toughness (T_S) as:

$$T_S = p_1 \ln \left(\frac{2\varepsilon_b + q_1}{q_1} \right) + \frac{\varepsilon_b(2p_2 - p_1 q_1)}{q_1(\varepsilon_b + q_1)} \quad (3.56)$$

A MATLAB 7.9 program code that computes all mechanical properties given the values of the constants in the linear-quadratic rational model is given in the appendices (A 7.10).

CHAPTER FOUR

RESULTS AND DISCUSSION

The results obtained in this work are presented and discussed in the sections of this chapter.

4.1 Percentage Reduction in Area and Poisson Ratio Model Analysis

A simple sensitivity analysis was performed for the reduction in area model (Eqn. 3.12), the Poisson ratio model for circular cross-sections (Eqn. 3.23) and the Poisson ratio model for non-circular cross-sections (Eqn. 3.27) for percentage elongation values varying from zero to fifty percent by simulating the equation using a MATLAB 7.9 code and the results are presented as Figure 4.1, Figure 4.2 and Figure 4.3 respectively. Figure 4.1 shows how percentage reduction in area increases somewhat with increase in percentage elongation (as a fraction) while Figure 4.2 and Figure 4.3 respectively show how Poisson ratio – for both circular and non-circular cross-sections – decreases somewhat with increase in percentage elongation. It can be observed from the figures that the values of percentage reduction in area and Poisson ratio will remain within acceptable limits (Greaves et al, 2011).

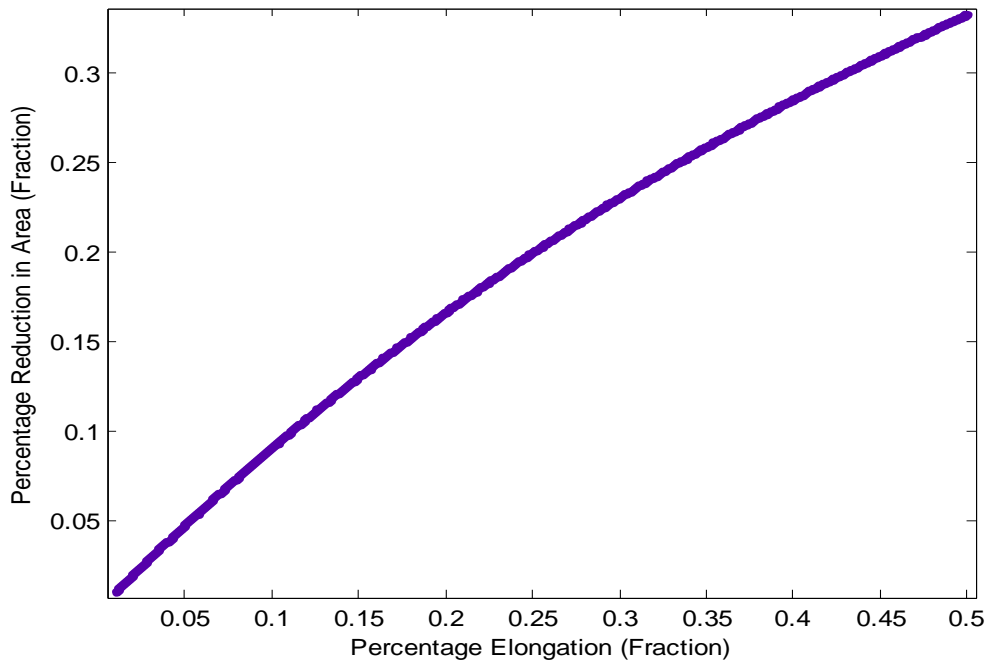


Figure 4.1: Percentage Reduction in Area vs. Percentage Elongation (Eqn. 3.12)

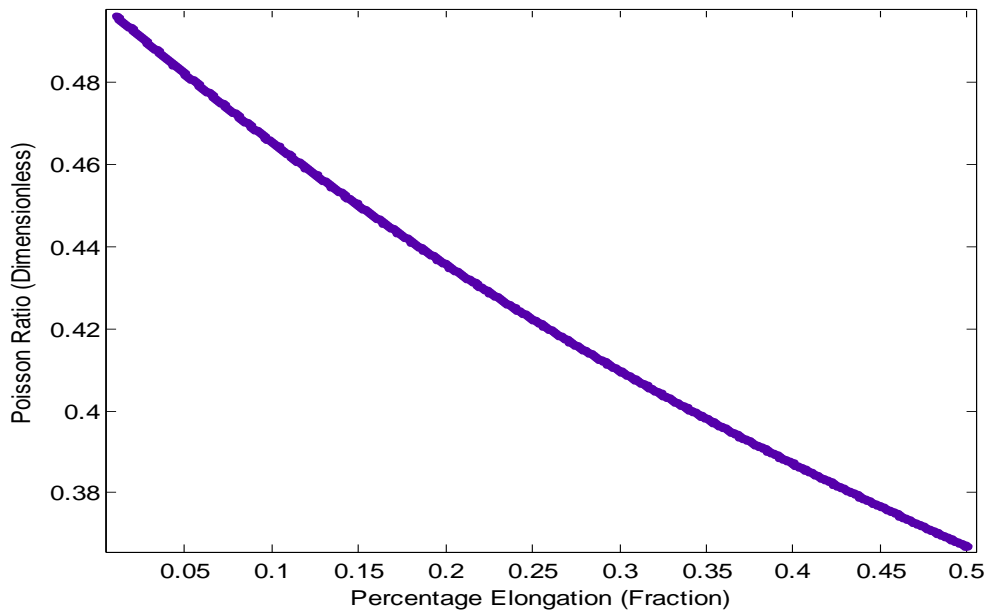


Figure 4.2: Poisson Ratio versus Percentage Elongation (Circular Cross-Sections)

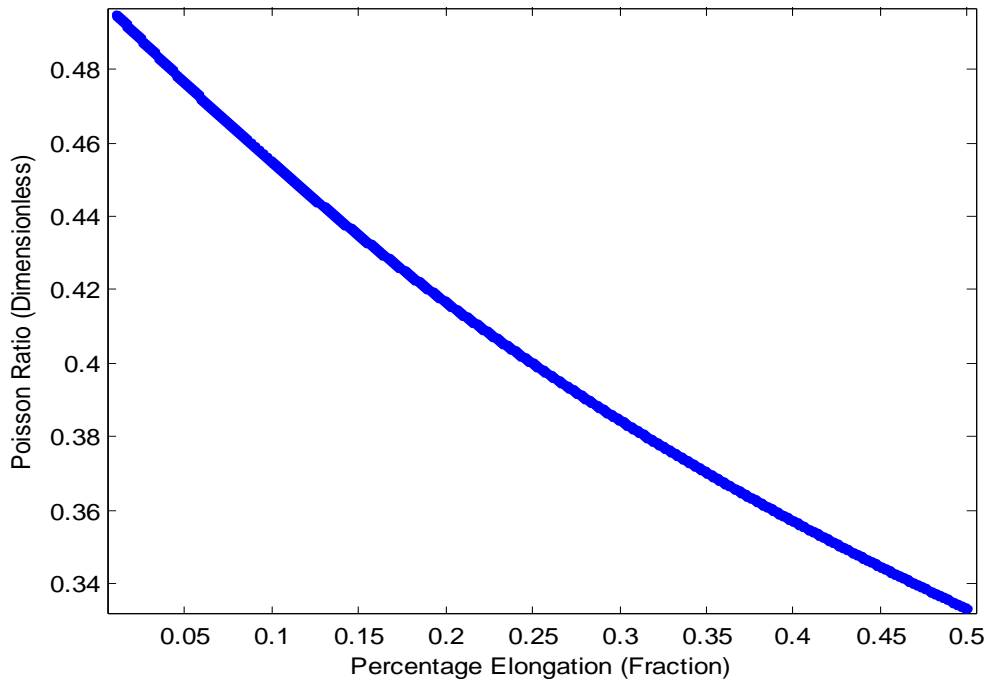


Figure 4.3: Poisson Ratio versus Percentage Elongation (Noncircular Cross-Sections)

4.2 Chemical Composition of Natural Fiber Sources

Table 4.1 shows the results from the analysis of the chemical composition of the different sources of natural fibers studied using the method of analysis described in section 3.1 of this work. The table shows the percentage composition of pectin, lignin, hemicellulose and cellulose in the natural fiber sources. Natural fibres are seen as composites of cellulose fibers, with hemicellulose as a compatibilizer in a lignin matrix. Cellulose and hemicellulose are known to contribute significantly to fiber strength (Kalia et al, 2009). It can be seen from the table that empty plantain bunch fiber has the highest hemicelluloses content (53.63%), followed by empty palm bunch fiber (42.85%) and rattan palm fiber (33.06%), thus empty plantain bunch fiber should have the most strength based on hemicelluloses content. Rattan palm fiber has the highest cellulose content (58.64%) followed by empty palm bunch fiber (46.9%) and empty plantain

bunch fiber (41.06%), thus rattan palm fiber should have the most strength based on cellulose content. Empty plantain bunch, rattan palm and empty palm bunch have the sum of cellulose and hemicelluloses content as 94.68%, 91.7% and 89.75% respectively. Empty plantain bunch fiber should have the most strength based on the sum of cellulose and hemicelluloses content.

The hemicelluloses content is also known to be responsible for the water absorption property of natural fibers (Kalia et al, 2009). Thus, the water absorption tendencies of the fibers, from the most to the least, based on the hemicelluloses content would be: Empty plantain bunch fiber, empty palm bunch fiber and rattan palm fiber.

Mercerization is believed to improve fiber strength by removal of cementing substances like lignin and hemicelluloses, thus increasing the amount of cellulose exposed on the fiber surface. The fibers will then yield to mercerization treatment based on their hemicelluloses content. It is expected therefore that mercerization will improve the strength of empty plantain bunch fiber the most, since it has the highest hemicelluloses content, followed by empty palm bunch fiber and the rattan palm fiber.

Table 4.1: Chemical composition of natural fiber sources

Sample	Pectin (%)	Lignin (%)	Hemicellulose (%)	Cellulose (%)
Plantain Bunch	1.26±0.03	2.74±0.04	53.62±0.04	41.06±0.19
Palm Bunch	0.86±0.02	8.64±0.22	42.85±0.26	46.9±0.47
Rattan palm	0.24±0.02	5.32±0.02	33.06±0.2	58.64±0.06

4.3 Mechanical Properties of Empty Plantain Bunch Fiber

This section presents and discusses the mechanical properties of empty plantain bunch fiber. These results were obtained from stress-strain analysis from the plots given in Appendix 7.1. Table 4.2 shows the mechanical properties of untreated empty plantain bunch fiber, with the modulus measured using the new approach in parentheses.

Table 4.2: Mechanical Properties of Untreated Empty Plantain Bunch Fiber

Toughness (MPa)	%El (%RA) (%)	Tensile Strength (MPa)	Yield Strength (MPa)	Young Modulus (GPa)	Poisson Ratio	Shear Modulus (GPa)
3.5669	9.25(8.47)	51.6471	19.7363	1.3070(1.0162)	0.4678	0.4452

Table 4.3 shows the mechanical properties of empty plantain bunch fiber treated with 2wt% NaOH. Modulus measured using the new approach is presented with that of the traditional approach and maximum values of mechanical properties highlighted. It can be observed from Tables 4.2 and 4.3, that empty plantain bunch fiber treated with 2wt % NaOH had its toughness increased 3.4 times relative to the untreated sample, the tensile strength of the treated sample was more than 12.5 times the untreated one, yield strength was increased almost 8 times, modulus of elasticity and shear modulus increased 20 times, while there was no significant improvement in ductility (percentage elongation and reduction in area) and Poisson ratio. Eighty percent of the mechanical properties had their maximum values after the fiber had been treated at this concentration for 120 minutes.

Table 4.3: Mechanical Properties of Empty Plantain Bunch Fiber Treated with 2 wt% NaOH

Time (mins)	30	60	90	120	150
Variables (Units)					
Toughness (MPa)	3.6740	1.8963	1.6332	*15.7895	11.2058
Tensile Strength (MPa)	144.0551	149.8745	189.5307	383.8447	*647.1856
Modulus of Elasticity (GPa)	24.6400	26.3800	19.9000	*27.4700	25.5600
Modulus (New Approach)(GPa)	38.0690	*38.2410	19.9580	21.9320	23.2900
Yield Strength (MPa)	92.5748	99.9599	150.3280	*172.9783	72.6703
Percentage Elongation (%)	3.1250	1.7500	1.4500	*5.7000	3.2500
Percentage Reduction in Area (%)	3.0303	1.7199	1.4293	*5.3926	3.1477
Poisson Ratio (Dimensionless)	0.4886	0.4935	*0.4946	0.4796	0.4881
Shear Modulus (GPa)	8.2764	8.8314	6.6572	*9.2830	8.5879

*Maximum values

Table 4.4 shows the mechanical properties of empty plantain bunch fiber treated with 4wt% NaOH. Modulus measured using the new approach is presented with that of the traditional approach and maximum values of mechanical properties highlighted. It can be observed from Tables 4.2 and 4.4 that empty plantain bunch fiber treated with 4wt % NaOH had its toughness increased more than 13 times relative to the untreated sample, the tensile strength of the treated sample was more than 16.5 times the untreated one, yield strength was increased more than 32 times, modulus of elasticity and shear modulus increased more than 50 times, while there was no significant improvement in ductility (percentage elongation and reduction in area) and Poisson ratio. Treatment at this concentration resulted in increase in all mechanical properties in comparison with that of 2 wt % NaOH. Eighty percent of the mechanical properties also had their maximum values after the fiber had been treated at this concentration for 120 minutes.

Table 4.4: Mechanical Properties of Empty Plantain Bunch Fiber Treated with 4 wt% NaOH

Time (mins)	30	60	90	120	150
Variables (Units)					
Toughness (MPa)	13.5841	24.8134	35.3623	*51.9357	40.0158
Tensile Strength (MPa)	288.1098	576.4851	615.0219	*860.5139	718.4211
Modulus of Elasticity (GPa)	28.0100	27.7800	*70.3500	48.1400	27.5100
Modulus (New Approach)(GPa)	43.2650	37.4830	74.0800	*76.4560	37.6550
Yield Strength (MPa)	194.2555	354.6910	308.4525	*661.5980	465.2110
Percentage Elongation (%)	5.7500	5.7500	6.9500	*7.2750	7.2500
Percentage Reduction in Area (%)	5.4374	5.4374	6.4984	*6.7816	6.7599
Poisson Ratio (Dimensionless)	0.4794	*0.4794	0.4754	0.4743	0.4744
Shear Modulus (GPa)	9.4665	9.3888	*23.8416	16.3267	9.3295

*Maximum values

Table 4.5 shows the mechanical properties of empty plantain bunch fiber treated with 6wt% NaOH. Modulus measured using the new approach is presented with that of the traditional approach and maximum values of mechanical properties highlighted. It can also be observed from Tables 4.2 and 4.5, that Empty Plantain Bunch Fiber treated with 6wt % NaOH had its toughness increased about 13 times relative to the untreated sample, the tensile strength of the treated sample was more than 16.5 times the untreated one, yield strength was increased almost 24 times, modulus of elasticity and shear modulus increased more than 40 times, while there was no significant improvement in ductility (percentage elongation and reduction in area) and Poisson ratio. Treatment at this concentration resulted in a slight drop in all mechanical properties in comparison with that of 4 wt %, indicating that the optimum concentration of NaOH for mercerization of empty plantain bunch fiber would lie between 4wt% and 6wt %. Eighty percent of the mechanical properties also had their maximum values after the fiber had been treated at this concentration for 120 minutes.

Table 4.5: Mechanical Properties of Empty Plantain Bunch Fiber Treated with 6 wt% NaOH

Time (mins) Variables (Units)	30	60	90	120	150
Toughness (MPa)	9.0455	9.7172	16.1488	*50.9526	9.6217
Tensile Strength (MPa)	379.2531	481.8816	588.1484	*855.6013	484.8420
Modulus of Elasticity (GPa)	53.0300	22.2200	38.9300	40.1300	*58.2800
Modulus (New Approach)(GPa)	74.1680	22.3080	21.0930	57.5510	*85.4490
Yield Strength (MPa)	311.9990	301.5460	394.3195	*487.3150	369.0740
Percentage Elongation (%)	2.8750	3.3750	3.8000	*7.5250	2.5000
Percentage Reduction in Area (%)	2.7776	3.2648	3.6609	*6.9984	2.4390
Poisson Ratio (Dimensionless)	0.4895	0.4877	0.4862	0.4734	*0.4908
Shear Modulus (GPa)	17.8016	7.4680	13.0973	13.6178	*19.5463

*Maximum values

Table 4.6 shows the mechanical properties of empty plantain bunch fiber treated with 8wt% NaOH. Modulus measured using the new approach is presented with that of the traditional approach and maximum values of mechanical properties highlighted. Observations from Tables 4.2 and 4.6 show that empty plantain bunch fiber treated with 8wt % NaOH had its toughness increased almost 9 times relative to the untreated sample, the tensile strength of the treated sample was more than 15 times the untreated one, yield strength was increased almost 30 times, modulus of elasticity and shear modulus increased more than 20 times, while there was no significant improvement in ductility (percentage elongation and reduction in area) and Poisson ratio. Treatment at this concentration resulted in a slight drop in almost all mechanical properties in comparison with that of 6 wt %. Forty percent of the mechanical properties had their maximum values after the fiber had been treated at this concentration for 30 minutes.

Table 4.6: Mechanical Properties of Empty Plantain Bunch Fiber Treated with 8 wt% NaOH

Time (mins) Variables (Units)	30	60	90	120	150
Toughness (MPa)	*35.2483	19.1183	17.6685	5.6792	10.8406
Tensile Strength (MPa)	665.1185	*783.1146	703.5303	529.9170	491.8404
Modulus of Elasticity (GPa)	24.6500	21.1600	23.9700	25.8100	*29.9200
Modulus (New Approach)(GPa)	29.6750	18.1380	21.7260	32.5980	*36.8490
Yield Strength (MPa)	425.2360	327.1095	*611.1310	529.9170	459.4035
Percentage Elongation (%)	*7.1250	4.6250	4.0500	2.0000	3.0000
Percentage Reduction in Area (%)	*6.6510	4.4206	3.8924	1.9608	2.9126
Poisson Ratio (Dimensionless)	0.4748	0.4833	0.4853	*0.4926	0.4890
Shear Modulus (GPa)	8.3572	7.1328	8.0690	8.6459	*10.0468

*Maximum values

Table 4.7 shows the mechanical properties of empty plantain bunch fiber treated with 10wt% NaOH. Modulus measured using the new approach is presented with that of the traditional approach and maximum values of mechanical properties highlighted. Observations from Tables 4.2 and 4.7 reveal that empty plantain bunch fiber treated with 10wt % NaOH had its toughness increased 9.5 times relative to the untreated sample, the tensile strength of the treated sample was more than 11 times the untreated one, yield strength was increased more than 19 times, modulus of elasticity and shear modulus increased 17 times, while there was no significant improvement in ductility (percentage elongation and reduction in area) and Poisson ratio. Treatment at this concentration resulted in a slight drop in all mechanical properties in comparison with that of 8 wt %. Eighty percent of the mechanical properties had their maximum values after the fiber had been treated at this concentration for 30 minutes. Generally, a slight increase in Poisson ratio (5%) and a slight decrease in ductility were observed after treatment.

Table 4.7: Mechanical Properties of Empty Plantain Bunch Fiber Treated with 10 wt% NaOH

Time (mins)	30	60	90	120	150
Variables (Units)					
Toughness (MPa)	*37.3020	5.3062	7.3692	5.1919	0.6821
Tensile Strength (MPa)	*614.2335	353.2127	267.1565	262.9740	177.0635
Modulus of Elasticity (GPa)	14.6400	21.6100	*23.6000	21.8300	17.5600
Modulus (New Approach)(GPa)	17.2560	*25.2670	21.0930	23.9610	9.1493
Yield Strength (MPa)	*404.1075	250.8445	144.2045	210.5690	177.0635
Percentage Elongation (%)	*8.5000	2.5000	3.6250	2.7500	1.0000
Percentage Reduction in Area (%)	*7.8341	2.4390	3.4982	2.6764	0.9901
Poisson Ratio (Dimensionless)	0.4702	0.4908	0.4868	0.4899	*0.4963
Shear Modulus (GPa)	4.9788	7.2477	*7.9365	7.3259	5.8679

*Maximum values

The general observation is that the best results are obtained for long-time treatments (120mins) with low concentration of NaOH (2wt%-6wt %) and short-time treatments (30mins) with high concentration of NaOH (8wt%-10wt %), though low concentration NaOH gave best results overall. This is similar to the observation of Wlodek et al (2012) on treatment of Jute fiber.

4.3.1 Response Surface Model for Tensile Properties of Treated Empty Plantain Bunch Fiber

A general response surface model of the form: $y = c_0 + c_1x_1 + c_2x_2 + c_3x_1x_2 + c_4x_1^2 + c_5x_2^2$, where y represents the response, which in this case are the mechanical properties, x_1 and x_2 represent NaOH concentration and treatment time respectively and c_i are model constants, was fit to the data from Table 4.3 to Table 4.7. The model coefficients obtained and statistical fit results are given in Tables 4.8 to 4.13.

Tables 4.8 to 4.13 reveal that NaOH concentration and treatment time contribute from 38% to 73% of the variability observed in the mechanical properties of the fibers, based on the values of the R^2 . This is not out of place, considering that factors like plant variety, climate, maturity,

harvesting technique, retting degree, size (fiber diameter) and other factors that affect the mechanical properties of natural fibers were not factored into our model.

The R^2 values reveal that NaOH concentration and treatment time contribute to variations in mechanical properties of empty plantain bunch fiber in this order (from the most to the least): tensile strength (73%), yield strength (61%), modulus of elasticity (40%), toughness and percentage reduction in area (39%) and percentage elongation (38%).

The significance of each model coefficient can be judged based on the value of the t-statistics (which must have a magnitude of 2 or more to be significant) or the p-value. The coefficient of NaOH concentration is significant for all mechanical properties, the coefficient of the interaction between NaOH concentration and treatment time is significant for toughness, tensile strength, percentage elongation and percentage reduction in area while the coefficient of NaOH concentration squared is significant for toughness, tensile strength, modulus of elasticity and yield strength. Only for tensile strength did the coefficient of treatment time show some significance. The significant interaction between NaOH concentration and time for most mechanical properties indicate that the variables do not function independently; rather the choice of NaOH Concentration could determine whether or not a mechanical property will increase or reduce with treatment time and vice versa.

In general, a model of the reduced form: $y = c_0 + c_1x_1 + c_2x_1x_2 + c_3x_1^2$ may be used to effectively model the mechanical properties of mercerized empty plantain bunch fiber.

The statistical model based on tensile strength and yield strength are adequate at 95% confidence bound, while the other models are adequate at 90% confidence bound based on the F-statistics.

Table 4.8: Response Surface Model Based on Toughness

Variables	Coefficients	Std. Error	t-stat	P-value	F-stat
Constant	-39.4839	21.8280	-1.8089	0.08632	SSE = 3468.5
NaOH Conc.(wt %)	16.2275	5.3376	3.0402	0.006734	DFE =19
Time (mins)	0.3697	0.35584	1.0389	0.31187	DFR =5
NaOH Conc. * Time	-0.0578	0.022518	-2.5673	0.018855	SSR =2235.5
NaOH Conc.^2	-0.9469	0.40372	-2.3455	0.030009	F =2.4493
Time^2	-6.8642e-5	0.0017943	-0.038256	0.96988	P-val=0.0712
	R ² = 0.3919	Adj.R ² = 0.2319			

Table 4.9: Response Surface Model Based on Tensile Strength

Variables	Coefficients	Std. Error	t-stat	P-value	F-stat
Constant	-793.5894	208.33	-3.8093	0.0011844	SSE = 3.1595e5
NaOH Conc.(wt %)	329.5172	50.944	6.4682	3.3705e-6	DFE =19
Time (mins)	9.2166	3.3963	2.7137	0.013775	DFR =5
NaOH Conc. * Time	-1.0257	0.21492	-4.7723	0.0001324	SSR =8.5164e5
NaOH Conc.^2	-19.4045	3.8532	-5.0359	7.3374e-5	F =10.243
Time^2	-0.0118	0.017125	-0.68955	0.49882	P-val=7.039e-5
	R ² = 0.7294	Adj.R ² = 0.6542			

Table 4.10: Response Surface Model Based on Modulus of Elasticity

Variables	Coefficients	Std. Error	t-stat	P-value	F-stat
Constant	483.30	19145	0.025244	0.98012	SSE = 2.6682e9
NaOH Conc. (wt %)	1.1830e4	4681.6	2.527	0.020538	DFE = 19
Time (mins)	127.1052	312.11	0.40725	0.68838	DFR = 5
NaOH Conc. * Time	0.3483	19.751	0.017636	0.98611	SSR = 1.7697e9
NaOH Conc.^2	-1.0932e3	354.1	-3.0873	0.0060642	F = 2.5203
Time^2	-0.4513	1.5738	-0.28674	0.77741	P-val= 0.065262
	R ² =0.3988	Adj. R ² =0.2405			

Table 4.11: Response Surface Model Based on Yield Strength

Variables	Coefficients	Std. Error	t-stat	P-value	F-stat
Constant	-497.8359	183.76612	-2.70907	0.01391	SSE = 245835.1551
NaOH Conc. (wt %)	233.6400	44.93729	5.1992	5.1044e-5	DFE = 19
Time (mins)	4.1869	2.99582	1.39757	0.17835	DFR = 5
NaOH Conc. * Time	-0.2721	0.18958	-1.43547	0.16741	SSR = 391660.7
NaOH Conc.^2	-16.1247	3.39888	-4.74411	0.00014	F = 6.0541
Time^2	-0.0106	0.01571	-0.70423	0.48983	P-val = 0.0016
	R ² =0.6144	Adj. R ² =0.5129			

Table 4.12: Response Surface Model Based on Ductility (% Elongation)

Variables	Coefficients	Std. Error	t-stat	P-value	F-stat
Constant	-1.4160	3.1233	-0.45336	0.65542	SSE = 71.015
NaOH Conc. (wt %)	1.8808	0.76377	2.4626	0.023521	DFE = 19
Time (mins)	0.0279	0.050918	0.54738	0.59049	DFR = 5
NaOH Conc. * Time	-0.0089	0.0032222	-2.7569	0.012545	SSR = 43.367
NaOH Conc.^2	-0.0951	0.057768	-1.646	0.1162	F = 2.3206
Time^2	9.1270e-5	0.00025675	0.35548	0.72614	P-val = 0.083484
	R ² = 0.3791	Adj. R ² = 0.2158			

Table 4.13: Response Surface Model Based on Ductility (% Reduction in Area)

Variables	Coefficients	Std. Error	t-stat	P-value	F-stat
Constant	-1.1914	2.8441	-0.41891	0.67998	SSE = 58.884
NaOH Conc. (wt %)	1.7325	0.69548	2.4911	0.02215	DFE = 19
Time (mins)	0.0263	0.046365	0.56719	0.57723	DFR = 5
NaOH Conc. * Time	-0.0081	0.0029341	-2.7651	0.012324	SSR = 36.492
NaOH Conc.^2	-0.0882	0.052603	-1.6770	0.10992	F = 2.355
Time^2	7.8218e-5	0.00023379	0.33456	0.74162	P-val = 0.079997
	R ² = 0.3826	Adj. R ² = 0.2201			

The response surface models were optimized using a MATLAB 7.9 code and the optimum NaOH concentrations and time obtained are presented in Table 4.14. It can be observed from Table 4.14 that NaOH concentrations of approximately 4-6wt% give the best results for times of approximately 120-150mins, for the major mechanical properties.

Table 4.14: Optimum NaOH Concentration and Time predicted with Response Surface Models

	Toughness	Tensile Strength	Young Modulus	Yield Strength	%El	%RA
NaOH Conc. (wt %)	3.9907	4.5263	5.4335	6.2559	8.4848	8.4439
Time (mins)	150	150	142.9179	117.2018	30	30

4.3.2 Surface Plot Study for Tensile Properties of Treated Empty Plantain Bunch Fiber

The response surface models were used to obtain the surface plot and study the interaction of the variables (NaOH concentration and time) with respect to all mechanical properties studied and the results are presented in Figures 4.4 to 4.9. It can be observed from the surface plots that there is a significant linear relationship between time and all the mechanical properties, while a quadratic relationship exists for NaOH concentration, indicating the existence of an optimum concentration. The nature of the contour lines - not being parallel one to another - except for yield strength and young's modulus, reveal a high level of interaction between the two variables for these mechanical properties. This corroborates the numerical values obtained from the response surface models.

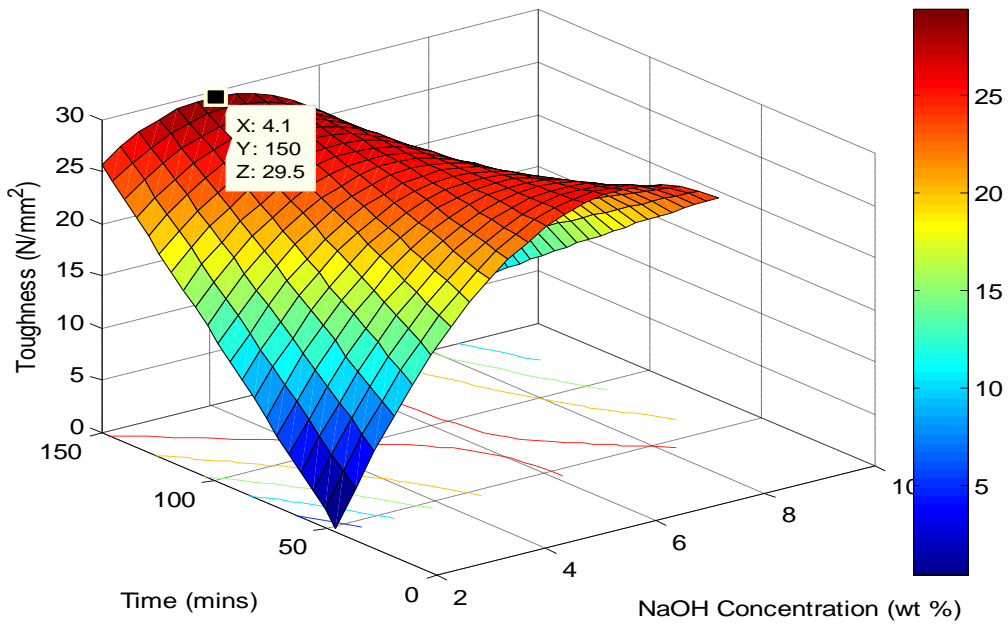


Figure 4.4: Surface plot of NaOH conc. and time interaction on Toughness

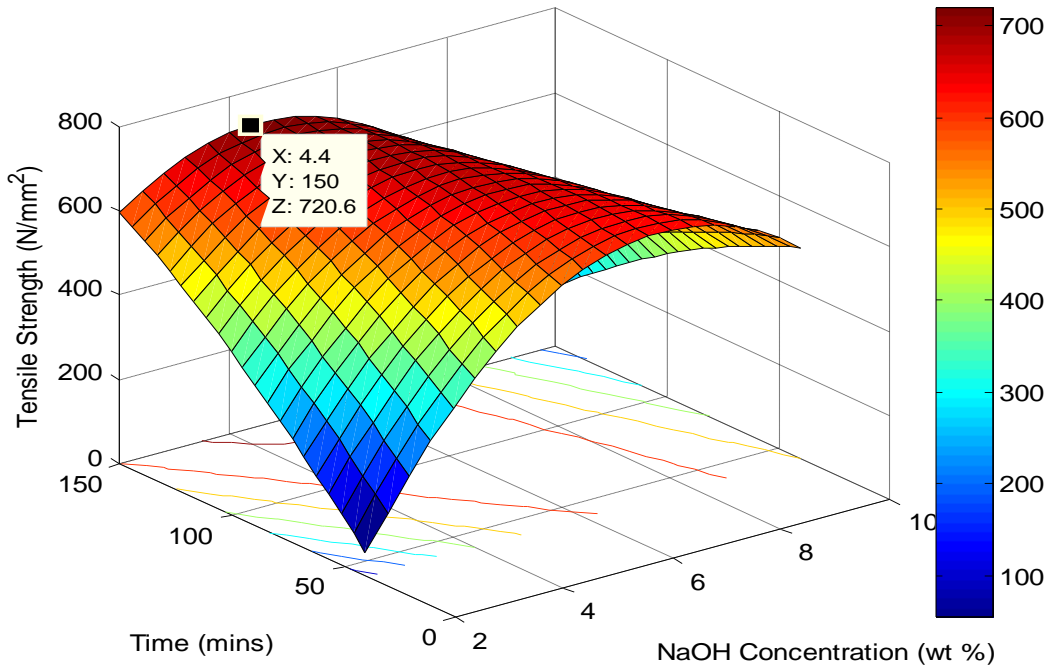


Figure 4.5: Surface plot of NaOH conc. and time interaction on Tensile Strength

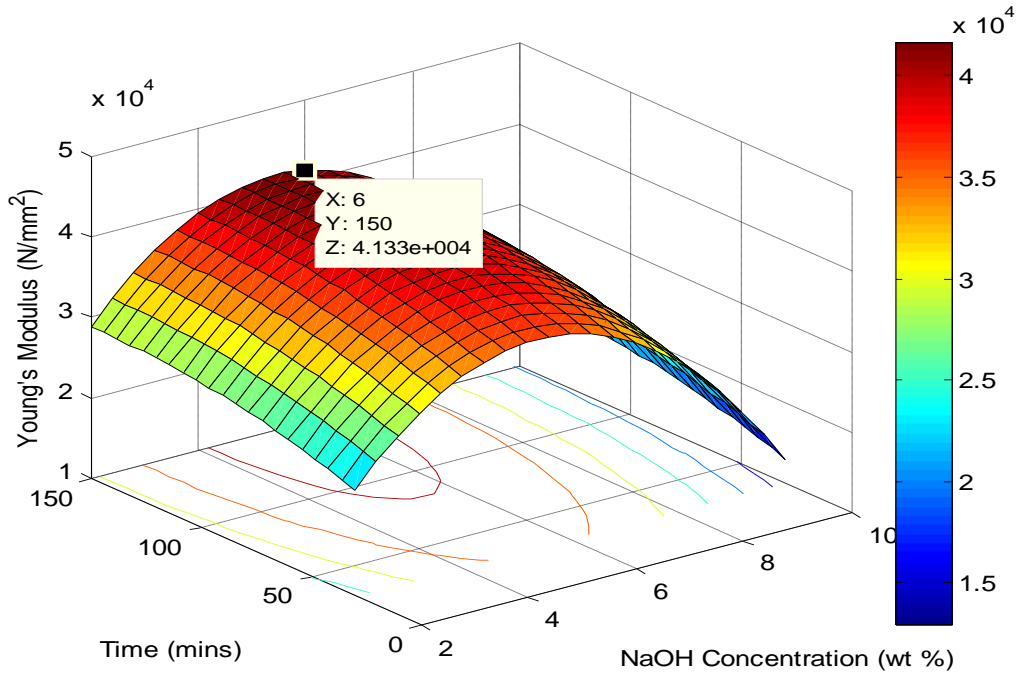


Figure 4.6: Surface plot of NaOH conc. and time interaction on Modulus of Elasticity

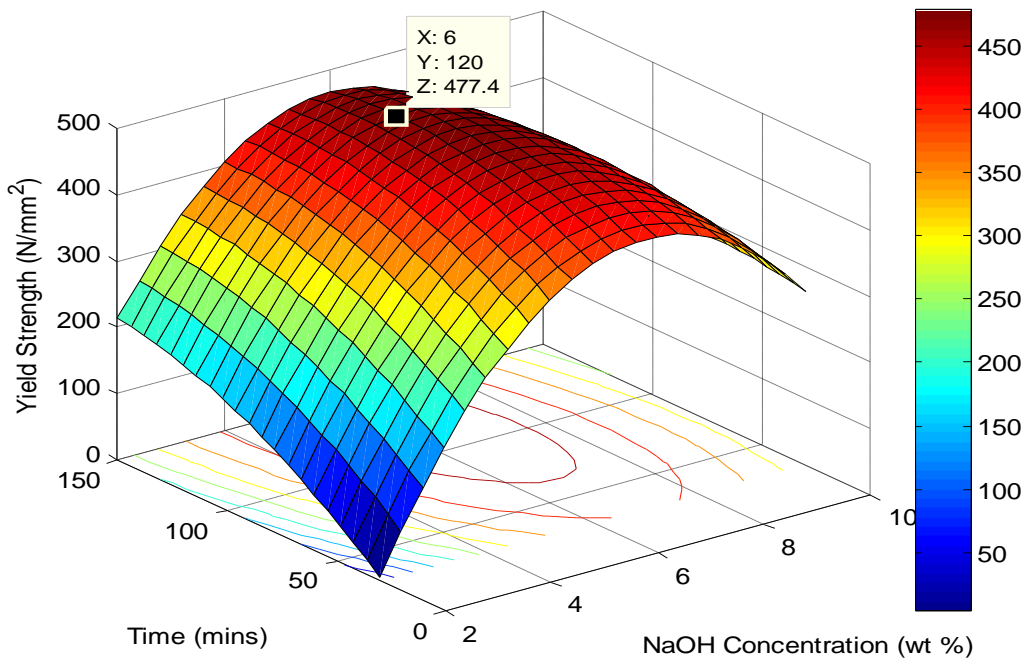


Figure 4.7: Surface plot of Effect of NaOH Conc. and Time interaction on Yield Strength

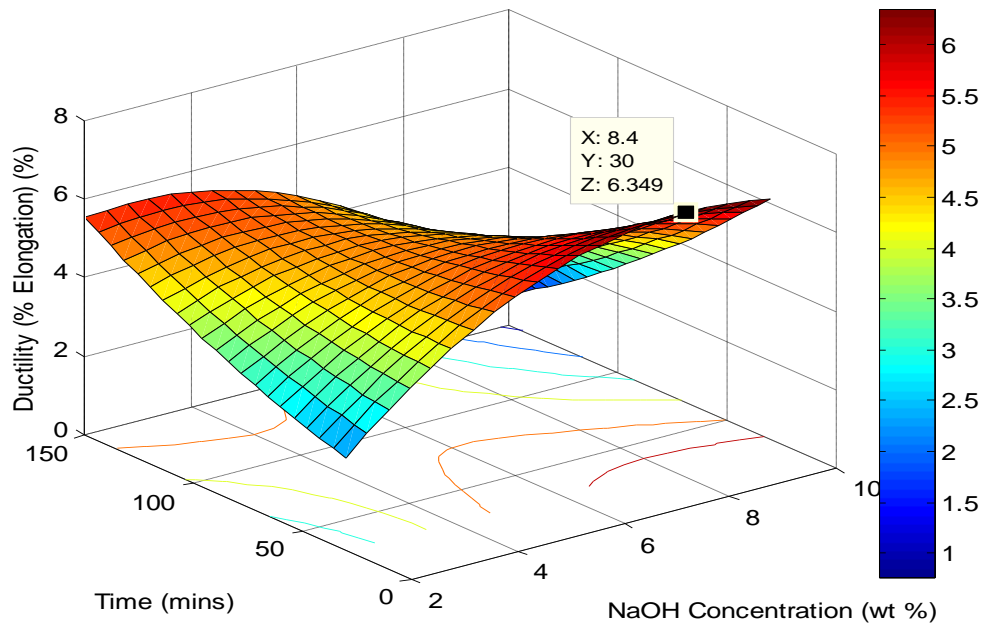


Figure 4.8: Surface plot of NaOH conc. and time interaction on Percentage Elongation

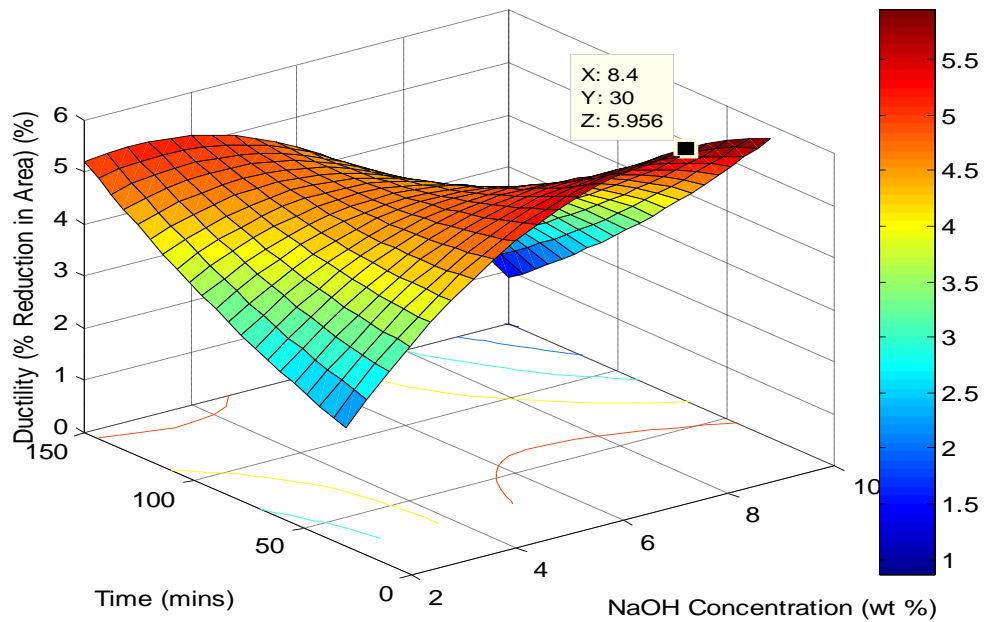


Figure 4.9: Surface plot of NaOH conc. and time interaction on %Reduction in Area

4.3.3 Analysis of Variance Study for Tensile Properties of Treated Empty Plantain Bunch Fiber

Data from Tables 4.3 to 4.7 were used for analysis of variance study using MATLAB 7.9 software. Tables 4.15 to 4.20 show results from analysis of variance study on the contributions of varying NaOH concentration and time on the observed improvement and variation in mechanical properties of empty plantain bunch fiber. The Tables reveal that NaOH concentration has significant effect on the observed changes in fiber toughness and ductility at 90% confidence, it also has significant effect on observed changes in fiber tensile strength, modulus of elasticity and yield strength at 95% confidence, while the contribution of time is not significant for all mechanical properties of empty plantain bunch fiber studied.

The above observation explains why several authors studied the mechanical properties of some natural fibers as functions of NaOH concentration alone, while keeping time constant (Sreekala et al, 2000; Mishra et al, 2003; Edeerozey et al, 2007; Paul et al, 2008; John et al, 2008; Hai et al, 2009).

Table 4.15: ANOVA for Empty Plantain Bunch Fiber Based on Tensile Strength

Source	Sum Sq.	Df	Mean Sq.	F	Prob>F
NaOH Concentration (wt %)	497057.4	4	124264.4	3.31	0.0372
Time (mins)	68657	4	17414.3	0.46	0.7614
Error	600875.8	16	37554.7		
Total	1167590.2	24			

Table 4.16: ANOVA for Empty Plantain Bunch Fiber Based on Toughness

Source	Sum Sq.	Df	Mean Sq.	F	Prob>F
NaOH Concentration (wt %)	2004.7	4	501.175	2.57	0.0776
Time (mins)	584.39	4	146.099	0.75	0.5720
Error	3114.81	16	194.676		
Total	5703.9	24			

Table 4.17: ANOVA for Empty Plantain Bunch Fiber Based on Modulus of Elasticity

Source	Sum Sq.	Df	Mean Sq.	F	Prob>F
NaOH Concentration (wt %)	2.08409e9	4	5.21022e8	4.23	0.0159
Time (mins)	3.83072e9	4	9.57681e7	0.78	0.5558
Error	1.97073e9	16	1.23171e8		
Total	4.43789e9	24			

Table 4.18: ANOVA for Empty Plantain Bunch Fiber Based on Yield strength

Source	Sum Sq.	Df	Mean Sq.	F	Prob>F
NaOH Concentration (wt %)	395578.4	4	98894.6	8.87	0.0006
Time (mins)	63431.1	4	15857.8	1.42	0.2720
Error	178486.3	16	11155.4		
Total	637495.8	24			

Table 4.19: ANOVA for Empty Plantain Bunch Fiber Based on Ductility (%El)

Source	Sum Sq.	Df	Mean Sq.	F	Prob>F
NaOH Concentration (wt %)	36.542	4	9.13562	2.39	0.0939
Time (mins)	16.744	4	4.18594	1.10	0.3919
Error	61.096	16	3.81852		
Total	114.383	24			

Table 4.20: ANOVA for Empty Plantain Bunch Fiber Based on Ductility (%RA)

Source	Sum Sq.	Df	Mean Sq.	F	Prob>F
NaOH Concentration (wt %)	30.6889	4	7.67222	2.41	0.0918
Time (mins)	13.8213	4	3.45534	1.09	0.3960
Error	50.8652	16	3.17908		
Total	95.3754	24			

4.4 Mechanical Properties of Empty Palm Bunch Fibers

This section presents and discusses the mechanical properties of empty palm bunch fiber. These results were obtained from stress-strain analysis from the plots given in Appendix 7.2. Table 4.21 shows the mechanical properties of untreated empty palm bunch fiber. The tensile strength of empty palm bunch fiber is less than that of empty plantain bunch fiber, this could be due to its lower cellulose content, but its yield strength and modulus are higher than that of empty plantain bunch fiber.

Table 4.21: Mechanical Properties of Untreated Empty Palm Bunch Fiber

Toughness (MPa)	%El (%RA) (%)	Tensile Strength (MPa)	Yield Strength (MPa)	Young Modulus (GPa)	Poisson Ratio	Shear Modulus (GPa)
2.3699	15.12 (13.14)	36.1078	26.5766	1.8909	0.4496	0.6522

Table 4.22 shows the mechanical properties of empty palm bunch fiber treated with 2wt% NaOH. The mechanical properties were obtained using the traditional approach and maximum values of the properties are highlighted. It can be observed from Tables 4.21 and 4.22, that empty palm bunch fiber treated with 2wt % NaOH had its toughness increased by 14% relative to the untreated sample, the tensile strength of the treated sample was more than 2.3 times the untreated one, yield strength was 2.7 times the untreated, modulus of elasticity and shear modulus increased more than 3.5 times, while there was no significant improvement in ductility (percentage elongation and reduction in area). Eighty percent of the mechanical properties had their maximum values after the fiber had been treated at this concentration for 120 minutes.

Table 4.22: Mechanical Properties of Empty Palm Bunch Fiber Treated with 2 wt% NaOH

Time (mins)	30	60	90	120	150
Variables (Units)					
Toughness (MPa)	2.0761	0.7917	2.2744	*2.7092	1.5499
Tensile Strength (MPa)	43.3645	49.7159	55.0786	*85.1043	36.4263
Modulus of Elasticity (GPa)	3.2450	7.1210	3.3660	*9.0780	8.3260
Yield Strength (MPa)	32.7285	34.9675	42.8189	*72.0920	23.2409
Percentage Elongation (%)	*5.7500	2.1250	5.0000	3.7500	5.0000
Percentage Reduction in Area (%)	*5.4374	2.0808	4.7619	3.6145	4.7619
Poisson Ratio (Dimensionless)	0.4794	*0.4922	0.4820	0.4864	0.4820
Shear Modulus (GPa)	1.0967	2.3861	1.1356	*3.0537	2.8090

*Maximum values

Table 4.23 shows the mechanical properties of empty palm bunch fiber treated with 4wt% NaOH. The mechanical properties were obtained using the traditional approach and maximum values of the properties are highlighted. It can be observed from Tables 4.21 and 4.23, that empty palm bunch fiber treated with 4wt % NaOH had its toughness increased more than 5 times relative to the untreated sample, the tensile strength of the treated sample was more than 3.5 times the untreated one, yield strength was increased nearly 5 times, modulus of elasticity and shear modulus increased more than 6.5times, while there was no significant improvement in ductility (percentage elongation and reduction in area). Treatment at this concentration resulted in increase in all mechanical properties in comparison with that of 2 wt % NaOH. Forty percent of the mechanical properties had their maximum values after the fiber had been treated at this concentration for 60 minutes and another forty percent after treatment for 90 minutes.

Table 4.23: Mechanical Properties of Empty Palm Bunch Fiber Treated with 4 wt% NaOH

Time (mins)	30	60	90	120	150
Variables (Units)					
Toughness (MPa)	0.6843	*14.3601	2.5243	6.8328	3.0796
Tensile Strength (MPa)	50.5294	140.8620	*169.8607	137.5546	85.8809
Modulus of Elasticity (GPa)	5.8290	5.2700	12.8400	3.1810	*14.6800
Yield Strength (MPa)	32.4204	51.5168	*157.1335	82.5811	71.6270
Percentage Elongation (%)	2.0000	*15.5750	2.1875	8.0000	4.1250
Percentage Reduction in Area (%)	1.9608	*13.4761	2.1407	7.4074	3.9616
Poisson Ratio (Dimensionless)	*0.4926	0.4483	0.4919	0.4719	0.4850
Shear Modulus (GPa)	1.9526	1.8194	4.3032	1.0806	*4.9428

*Maximum values

Table 4.24 shows the mechanical properties of empty palm bunch fiber treated with 6wt% NaOH. The mechanical properties were obtained using the traditional approach and maximum values of the properties are highlighted. It can be observed from Tables 4.21 and 4.24, that empty palm bunch fiber treated with 6wt % NaOH had its toughness increased by about 19% relative to the untreated sample, the tensile strength of the treated sample was more than six times the untreated one, yield strength was increased approximately seven times, modulus of elasticity and shear modulus increased more than eleven times, while there was no significant improvement in ductility (percentage elongation and reduction in area). Treatment at this concentration resulted in increase in all mechanical properties in comparison with that of 4 wt %, except for toughness and ductility. Forty percent of the mechanical properties had their maximum values after the fiber had been treated at this concentration for 60 minutes and another forty percent after treatment for 90 minutes.

Table 4.24: Mechanical Properties of Empty Palm Bunch Fiber Treated with 6 wt% NaOH

Time (mins) Variables (Units)	30	60	90	120	150
Toughness (MPa)	0.9421	*2.8331	2.1540	1.0595	0.6943
Tensile Strength (MPa)	56.7366	151.2424	*221.6477	42.3879	39.5472
Modulus of Elasticity (GPa)	6.3020	*23.3800	16.5100	4.5150	7.7410
Yield Strength (MPa)	41.4708	119.0245	*216.3740	25.6929	31.0433
Percentage Elongation (%)	2.2500	2.3250	1.7000	*3.2500	2.1250
Percentage Reduction in Area (%)	2.2000	2.2700	1.6700	*3.1500	2.0800
Poisson Ratio (Dimensionless)	0.4917	0.4914	*0.4937	0.4881	0.4922
Shear Modulus (GPa)	2.1124	*7.8383	5.5265	1.5170	2.5938

*Maximum values

Table 4.25 shows the mechanical properties of empty palm bunch fiber treated with 8wt% NaOH. The mechanical properties were obtained using the traditional approach and maximum values of the properties are highlighted. It can be observed from Tables 4.21 and 4.25 that empty palm bunch fiber treated with 8wt % NaOH had its toughness increased by more than 1.2 times relative to the untreated sample, the tensile strength of the treated sample was almost six times the untreated one, yield strength was increased more than 3.5 times, modulus of elasticity and shear modulus increased nearly 17 times, while there was no significant improvement in ductility (percentage elongation and reduction in area). Treatment at this concentration resulted in a slight drop in tensile strength and yield strength, while other mechanical properties increased slightly in comparison with that treated with 6 wt % NaOH. All mechanical properties had their maximum values after the fiber had been treated at this concentration for 90 minutes.

Table 4.25: Mechanical Properties of Empty Palm Bunch Fiber Treated with 8 wt% NaOH

Time (mins) Variables (Units)	30	60	90	120	150
Toughness (MPa)	2.1576	1.1098	*5.3847	1.9992	1.1022
Tensile Strength (MPa)	84.1348	98.9586	*211.2172	98.9812	81.4439
Modulus of Elasticity (GPa)	8.4820	10.9000	*34.6600	5.2110	11.7800
Yield Strength (MPa)	65.1417	88.9040	*126.2990	63.9426	57.4827
Percentage Elongation (%)	3.3000	1.6250	*3.3250	3.2500	1.8750
Percentage Reduction in Area (%)	3.1900	1.6000	*3.2200	3.1500	1.8400
Poisson Ratio (Dimensionless)	0.4880	*0.4940	0.4879	0.4881	0.4931
Shear Modulus (GPa)	2.8501	3.6479	*11.6473	1.7509	3.9448

*Maximum values

Table 4.26 shows the mechanical properties of empty palm bunch fiber treated with 10wt% NaOH. The mechanical properties were obtained using the traditional approach and maximum values of the properties are highlighted. It can be observed from Tables 4.21 and 4.26 that empty palm bunch fiber treated with 10wt % NaOH had its toughness increased by 50% relative to the untreated sample, the tensile strength of the treated sample was more than five times the untreated one, yield strength was increased more than two times, modulus of elasticity and shear modulus increased 4.5 times, while there was no significant improvement in ductility (percentage elongation and reduction in area). Treatment at this concentration resulted in a slight drop in all mechanical properties in comparison with that of 8 wt %, except for ductility. Sixty percent of the mechanical properties had their maximum values after the fiber had been treated for 60 minutes at this concentration. Generally, a slight increase in Poisson ratio (9%) and a slight decrease in ductility were observed after treatment.

Table 4.26: Mechanical Properties of Empty Palm Bunch Fiber Treated with 10 wt% NaOH

Time (mins) Variables (Units)	30	60	90	120	150
Toughness (MPa)	1.4199	*3.5656	0.9490	2.4830	0.6604
Tensile Strength (MPa)	97.8939	*184.0318	89.1509	84.4281	76.1398
Modulus of Elasticity (GPa)	6.8400	*10.7900	7.5530	3.2560	6.5260
Yield Strength (MPa)	*86.1386	78.1704	73.4620	62.8273	72.0961
Percentage Elongation (%)	2.2750	3.0250	1.7500	*4.4500	1.5000
Percentage Reduction in Area (%)	2.2200	2.9400	1.7200	*4.2600	1.4800
Poisson Ratio (Dimensionless)	0.4880	*0.4940	0.4879	0.4881	0.4931
Shear Modulus (GPa)	2.2984	*3.6111	2.5381	1.0940	2.1854

*Maximum values

The general observation is that the best results are obtained for long-time treatments (90-120mins) with low concentration of NaOH (2wt%-8wt %) and short-time treatments (60mins) with high concentration of NaOH (10wt %), though low concentration NaOH gave best results overall. This is similar to the observation of Wlodek et al (2012) on treatment of Jute fiber.

4.4.1 Response Surface Model for Tensile Properties of Treated Empty Palm bunch Fiber

A general response surface model of the form: $y = c_0 + c_1x_1 + c_2x_2 + c_3x_1x_2 + c_4x_1^2 + c_5x_2^2$, where y represents the response, which in this case are the mechanical properties, x_1 and x_2 represent NaOH concentration and treatment time respectively and c_i are model constants, was fit to the data from Tables 4.22 to 4.26. The model coefficients obtained and statistical fit results are given in Tables 4.27 to 4.32. It can be observed from Tables 4.27 to 4.32 that NaOH concentration and treatment time contribute from 14% to 51% of the variability observed in the mechanical properties of the fibers, based on the values of the R^2 . This is not out of place, considering that factors like plant variety, climate, maturity, harvesting technique, retting degree, size (fiber diameter) and other factors that affect the mechanical properties of natural fibers were not factored into our model. This result reveals that empty plantain bunch fiber responds better to

mercerization treatment (38 - 73%) than empty palm bunch fiber. This is most probably due to the higher hemicelluloses content of empty plantain bunch fiber.

The R^2 values reveal that NaOH concentration and treatment time contribute to variations in mechanical properties of Empty Plantain Bunch Fiber in this order (from the most to the least): tensile strength (51%), yield strength (38%), modulus of elasticity (23%), toughness and percentage reduction in area (15%) and percentage elongation (14%).

The significance of each model coefficient can be judged based on the value of the t-statistics (which must have a magnitude of 2 or more to be significant) or the p-value. The coefficient of NaOH concentration is significant for tensile strength, modulus of elasticity and yield strength at 90% confidence, the coefficients of time and time squared are significant for tensile strength and yield strength at 95% confidence. The coefficients of NaOH concentration squared and the interaction between NaOH concentration and treatment time are not significant. No coefficient of the RSM model was significant for toughness, percentage elongation and percentage reduction in area. The non-significant interaction between NaOH concentration and time for most mechanical properties indicate that the variables do function almost independently.

In general, a model of the reduced form: $y = c_0 + c_1x_1 + c_2x_2 + c_3x_2^2$ may be used to effectively model the mechanical properties of mercerized empty palm bunch fiber.

The statistical model based on tensile strength is adequate at 95% confidence bound, while that of yield strength is significant at 90% confidence bound based on the F-statistics. The statistical models for other mechanical properties are not adequate.

Table 4.27: Response Surface Model Based on Toughness

Variables	Coefficients	Std. Error	t-stat	P-value	F-stat
Constant	-1.7341	4.7757	-0.36311	0.72053	SSE=166.03
NaOH Conc. (wt %)	0.67362	1.1678	0.57682	0.57083	DFE=19
Time (mins)	0.10178	0.077855	1.3073	0.20672	DFR=5
NaOH Conc. * Time	-9.0302e-4	0.0049268	-0.18329	0.85651	SSR=29.46
NaOH Conc.^2	-0.063008	0.08833	-0.71332	0.48432	F=67426
Time^2	-5.6483e-4	0.00039258	-1.4388	0.16649	P-val =0.64801
	$R^2=0.1507$	Adj. $R^2=$ -0.0728			

Table 4.28: Response Surface Model Based on Tensile Strength

Variables	Coefficients	Std. Error	t-stat	P-value	F-stat
Constant	-140.2432	68.855	-2.0368	0.05585	SSE=34513
NaOH Conc. (wt %)	36.0216	16.838	2.1394	0.045603	DFE=19
Time (mins)	3.8753	1.1225	3.4524	0.0026684	DFR=5
NaOH Conc. * Time	-0.0670	0.071034	-0.94322	0.35741	SSR=35313
NaOH Conc.^2	-2.0710	1.2735	-1.6262	0.12038	F=3.888
Time^2	-0.020047	0.0056601	-3.5419	0.0021781	P-val =0.013511
	$R^2 = 0.5057$	Adj. $R^2 =$ 0.3757			

Table 4.29: Response Surface Model Based on Modulus of Elasticity

Variables	Coefficients	Std. Error	t-stat	P-value	F-stat
Constant	-15.0202	11.26	-1.334	0.19798	SSE=922.9
NaOH Conc. (wt %)	5.3777	2.7534	1.9531	0.065692	DFE=19
Time (mins)	0.2670	0.18356	1.4546	0.16211	DFR=5
NaOH Conc. * Time	-0.0092113	0.011616	-0.793	0.43757	SSR=270.3
NaOH Conc.^2	-0.34831	0.20825	-1.6725	0.11081	F=1.1129
Time^2	-0.0011597	0.00092557	-1.2529	0.22544	P-val =0.38653
	$R^2 = 0.2265$	Adj. $R^2 =$ 0.0230			

Table 4.30: Response Surface Model Based on Yield Strength

Variables	Coefficients	Std. Error	t-stat	P-value	F-stat
Constant	-107.6181	63.28	-1.7007	0.10532	SSE=29151
NaOH Conc. (wt %)	29.2316	15.474	1.889	0.074247	DFE=19
Time (mins)	2.7550	1.0316	2.6705	0.015119	DFR=5
NaOH Conc. * Time	-0.045485	0.065282	-0.69675	0.4944	SSR=18025
NaOH Conc.^2	-1.8113	1.1704	-1.5476	0.13821	F=2.3496
Time^2	-0.014049	0.0052018	-2.7009	0.014163	P-val =0.080527
	$R^2 = 0.3821$	Adj. $R^2 = 0.2195$			

Table 4.31: Response Surface Model Based on Ductility (% Elongation)

Variables	Coefficients	Std. Error	t-stat	P-value	F-stat
Constant	4.7625	4.9214	0.96771	0.34535	SSE=176.32
NaOH Conc. (wt %)	-0.411109	1.2035	-0.34159	0.73641	DFE=19
Time (mins)	0.038388	0.08023	0.47847	0.63777	DFR=5
NaOH Conc. * Time	2.6667e-4	0.0050771	0.052523	0.95866	SSR=29.083
NaOH Conc.^2	0.0024554	0.091025	0.026975	0.97876	F=0.62681
Time^2	-2.3651e-4	0.00040455	-0.58461	0.56569	P-val =0.68142
	$R^2 = 0.1416$	Adj. $R^2 = -0.0843$			

Table 4.32: Response Surface Model Based on Ductility (% Reduction in Area)

Variables	Coefficients	Std. Error	t-stat	P-value	F-stat
Constant	4.4746	4.2306	1.0577	0.30346	SSE=130.29
NaOH Conc. (wt %)	-0.40366	1.0345	-0.39019	0.70074	DFE=19
Time (mins)	0.034381	0.068968	0.49851	0.62385	DFR=5
NaOH Conc. * Time	3.8617e-5	0.0043644	0.008848	0.99303	SSR=22.994
NaOH Conc.^2	0.0067	0.078248	0.085187	0.933	F=0.67063
Time^2	-2.0176e-4	0.00034777	-0.58015	0.56863	P-val =0.65054
	$R^2 = 0.1500$	Adj. $R^2 = -0.0737$			

The response surface models were optimized using a MATLAB 7.9 code and the optimum NaOH concentrations and time obtained are presented in Table 4.33. It can be observed from Table 4.33 that NaOH concentrations of approximately 5-7wt% give the best results for times of approximately 80-90mins, for the major mechanical properties.

Table 4.33: Optimum NaOH concentration and time predicted with response surface model

	Toughness	Tensile Strength	Young Modulus	Yield Strength	%El	%RA
NaOH Conc.(wt %)	4.7263	7.3314	6.5411	6.9800	2	2
Time (mins)	86.3195	84.4037	89.1388	86.7504	82.2827	85.3941

4.4.2 Surface Plot Study for Tensile Properties of Treated Empty Palm Bunch Fiber

The response surface models were used to obtain the surface plot and study the interaction of the variables (NaOH concentration and time) with respect to all mechanical properties studied and the results are presented in Figures 4.10 to 4.15. It can be observed from Figures 4.10 to 4.15 that NaOH concentration and time have a significant quadratic relationship with most of the mechanical properties, indicating the existence of a global optimum NaOH concentration and time, except for ductility (percentage elongation and percentage reduction in area), which relates linearly with NaOH concentration. The nature of the contour lines, which are parallel one to another for all mechanical properties, reveal that there is no significant interaction between the two variables (NaOH concentration and treatment time) for all mechanical properties. This corroborates the numerical values obtained from the response surface models.

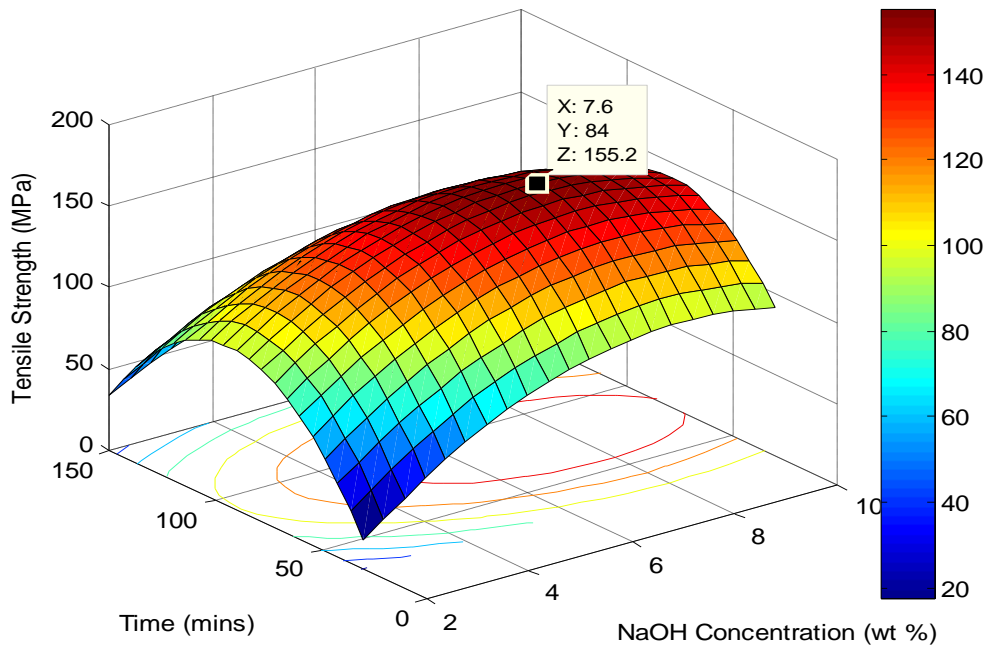


Figure 4.10: Surface plot of NaOH conc. and time interaction on Tensile Strength

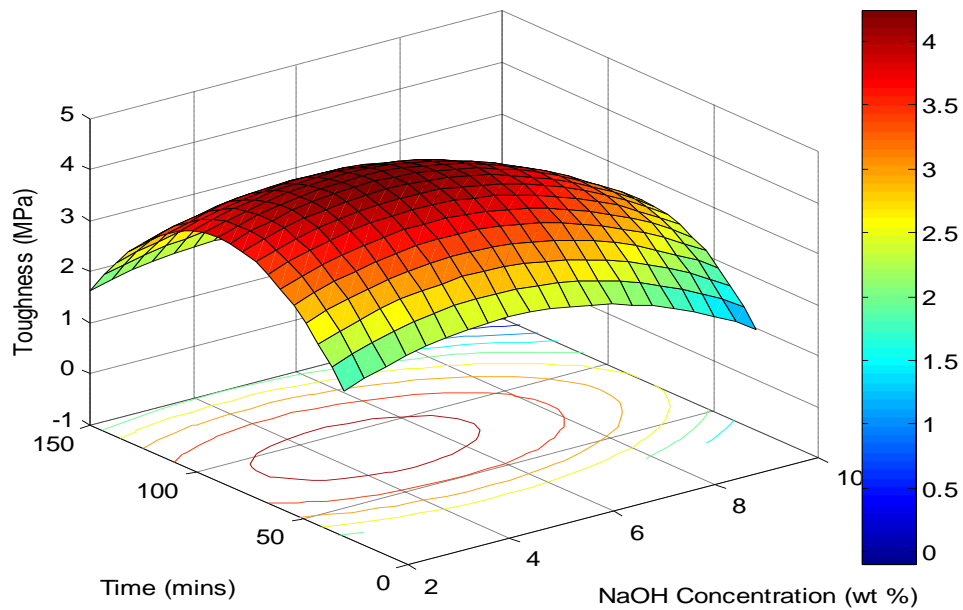


Figure 4.11: Surface plot of NaOH conc. and time interaction on Toughness

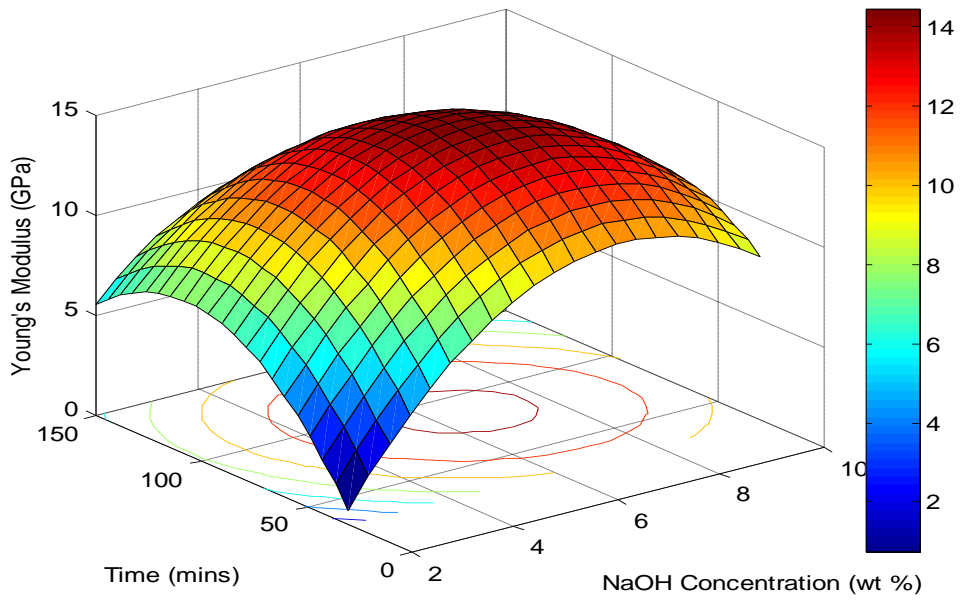


Figure 4.12: Surface Plot of NaOH conc. and time interaction on Young's Modulus

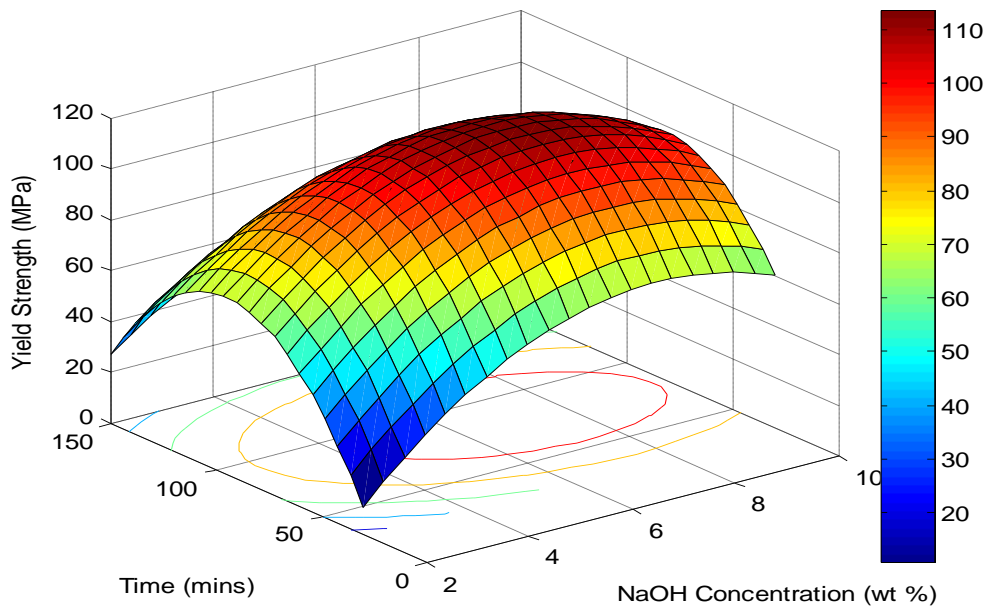


Figure 4.13: Surface plot of NaOH conc. and time interaction on Yield Strength

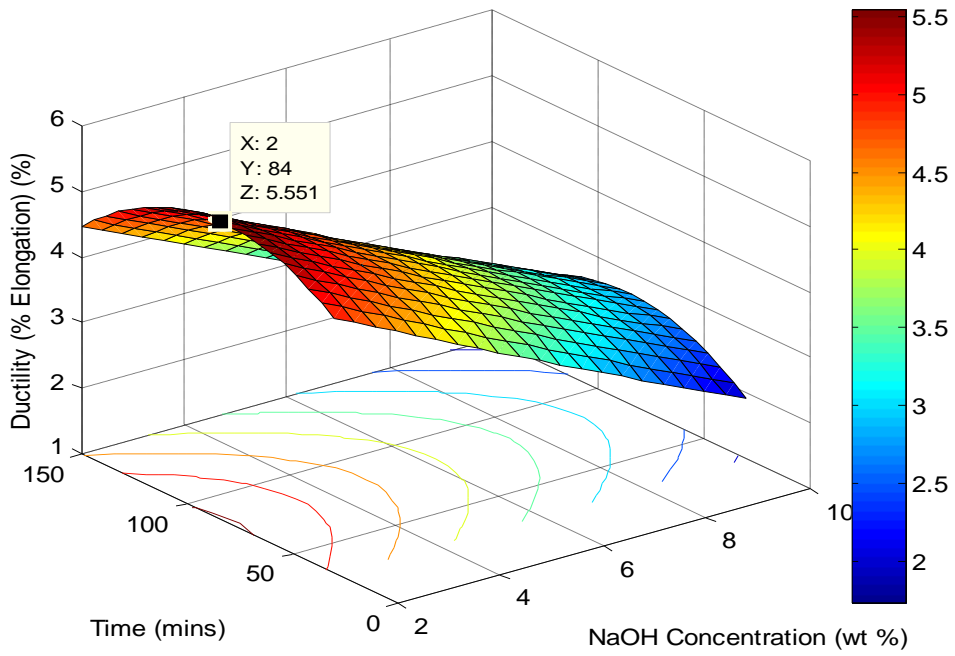


Figure 4.14: Surface plot of NaOH conc. and time interaction on %Elongation

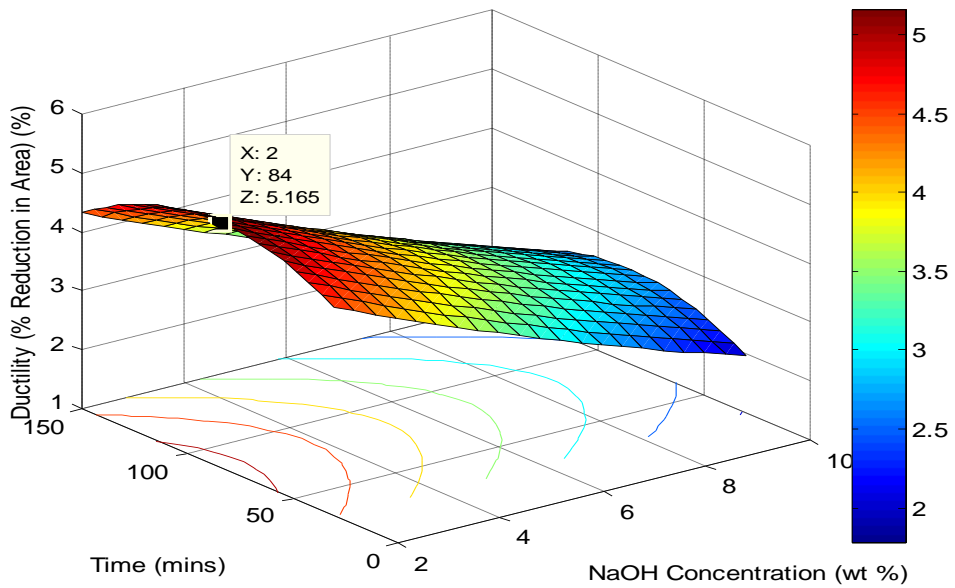


Figure 4.15: Surface plot of NaOH conc. and time interaction on %Reduction in Area

4.4.3 Analysis of Variance Study for Tensile Properties of Treated Empty Palm Bunch Fiber

Data from Tables 4.22 to 4.26 were used for analysis of variance study using MATLAB 7.9 software. Tables 4.34 to 4.39 show results from analysis of variance study on the contributions of varying NaOH concentration and time on the observed improvement and variation in mechanical properties of empty palm bunch fiber. It can be observed from the results of Tables 4.34 to 4.39 that time has significant effect on the observed changes in fiber tensile strength and yield strength at 95% confidence, while the contribution of NaOH concentration is not significant for all mechanical properties of empty palm bunch fiber studied, though it plays more role in improvement of toughness and ductility than time does. Based on the above observation it will be wrong to study the mechanical properties of empty palm bunch fiber as a function of NaOH concentration alone, while keeping time constant, as some authors do with certain fibers. It will be more appropriate to keep NaOH concentration constant and vary time in the study of the mercerization of empty palm bunch fiber as observed in some studies (Ray et al, 2001).

Table 4.34: ANOVA for Empty Palm Bunch Fiber Based on Tensile Strength

Source	Sum Sq.	Df	Mean Sq.	F	Prob>F
NaOH Concentration (wt %)	13356.4198	4	3339.105	1.8723	0.16456
Time (mins)	27934.7207	4	6983.6802	3.9158	0.021075
Error	28535.0281	16	1783.4393		
Total	69826.1686	24			

Table 4.35: ANOVA for Empty Palm Bunch Fiber Based on Toughness

Source	Sum Sq.	Df	Mean Sq.	F	Prob>F
NaOH Concentration (wt %)	53.5657	4	13.3914	1.9685	0.14807
Time (mins)	33.0806	4	8.2701	1.2157	0.34281
Error	108.8433	16	6.8027		
Total	195.4896	24			

Table 4.36: ANOVA for Empty Palm Bunch Fiber Based on Modulus of Elasticity

Source	Sum Sq.	Df	Mean Sq.	F	Prob>F
NaOH Concentration (wt %)	226.2109	4	56.5527	1.4124	0.27478
Time (mins)	326.3502	4	81.5875	2.0377	0.13732
Error	640.6368	16	40.0398		
Total	1193.1979	24			

Table 4.37: ANOVA for Empty Palm Bunch Fiber Based on Yield strength

Source	Sum Sq.	Df	Mean Sq.	F	Prob>F
NaOH Concentration (wt %)	6462.8459	4	1615.7115	1.1368	0.37451
Time (mins)	17972.7083	4	4493.1771	3.1615	0.042926
Error	22739.7141	16	1421.2321		
Total	47175.2683	24			

Table 4.38: ANOVA for Empty Palm Bunch Fiber Based on Ductility (%El)

Source	Sum Sq.	Df	Mean Sq.	F	Prob>F
NaOH Concentration (wt %)	58.4487	4	14.6122	1.8409	0.17036
Time (mins)	58.4487	4	4.9873	0.62831	0.64926
Error	127.0015	16	7.9376		
Total	205.3994	24			

Table 4.39: ANOVA for Empty Palm Bunch Fiber Based on Ductility (%RA)

Source	Sum Sq.	Df	Mean Sq.	F	Prob>F
NaOH Concentration (wt %)	44.493	4	11.1232	1.8923	0.16099
Time (mins)	14.7387	4	3.6847	0.62682	0.65024
Error	94.0529	16	5.8783		
Total	153.2846	24			

4.5 Mechanical Properties of Rattan Palm Fiber

This section presents and discusses the mechanical properties of rattan palm fiber. These results were obtained from stress-strain analysis from the plots given in Appendix 7.3. Table 4.40 shows the mechanical properties of untreated rattan palm fiber. The tensile strength of rattan palm fiber is less than that of empty plantain bunch fiber and empty palm bunch fiber, this could be due to its lower cellulose content, but its modulus is in the same range with that of empty plantain bunch fiber.

Table 4.40: Mechanical Properties of Untreated Rattan Palm Fiber

Toughness (MPa)	%El (%RA) (%)	Tensile Strength (MPa)	Yield Strength (MPa)	Young Modulus (GPa)	Poisson Ratio	Shear Modulus (GPa)
0.1757	2.85 (2.77)	3.7506	3.7506	1.2402	0.4896	0.4163

Table 4.41 shows the mechanical properties of rattan palm fiber treated with 2wt% NaOH. The mechanical properties were obtained using the traditional approach and maximum values of the properties are highlighted. It can be observed from Tables 4.40 and 4.41, that rattan palm fiber treated with 2wt % NaOH had its toughness increased nearly thirteen times relative to the untreated sample, the tensile strength of the treated sample was more than sixteen times the untreated one, yield strength was increased almost ten times, modulus of elasticity and shear modulus increased nine times, while ductility (percentage elongation and reduction in area) increased by 60%. All the mechanical properties had their maximum values after the fiber had been treated at this concentration for 120 minutes.

Table 4.41: Mechanical Properties of Rattan Palm Fiber Treated with 2 wt% NaOH

Time (mins) Variables (Units)	30	60	90	120	150
Toughness (MPa)	0.1484	0.1649	0.2488	*2.4336	0.3319
Tensile Strength (MPa)	9.4291	12.6120	19.1756	*60.7914	36.5405
Modulus of Elasticity (GPa)	1.0790	1.2270	7.7420	*12.8300	11.5500
Yield Strength (MPa)	4.8984	7.7092	17.3321	*40.3797	24.6398
Percentage Elongation (%)	2.5000	2.0500	1.5000	*4.6250	1.2500
Percentage Reduction in Area (%)	2.4400	2.0100	1.4800	*4.4200	1.2300
Poisson Ratio (Dimensionless)	0.4908	0.4924	0.4944	0.4833	*0.4954
Shear Modulus (GPa)	0.3619	0.4111	2.5903	*4.3248	3.8618

*Maximum values

Table 4.42 shows the mechanical properties of rattan palm fiber treated with 4wt% NaOH. The mechanical properties were obtained using the traditional approach and maximum values of the properties are highlighted. It can be observed from Tables 4.40 and 4.42 that rattan palm fiber treated with 4wt % NaOH had its toughness increased more than twenty-five times relative to the untreated sample, the tensile strength of the treated sample was more than twenty-five times the untreated one, yield strength was increased more than three times, modulus of elasticity and shear modulus increased more than three times, while ductility (percentage elongation and reduction in area) increased by 120%.

Treatment at this concentration resulted in increase in all mechanical properties in comparison with that of 2 wt % NaOH, except for modulus of elasticity and shear modulus. Eighty percent of the mechanical properties had their maximum values after the fiber had been treated at this concentration for 120 minutes.

Table 4.42: Mechanical Properties of Rattan Palm Fiber Treated with 4 wt% NaOH

Time (mins) Variables (Units)	30	60	90	120	150
Toughness (MPa)	0.5959	1.3584	2.0742	*4.6102	1.6673
Tensile Strength (MPa)	16.4274	40.9197	72.9939	*96.4275	45.9959
Modulus of Elasticity (GPa)	1.5180	1.5750	*5.1340	3.4110	1.2480
Yield Strength (MPa)	9.5555	15.7245	43.8901	*60.6704	14.5682
Percentage Elongation (%)	4.7500	5.8750	4.2500	*6.5000	6.3750
Percentage Reduction in Area (%)	4.5300	5.5500	4.0800	*6.1000	5.9900
Poisson Ratio (Dimensionless)	0.4829	0.4790	*0.4846	0.4769	0.4773
Shear Modulus (GPa)	0.5118	0.5325	*1.7291	1.1548	0.4224

*Maximum values

Table 4.43 shows the mechanical properties of rattan palm fiber treated with 6wt% NaOH. The mechanical properties were obtained using the traditional approach and maximum values of the properties are highlighted. It can be observed from Tables 4.40 and 4.43 that rattan palm fiber treated with 6wt % NaOH had its toughness increased about fifteen times relative to the untreated sample, the tensile strength of the treated sample was more than twenty-three times the untreated one, yield strength was increased about six times, modulus of elasticity and shear modulus increased more than 2.5 times, while ductility (percentage elongation and reduction in area) increased by 180%. Treatment at this concentration resulted in decrease in most mechanical properties in comparison with that of 4 wt %. Forty percent of the mechanical properties had their maximum values after the fiber had been treated at this concentration for 60 minutes and another forty percent after treatment for 90minutes.

Table 4.43: Mechanical Properties of Rattan Palm Fiber Treated with 6 wt% NaOH

Time (mins) Variables (Units)	30	60	90	120	150
Toughness (MPa)	0.2747	*2.8925	2.8924	1.0683	0.1453
Tensile Strength (MPa)	25.3175	56.7078	*88.4611	24.7215	15.8163
Modulus of Elasticity (GPa)	2.6520	2.5140	3.9420	*4.7970	1.6070
Yield Strength (MPa)	22.0831	17.0391	*27.1237	13.9210	14.5614
Percentage Elongation (%)	1.6250	*8.2500	5.8000	5.0000	1.4500
Percentage Reduction in Area (%)	1.6000	*7.6200	5.4800	4.7600	1.4300
Poisson Ratio (Dimensionless)	0.4940	0.4710	0.4793	0.4820	*0.4946
Shear Modulus (GPa)	0.8876	0.8545	1.3324	*1.6184	0.5376

*Maximum values

Table 4.44 shows the mechanical properties of rattan palm fiber treated with 8wt% NaOH. The mechanical properties were obtained using the traditional approach and maximum values of the properties are highlighted. It can be observed from Tables 4.40 and 4.44 that rattan palm fiber treated with 8wt % NaOH had its toughness increased about twenty-six times relative to the untreated sample, the tensile strength of the treated sample was more than eighteen times the untreated one, yield strength was increased about 2.5 times, modulus of elasticity and shear modulus increased more than 100%, while ductility (percentage elongation and reduction in area) increased by nearly 300%. Treatment at this concentration resulted in decrease all mechanical properties, except toughness and percentage elongation, in comparison with that treated with 6 wt % NaOH. All mechanical properties had their maximum values after the fiber had been treated at this concentration for 30 minutes.

Table 4.44: Mechanical Properties of Rattan Palm Fiber Treated with 8 wt% NaOH

Time (mins) Variables (Units)	30	60	90	120	150
Toughness (MPa)	*4.7781	0.1220	0.1832	0.1072	0.2210
Tensile Strength (MPa)	*68.6536	13.4102	13.1627	7.9880	7.5725
Modulus of Elasticity (GPa)	*2.6590	0.8894	1.0140	1.4630	0.8496
Yield Strength (MPa)	*13.6676	13.4102	11.3163	7.3728	3.6337
Percentage Elongation (%)	*11.2500	1.7000	2.1250	1.6500	3.7500
Percentage Reduction in Area (%)	*10.1100	1.6700	2.0800	1.6200	3.6100
Poisson Ratio (Dimensionless)	0.4614	0.4937	0.4922	*0.4939	0.4864
Shear Modulus (GPa)	*0.9097	0.2977	0.3398	0.4897	0.2858

*Maximum values

Table 4.45 shows the mechanical properties of rattan palm fiber treated with 10wt% NaOH. The mechanical properties were obtained using the traditional approach and maximum values of the properties are highlighted. It can be observed from Tables 4.40 and 4.45 that rattan palm fiber treated with 10wt % NaOH had its toughness increased 3.5 times relative to the untreated sample, the tensile strength of the treated sample was more than six times the untreated one, yield strength was increased more than two times, modulus of elasticity and shear modulus increased by about 40%, while ductility (percentage elongation and reduction in area) increased by 70%. Treatment at this concentration resulted in a slight drop in all mechanical properties in comparison with that of 8 wt %. Sixty percent of the mechanical properties had their maximum values after the fiber had been treated at this concentration for 30 minutes at this concentration.

Generally, a slight increase in Poisson ratio (1%) and increase in ductility were observed after treatment.

Table 4.45: Mechanical Properties of Rattan Palm Fiber Treated with 10 wt% NaOH

Time (mins) Variables (Units)	30	60	90	120	150
Toughness (MPa)	*0.7987	0.4448	0.3747	0.3411	0.2712
Tensile Strength (MPa)	*24.4897	17.2158	16.0657	15.2872	12.4301
Modulus of Elasticity (GPa)	1.4230	1.4090	*1.7810	1.2270	1.1340
Yield Strength (MPa)	11.5612	*12.7215	11.7222	10.2263	7.8279
Percentage Elongation (%)	*4.9375	3.3750	3.0000	3.2500	3.1250
Percentage Reduction in Area (%)	*4.7100	3.2600	2.9100	3.1500	3.0300
Poisson Ratio (Dimensionless)	0.4822	0.4877	*0.4890	0.4881	0.4886
Shear Modulus (GPa)	0.4800	0.4735	*0.5981	0.4123	0.3809

*Maximum values

The general observation is that the best results are obtained for long-time treatments (90-120mins) with low concentration of NaOH (2wt%-6wt %) and short-time treatments (30mins) with high concentration of NaOH (8wt%-10wt %), though low concentration NaOH giving best results overall. This is similar to the observation of Wlodek et al (2012) on treatment of Jute fiber.

4.5.1 Response Surface Model for Tensile Properties of Treated Empty Palm bunch Fiber

A general response surface model of the form: $y = c_0 + c_1x_1 + c_2x_2 + c_3x_1x_2 + c_4x_1^2 + c_5x_2^2$, where y represents the response, which in this case are the mechanical properties, x_1 and x_2 represent NaOH concentration and treatment time respectively and c_i are model constants, was fit to the data from Tables 4.41 to 4.45. The model coefficients obtained and statistical fit results are given in Tables 4.46 to 4.51.

Tables 4.46 to 4.51 reveal that NaOH concentration and treatment time contribute from 21% to 44% of the variability observed in the mechanical properties of the fibers, based on the values of the R^2 . This is not out of place, considering that factors like plant variety, climate, maturity,

harvesting technique, retting degree, size (fiber diameter) and other factors that affect the mechanical properties of natural fibers were not factored into our model. This result reveals that empty palm bunch fiber responds better to mercerization treatment than rattan palm fiber (21-44%), but less than empty plantain bunch fiber. This observation is in agreement with the order of the hemicelluloses content of the fibers from the most to the least: empty plantain bunch fiber, empty palm bunch fiber and rattan palm fiber.

The R^2 values reveal that NaOH concentration and treatment time contribute to variations in mechanical properties of rattan palm fiber in this order (from the most to the least): yield strength (44%), tensile strength (39%), toughness (26%), modulus of elasticity (23%), percentage elongation (22%) and percentage reduction in area (21%).

The significance of each model coefficient can be judged based on the value of the t-statistics (which must have a magnitude of 2 or more to be significant) or the p-value. The coefficient of NaOH concentration is significant for tensile strength at 95% confidence and for toughness and ductility at 90% confidence; the coefficients of time are significant for tensile strength at 90% confidence and for modulus of elasticity and yield strength at 95% confidence. The coefficients of NaOH concentration squared are significant for tensile strength and for modulus of elasticity at 90% confidence and the coefficients of interaction between NaOH concentration and treatment time are significant for tensile strength, modulus of elasticity and yield strength at 95% confidence, while coefficient of time squared is only significant at 90% confidence for yield strength. The significant interaction between NaOH concentration and time for some mechanical properties indicate that the variables do not function independently.

In general, a model of the reduced form: $y = c_0 + c_1x_1 + c_2x_2 + c_3x_1x_2 + c_4x_2^2$ may be used to effectively model the most mechanical properties of mercerized rattan palm fiber.

The statistical model based on tensile strength is adequate at 90% confidence bound, while that of modulus of elasticity and yield strength is significant at 95% confidence bound based on the F-statistics. The statistical models for other mechanical properties are not adequate.

Table 4.46: Response Surface Model Based on Toughness

Variables	Coefficients	Std. Error	t-stat	P-value	F-stat
Constant	-2.7396	2.1617	-1.2673	0.22035	SSE=34.018
NaOH Conc. (wt %)	1.0814	0.52862	2.0457	0.054879	DFE=19
Time (mins)	0.038146	0.035241	1.0824	0.29261	DFR=5
NaOH Conc. * Time	-0.0036854	0.0022301	-1.6526	0.11485	SSR=12.136
NaOH Conc.^2	-0.068385	0.039983	-1.7104	0.10348	F=1.3556
Time^2	-1.0515e-4	0.0001777	-0.59174	0.561	P-val=0.28451
	$R^2 = 0.2629$	Adj. $R^2 = 0.0690$			

Table 4.47: Response Surface Model Based on Tensile Strength

Variables	Coefficients	Std. Error	t-stat	P-value	F-stat
Constant	-56.6348	37.464	-1.5117	0.14706	SSE=10217
NaOH Conc. (wt %)	20.1285	9.1611	2.1972	0.040613	DFE=19
Time (mins)	1.1944	0.61074	1.9557	0.065369	DFR=5
NaOH Conc. * Time	-0.083188	0.038649	-2.1524	0.04443	SSR=6584
NaOH Conc.^2	-1.2769	0.69291	-1.8428	0.081023	F=2.4487
Time^2	-0.0038167	0.0030796	-1.2394	0.23031	P-val=0.071252
	$R^2 = 0.3919$	Adj. $R^2 = 0.2318$			

Table 4.48: Response Surface Model Based on Modulus of Elasticity

Variables	Coefficients	Std. Error	t-stat	P-value	F-stat
Constant	-0.18822	3.3826	-0.055643	0.95621	SSE=83.292
NaOH Conc. (wt %)	-0.91716	0.82716	-1.1088	0.28135	DFE=19
Time (mins)	0.14576	0.055144	2.6433	0.016031	DFR=5
NaOH Conc. * Time	-0.011825	0.0034896	-3.3887	0.0030822	SSR=162.71
NaOH Conc.^2	0.11435	0.062563	1.8278	0.083324	F=7.4233
Time^2	-3.0364e-4	0.000278	-1.092	0.28849	P-val =0.00052117
	$R^2 = 0.2265$	Adj. $R^2 =$ 0.0230			

Table 4.49: Response Surface Model Based on Yield Strength

Variables	Coefficients	Std. Error	t-stat	P-value	F-stat
Constant	-23.6586	18.012	-1.3135	0.20467	SSE=2361.9
NaOH Conc. (wt %)	5.5642	4.4046	1.2633	0.22178	DFE=19
Time (mins)	0.77376	0.29364	2.635	0.016316	DFR=5
NaOH Conc. * Time	-0.040884	0.018582	-2.2002	0.040366	SSR=1840
NaOH Conc.^2	-0.30439	0.33315	-0.91367	0.37234	F=2.9604
Time^2	-0.0026659	0.0014807	-1.8005	0.087687	P-val =0.038474
	$R^2 = 0.4379$	Adj. $R^2 = 0.2900$			

Table 4.50: Response Surface Model Based on Ductility (% Elongation)

Variables	Coefficients	Std. Error	t-stat	P-value	F-stat
Constant	-0.22625	3.8991	-0.058026	0.95433	SSE=110.67
NaOH Conc. (wt %)	1.8661	0.95347	1.9572	0.065179	DFE=19
Time (mins)	-0.0040107	0.063564	-0.063097	0.95035	DFR=5
NaOH Conc. * Time	-0.0044292	0.0040225	-1.1011	0.2846	SSR=30.61
NaOH Conc.^2	-0.11875	0.072116	-1.6466	0.11607	F=1.051
Time^2	1.0159e-4	0.00032052	0.31695	0.75474	P-val =0.41735
	$R^2 = 0.2167$	Adj. $R^2 = 0.0105$			

Table 4.51: Response Surface Model Based on Ductility (% Reduction in Area)

Variables	Coefficients	Std. Error	t-stat	P-value	F-stat
Constant	-0.0372	3.5324	-0.010531	0.99171	SSE=90.836
NaOH Conc. (wt %)	1.6685	0.8638	1.9315	0.068473	DFE=19
Time (mins)	-0.0020857	0.057587	-0.036219	0.97149	DFR=5
NaOH Conc. * Time	-0.0039067	0.0036442	-1.072	0.29714	SSR=24.169
NaOH Conc.^2	-0.10657	0.065335	-1.6312	0.11932	F=1.0111
Time^2	8.1587e-5	0.00029038	0.28097	0.78177	P-val =0.43833
	$R^2 = 0.2102$	Adj. $R^2 =$ 0.0023			

The response surface models were optimized using a MATLAB 7.9 code and the optimum NaOH concentrations and time obtained are presented in Table 4.52. It can be observed from Table 4.52 that NaOH concentrations of approximately 2-5wt% give the best results for times of approximately 90-150mins, for the major mechanical properties.

Table 4.52: Optimum NaOH Concentration and Time predicted with Response Surface Models

	Toughness	Tensile Strength	Young Modulus	Yield Strength	%El	%RA
NaOH Conc. (wt %)	5.4819	4.3175	2	2	7.2978	7.2783
Time (mins)	89.9779	109.4184	150	129.7858	30	30

4.5.2 Surface Plot Study for Tensile Properties of Treated Rattan Palm Fiber

The response surface models were used to obtain the surface plot and study the interaction of the variables (NaOH concentration and time) with respect to all mechanical properties studied and the results are presented in Figures 4.16 to 4.21. It can be observed from Figures 4.16 to 4.21 that NaOH concentration has a significant quadratic relationship with most of the mechanical

properties, except for yield strength, while time has a quadratic relationship with toughness, tensile strength and yield strength, but a linear relationship for other mechanical properties. The cases where both variables have a quadratic relationship indicate the existence of a global optimum NaOH concentration and time. The nature of the contour lines, which are not parallel one to another for most mechanical properties, except for ductility, reveal a good level of interaction between the two variables for all mechanical properties. This corroborates the numerical values obtained from the response surface models.

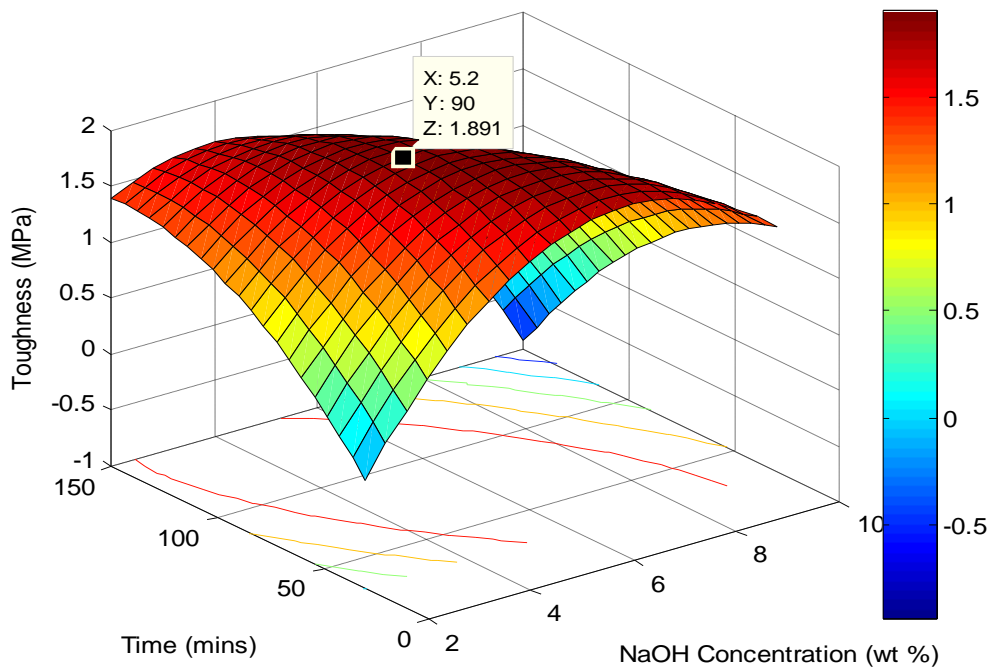


Figure 4.16: Surface Plot of NaOH Conc. and Time interaction on Toughness

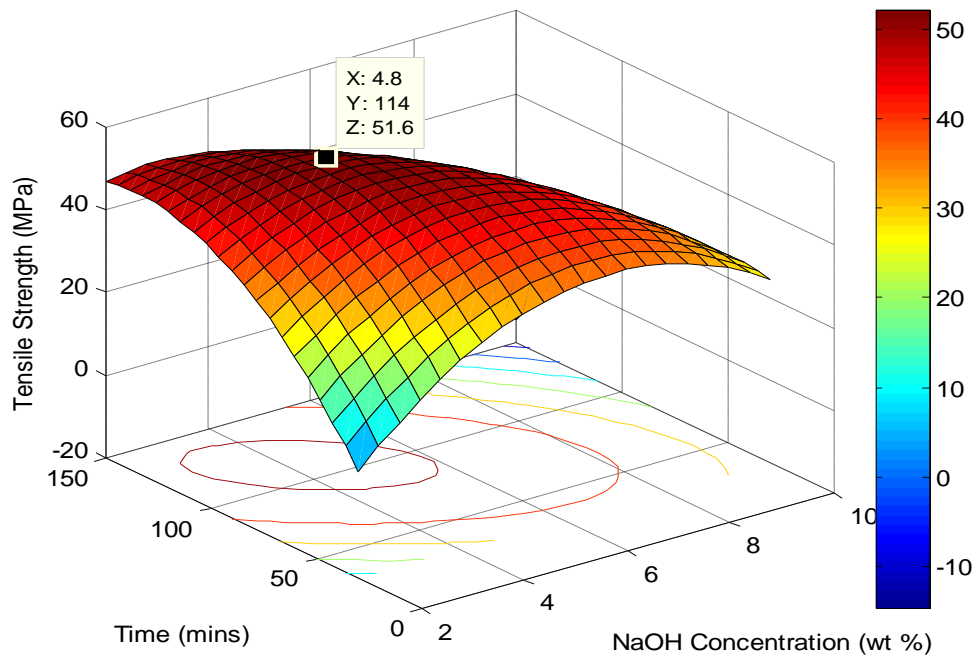


Figure 4.17: Surface Plot of NaOH Conc. and Time interaction on Tensile Strength

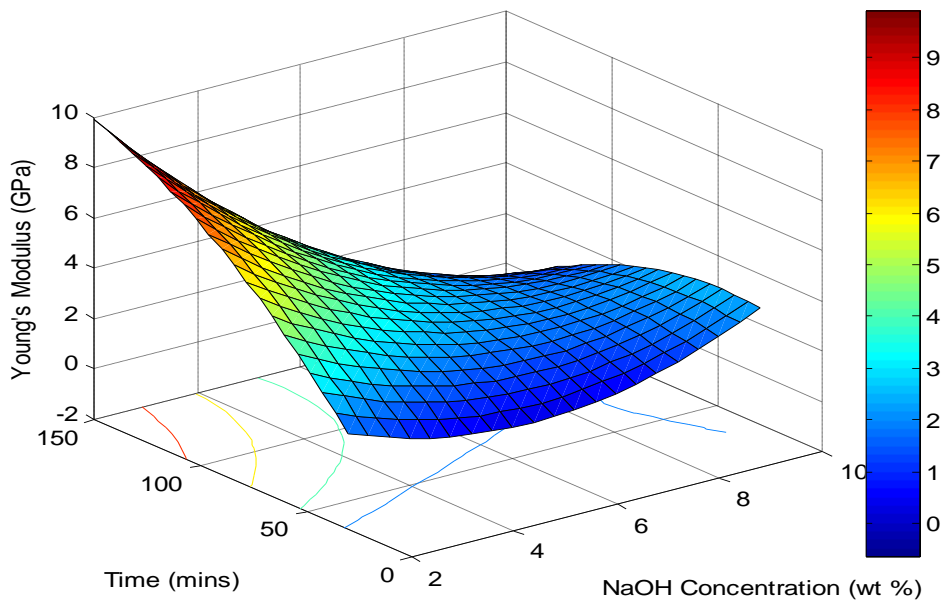


Figure 4.18: Surface Plot of NaOH Conc. and Time interaction on Young's Modulus

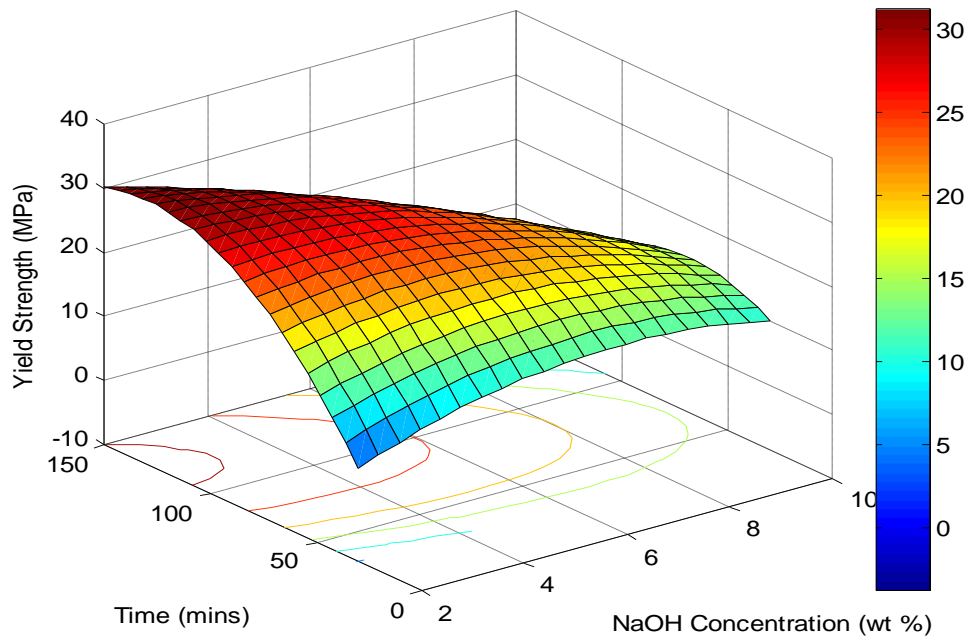


Figure 4.19: Surface Plot of NaOH Conc. and Time interaction on Yield Strength

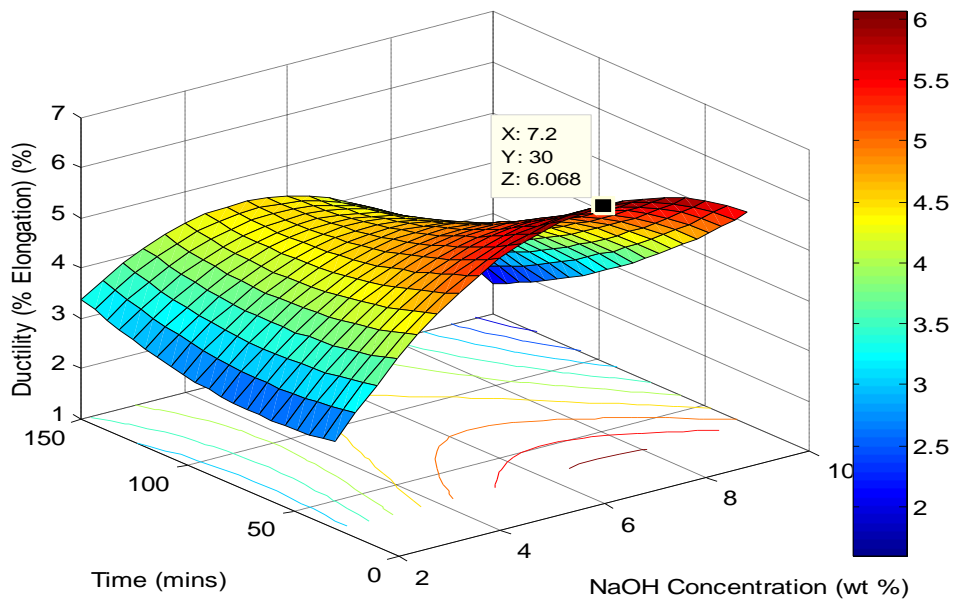


Figure 4.20: Surface Plot of NaOH Conc. and Time interaction on %Elongation

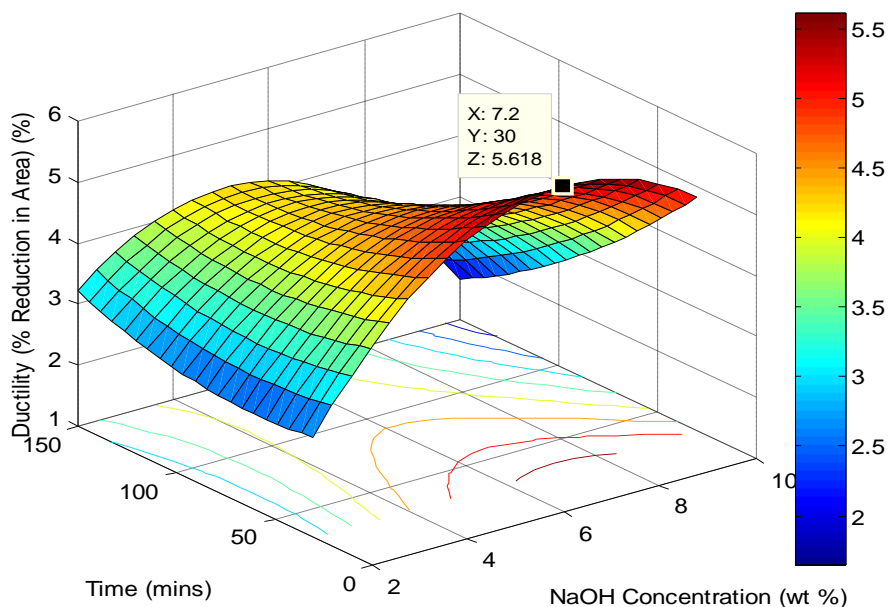


Figure 4.21: Surface Plot of NaOH Conc. and Time interaction on %Reduction in Area

4.5.3 Analysis of Variance Study for Tensile Properties of Treated Rattan Palm Fiber

Data from Tables 4.41 to 4.45 were used for analysis of variance study using MATLAB 7.9 software. Tables 4.53 to 4.58 show results from analysis of variance study on the contributions of varying NaOH concentration and time on the observed improvement and variation in mechanical properties of empty palm bunch fiber. The Tables reveal that NaOH concentration has more effect on all the mechanical properties than time; this effect is significant at 95% confidence for young's modulus. Time has no significant effect on the observed changes in fiber mechanical properties studied. Mercerization of rattan palm fiber can thus be studied in a similar way as empty plantain bunch fiber as a function of NaOH concentration alone, while keeping time constant (Sreekala et al, 2000; Mishra et al, 2003; Edeerozey et al, 2007; Paul et al, 2008; John et al, 2008; Hai et al, 2009).

Table 4.53: ANOVA for Rattan Palm Fiber Based on Toughness

Source	Sum Sq.	Df	Mean Sq.	F	Prob>F
NaOH Concentration (wt %)	8.2877	4	2.0719	0.97248	0.44969
Time (mins)	3.7775	4	0.94439	0.44326	0.77567
Error	34.089	16	2.1306		
Total	46.1543	24			

Table 4.54: ANOVA for Rattan Palm Fiber Based on Tensile Strength

Source	Sum Sq.	Df	Mean Sq.	F	Prob>F
NaOH Concentration (wt %)	4736.8076	4	1184.2019	1.7703	0.18419
Time (mins)	1361.4882	4	340.3721	0.50883	0.73007
Error	10702.8111	16	668.9257		
Total	16801.1069	24			

Table 4.55: ANOVA for Rattan Palm Fiber Based on Modulus of Elasticity

Source	Sum Sq.	Df	Mean Sq.	F	Prob>F
NaOH Concentration (wt %)	102.4099	4	25.6025	3.8466	0.022446
Time (mins)	37.1019	4	9.2755	1.3936	0.28066
Error	106.4927	16	6.6558		
Total	246.0045	24			

Table 4.56: ANOVA for Rattan Palm Bunch Based on Yield strength

Source	Sum Sq.	Df	Mean Sq.	F	Prob>F
NaOH Concentration (wt %)	1183.2691	4	295.8173	2.1719	0.11876
Time (mins)	839.3132	4	209.8283	1.5406	0.23796
Error	2179.2534	16	136.2033		
Total	4201.8357	24			

Table 4.57: ANOVA for Rattan Palm Fiber Based on Ductility (%El)

Source	Sum Sq.	Df	Mean Sq.	F	Prob>F
NaOH Concentration (wt %)	27.0714	4	6.7678	1.0506	0.41238
Time (mins)	11.14	4	2.785	0.43232	0.7833
Error	103.0719	16	6.442		
Total	141.2832	24			

Table 4.58: ANOVA for Rattan Palm Fiber Based on Ductility (%RA)

Source	Sum Sq.	Df	Mean Sq.	F	Prob>F
NaOH Concentration (wt %)	22.9919	4	5.748	1.1057	0.38779
Time (mins)	8.8377	4	2.2094	0.42501	0.78839
Error	83.1755	16	5.1985		
Total	115.005	24			

4.6 Mechanical Properties of Silane Treated Fiber

This section presents and discusses the mechanical properties of fibers treated with Silane coupling agent. These results were obtained from stress-strain analysis of the plots given in the Appendix. Table 4.59 to 4.61 present mechanical properties of Silane treated Empty Plantain Bunch fibers after pretreatment with NaOH at optimum conditions (4wt% for 120mins).

Table 4.59 shows the mechanical properties of Empty Plantain Bunch fiber treated with 0.25wt% silane for 20mins to 100min. The general observation is that sixty percent of the mechanical properties had their maximum values after treatment with 0.25wt% silane for 60mins. The maximum mechanical properties obtained after treatment of Empty Plantain Bunch fiber with 0.25wt% silane were only a fraction (10-53%) of the maximum mechanical properties obtained from mercerization alone.

Table 4.59: Mechanical Properties of Empty Plantain Bunch Fiber treated with 0.25 wt% Silane

Time (mins)	20	60	100
Variables (Units)			
Toughness (MPa)	1.3567	2.6315	*5.2714
Tensile Strength (MPa)	158.3096	*351.1372	339.2346
Modulus of Elasticity (GPa)	11.9462	*29.4617	19.3580
Yield Strength (MPa)	158.3096	*351.1372	284.2130
Percentage Elongation (%)	1.5000	1.3750	*2.5000

*Maximum values

Table 4.60 shows the mechanical properties of Empty Plantain Bunch fiber treated with 0.75wt% silane for 20mins to 100min. The general observation is that sixty percent of the mechanical properties had their maximum values after treatment with 0.75wt% silane for 60mins. The maximum mechanical properties obtained after treatment of Empty Plantain Bunch fiber with 0.75wt% silane were only a fraction (17-71%) of the maximum mechanical properties obtained from mercerization alone.

Table 4.60: Mechanical Properties of Empty Plantain Bunch Fiber treated with 0.75 wt% Silane

Time (mins)	20	60	100
Variables (Units)			
Toughness (MPa)	2.4196	*8.6406	5.8243
Tensile Strength (MPa)	244.0109	*404.7007	339.2346
Modulus of Elasticity (GPa)	15.1898	*49.9709	15.8084
Yield Strength (MPa)	*244.0900	212.4425	108.2575
Percentage Elongation (%)	1.5000	3.0000	*3.2500

*Maximum values

Table 4.61 shows the mechanical properties of Empty Plantain Bunch fiber treated with 1.25wt% silane for 20mins to 100min. The general observation is that sixty percent of the mechanical properties had their maximum values after treatment with 1.25wt% silane for 60mins. The

maximum mechanical properties obtained after treatment of Empty Plantain Bunch fiber with 1.25wt% silane were only a fraction (18-53%) of the maximum mechanical properties obtained from mercerization alone.

Table 4.61: Mechanical Properties of Empty Plantain Bunch Fiber treated with 1.25 wt% Silane

Time (mins)	20	60	100
Variables (Units)			
Toughness (MPa)	5.1586	*9.1412	2.9844
Tensile Strength (MPa)	321.3803	*452.3126	244.0109
Modulus of Elasticity (GPa)	*17.8169	15.4284	16.0115
Yield Strength (MPa)	*239.1485	219.3470	176.1500
Percentage Elongation (%)	2.5000	*3.7500	2.1250

*Maximum values

Generally, silane treatment of Empty Plantain Bunch fiber that was pre-treated with NaOH at optimum conditions produced fibers that were slightly weaker, for all mechanical properties, than that obtained from NaOH treatment alone.

4.6.1 RSM Model for Tensile Properties of Silane Treated Empty Plantain bunch Fiber

A general response surface model of the form: $y = c_0 + c_1x_1 + c_2x_2 + c_3x_1x_2 + c_4x_1^2 + c_5x_2^2$, where y represents the response, which in this case are the mechanical properties, x_1 and x_2 represent silane concentration and treatment time respectively and c_i are model constants, was fit to the data from Tables 4.59 to 4.61. The model coefficients obtained and statistical fit results are given in Tables 4.62 to 4.66.

Tables 4.62 to 4.66 reveal that Silane concentration and treatment time contribute from 43% to 96% of the variability observed in the mechanical properties of the fibers, based on the values of the R^2 . The R^2 values reveal that Silane concentration and treatment time contribute to variations

in mechanical properties of empty plantain bunch fiber in this order (from the most to the least): tensile strength (96%), toughness (74%), yield strength (64%), modulus of elasticity (59%) and percentage elongation (43%).

The significance of each model coefficient can be judged based on the value of the t-statistics (which must have a magnitude of 2 or more to be significant) or the p-value. The coefficient of silane concentration is significant for tensile strength at 90% confidence while the coefficient of time is significant for tensile strength at 95% confidence. The coefficient of interaction between silane concentration and treatment time is significant for tensile strength at 95% confidence, while other coefficients are not significant. The statistical model based on tensile strength is adequate at 95% confidence bound based on the F-statistics. The statistical models for other mechanical properties are not adequate.

Table 4.62: Response Surface Model Based on Toughness

Variables	Coefficients	Std. Error	t-stat	P-value	F-stat
Constant	-8.4991	4.9045	-1.7329	0.1815	SSE=15.5730
Silane Conc. (wt %)	14.4670	10.4200	1.3883	0.2592	DFE=3
Time (mins)	0.3012	0.1303	2.3122	0.1038	DFR=5
Silane Conc. * Time	-0.0761	0.0570	-1.3362	0.2738	SSR=44.9390
Silane Conc.^2	-4.8169	6.4443	-0.7475	0.5090	F=1.7314
Time^2	-0.0019	0.0010	-1.8426	0.1626	P-val =0.3455
	$R^2 = 0.7426$	Adj. $R^2 =$ 0.3137			

Table 4.63: Response Surface Model Based on Tensile Strength

Variables	Coefficients	Std. Error	t-stat	P-value	F-stat
Constant	-152.2200	60.5050	-2.5158	0.0865	SSE=2370.1
Silane Conc. (wt %)	359.5700	128.5500	2.7971	0.0680	DFE=3
Time (mins)	12.8760	1.6069	8.0132	0.0041	DFR=5
Silane Conc. * Time	-3.2287	0.7027	-4.5947	0.0194	SSR=61641
Silane Conc.^2	-73.0050	79.5010	-0.9183	0.4262	F=15.605
Time^2	-0.0802	0.0124	-6.4580	0.0075	P-val =0.0234
	$R^2 = 0.9630$	Adj. $R^2 = 0.9013$			

Table 4.64: Response Surface Model Based on Modulus of Elasticity

Variables	Coefficients	Std. Error	t-stat	P-value	F-stat
Constant	-15.8550	19.6170	-0.8082	0.4643	SSE=457.02
Silane Conc. (wt %)	48.0780	46.1820	1.0411	0.3566	DFE=4
Time (mins)	1.1958	0.5773	2.0715	0.1071	DFR=4
Silane Conc.^2	-34.6100	30.2330	-1.1448	0.3162	SSR=664.89
Time^2	-0.0097	0.0047	-2.0638	0.1080	F=1.4549
	$R^2 = 0.5926$	Adj. $R^2 = 0.1853$			P-val=0.3626

Table 4.65: Response Surface Model Based on Ductility (% Elongation)

Variables	Coefficients	Std. Error	t-stat	P-value	F-stat
Constant	1.0451	0.6809	1.5350	0.1757	SSE=3.23
Silane Conc. (wt %)	1	0.5991	1.6692	0.1461	DFE=6
Time (mins)	0.0099	0.0075	1.3215	0.2345	DFR=2
					SSR=2.4401
					F=2.2663
	$R^2 = 0.4303$	Adj. $R^2 = 0.2405$			P-val = 0.18486

Table 4.66: Response Surface Model Based on Yield Strength

Variables	Coefficients	Std. Error	t-stat	P-value	F-stat
Constant	158.1500	149.7200	1.0563	0.3684	SSE=14513
Silane Conc. (wt %)	-210.0500	318.1000	-0.6603	0.5562	DFE=3
Time (mins)	5.9132	3.9763	1.4871	0.2337	DFR=5
Silane Conc. * Time	-2.3613	1.7388	-1.3580	0.2676	SSR=26008
Silane Conc.^2	199.1500	196.7300	1.0123	0.3859	F=1.0752
Time^2	-0.0371	0.0307	-1.2053	0.3145	P-val =0.5090
	$R^2 = 0.6418$	$Adj. R^2 = 0.0449$			

4.6.2 Surface Plot for Tensile Properties of Silane Treated Empty Plantain Bunch Fiber

The response surface models were used to obtain the surface plot and study the interaction of the variables (silane concentration and time) with respect to all mechanical properties studied and the results are presented in Figures 4.22 to 4.26. It can be observed from Figures 4.22 to 4.26 that silane concentration has a significant quadratic relationship with the Toughness, Yield Strength and Young's modulus, while time has a quadratic relationship most mechanical properties and a linear relationship with Elongation. The nature of the contour lines, which are mostly parallel one to another for most mechanical properties, except for tensile strength, reveal low interaction between the two variables for all mechanical properties. This corroborates the numerical values obtained from the response surface models.

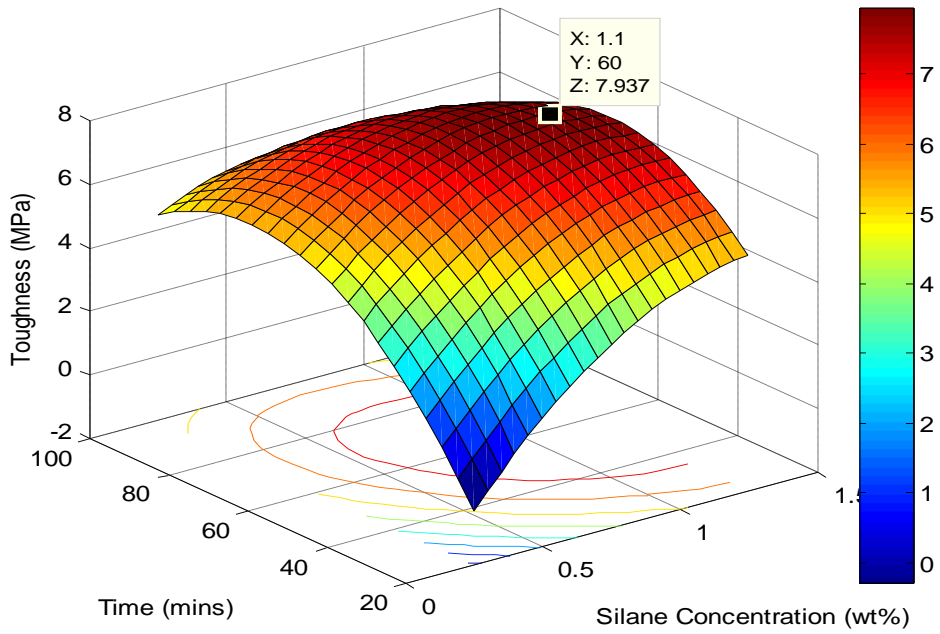


Figure 4.22: Surface Plot of Silane Conc. and Time interaction on Toughness

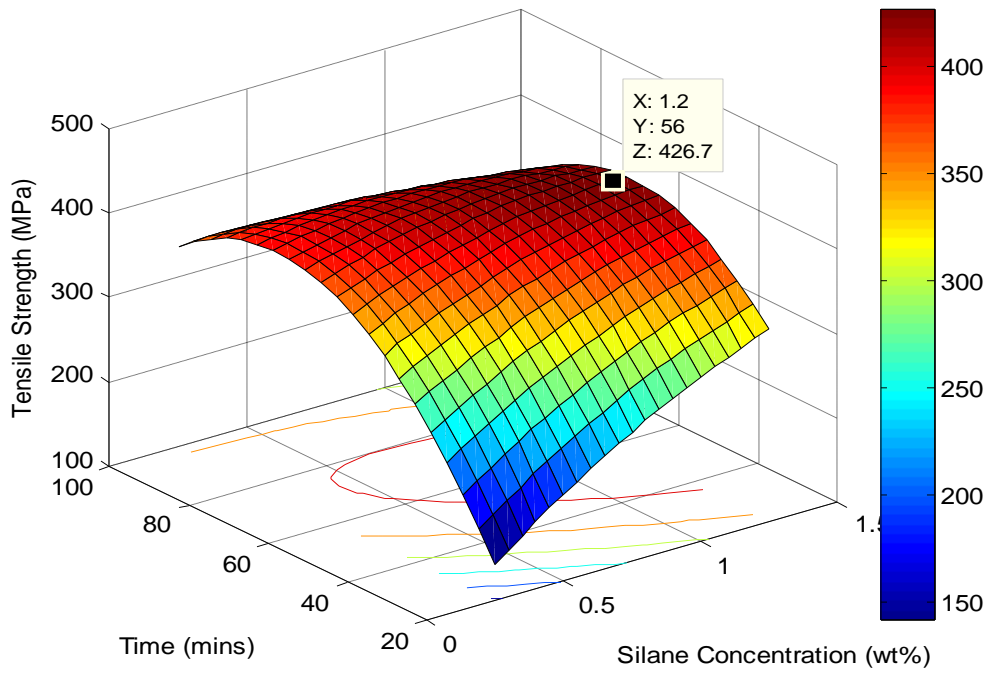


Figure 4.23: Surface Plot of Silane Conc. and Time interaction on Tensile Strength

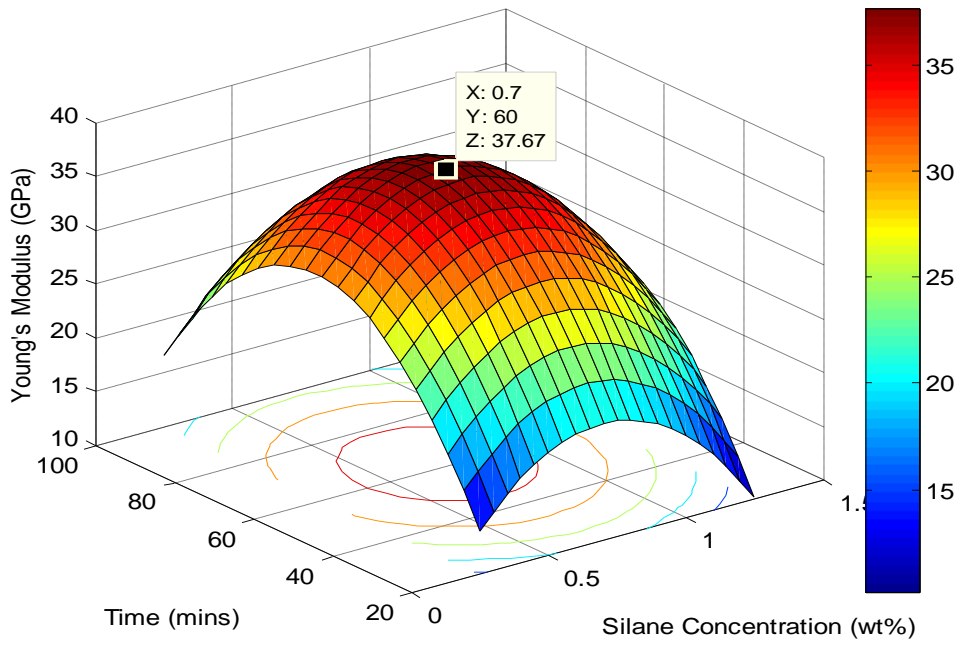


Figure 4.24: Surface Plot of Silane Conc. and Time interaction on Young's Modulus

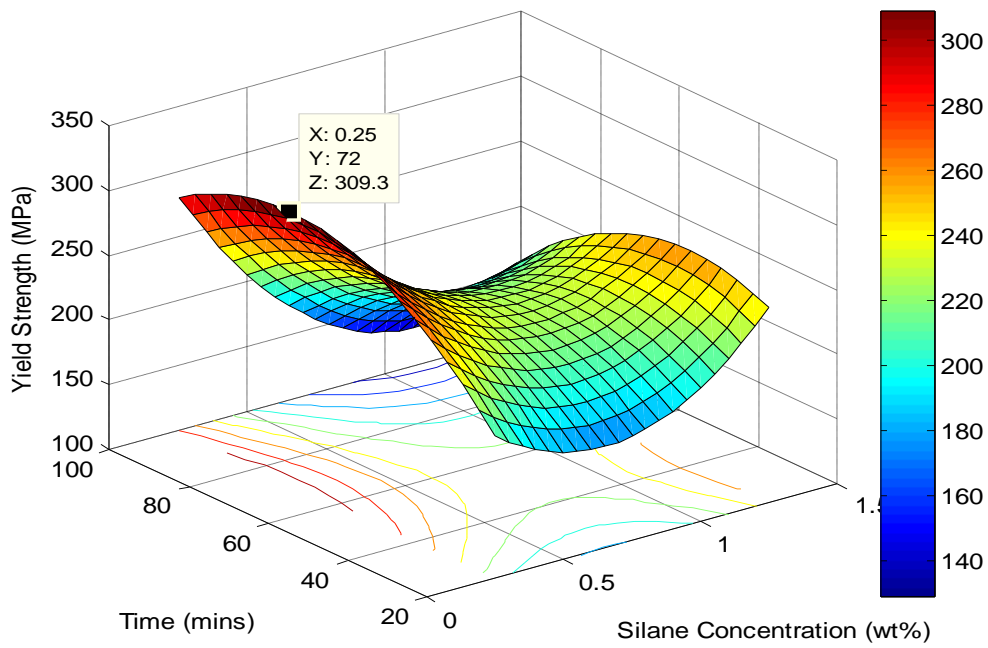


Figure 4.25: Surface Plot of Silane Conc. and Time interaction on Yield Strength

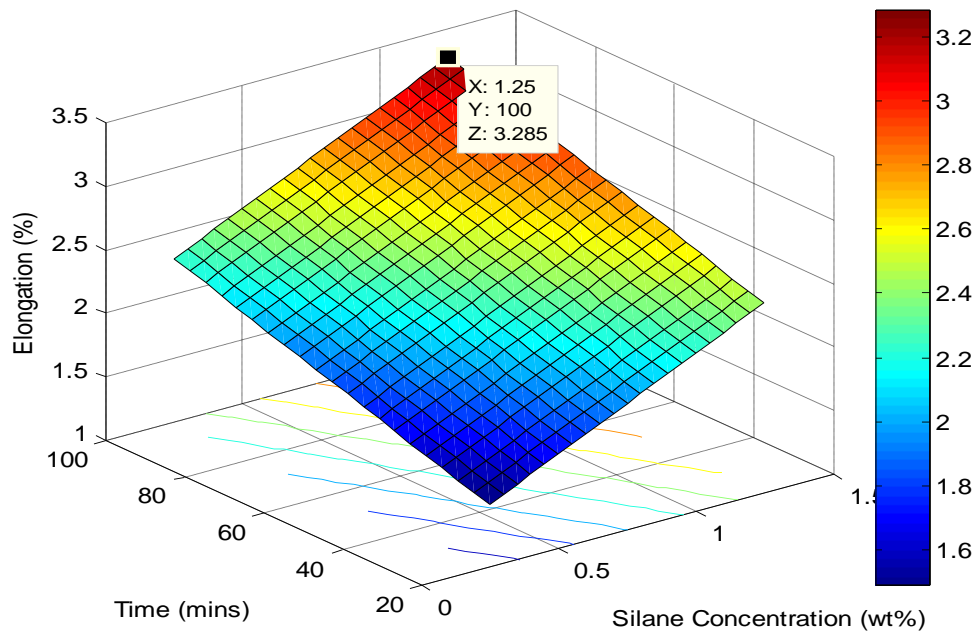


Figure 4.26: Surface Plot of Silane Conc. and Time interaction on %Elongation

The optimum conditions for silane treatment varied based on the mechanical property of interest. It can be observed from Table 4.67, that Tensile Strength and Toughness which have the highest R-squared values have optimum values for silane concentration of 1.1-1.2wt% after treatment for 56-60mins.

Table 4.67: Optimum Silane Concentration and Time predicted with Response Surface Models

	Toughness	Tensile Strength	Young Modulus	Yield Strength	%EI
Silane Conc. (wt %)	1.10	1.20	0.70	0.25	1.25
Time (mins)	60	56	60	72	100

4.6.3 ANOVA Study for Tensile Properties of Silane Treated Empty Plantain Bunch fiber

Data from Tables 4.59 to 4.61 were used for analysis of variance study using MATLAB 7.9 software. Tables 4.68 to 4.72 show results from analysis of variance study on the contributions of varying silane concentration and time on the observed improvement and variation in mechanical properties of empty plantain bunch fiber after mercerization treatment at optimum conditions. The Tables reveal that silane concentration and time has no significant effect on most of the mechanical properties.

Table 4.68: ANOVA for Silane treated Empty Plantain Bunch Fiber (Toughness)

Source	Sum Sq.	Df	Mean Sq.	F	Prob>F
Silane Concentration (wt %)	13.6326	2	6.8163	1.10	0.4169
Time (mins)	22.0375	2	11.0188	1.77	0.2808
Error	24.8420	4	6.2105		
Total	60.5122	8			

Table 4.69: ANOVA for Silane treated Empty Plantain Bunch Fiber (Tensile Strength)

Source	Sum Sq.	Df	Mean Sq.	F	Prob>F
Silane Concentration (wt %)	5427.6	2	2713.8	0.57	0.6057
Time (mins)	39534.7	2	19767.3	4.15	0.1057
Error	19049.1	4	4762.3		
Total	64011.5	8			

Table 4.70: ANOVA for Silane treated Empty Plantain Bunch Fiber (Young's Modulus)

Source	Sum Sq.	Df	Mean Sq.	F	Prob>F
Silane Concentration (wt %)	171.81	2	85.905	0.75	0.5282
Time (mins)	493.08	2	246.541	2.16	0.2314
Error	457.02	4	114.254		
Total	1121.91	8			

Table 4.71: ANOVA for Silane treated Empty Plantain Bunch Fiber (Yield strength)

Source	Sum Sq.	Df	Mean Sq.	F	Prob>F
Silane Concentration (wt %)	9171.9	2	4585.93	0.78	0.5165
Time (mins)	7914.8	2	3957.42	0.68	0.5588
Error	23434	4	5858.49		
Total	40520.7	8			

Table 4.72: ANOVA for Silane treated Empty Plantain Bunch Fiber (%Elongation)

Source	Sum Sq.	Df	Mean Sq.	F	Prob>F
Silane Concentration (wt %)	1.67014	2	0.83507	1.28	0.3708
Time (mins)	1.39931	2	0.69965	1.08	0.4227
Error	2.60069	4	0.65017		
Total	5.67014	8			

Generally, fibers treated with silane after pre-treatment with NaOH at optimum condition were weaker than those obtained using NaOH treatment alone. This is similar to observations by John et al (2008) who studied sisal and oil palm fiber and reported better tensile properties for NaOH treated fibers over silane treated fibers and Yu et al (2010) who studied ramie fibers and also reported better tensile properties for NaOH treated fibers over silane treated fibers.

4.7 Water Absorption Analysis of Treated and Untreated Fibers

The water absorption test results obtained for untreated and treated fibers (Appendix 7.4) were studied using Becker's model (Eqn. 2.37), Peleg's model (Eqn. 2.49) and the general water transport model (Eqn. 2.36) and the results are presented and discussed in this section.

4.7.1 Analysis of Empty Plantain Bunch Fiber Water Sorption using Peleg's Model

Water absorption results for untreated and treated empty plantain bunch fiber were fit to Peleg's model (Eqn. 2.49) and the numerical results are presented in Tables 4.73 and 4.74 respectively, while the graphical fit results are presented in Figures 4.27 and 4.28 respectively. It can be observed from Tables 4.73 and 4.74 that Peleg's model accurately describes the water absorption kinetics of untreated and treated empty plantain bunch fiber with R^2 between 0.9654 and 0.9974. The Peleg's rate constant (k_1) for untreated empty plantain bunch (Table 4.73) increases slightly with temperature to a maximum at 50°C before dropping to a minimum at 70°C, though the value remains relatively constant with temperature ($\cong 0.02$), thus the initial water sorption does not change significantly with temperature. The Peleg's capacity constant (k_2) does not follow any definite profile. It can be observed from Table 4.74 that the Peleg's rate constant for treated empty plantain bunch fiber is higher than untreated with a factor of about ten and tends to reduce with temperature. The Peleg's capacity constant (k_2) - which is inversely proportional to maximum water sorption capacity - for the treated samples is also higher than the untreated by a factor of about three. Thus, the treatment tends to increase initial water sorption rate about ten times but reduces maximum water capacity (equilibrium moisture content) by about three times.

Table 4.73: Peleg's Model fit to Untreated Plantain Bunch Fiber Water sorption

Temp. (°C)	K_1 (min % ⁻¹)	K_2 (% ⁻¹)	R^2	Adj- R^2
30	0.01991	0.001584	0.9963	0.9953
40	0.01992	0.0007824	0.9890	0.9863
50	0.02455	0.001644	0.9951	0.9938
60	0.02359	0.0008738	0.9969	0.9961
70	0.01633	0.001333	0.9971	0.9963

Table 4.74: Peleg's Model fit to Treated Plantain Bunch Fiber Water sorption

Temp. (°C)	K ₁ (min % ⁻¹)	K ₂ (% ⁻¹)	R ²	Adj-R ²
30	0.2397	6.149e-5	0.9654	0.9567
40	0.0703	0.003574	0.9962	0.9952
50	0.1036	0.003366	0.9974	0.9968
60	0.0598	0.003941	0.9934	0.9918
70	0.1019	0.003393	0.9963	0.9954

The graphical fit results of Peleg's model to the water sorption data of untreated and treated empty plantain bunch fibers are presented in Figures 4.27 and 4.28 respectively. It can be observed from the Figures 4.27 and 4.28 that the Peleg's model has a good fit to the water sorption data and that fiber treatment reduces water sorption more than three times even within the first twenty five minutes as observed by Dhakal et al (2006) and Srubar et al (2012).

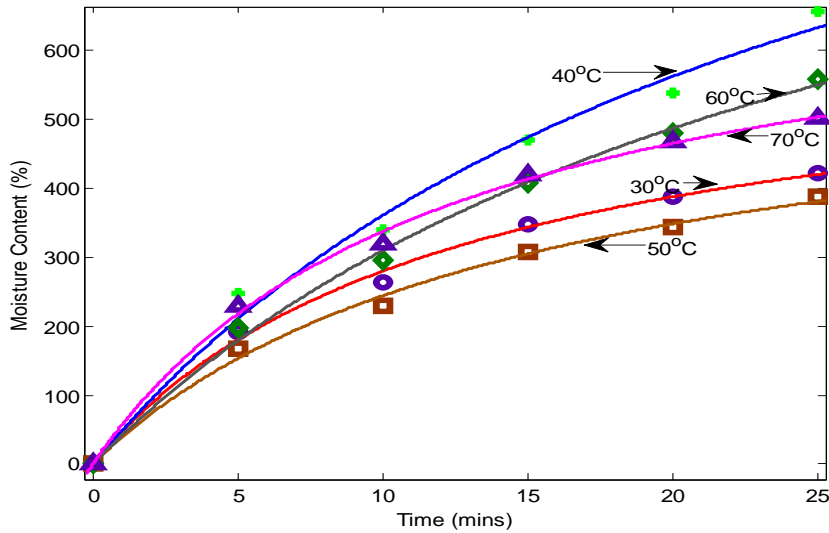


Figure 4.27: Peleg Model Graphical fit to Untreated Empty Plantain Bunch Fiber

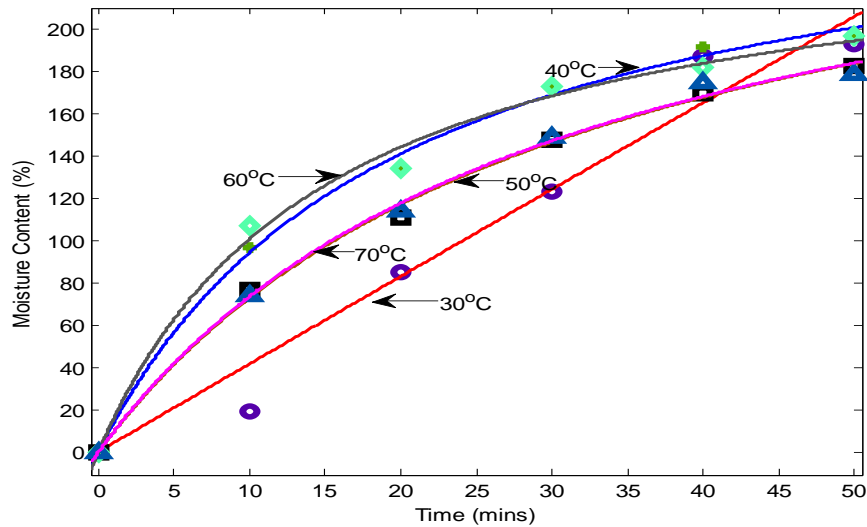


Figure 4.28: Peleg Model Graphical fit to Treated Empty Plantain Bunch Fiber

4.7.2 Analysis of Empty Plantain Bunch Fiber Water Sorption using Becker's Model

Water absorption results for untreated and treated empty plantain bunch fiber were fit to Becker's model (Eqn. 2.37) to study the mechanism of the water sorption and the numerical results are presented in Tables 4.75 and 4.76 respectively, while the graphical fit results are presented in Figures 4.29 and 4.30 respectively. It can be observed from Tables 4.75 and 4.76 that Becker's model fits the water absorption kinetics of untreated and treated empty plantain bunch fiber with R^2 between 0.9813 and 0.9968 except for treated empty plantain bunch fiber at 30°C with R^2 of 0.8340. The rate constant (α) for untreated empty plantain bunch (Table 4.75) does not follow any definite profile while that treated empty plantain bunch fiber (Table 4.76) remains relatively constant with temperature, but the values are at most one-third of the untreated. Treatment of the fiber thus reduces water sorption rate. Initial water sorption due to fast capillary action seemed also slightly higher for the treated sample. The water sorption mechanism is

therefore majorly Fickian diffusion controlled and especially intra particle diffusion since the value of M_p is very small (Hamdaoui et al, 2014).

Table 4.75: Becker’s Model fit to Untreated Plantain Bunch Fiber Water sorption

Temp. (°C)	α (% min ^{-1/2})	M_p (%)	R^2	Adj- R^2
30	86.04	0.0491	0.9969	0.9961
40	121.9	2.456e-10	0.9813	0.9813
50	76.8	4.214e-13	0.9968	0.9968
60	105.3	1.8e-11	0.9814	0.9814
70	103.2	0.6961	0.9961	0.9952

Table 4.76: Becker’s Model fit to Treated Plantain Bunch Fiber Water sorption

Temp. (°C)	α (% min ^{-1/2})	M_p (%)	R^2	Adj- R^2
30	24.41	3.945e-8	0.8340	0.8340
40	29.11	3.568	0.9898	0.9873
50	26.13	4.244e-14	0.9951	0.9951
60	28.15	7.815	0.9850	0.9812
70	26.22	5.426e-9	0.9897	0.9897

The graphical fit results of Becker’s model to the water sorption data of untreated and treated empty plantain bunch fibers are presented in Figures 4.29 and 4.30 respectively. It can be observed from the Figures 4.29 and 4.30 that the Becker’s model has a good fit to the water sorption data except for water sorption of treated fiber at 30°C which showed deviation from Fickian diffusion. Fiber treatment reduces water sorption more than three times even within the first twenty five minutes as also observed by Srubar et al (2014).

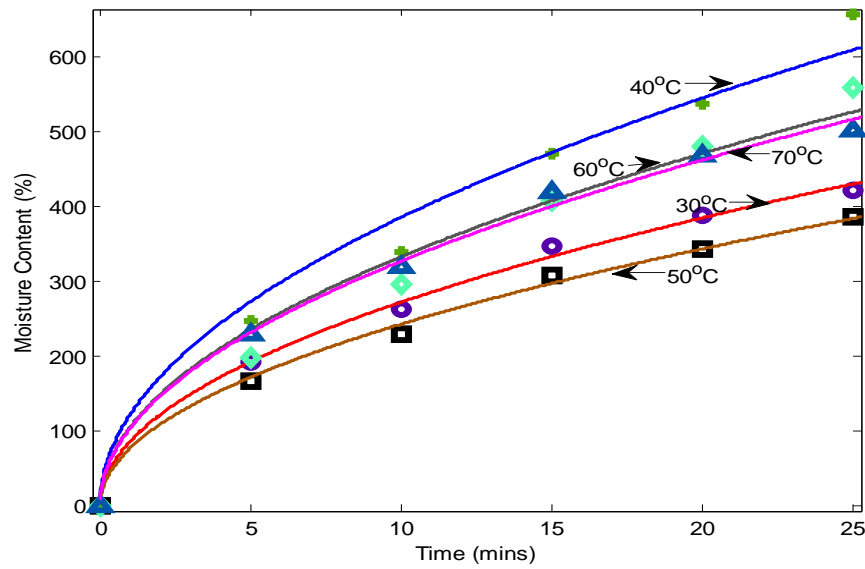


Figure 4.29: Becker's Model Graphical fit to Untreated Empty Plantain Bunch Fiber

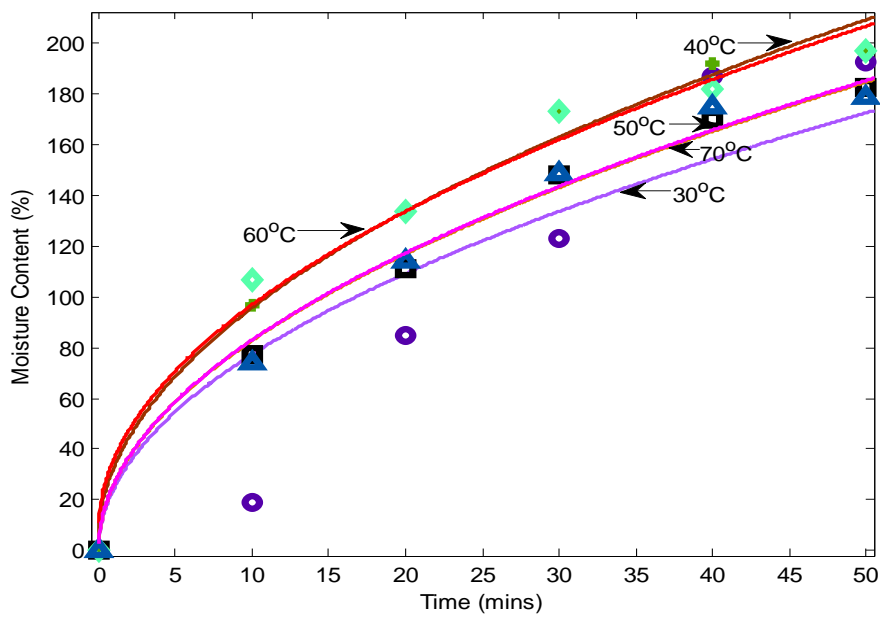


Figure 4.30: Becker's Model Graphical fit to Treated Empty Plantain Bunch Fiber

4.7.3 Analysis of Empty Palm Bunch Fiber Water Sorption using Peleg's Model

Water absorption results for untreated and treated empty palm bunch fiber were fit to Peleg's model (Eqn. 2.49) and the numerical results are presented in Tables 4.77 and 4.78 respectively, while the graphical fit results are presented in Figures 4.31 and 4.32 respectively. It can be observed from Tables 4.77 and 4.78 that Peleg's model accurately describes the water absorption kinetics of untreated and treated empty palm bunch fiber with R^2 between 0.9594 and 0.9986. The Peleg's rate constant (k_1) for untreated empty palm bunch fiber (Table 4.77) does not vary widely, it lies between 0.03693 and 0.05455 for the temperatures studied, giving an indication of the initial water sorption. The Peleg's capacity constant (k_2) also does not follow any definite profile. It can be observed from Table 4.78 that the Peleg's rate constant for treated empty palm bunch fiber is higher than untreated with a factor of between two and ten. The Peleg's capacity constant (k_2) - which is inversely proportional to maximum water sorption capacity - for the treated samples is slightly higher than that of untreated. Thus, the treatment tends to increase initial water sorption rate but reduces maximum water capacity (equilibrium moisture content).

Table 4.77: Peleg's Model fit to Untreated Palm Bunch Fiber Water sorption

Temp. (°C)	K_1 (min % ⁻¹)	K_2 (% ⁻¹)	R^2	Adj- R^2
30	0.04485	0.001009	0.9973	0.9966
40	0.05455	0.0006718	0.9986	0.9983
50	0.03693	0.003085	0.9973	0.9966
60	0.04740	0.002508	0.9767	0.9709
70	0.04112	0.002302	0.9969	0.9962

Table 4.78: Peleg's Model fit to Treated Palm Bunch Fiber Water sorption

Temp. (°C)	K ₁ (min % ⁻¹)	K ₂ (% ⁻¹)	R ²	Adj-R ²
30	0.4344	3.682e-13	0.9594	0.9594
40	0.1210	0.004857	0.9973	0.9967
50	0.1202	0.004958	0.9942	0.9928
60	0.1245	0.007169	0.9949	0.9936
70	0.2493	0.002229	0.9829	0.9786

The graphical fit results of Peleg's model to the water sorption data of untreated and treated empty palm bunch fibers are presented in Figures 4.31 and 4.32 respectively. It can be observed from the Figures 4.31 and 4.32 that the Peleg's model has a good fit to the water sorption data and that fiber treatment reduces water sorption about three times for most of the temperatures. This observation is in agreement with those of Dhakal et al (2006) and Srubar et al (2012).

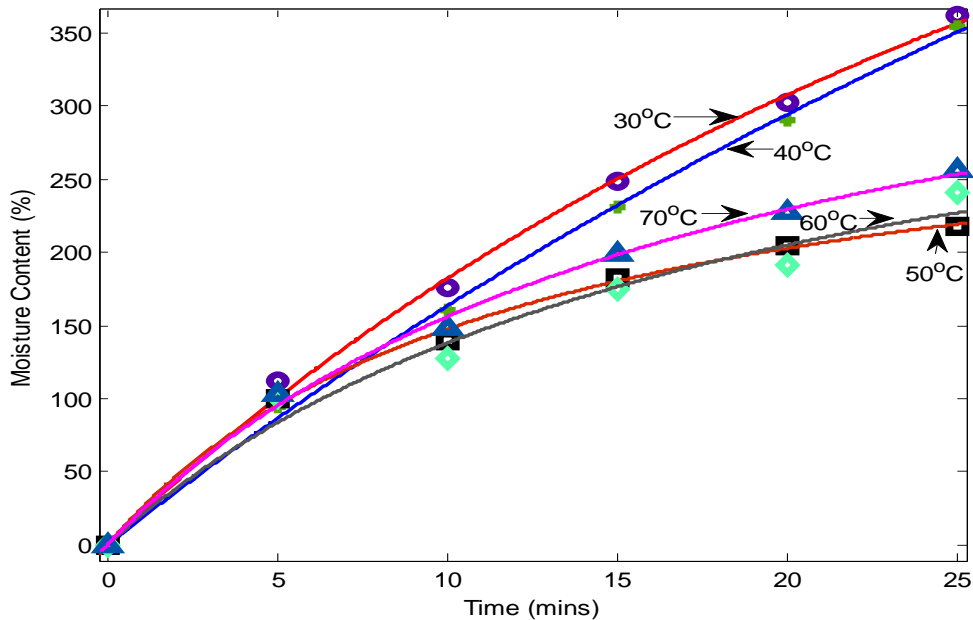


Figure 4.31: Peleg Model Graphical fit to Untreated Empty Palm Bunch Fiber

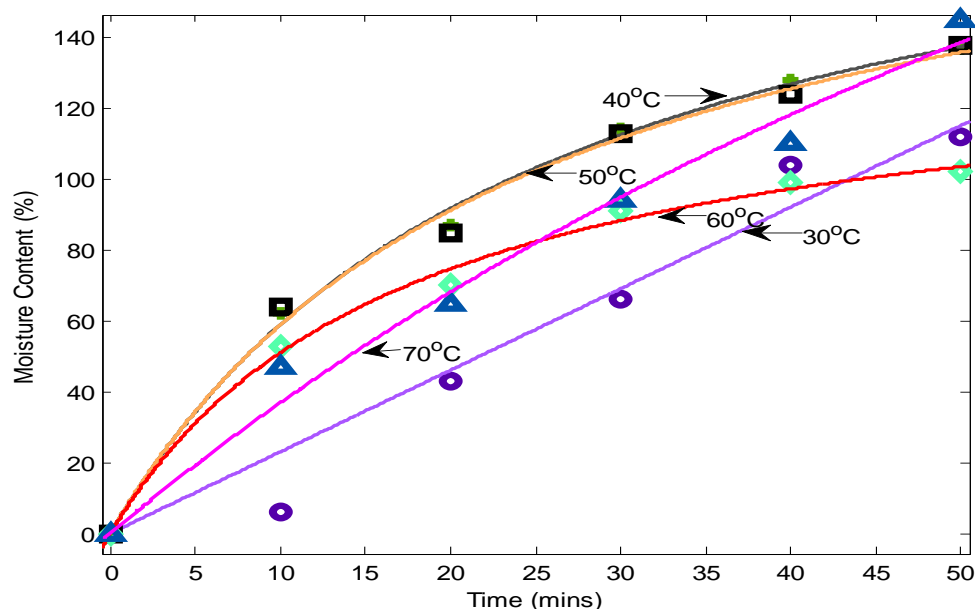


Figure 4.32: Peleg Model Graphical fit to Treated Empty Palm Bunch Fiber

4.7.4 Analysis of Empty Palm Bunch Fiber Water Sorption using Becker's Model

Water absorption results for untreated and treated empty palm bunch fiber were fit to Becker's model (Eqn. 2.37) to study the mechanism of the water sorption and the numerical results are presented in Tables 4.79 and 4.80 respectively, while the graphical fit results are presented in Figures 4.33 and 4.34 respectively. It can be observed from Tables 4.79 and 4.80 that Becker's model fits the water absorption kinetics of untreated and treated empty palm bunch fiber with R^2 between 0.9365 and 0.9969 except for treated empty palm bunch fiber at 30°C with R^2 of 0.7944. The rate constant (α) for untreated empty palm bunch (Table 4.79) reduces with temperature except at 70°C while that treated empty palm bunch fiber (Table 4.80) varies between 13.48 and 19.92 with the values about one-third of the untreated. Treatment of the fiber thus reduces water sorption rate. Initial water sorption due to fast capillary action seemed also slightly higher for the treated sample. The water sorption mechanism is therefore majorly Fickian

diffusion controlled and especially intra particle diffusion since the value of M_p is very small (Hamdaoui et al, 2014).

Table 4.79: Becker’s Model fit to Untreated Empty Palm Bunch Fiber Water sorption

Temp. (°C)	α (% min ^{-1/2})	M_p (%)	R^2	Adj- R^2
30	65.76	3.071e-8	0.9606	0.9606
40	62.40	4.078e-9	0.9365	0.9365
50	44.93	0.6288	0.9957	0.9946
60	44.86	4.629e-11	0.9832	0.9832
70	50.25	1.907e-11	0.9941	0.9941

Table 4.80: Becker’s Model fit to Treated Empty Palm Bunch Fiber Water sorption

Temp. (°C)	α (% min ^{-1/2})	M_p (%)	R^2	Adj- R^2
30	13.48	1.406e-10	0.7944	0.7944
40	19.92	0.005412	0.9963	0.9954
50	19.65	0.5008	0.9969	0.9961
60	14.99	2.9490	0.9865	0.9832
70	17.83	6.45e-13	0.9473	0.9473

The graphical fit results of Becker’s model to the water sorption data of untreated and treated empty palm bunch fibers are presented in Figures 4.33 and 4.34 respectively. It can be observed from the Figures 4.33 and 4.34 that the Becker’s model has a good fit to the water sorption data except for water sorption of treated fiber at 30°C which showed deviation from Fickian diffusion. Fiber treatment reduces water sorption about three times even within the first twenty five minutes as observed also by Srubar et al (2012).

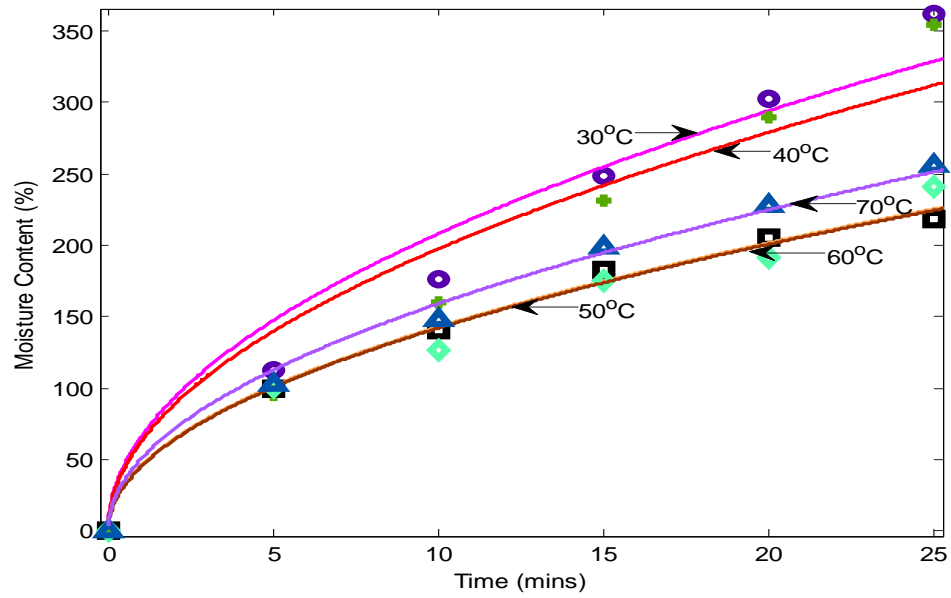


Figure 4.33: Becker's Model Graphical fit to Untreated Empty Palm Bunch Fiber

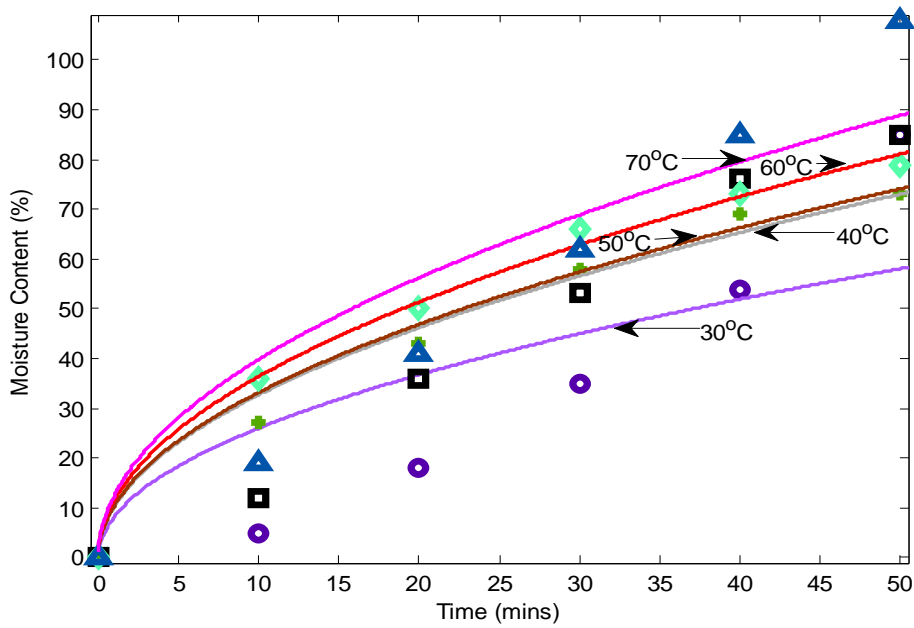


Figure 4.34: Becker's Model Graphical fit to Treated Empty Palm Bunch Fiber

Generally, the water sorption capacity and rate of empty plantain fiber is about twice that of empty palm bunch fiber. This is due to the higher hemicelluloses content of empty plantain bunch fiber (Hamdaoui et al, 2014).

4.7.5 Analysis of Rattan Palm Fiber Water Sorption using Peleg's Model

Water absorption results for untreated and treated rattan palm fiber were fit to Peleg's model (Eqn. 2.49) and the numerical results are presented in Tables 4.81 and 4.82 respectively, while the graphical fit results are presented in Figures 4.35 and 4.36 respectively. It can be observed from Tables 4.81 and 4.82 that Peleg's model accurately describes the water absorption kinetics of untreated and treated rattan palm fiber with R^2 between 0.9135 and 0.9990. The Peleg's rate constant (k_1) for untreated rattan palm fiber (Table 4.81) reduces with increase in temperature. The Peleg's capacity constant (k_2) initially increases with temperature before dropping. It can be observed from Table 4.82 that the Peleg's rate constant for treated empty palm bunch fiber is higher than untreated with a factor of between two and seven. The Peleg's capacity constant (k_2) - which is inversely proportional to maximum water sorption capacity - for the treated samples is not significantly different from that of untreated.

Table 4.81: Peleg's Model fit to Untreated Rattan Palm Fiber Water sorption

Temp. (°C)	K_1 (min % ⁻¹)	K_2 (% ⁻¹)	R^2	Adj- R^2
30	0.2475	0.0001654	0.9973	0.9966
40	0.1030	0.003097	0.9990	0.9987
50	0.07475	0.005373	0.9944	0.9930
60	0.09023	0.003273	0.9934	0.9918
70	0.06653	0.004335	0.9903	0.9879

Table 4.82: Peleg's Model fit to Treated Rattan Palm Fiber Water sorption

Temp. (°C)	K ₁ (min % ⁻¹)	K ₂ (% ⁻¹)	R ²	Adj-R ²
30	0.6989	1.012e-13	0.9135	0.9135
40	0.3009	0.007406	0.9976	0.9970
50	0.5612	0.0001147	0.9876	0.9845
60	0.2077	0.008516	0.9969	0.9961
70	0.4713	2.795e-14	0.9984	0.9984

The graphical fit results of Peleg's model to the water sorption data of untreated and treated rattan palm fibers are presented in Figures 4.35 and 4.36 respectively. It can be observed from the Figures 4.35 and 4.36 that the Peleg's model has a good fit to the water sorption data and that fiber treatment reduces water sorption about three times for most of the temperatures which agree with observation of Dhakal et al (2006) and Srubar et al (2012).

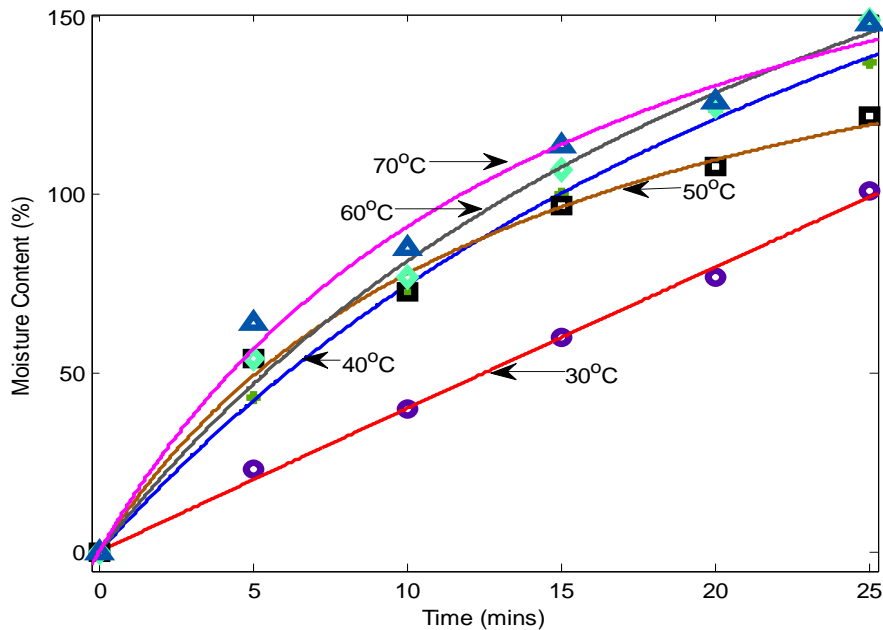


Figure 4.35: Peleg Model Graphical fit to Untreated Rattan Palm Fiber

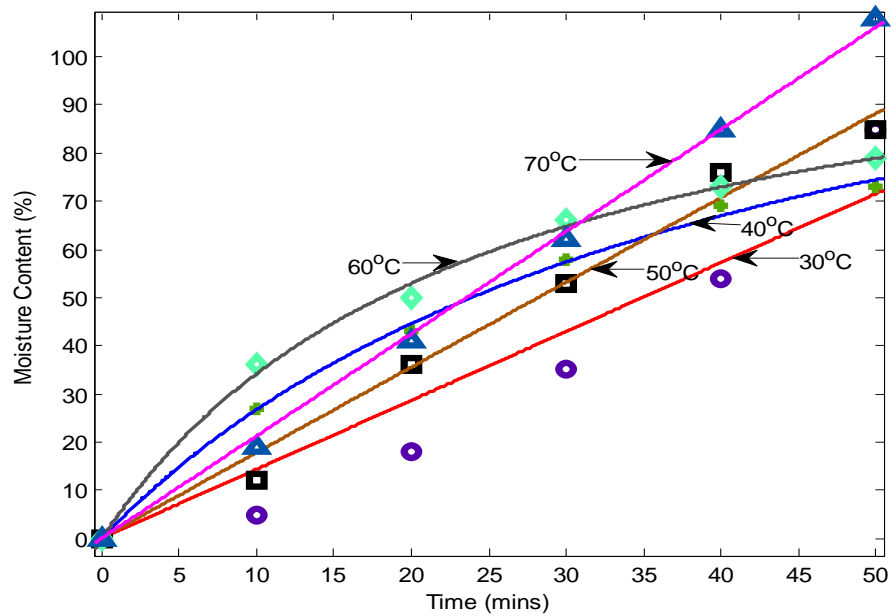


Figure 4.36: Peleg Model Graphical fit to Treated Rattan Palm Fiber

4.7.6 Analysis of Rattan Palm Fiber Water Sorption using Becker's Model

Water absorption results for untreated and treated rattan palm fiber were fit to Becker's model (Eqn. 2.37) to study the mechanism of the water sorption and the numerical results are presented in Tables 4.83 and 4.84 respectively, while the graphical fit results are presented in Figures 4.37 and 4.38 respectively. It can be observed from Tables 4.83 and 4.84 that Becker's model fits the water absorption kinetics of untreated and treated rattan palm fiber with R^2 between 0.8627 and 0.9976 except for treated rattan palm fiber at 30°C with R^2 of 0.67413. The rate constant (α) for untreated rattan palm (Table 4.83) increased with temperature likewise that of treated rattan palm fiber (Table 4.84), with values for the treated being about one-half that of the untreated. Treatment of the fiber thus reduces water sorption rate. Initial water sorption due to fast capillary action (M_p) was about the same for treated and untreated samples. The water sorption

mechanism is therefore majorly Fickian diffusion controlled and especially intra particle diffusion since the value of M_p is very small (Hamdaoui et al, 2014).

Table 4.83: Becker's Model fit to Untreated Rattan Palm Fiber Water sorption

Temp. (°C)	α (% min ^{-1/2})	M_p (%)	R^2	Adj- R^2
30	16.8	7.212e-9	0.8960	0.8960
40	26.05	6.538e-11	0.9684	0.9684
50	24.27	1.111e-7	0.9976	0.9976
60	27.77	3.227e-10	0.9801	0.9801
70	28.76	2.609e-10	0.9952	0.9952

Table 4.84: Becker's Model fit to Treated Rattan Palm Fiber Water sorption

Temp. (°C)	α (% min ^{-1/2})	M_p (%)	R^2	Adj- R^2
30	8.204	5.955e-11	0.6913	0.6913
40	10.32	4.984e-14	0.9851	0.9851
50	10.47	4.585e-10	0.8627	0.8627
60	11.44	0.1384	0.9962	0.9952
70	12.56	1.302e-9	0.8659	0.8659

The graphical fit results of Becker's model to the water sorption data of untreated and treated rattan palm fibers are presented in Figures 4.37 and 4.38 respectively. It can be observed from the Figures 4.37 and 4.38 that the Becker's model has a good fit to the water sorption data except for water sorption of treated fiber at 30°C which showed deviation from Fickian diffusion. Fiber treatment reduces water sorption about three times even within the first twenty five minutes as observed by Srubar et al (2012).

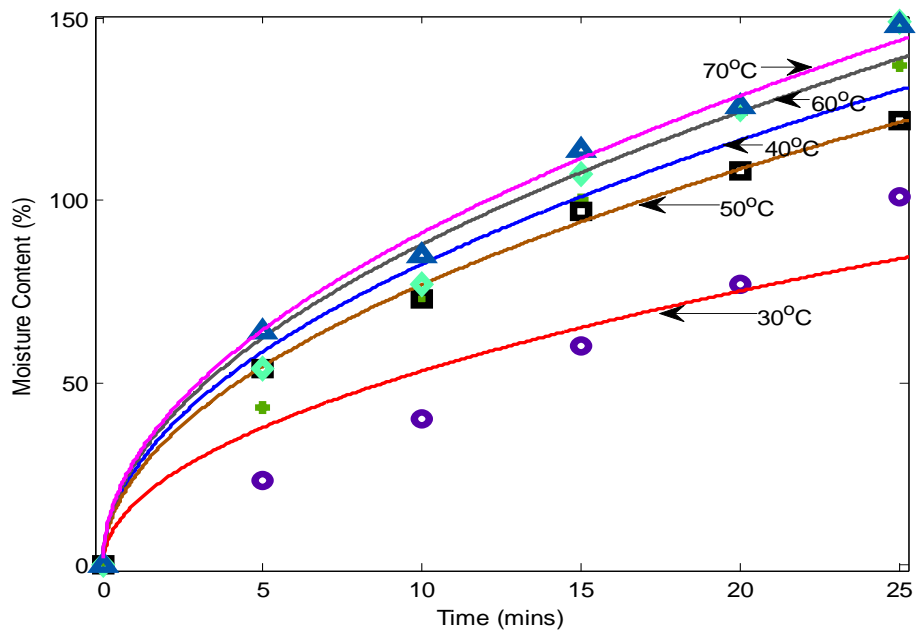


Figure 4.37: Becker's Model Graphical fit to Untreated Rattan Palm Fiber

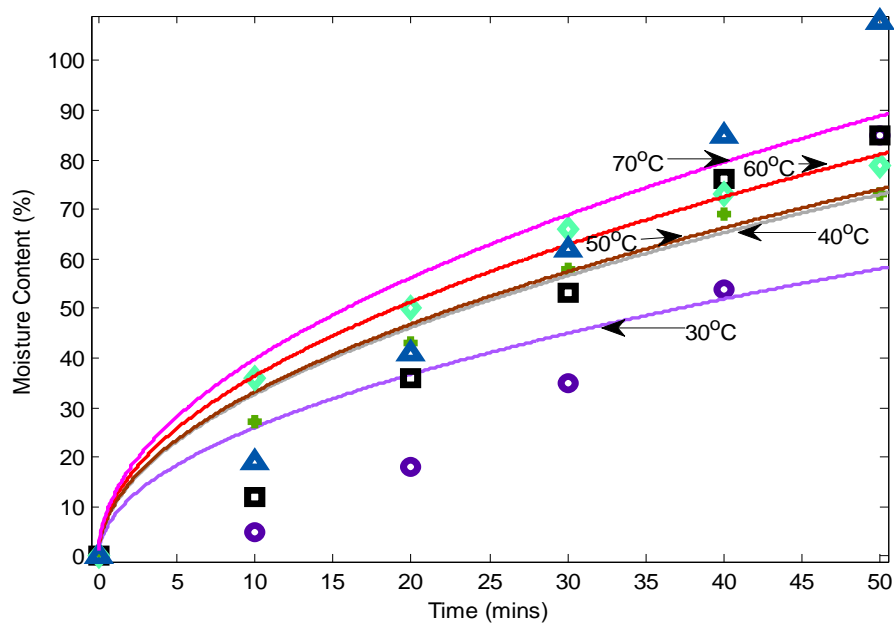


Figure 4.38: Becker's Model Graphical fit to Treated Rattan Palm Fiber

Generally, the water sorption capacity and rate of rattan palm fiber are less than those of empty palm bunch fiber, though this is more prominent before treatment. This is due to the low hemicelluloses content of rattan palm fiber (Dhakal et al, 2006).

4.8 Scanning Electron Microscopy(SEM) Analysis

SEM analysis was done on treated and untreated fiber samples at different magnifications and the results are presented in Figures 4.39 to 4.56.

4.8.1 SEM Analysis for Treated and Untreated Empty Plantain Bunch Fiber

Figure 4.39, Figure 4.41 and Figure 4.43 present SEM analysis for untreated empty plantain bunch fiber at magnifications of 500, 1500 and 2500 respectively, while Figure 4.40, Figure 4.42 and Figure 4.44 present SEM analysis for treated empty plantain bunch fiber at magnifications of 500, 1000 and 2000 respectively. It can be observed by comparing the SEM analysis results of untreated and treated empty plantain bunch fiber that the treatment brought about increase in fiber surface roughness, which is often responsible for increased exposure of cellulose on fiber surface, increased number of possible sites and allowing for better fiber wetting. It can also be observed by comparing the SEM analysis of untreated and treated fiber that the fiber bundles have started undergoing fibrillation (micro-fibrillation) - breakdown of fiber bundle into smaller fibers.

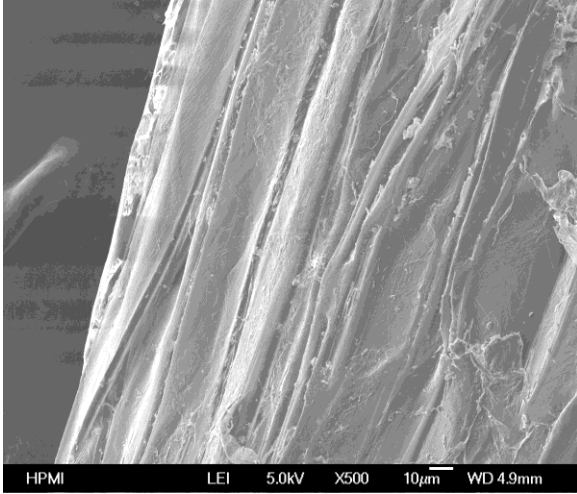


Fig. 4.39:SEM for Untreated Empty Plantain Bunch Fiber(x500)

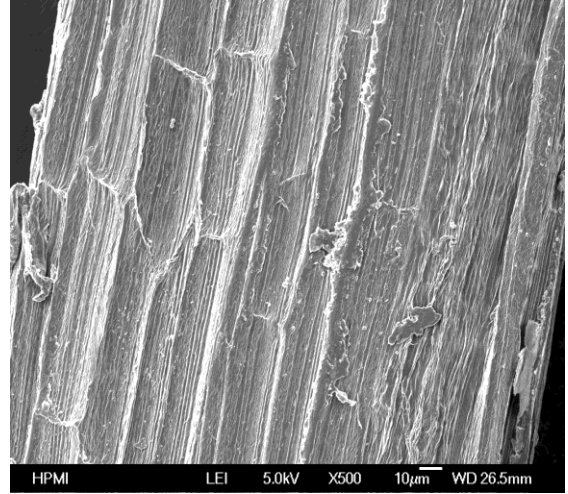


Fig. 4.40:SEM for Treated Empty Plantain Bunch Fiber(x500)

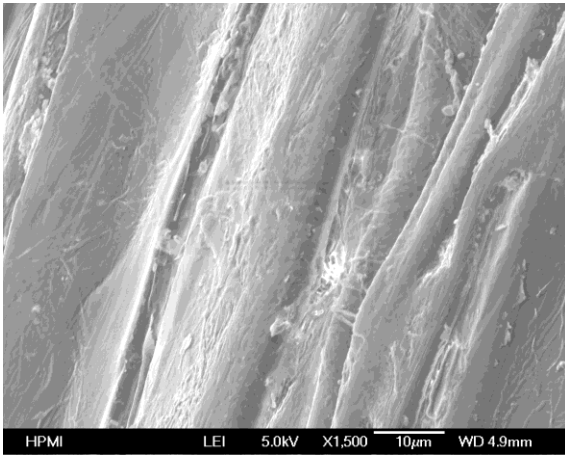


Fig. 4.41:SEM for Untreated Plantain Bunch Fiber(x1500)

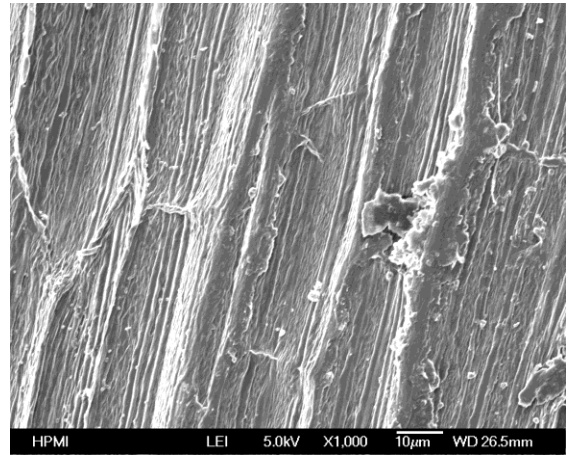


Fig. 4.42:SEM for Treated Plantain Bunch Fiber(x1000)

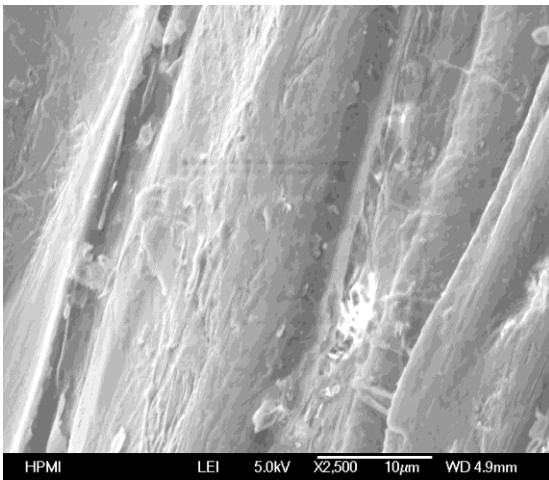


Fig. 4.43:SEM for Untreated Plantain Bunch Fiber(x2500)

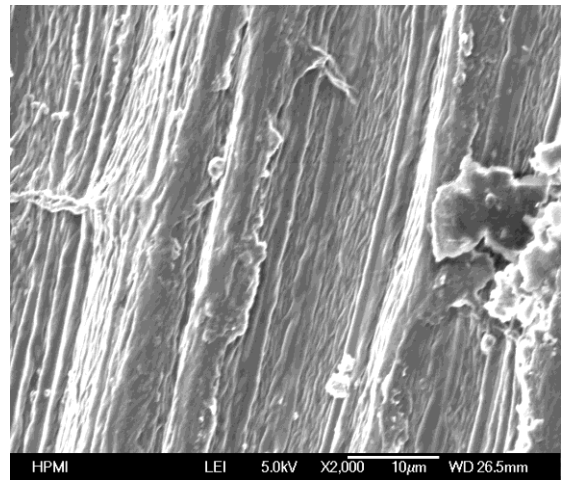


Fig. 4.44:SEM for Treated Plantain Bunch Fiber(x2000)

4.8.2 SEM Analysis for Treated and Untreated Empty Palm Bunch Fiber

Figure 4.45, Figure 4.47 and Figure 4.49 present SEM analysis for untreated empty palm bunch fiber at magnifications of 250, 500 and 1500 respectively, while Figure 4.46, Figure 4.48 and Figure 4.50 present SEM analysis for treated empty palm bunch fiber at magnifications of 250, 500 and 1000 respectively. It can be observed by comparing the SEM analysis results of untreated and treated empty palm bunch fiber that the treatment brought about increase in fiber surface roughness, which is often responsible for increased exposure of cellulose on fiber surface, increased number of possible sites and allowing for better fiber wetting. It can also be observed by comparing the SEM analysis of untreated and treated fiber that the fiber bundles have started undergoing fibrillation (micro-fibrillation) - breakdown of fiber bundle into smaller fibers and thus increase in aspect ratio.

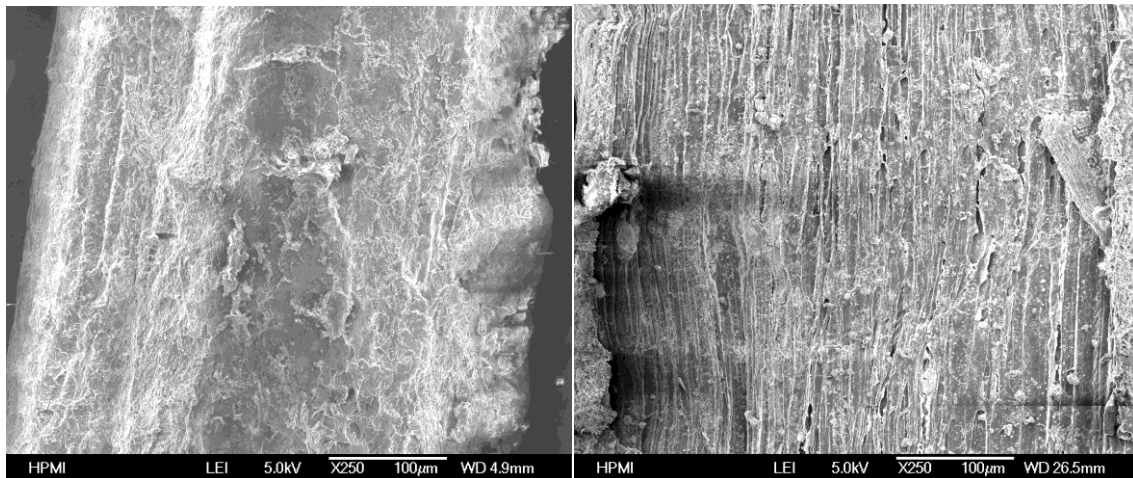


Fig. 4.45: SEM for Untreated Empty Palm Bunch Fiber (x250) Fig. 4.46: SEM for Treated Empty Palm Bunch Fiber (x250)

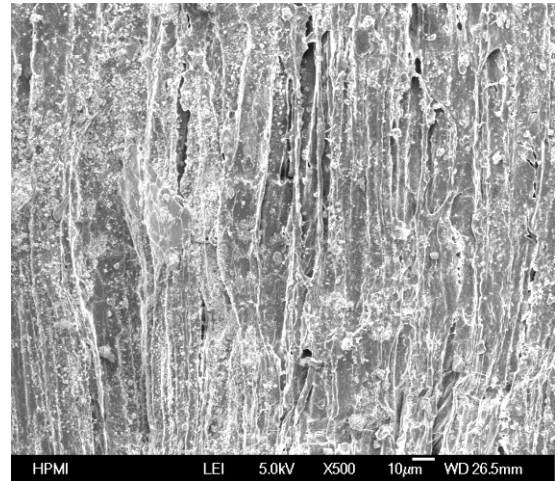
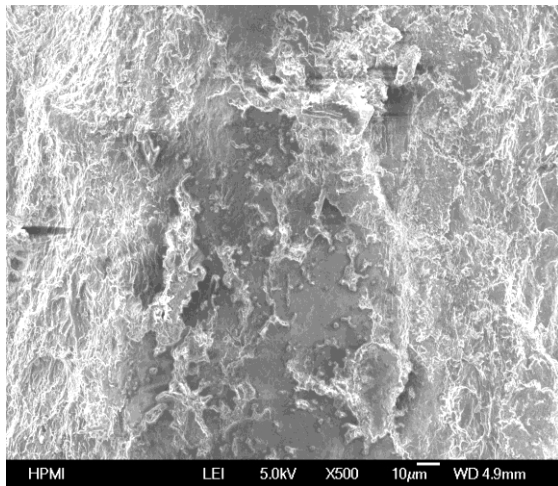


Fig. 4.47: SEM for Untreated Empty Palm Bunch Fiber (x500) Fig. 4.48: SEM for Treated Empty Palm Bunch Fiber (x500)

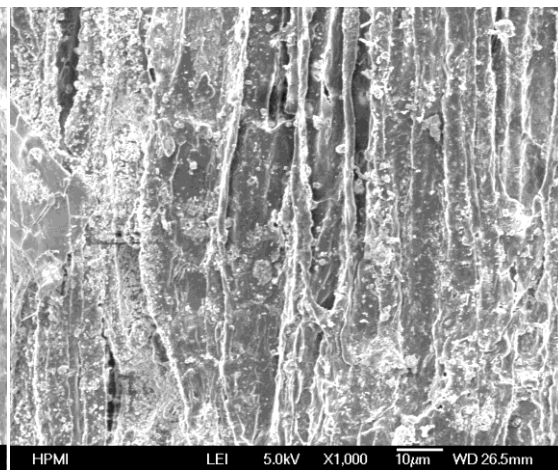
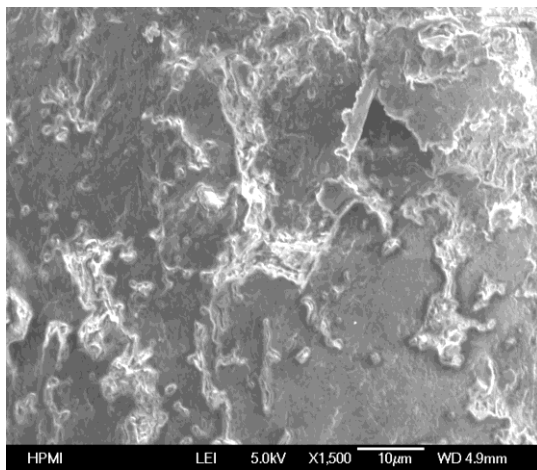


Fig. 4.49: SEM for Untreated Empty Palm Bunch Fiber (x1500) Fig. 4.50: SEM for Treated Empty Palm Bunch Fiber (x1000)

4.8.3 SEM Analysis for Treated and Untreated Rattan Palm Fiber

Figure 4.51, Figure 4.53 and Figure 4.55 present SEM analysis for untreated rattan palm fiber at magnifications of 250, 500 and 1000 respectively, while Figure 4.52, Figure 4.54 and Figure 4.56 present SEM analysis for treated rattan palm fiber at magnifications of 250, 500 and 1000 respectively. It can be observed by comparing the SEM analysis results of untreated and treated rattan palm bunch fiber that the treatment brought about increase in fiber surface roughness,

which is often responsible for increased exposure of cellulose on fiber surface, increased number of possible sites and allowing for better fiber wetting. It can also be observed by comparing the SEM analysis of untreated and treated fiber that the fiber bundles have started undergoing fibrillation (micro-fibrillation) - breakdown of fiber bundle into smaller fibers and thus increase in aspect ratio, though this is not prominent as in other fibers. This is due to the low hemicelluloses content of rattan palm fiber in comparison to empty plantain bunch fiber and empty palm bunch fiber, making it the least of the three fibers in observed change in property due to mercerization.

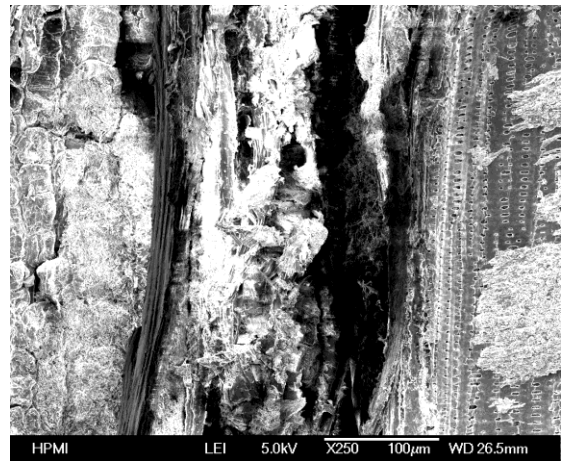
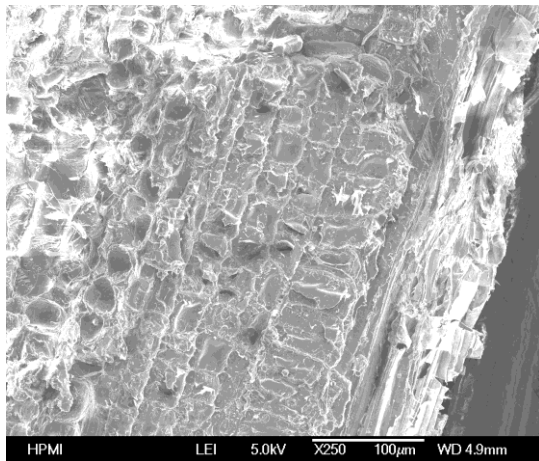


Fig. 4.51: SEM for Untreated Rattan Palm Fiber (x250) Fig. 4.52: SEM for Treated Rattan Palm Fiber (x250)

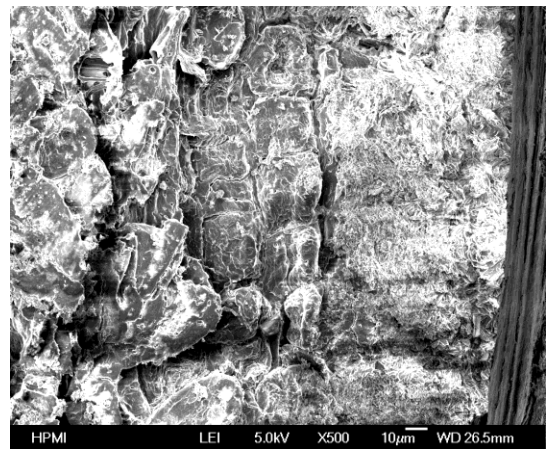
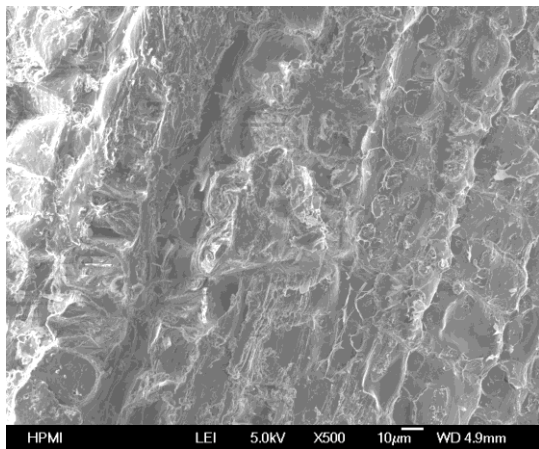


Fig. 4.53: SEM for Untreated Rattan Palm Fiber (x500) Fig. 4.54: SEM for Treated Rattan Palm Fiber (x500)

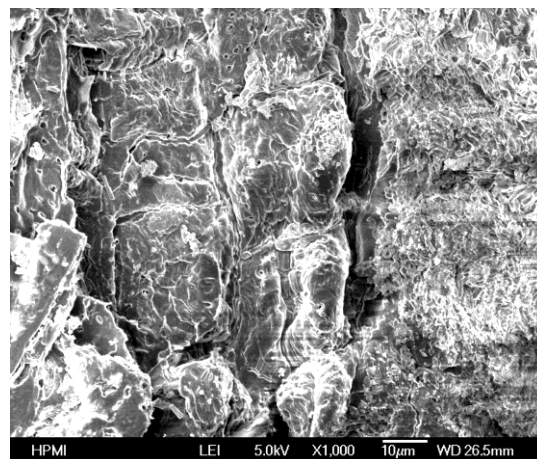
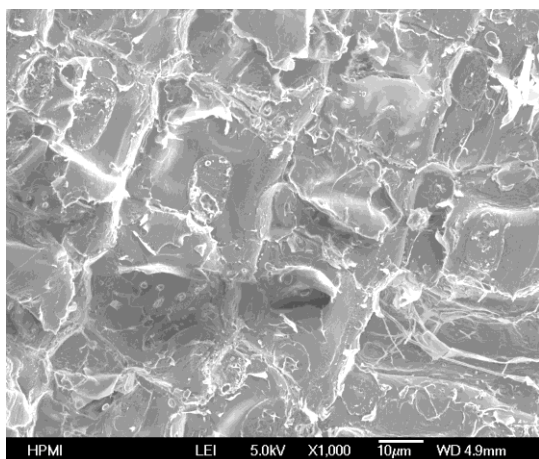


Fig. 4.55: SEM for Untreated RattanPalm Fiber (x1000) Fig. 4.56:SEM for Treated RattanPalm Fiber (x1000)

4.9 Mechanical Properties of Empty Plantain Fiber-Polyester Composite

The tensile test data for empty plantain bunch-polyester composite for fiber lengths of 10mm, 30mm and 50mm (fiber aspect ratios of 23.6183m/m, 70.8550m/m and 118.0916m/m) and fiber volume fractions of 10%, 30% and 50% were analyzed using the traditional approach and the new approach (highlighted) for Young's modulus, tensile strength, yield strength, ultimate elongation and toughness, and the results are given in Table 4.85. It can be observed from Table 4.85 that the tensile strength and toughness obtained using the two techniques are close for most samples, but the Young's modulus and yield strength values differ, with the new approach having higher values of Young's modulus for most of the samples.

Table 4.85: Empty Plantain Bunch Fiber-Polyester Composite Analysis

Fiber Length (mm)	Fiber Aspect Ratio (m/m)	Volume Fraction (%)	Young Modulus (GPa)	Tensile Strength (MPa)	Yield Strength (MPa)	Ultimate Elongation (%)	Toughness (MPa)
10	23.6183	10	4.4744 *5.8391	24.9876 *25.6314	23.7218 *20.2284	1.8590	0.382525 *0.4059
10	23.6183	30	5.6100 *1.5807	29.2470 *68.3601	9.5765 *19.5267	2.5000	0.418183 *0.4230
10	23.6183	50	3.7312 *5.1957	26.9155 *27.2338	24.6540 *20.4248	2.0630	0.442986 *0.4727
30	70.8550	10	3.9542 *7.4504	31.4467 *43.2445	23.9238 *19.6140	1.3280	0.274723 *0.2808
30	70.8550	30	4.6690 *6.8053	34.8739 *34.6684	27.6724 *21.9523	2.5000	0.694539 *0.6976
30	70.8550	50	3.5700 *3.8078	33.2262 *34.5936	31.7125 *31.4061	2.1560	0.557679 *0.5687
50	118.0916	10	3.6803 *4.9718	28.0112 *28.7382	24.8942 *19.9416	2.2656	0.509741 *0.5865
50	118.0916	30	4.7661 0.9192	32.2706 *32.2706	8.6147 *32.2706	3.0200	0.512797 *0.5052
50	118.0916	50	3.1617 *4.1149	29.6589 *29.7586	21.8382 *18.1395	2.6600	0.6055 *0.8683

*Value computed using the new approach

4.9.1 Young's Modulus Analysis for Empty Plantain Bunch-Polyester Composite

Young's modulus results from the traditional approach in Table 4.85 were modeled using response surface methodology and the results are presented in Table 4.86, Table 4.87 and Figure 4.57. The pure quadratic model ($y = a_1 + a_2x_1 + a_3x_2 + a_4x_1^2 + a_5x_2^2$) gave the best fit, based on the Adjusted-R² and was therefore used. It can be observed from Table 4.86 that the response surface model for Young's modulus of empty plantain bunch-polyester composite explains 93% of the variability observed in the Young's modulus of the composite. The t-statistics value and its p-value show that most of the variable coefficients are significant except the quadratic term of

the aspect ratio. The model is adequate at 95% confidence interval based on the f-statistics. It can be observed from the ANOVA table (Table 4.87) that fiber aspect ratio and volume fraction are significant variables at 95% confidence interval, though fiber volume fraction is the more significant term, which corroborates observation from the surface plot (Figure 4.57) showing the significant change in Young's modulus (as observed from the colour variation) along the fiber volume fraction axis. The surface plot also reveals that the Young's modulus reduces slightly with increase in fiber aspect ratio.

Table 4.86: Empty Plantain Bunch-Polyester Young's Modulus RSM Model Statistics

Variables	Coefficients	Std. Error	t-stat	P-value	F-stat
Constant	3.4327	0.3687	9.3092	0.0007	SSE = 0.16149
Aspect Ratio (m/m)	-0.0188	0.0092	-2.0425	0.1106	DFE = 4
Volume Frac.(%)	0.1742	0.0217	8.0286	0.0013	DFR = 4
Aspect Ratio^2	7.7481e-05	6.3675e-05	1.2168	0.2906	SSR = 4.4639
Vf^2	-0.0031	0.0004	-8.8196	0.0009	F = 27.642
	R ² = 0.9651	Adj.R ² = 0.9302			P-val = 0.0035718

Table 4.87: Empty Plantain Bunch-Polyester Young's Modulus Analysis of Variance

Source	Sum Sq.	Df	Mean Sq.	F	Prob>F
Fiber Aspect Ratio (m/m)	0.87195	2	0.43598	10.8	0.0244
Fiber Volume Fraction (Vf) (%)	3.5919	2	1.79595	44.48	0.0019
Error	0.16149	4	0.04037		
Total	4.62535	8			

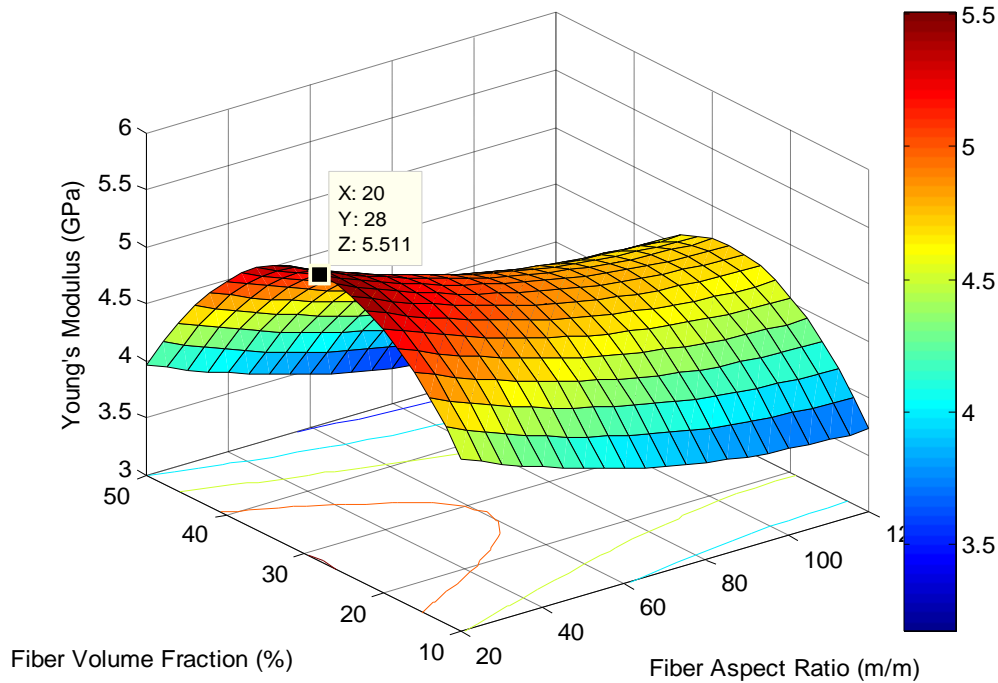


Figure 4.57: Surface plot for modulus of empty plantain bunch-polyester composite

4.9.2 Tensile Strength Analysis for Empty Plantain Bunch-Polyester Composite

Tensile strength results from the traditional approach in Table 4.85 were modeled using response surface methodology and the results are presented in Table 4.88, Table 4.89 and Figure 4.58. The pure quadratic model ($y = a_1 + a_2x_1 + a_3x_2 + a_4x_1^2 + a_5x_2^2$) gave the best fit, based on the Adjusted- R^2 and was therefore used. It can be observed from Table 4.88 that the response surface model for tensile strength of empty plantain bunch-polyester composite explains 99% of the variability observed in the tensile strength of the composite. The t-statistics value and its p-value show that fiber aspect ratio and volume fraction are significant in their linear and quadratic terms. The model is adequate based on the f-statistics. It can be observed from the ANOVA table (Table 4.88) that both variables are significant though fiber aspect ratio has higher significance. This corroborates observation from the surface plot (Figure 4.58) showing the significant change

in tensile strength (as observed from the colour variation) along the fiberaspect ratio axis. The surface plot also reveals initial increase and subsequent decrease in tensile strength with increase in fiberaspect ratio and volume fraction.

Table 4.88: Empty Plantain Bunch-PolyesterTensile Strength RSM Model Statistics

Variables	Coefficients	Std. Error	t-stat	P-value	F-stat
Constant	14.2531	0.5279	27.0010	1.1186e-05	SSE =0.33093
Aspect Ratio (m/m)	0.3274	0.0132	24.8913	1.5463e-05	DFE = 4
Vol. Frac.(%)	0.5080	0.0311	16.3527	8.1854e-05	DFR = 4
Asp. Ratio ^2	-0.0021	9.1152e-05	-22.9469	2.1369e-05	SSR = 80.313
Vf^2	-0.0077	0.0005	-15.1901	0.0001	F = 242.68
	R ² = 0.9959	Adj. R ² = 9918			P-val =5.0382e-5

Table 4.89: Empty Plantain Bunch-Polyester Tensile Strength Analysis of Variance

Source	Sum Sq.	Df	Mean Sq.	F	Prob>F
Fiber Aspect Ratio (m/m)	56.4434	2	28.2217	341.12	0
Fiber Volume Fraction (Vf) (%)	23.8693	2	11.9347	144.25	0.0002
Error	0.3309	4	0.0827		
Total	80.6436	8			

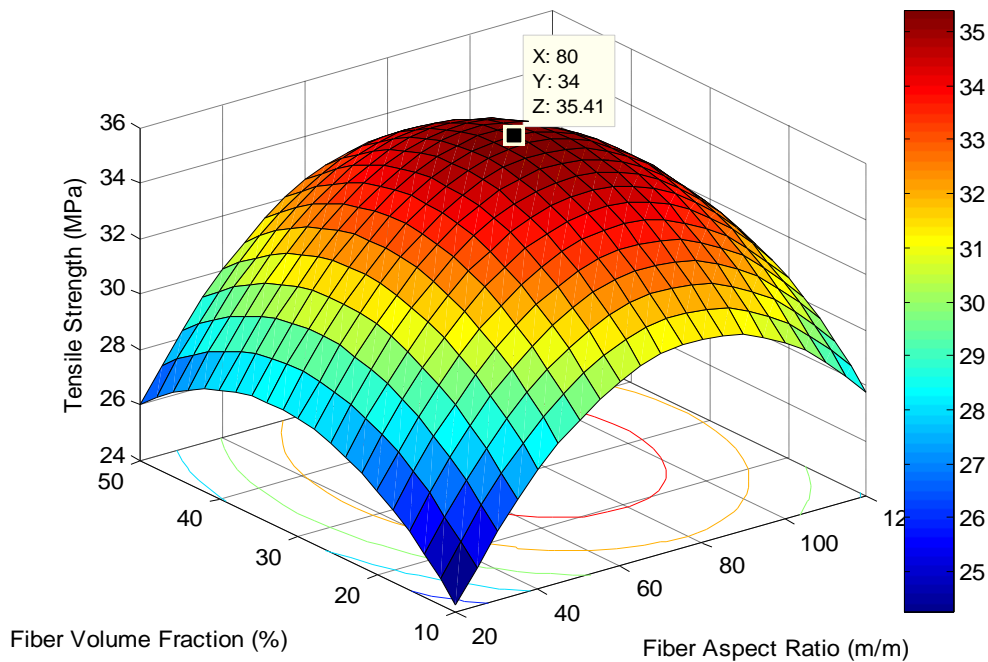


Figure 4.58: Surface plot for tensile strength of plantain bunch-polyester composite

4.9.3 Yield Strength Analysis for Empty Plantain Bunch-Polyester Composite

Yield strength results from the traditional approach in Table 4.85 were modeled using response surface methodology and the results are presented in Table 4.90, Table 4.91 and Figure 4.59. The pure quadratic model ($y = a_1 + a_2x_1 + a_3x_2 + a_4x_1^2 + a_5x_2^2$) gave the best fit, based on the Adjusted- R^2 and was therefore used. It can be observed from Table 4.90 that the response surface model for yield strength of empty plantain bunch-polyester fiber explains 74% of the variability observed in the yield strength of the composite. The t-statistics value and its p-value show that none of the variables is significant at 95% confidence, though all terms are significant at 90% confidence interval. The model is not adequate based on the f-statistics. It can be observed from the ANOVA table (Table 4.91) that none of the variables is significant though fiber volume fraction has higher significance. This corroborates observation from the surface plot (Figure

4.59) showing more significant change in yield strength along the fiber length axis. Yield strength does not change significantly with fiber aspect ratio and fiber volume fraction.

Table 4.90: Empty Plantain Bunch-Polyester Yield Strength RSM Model Statistics

Variables	Coefficients	Std. Error	t-stat	P-value	F-stat
Constant	22.5844	10.2181	2.2102	0.0916	SSE = 124
Aspect Ratio (m/m)	0.5552	0.2546	2.1804	0.0947	DFE = 4
Vol. Frac.(%)	-1.4282	0.6014	-2.3749	0.0764	DFR = 4
Asp. Ratio^2	-0.0040	0.0018	-2.2571	0.0870	SSR = 357.92
Vf^2	0.0246	0.0098	2.4984	0.0669	F = 2.8864
	$R^2 = 0.7427$	$Adj.R^2 = 0.4854$			P-val = 0.16455

Table 4.91: Empty Plantain Bunch-Polyester Yield Strength Analysis of Variance

Source	Sum Sq.	Df	Mean Sq.	F	Prob>F
Fiber Length (Fl) (mm)	159.065	2	79.5325	2.57	0.1919
Fiber Volume Fraction (Vf) (%)	198.851	2	99.4254	3.21	0.1475
Error	123.999	4	30.9998		
Total	481.915	8			

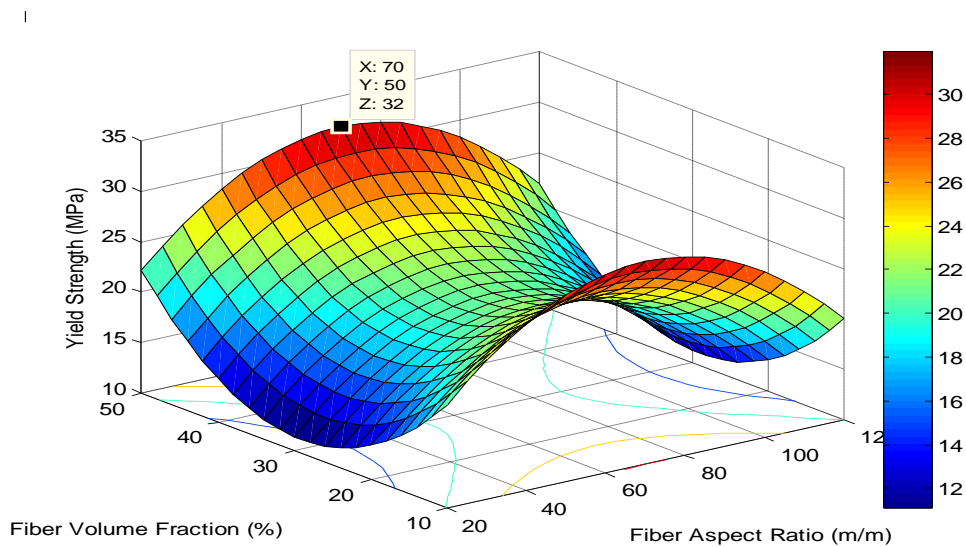


Figure 4.59: Surface plot for yield strength of empty plantain bunch-polyester composite

4.9.4 Ultimate Elongation Analysis for Empty Plantain Bunch-Polyester Composite

Ultimate elongation results from Table 4.85 were modeled using response surface methodology and the results are presented in Table 4.92, Table 4.93 and Figure 4.60. The pure quadratic model ($y = a_1 + a_2x_1 + a_3x_2 + a_4x_1^2 + a_5x_2^2$) gave the best fit, based on the Adjusted-R² and was therefore used. It can be observed from Table 4.92 that the response surface model for ultimate elongation of empty plantain bunch-polyester fiber explains 94% of the variability observed in the ultimate elongation of the composite. The t-statistics value and its p-value show that all the variables are significant at 95% confidence, except for the linear term of aspect ratio which is significant at 90% confidence. The model is adequate based on the f-statistics. It can be observed from the ANOVA table (Table 4.93) that both variables are significant, though fiber volume fraction has higher significance. This corroborates observation from the surface plot (Figure 4.60) showing the significant change in Ultimate Elongation (as observed from the colour variation) along the fibervolume fraction axis. The surface plot also reveals increase in the elongation with fiber volume fraction to a maximum before reduction.

Table 4.92: Empty Plantain Bunch-Polyester Ultimate Elongation RSM Model Statistics

Variables	Coefficients	Std. Error	t-stat	P-value	F-stat
Constant	1.1784	0.3205	3.6772	0.0213	SSE =0.12196
Aspect Ratio (m/m)	-0.0200	0.0080	-2.5075	0.0662	DFE = 4
Vol. Frac.(%)	0.1046	0.0189	5.5457	0.0052	DFR = 4
Asp. Ratio^2	0.0002	5.5337e-05	3.2390	0.0317	SSR = 1.8099
Vf^2	-0.0015	0.0003	-5.0057	0.0075	F = 14.84
	R ² = 0.9369	Adj. R ² =0.8737			P-val =0.011454

Table 4.93: Empty Plantain Bunch-Polyester Ultimate Elongation ANOVA Table

Source	Sum Sq.	Df	Mean Sq.	F	Prob>F
Fiber Length (Fl) (mm)	0.70679	2	0.35339	11.59	0.0217
Fiber Volume Fraction (Vf) (%)	1.10312	2	0.55156	18.09	0.0099
Error	0.12196	4	0.03049		
Total	1.93187	8			

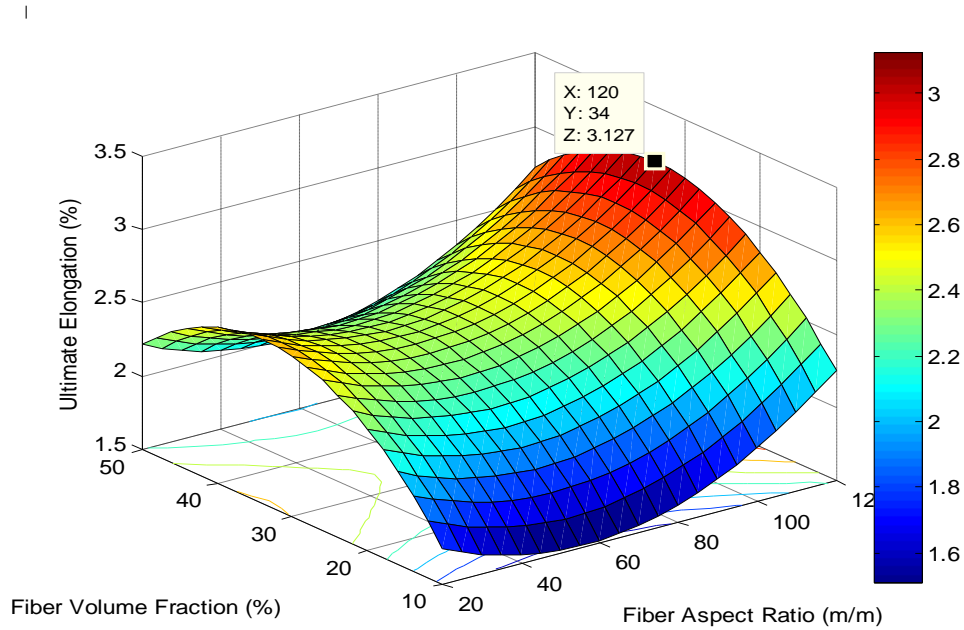


Figure 4.60: Surface plot for ultimate elongation plantain bunch-polyester

4.9.5 Empty Plantain Bunch-Polyester Composite Toughness Analysis

Results for toughness of empty plantain bunch-polyester composite from the traditional approach in Table 4.85 were modeled using response surface methodology and the results are presented in Table 4.94, Table 4.95 and Figure 4.61. The pure quadratic model ($y = a_1 + a_2x_1 + a_3x_2 + a_4x_1^2 + a_5x_2^2$) gave the best fit, based on the Adjusted-R² and was therefore used. It can be observed from Table 4.95 that the response surface model for toughness of empty plantain bunch-polyester fiber explains only 57% of the variability observed in the toughness of the

composite. The t-statistics value and its p-value show that none of the variables is significant. The model is not adequate based on the f-statistics. It can be observed from the ANOVA table (Table 4.95) that none of the variables is significant though fiber volume fraction has higher significance. This corroborates observation from the surface plot (Figure 4.61) showing the significant change in toughness (as observed from the colour variation) along the fiber volume fraction axis. The surface plot also reveals an initial drop followed by an increase in toughness with increase in fiber aspect ratio and volume fraction.

Table 4.94: Empty Plantain Bunch-Polyester Toughness RSM Model Statistics

Variables	Coefficients	Std. Error	t-stat	P-value	F-stat
Constant	0.1036	0.2124	0.4876	0.6513	SSE = 0.053563
Aspect Ratio (mm)	0.0033	0.0053	0.6311	0.5622	DFE = 4
Vol. Frac.(%)	0.0159	0.0125	1.2701	0.2729	DFR = 4
Asp. Ratio^2	-1.4199e-05	3.6671e-05	-0.3872	0.7183	SSR = 0.072071
Vf^2	-0.0002	0.0002	-0.9897	0.3783	F = 1.3455
	R ² =0.5737	Adj. R ² =0.1473			P-val =0.39301

Table 4.95: Empty Plantain Bunch-Polyester Toughness Analysis of Variance

Source	Sum Sq.	Df	Mean Sq.	F	Prob>F
Fiber Length (Fl) (mm)	0.02561	2	0.0128	0.96	0.4577
Fiber Volume Fraction (Vf) (%)	0.04646	2	0.02323	1.73	0.2867
Error	0.05356	4	0.01339		
Total	0.12563	8			

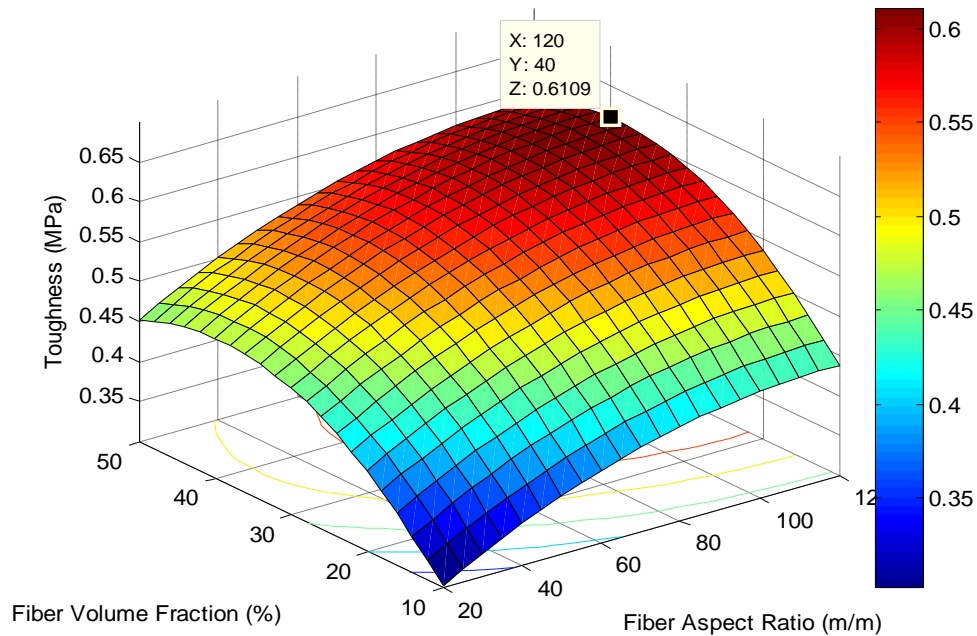


Figure 4.61: Surface plot for toughness of plantain bunch-polyester composite

4.9.6 Empty Plantain Bunch-Polyester Composite Tensile Properties Optimization

The RSM model coefficients from Table 4.86, Table 4.88, Table 4.90, Table 4.92 and Table 4.94 were used to run a MATLAB 7.9 optimization code and the optimal values for fiber aspect ratio and fiber volume fraction are presented alongside predicted optimal values of mechanical properties and the experimental values for validation. The optimization table (Table 4.96) reveals that most properties have their optimum values at fiber volume fractions between 28% and 40%. This observation is in agreement with observations from Gassan and Bledzki (1999), Mohanty et al (2000), Ratna Prasad et al (2008), Chimekwene et al (2012) and Ihueze et al (2012). It can also be observed from Table 4.97 that the model predicted values for mechanical properties are close to the experimentally validated values, except for toughness and yield strength. This may be due to the low fit of the RSM model for these properties.

Table 4.96: Optimal Values for Mechanical Properties Empty Plantain Bunch-Polyester

Variables	Toughness	Tensile Strength	Young Modulus	Yield Strength	%El
Fiber Aspect Ratio (m/m)	118	80	23.6	70	118
Fiber Volume Fraction (%)	40	34	28	50	34

Table 4.97: Predicted versus Experimental Optimum for Empty Plantain Bunch-Polyester

	Toughness (MPa)	Tensile Strength (MPa)	Young Modulus (GPa)	Yield Strength (MPa)	%El (%)
Model Predicted Values	0.6113	35.4100	5.5110	32.0000	3.4281
Experimental Values	0.5587	35.2648	5.6012	23.7664	3.0372

4.10 Mechanical Properties of Empty Plantain Bunch-Epoxy Composite

The tensile test data for empty plantain bunch-epoxy composite for fiber lengths of 10mm, 30mm and 50mm (fiber aspect ratios of 23.6183m/m, 70.8550m/m and 118.0916m/m) and fiber volume fractions of 10%, 30% and 50% were analyzed using the traditional approach for Young's modulus, tensile strength, yield strength, ultimate elongation and toughness, and the results are given in Table 4.98. It can be observed from Table 4.98 that the tensile strength, toughness and yield strength obtained using the two techniques are close but the Young's modulus values differ with the new approach having higher values of Young's modulus.

Table 4.98: Empty Plantain Bunch-Epoxy Composite Tensile Test Analysis

Fiber Length (mm)	Fiber Aspect Ratio (m/m)	Volume Fraction (%)	Young Modulus (GPa)	Tensile Strength (MPa)	Yield Strength (MPa)	Ultimate Elongation (%)	Toughness (MPa)
10	23.6183	10	1.1027 *3.1853	6.1541 *6.1659	5.0961 *4.1802	3.75	0.207652 *0.2097
10	23.6183	30	2.2720 *5.9769	7.1957 *7.0362	5.9000 *5.1321	4.72	0.307617 *0.3108
10	23.6183	50	1.7210 *5.1404	6.6817 *6.8770	5.1697 *4.7178	2.97	0.171523 *0.1754
30	70.8550	10	1.6760 *2.4598	7.5041 *7.6443	4.70274 *4.1900	5.16	0.324029 *0.3272
30	70.8550	30	2.9710 *7.6161	8.4293 *8.6801	6.79284 *6.1888	2.73	0.203074 *0.2056
30	70.8550	50	1.7710 *6.5704	7.1597 *7.0933	5.7389 *5.1165	4.22	0.26834 *0.2714
50	118.0916	10	1.6320 *3.7531	6.9901 *6.9738	5.6693 *4.7800	2.73	0.16571 *0.1670
50	118.0916	30	2.5850 *1.1567	8.0344 *9.4175	3.49882 *4.3142	4.45	0.29019 *0.2882
50	118.0916	50	1.6430 *2.7895	7.3104 *7.9823	4.54599 *4.3487	4.53	0.295807 *0.2960

*Value computed using the new approach

4.10.1 Young’s Modulus Analysis for Empty Plantain Bunch-Epoxy Composite

Young’s modulus results from the traditional approach in Table 4.98 were modeled using response surface methodology and the results are presented in Table 4.99, Table 4.100 and Figure 4.62. The quadratic model ($y = a_1 + a_2x_1 + a_3x_2 + a_4x_1x_2 + a_5x_1^2 + a_6x_2^2$) gave the best fit, based on the Adjusted-R² and was therefore used. It can be observed from Table 4.99 that the response surface model for Young’s modulus of empty plantain bunch-epoxy composite explains 97% of the variability observed in the Young’s modulus of the composite. The t-statistics value and its p-value show that most variables are significant at 95% or 90% confidence interval except the interaction term. The model is also adequate based on the f-statistics. It can be

observed from the ANOVA table (Table 4.100) that fiber volume fraction is significant. This corroborates observation from the surface plot (Figure 4.62). The surface plot also reveals a good level of interaction between the variables, though not significant. Young's modulus increases with increase in fiber aspect ratio and also fiber volume fraction to a maximum before an observed drop.

Table 4.99: Empty Plantain Bunch-Epoxy Modulus RSM Model Statistics

Variables	Coefficients	Std. Error	t-stat	P-value	F-stat
Constant	-0.8920	0.3314	-2.6913	0.0743	SSE = 0.07112
Aspect Ratio (m/m)	0.0274	0.0075	3.6788	0.0348	DFE = 3
Fiber Vol. Frac.(%)	0.1702	0.0176	9.6669	0.0024	DFR = 5
Asp. Ratio*Vf	-0.0002	8.1488e-05	-1.9721	0.1431	SSR = 2.5476
Asp. Ratio^2	-0.0001	4.8793e-05	-2.8784	0.0636	F = 21.493
Vf^2	-0.0025	0.0003	-9.3539	0.0026	P-val = 0.014826
	R ² = 0.9728	Adj. R ² = 0.9276			

Table 4.100: Empty Plantain Bunch-Epoxy Young's Modulus ANOVA Table

Source	Sum Sq.	Df	Mean Sq.	F	Prob>F
Fiber Aspect Ratio (m/m)	0.29378	2	0.14689	3.6	0.1277
Fiber Volume Fraction (Vf) (%)	2.16164	2	1.08082	26.47	0.0049
Error	0.16332	4	0.04083		
Total	2.61874	8			

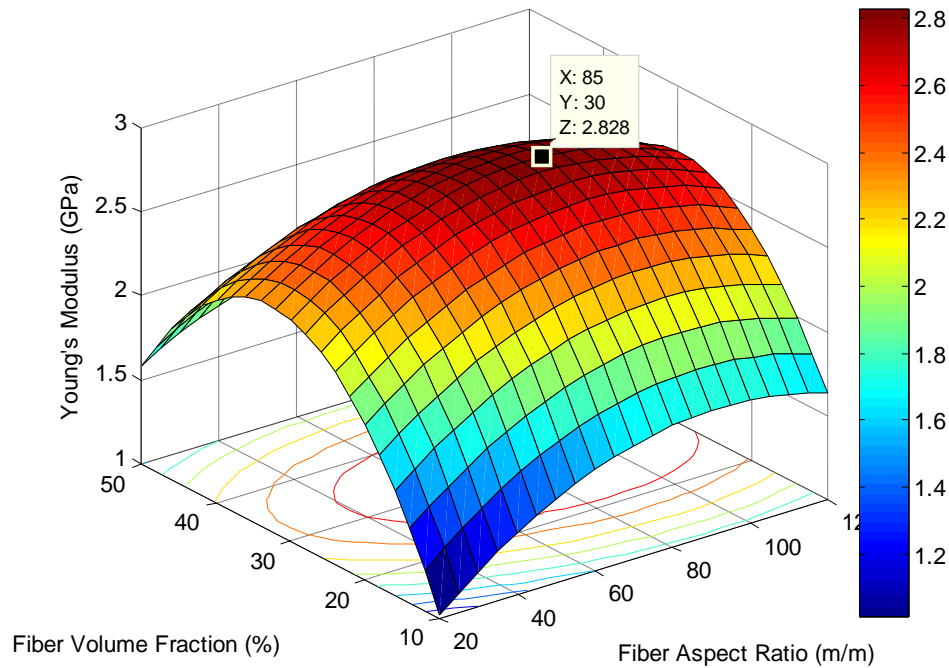


Figure 4.62: Surface plot for modulus of plantain bunch-epoxy composite

4.10.2 Tensile Strength Analysis for Empty Plantain Bunch-Epoxy Composite

Tensile strength results from the traditional approach in Table 4.98 were modeled using response surface methodology and the results are presented in Table 4.101, Table 4.102 and Figure 4.63. The pure quadratic model ($y = a_1 + a_2x_1 + a_3x_2 + a_4x_1^2 + a_5x_2^2$) gave the best fit, based on the Adjusted- R^2 and was therefore used. It can be observed from Table 4.101 that the response surface model for tensile strength of empty plantain bunch-epoxy composite explains 93% of the variability observed in the tensile strength of the composite. The t-statistics value and its p-value show that all the variables are significant at 95% confidence interval. The model is adequate based on the f-statistics. It can also be observed from the ANOVA table (Table 4.102) that the two variables (fiber aspect ratio and fiber volume fraction) are significant. This corroborates observation from the surface plot (Figure 4.83) which also reveals that the tensile

strength increases with increase in fiberspect ratio and fiber volume fraction to a maximum before a subsequent decrease.

Table 4.101: Empty Plantain Bunch-Epoxy Tensile Strength RSM Model Statistics

Variables	Coefficients	Std. Error	t-stat	P-value	F-stat
Constant	4.1072	0.4522	9.0828	0.0008	SSE = 0.24285
Aspect Ratio (m/m)	0.0486	0.0113	4.3094	0.0126	DFE = 4
Fiber Vol. Frac.(%)	0.1422	0.0266	5.3417	0.0059	DFR = 4
Asp. Ratio^2	-0.0003	7.8084e-05	-3.6540	0.0217	SSR= 3.4291
Vf^2	-0.0023	0.0004	-5.2791	0.0062	F = 14.12
	R ² = 0.9339	Adj.R ² = 0.8677			P-val= 0.012543

Table 4.102: Empty Plantain Bunch-Epoxy Tensile Strength ANOVA Table

Source	Sum Sq.	Df	Mean Sq.	F	Prob>F
Fiber Aspect Ratio (m/m)	1.69488	2	0.84744	13.96	0.0157
Fiber Volume Fraction (Vf) (%)	1.73425	2	0.86713	14.28	0.0151
Error	0.24285	4	0.06071		
Total	3.67198	8			

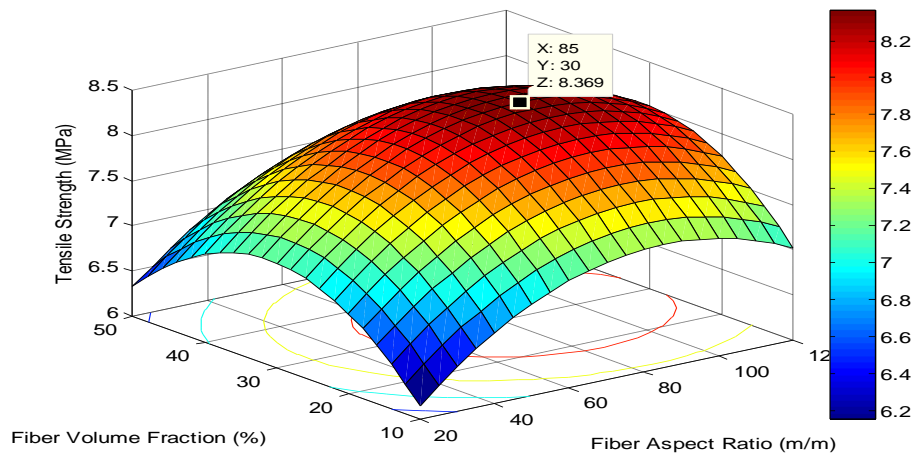


Figure 4.63: Surface plot fortensilestrength of empty plantainbunch-epoxy

4.10.3 Yield Strength Analysis for Empty Plantain Bunch-Epoxy Composite

Yield strength results from the traditional approach in Table 4.98 were modeled using response surface methodology and the results are presented in Table 4.103, Table 4.104 and Figure 4.64. The quadratic model ($y = a_1 + a_2x_1 + a_3x_2 + a_4x_1x_2 + a_5x_1^2 + a_6x_2^2$) gave the best fit, based on the Adjusted-R², and was therefore used. It can be observed from Table 4.103 that the response surface model for yield strength of empty plantain bunch-epoxy composite explains only 58% of the variability observed in the yield strength of the composite. The t-statistics value and its p-value show that none of the terms is significant. The model is not adequate based on the f-statistics. It can be observed from the ANOVA table (Table 4.104) that none of the variables is significant. This corroborates observation from the surface plot (Figure 4.64). The surface plot also reveals slight increase in the yield strength with increase in fiberspect ratio or volume fraction before a maximum.

Table 4.103: Empty Plantain Bunch-Epoxy Yield Strength RSM Model Statistics

Variables	Coefficients	Std. Error	t-stat	P-value	F-stat
Constant	2.8802	2.4666	1.1677	0.3273	SSE = 3.939
Aspect Ratio (m/m)	0.0644	0.0555	1.1614	0.3295	DFE = 3
Fiber Vol. Frac.(%)	0.0943	0.1310	0.7195	0.5238	DFR = 5
Asp. Ratio*Vf	-0.0006	0.0006	-0.9586	0.4085	SSR = 5.4353
Fl ²	-0.0004	0.0004	-1.1497	0.3336	F = 0.82791
Vf ²	-0.0010	0.0020	-0.5061	0.6476	P-val = 0.60297
	R ² = 0.5798	Adj.R ² = -0.1205			

Table 4.104: Empty Plantain Bunch-Epoxy Yield Strength ANOVA Table

Source	Sum Sq.	Df	Mean Sq.	F	Prob>F
Fiber Aspect Ratio (m/m)	3.72111	2	1.86055	1.45	0.3368
Fiber Volume Fraction (Vf) (%)	0.50758	2	0.25379	0.20	0.8285
Error	5.14562	4	1.28641		
Total	9.37431	8			

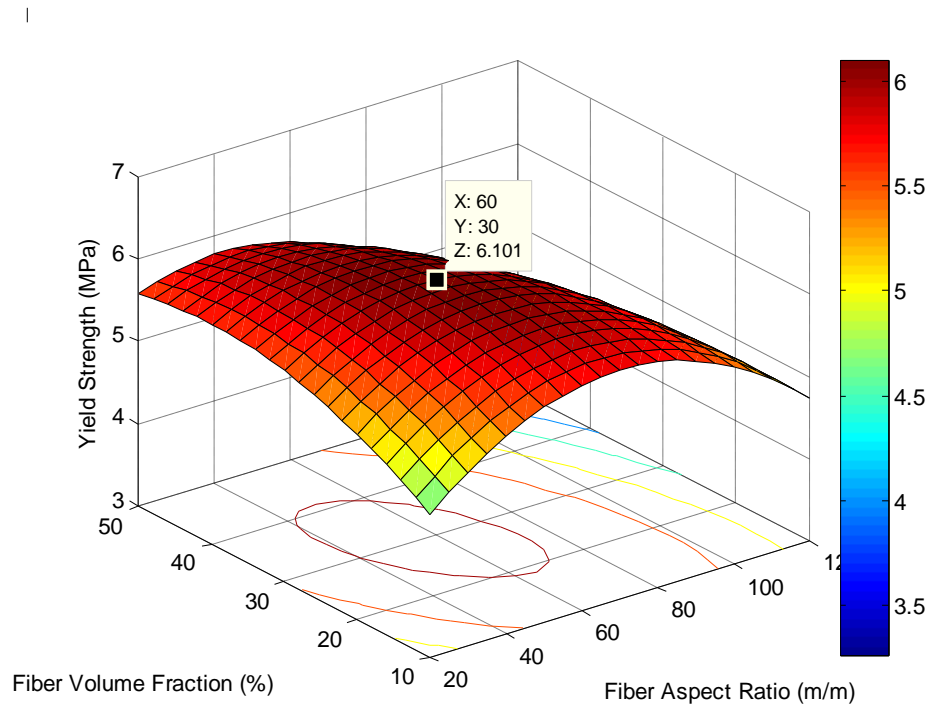


Figure 4.64: Surface plot for yield strength of plantain bunch-epoxy composite

4.10.4 Ultimate Elongation Analysis for Empty Plantain Bunch-Epoxy Composite

Ultimate elongation results from the traditional approach in Table 4.98 were modeled using response surface methodology and the results are presented in Table 4.105, Table 4.106 and Figure 4.65. The quadratic model ($y = a_1 + a_2x_1 + a_3x_2 + a_4x_1x_2 + a_5x_1^2 + a_6x_2^2$) gave the best fit, based on the Adjusted- R^2 and was therefore used. It can be observed from Table 4.105 that the response surface model for ultimate elongation of empty plantain bunch-epoxy

composite explains 26% of the variability observed in the ultimate elongation of the composite. The t-statistics and its p-value show that none of the terms is significant. The model is not adequate based on the f-statistics. It can be observed from the ANOVA table (Table 4.106) that none of the variables is significant. This corroborates observation from the surface plot (Figure 4.65). The surface plot also reveals that the elongation decreases with increase in fiber aspect ratio and fiber volume fraction.

Table 4.105: Empty Plantain Bunch-Epoxy Elongation RSM Model Statistics

Variables	Coefficients	Std. Error	t-stat	P-value	F-stat
Constant	4.8831	2.7602	1.7691	0.1750	SSE = 4.9325
Aspect Ratio (m/m)	-0.0082	0.0621	-0.1322	0.9032	DFE = 3
Fiber Vol. Frac.(%)	-0.0367	0.1466	-0.2504	0.8185	DFR = 5
Asp. Ratio*Vf	0.0007	0.0007	1.0060	0.3885	SSR = 1.7517
Asp. Ratio^2	-7.9923e-05	0.0004	-0.1967	0.8566	F = 0.21308
Vf^2	-0.0002	0.0023	-0.0809	0.9406	P-val = 0.9355
	R ² =0.2621	Adj. R ² =-0.9678			

Table 4.106: Empty Plantain Bunch-Epoxy Ultimate Elongation ANOVA Table

Source	Sum Sq.	Df	Mean Sq.	F	Prob>F
Fiber Aspect Ratio (m/m)	0.07576	2	0.03788	0.02	0.9774
Fiber Volume Fraction (Vf) (%)	0.01182	2	0.00591	0	0.9964
Error	6.59658	4	1.64914		
Total	6.68416	8			

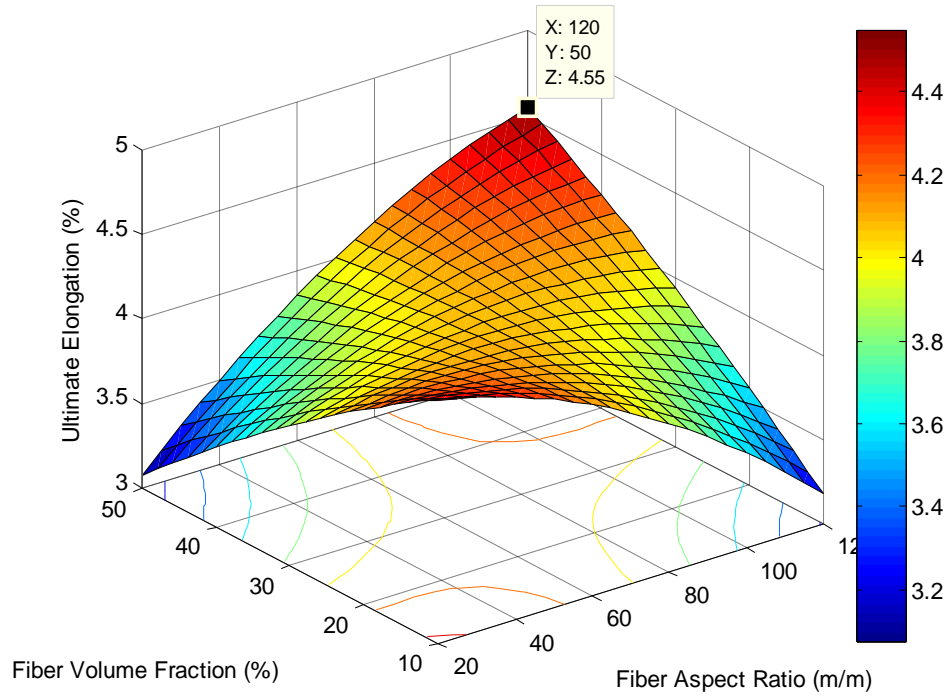


Figure 4.65: Surface plot forelongation of empty plantain bunch-epoxy composite

4.10.5 Toughness Analysis for Empty Plantain Bunch-Epoxy Composite

Results from the traditional approach for toughness of empty plantain bunch-epoxy composite in Table 4.98 were modeled using response surface methodology and the results are presented in Table 4.107, Table 4.108 and Figure 4.66. The quadratic model ($y = a_1 + a_2x_1 + a_3x_2 + a_4x_1x_2 + a_5x_1^2 + a_6x_2^2$) gave the best fit, based on the Adjusted- R^2 and was therefore used. It can be observed from Table 4.107 that the response surface model for toughness of empty plantain bunch-epoxy component explains 36% of the variability observed in the toughness of the composite. The t-statistics value and its p-value show that none of the variables is significant. The model is not adequate based on the f-statistics. It can be observed from the ANOVA table (Table 4.108) that none of the variables is significant. This corroborates observation from the surface plot (Figure 4.66). The surface plot also reveals that the toughness increases with

increase in the variables at high fiber aspect ratio and fiber volume fraction, but the reverse seems to be the case at low values of fiber aspect ratio and fiber volume fraction.

Table 4.107: Empty Plantain Bunch-Epoxy Toughness RSM Model Statistics

Variables	Coefficients	Std. Error	t-stat	P-value	F-stat
Constant	0.2312	0.1728	1.3379	0.2733	SSE = 0.01934
Aspect Ratio (m/m)	0.0005	0.0039	0.1340	0.9019	DFE = 3
Fiber Vol. Frac.(%)	0.0014	0.0092	0.1547	0.8869	DFR = 5
Asp. Ratio*Vf	4.4007e-05	4.2495e-05	1.0356	0.3765	SSR = 0.010731
Aspect Ratio^2	-1.1376e-05	2.5445e-05	-0.4471	0.6851	F = 0.3329
Vf^2	-7.0333e-05	0.0001	-0.4955	0.6543	P-val = 0.86641
	$R^2 = 0.3568$	Adj. $R^2 = -0.7151$			

Table 4.108: Empty Plantain Bunch-Epoxy Toughness ANOVA Table

Source	Sum Sq.	Df	Mean Sq.	F	Prob>F
Fiber Aspect Ratio (m/m)	0.00199	2	0.001	0.15	0.8640
Fiber Volume Fraction (Vf) (%)	0.00183	2	0.00091	0.14	0.8742
Error	0.02625	4	0.00656		
Total	0.03007	8			

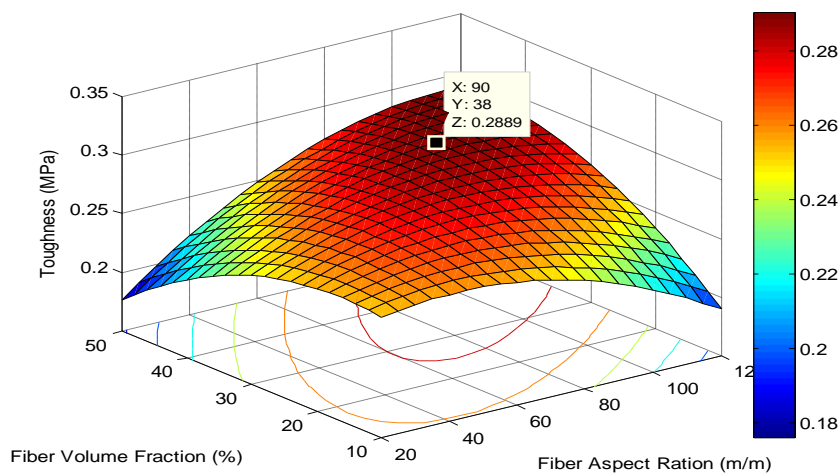


Figure 4.66: Surface plot for toughness of empty plantain bunch-epoxy composite

4.10.6 Empty Plantain Bunch-Epoxy Composite Tensile Properties Optimization

The RSM model coefficients from Table 4.98, Table 4.101, Table 4.103, Table 4.105 and Table 4.107 were used to run a MATLAB 7.9 optimization code and the optimal values for fiber aspect ratio and fiber volume fraction are presented alongside predicted optimal values of mechanical properties and the experimental values for validation. The optimization table (Table 4.109) reveals that most properties have their optimum values at high fiber aspect ratio and fiber volume fraction between 30% and 40%, except for ultimate elongation. This observation is in agreement with observations from Gassan and Bledzki (1999), Mohanty et al (2000), Ratna Prasad et al (2008), Chimekwene et al (2012) and Ihueze et al (2012). It can be observed from Table 4.110 that the model predicted values for mechanical properties are close to the experimentally validated values.

Table 4.109: Optimal Values for Mechanical Properties of Empty Plantain Bunch-Epoxy

Variables	Toughness	Tensile Strength	Young Modulus	Yield Strength	%El
Fiber Aspect ratio (m/m)	90	85	85	60	118
Fiber Volume Fraction (%)	38	30	30	30	50

Table 4.110: Predicted versus Experimental Optimum for Empty Plantain Bunch-Epoxy

	Toughness (MPa)	Tensile Strength (MPa)	Young Modulus (GPa)	Yield Strength (MPa)	%El (%)
Model Predicted Values	0.2889	8.3690	2.8280	6.1010	4.5500
Experimental Values	0.2371	8.4820	2.9696	6.2508	4.5300

4.11 Mechanical Properties of Empty Palm Bunch Fiber-Polyester Composite

The tensile test data for empty palm bunch-polyester composite for fiber lengths of 10mm, 30mm and 50mm (fiber aspect ratios of 22.2222m/m, 66.6667m/m and 111.1111m/m) and fiber volume fractions of 10%, 30% and 50% were analyzed using the traditional approach for Young's modulus, tensile strength, yield strength, ultimate elongation and toughness, and the results are given in Table 4.111.

Table 4.111: Empty Palm Bunch-Polyester Composite Tensile Test Analysis

Fiber Length (mm)	Fiber Aspect Ratio (m/m)	Volume Fraction (%)	Young Modulus (GPa)	Tensile Strength (MPa)	Yield Strength (MPa)	Ultimate Elongation (%)	Toughness (MPa)
10	22.2222	10	2.9470	12.3904	12.3904	0.3906	0.022783
10	22.2222	30	4.4500	27.1930	18.0963	1.2187	0.237184
10	22.2222	50	2.4989	24.8026	10.5728	2.2657	0.318504
30	66.6667	10	3.6756	23.0263	11.3469	1.7188	0.243891
30	66.6667	30	4.4643	30.1535	12.1616	2.1562	0.393466
30	66.6667	50	3.1069	26.6447	12.7924	2.1094	0.348053
50	111.1111	10	3.5699	18.0921	8.73516	2.1094	0.235159
50	111.1111	30	4.3021	29.6053	12.4802	0.9844	0.113700
50	111.1111	50	3.1357	23.3553	13.3923	1.9844	0.317844

4.11.1 Young's Modulus Analysis for Empty Palm Bunch-Polyester Composite

Young's modulus results from the traditional approach in Table 4.111 were modeled using response surface methodology and the results are presented in Table 4.112, Table 4.113 and Figure 4.67. The pure quadratic model ($y = a_1 + a_2x_1 + a_3x_2 + a_4x_1^2 + a_5x_2^2$) gave the best fit, based on the Adjusted-R² and was therefore used. It can be observed from Table 4.112 that the response surface model for Young's modulus of empty palm bunch-polyester composite explains 94% of the variability observed in the Young's modulus of the composite. The t-statistics and its

p-values show that the constant term, fiber volume fraction and its quadratic term are significant. The model is adequate based on the f-statistics. The ANOVA table (Table 4.113) reveals that only fiber volume fraction is significant at 95% confidence which corroborates observation from the surface plot (Figure 4.67). The surface plot also reveals a low level of interaction between the variables. Young's modulus increases with increase in fiber aspect ratio and also with increase in fiber volume fraction to a maximum before an observed drop.

Table 4.112: Empty Palm Bunch-Polyester Modulus RSM Model Statistics

Variables	Coefficients	Std. Error	t-stat	P-value	F-stat
Constant	1.2586	0.4480	2.8096	0.0483	SSE =0.23834
Aspect Ratio (m/m)	0.0221	0.0119	1.8590	0.1366	DFE = 4
Fiber Vol. Frac.(%)	0.1754	0.0264	6.6517	0.0027	DFR = 4
Aspect ratio^2	-0.0001	8.7382e-05	-1.5353	0.1995	SSR = 3.8214
Vf^2	-0.0031	0.0004	-7.2408	0.0019	F = 16.033
					P-val= 0.009936
	R ² = 0.9413	Adj.R ² =0.8826			

Table 4.113: Empty Palm Bunch-Polyester Young's Modulus ANOVA Table

Source	Sum Sq.	Df	Mean Sq.	F	Prob>F
Fiber Aspect Ratio (m/m)	0.34647	2	0.17323	2.91	0.1661
Fiber Volume Fraction (Vf) (%)	3.4749	2	1.73745	29.16	0.0041
Error	0.23834	4	0.05959		
Total	4.05971	8			

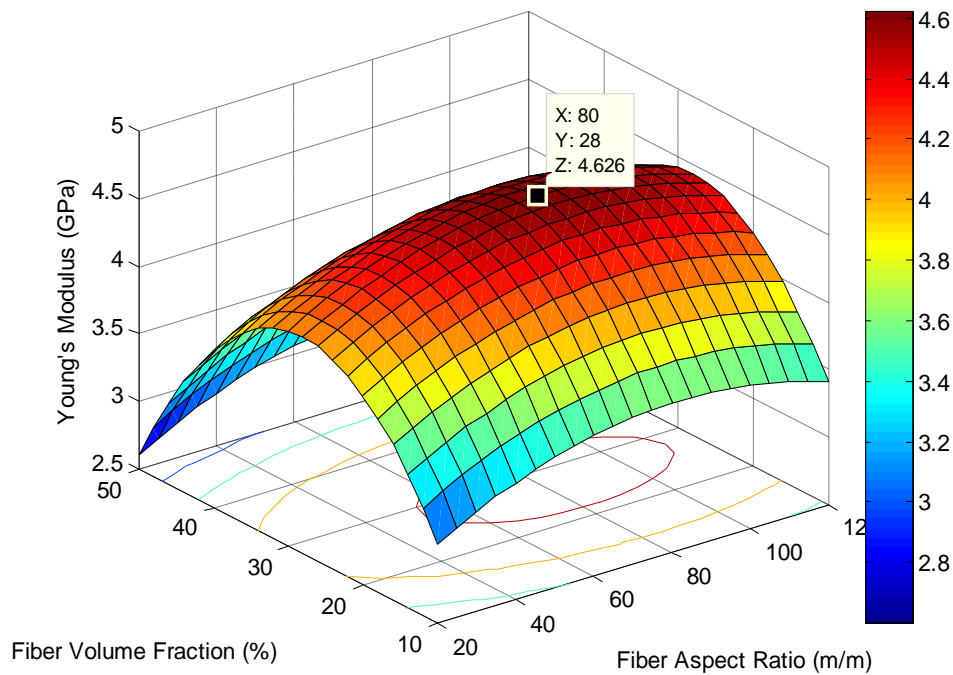


Figure 4.67: Surface plot of modulus of empty palm bunch-polyester composite

4.11.2 Tensile Strength Analysis for Empty Palm Bunch-Polyester Composite

Tensile Strength results from the traditional approach in Table 4.111 were modeled using response surface methodology and the results are presented in Table 4.114, Table 4.115 and Figure 4.68. The quadratic model ($y = a_1 + a_2x_1 + a_3x_2 + a_4x_1x_2 + a_5x_1^2 + a_6x_2^2$) gave the best fit, based on the Adjusted- R^2 and was therefore used. It can be observed from Table 4.114 that the response surface model for tensile strength of empty palm bunch-polyester composite explains 94% of the variability observed in the tensile strength of the composite. The t-statistics values reveal that fiber aspect ratio, fiber volume fraction and their quadratic terms are significant. All terms are significant at 95% confidence except the quadratic term of fiber aspect ratio which is significant at 90% confidence based on its p-value. The model is adequate based on the f-statistics at 95% confidence. It can be observed from the ANOVA table (Table 4.115)

that fiber volume fraction is significant. This corroborates observation from the surface plot (Figure 4.68) showing the significant change in tensile strength along the fibervolume fraction. The surface plot also shows that the tensile strength increases with increase in fiber aspect ratio and fiber volume fraction to a maximum before an observed drop.

Table 4.114: Empty Palm Bunch-Polyester Tensile Strength RSM Model Statistics

Variables	Coefficients	Std. Error	t-stat	P-value	F-stat
Constant	-5.5134	4.7012	-1.1728	0.3255	SSE =14.309
Aspect Ratio (m/m)	0.3577	0.1124	3.1832	0.0500	DFE =3
Fiber Vol. Frac.(%)	1.4513	0.2497	5.8120	0.0101	DFR =5
Asp. Ratio*Vf	-0.0020	0.0012	-1.6367	0.2002	SSR = 243.8
Aspect Ratio^2	-0.0020	0.0008	-2.6129	0.0795	F = 10.223
Vf^2	-0.0190	0.0039	-4.9205	0.0161	P-val= 0.04213
	R ² = 0.9446	Adj. R ² =0.8522			

Table 4.115:Empty Palm Bunch-Polyester Tensile Strength ANOVA Table

Source	Sum Sq.	Df	Mean Sq.	F	Prob>F
Fiber Aspect Ratio (m/m)	39.971	2	19.9854	2.95	0.1632
Fiber Volume Fraction (Vf) (%)	191.051	2	95.5257	14.11	0.0154
Error	27.086	4	6.7715		
Total	258.108	8			

1

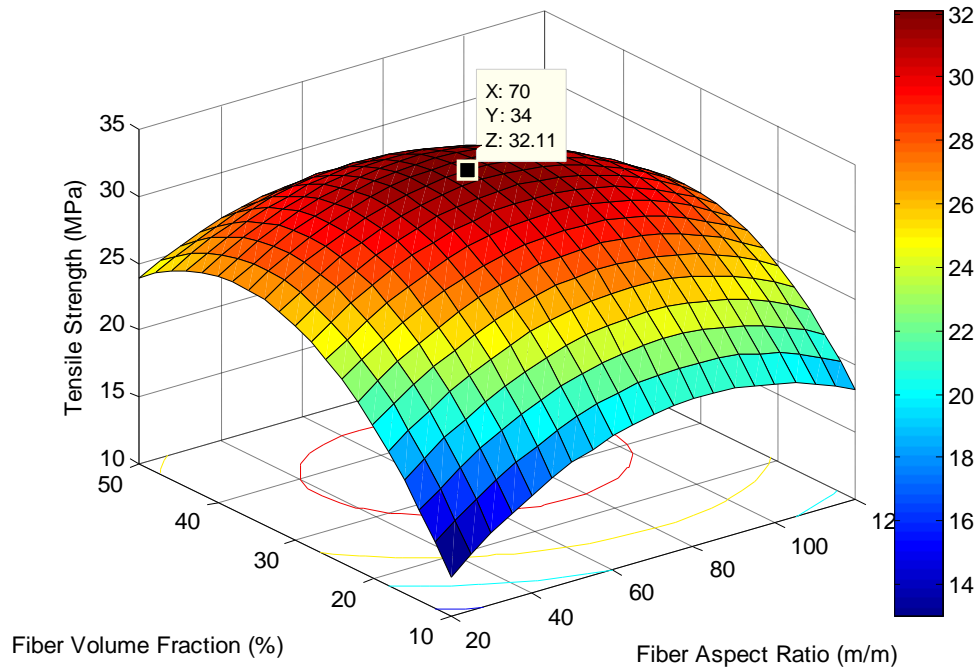


Figure 4.68: Surface plot for tensile strength of empty palm bunch-polyester composite

4.11.3 Yield Strength Analysis for Empty Palm Bunch-Polyester Composite

Yield strength results from the traditional approach in Table 4.111 were modeled using response surface methodology and the results are presented in Table 4.116, Table 4.117 and Figure 4.69. The quadratic model ($y = a_1 + a_2x_1 + a_3x_2 + a_4x_1x_2 + a_5x_1^2 + a_6x_2^2$) gave the best fit, based on the Adjusted- R^2 and was therefore used. It can be observed from Table 4.116 that the response surface model for yield strength of empty palm bunch-polyester composite explains only 69% of the variability observed in the yield strength of the composite. The t-statistics value and its p-value show that only the constant term is significant. The model is not adequate based on the f-statistics. It can be observed from the ANOVA table (Table 4.117) that none of the

variables is significant though fiber volume fraction has more effect. This corroborates observation from the surface plot (Figure 4.69). The surface plot also reveals drop in the yield strength with increase as fiber aspect ratio, but an initial increase with fiber aspect ratio to a maximum before a decrease.

Table 4.116: Empty Palm Bunch-Polyester Yield Strength RSM Model Statistics

Variables	Coefficients	Std. Error	t-stat	P-value	F-stat
Constant	13.1463	4.9478	2.6570	0.0765	SSE = 15.85
Aspect ratio (m/m)	-0.1133	0.1183	-0.9581	0.4087	DFE = 3
Fiber Vol. Frac.(%)	0.3205	0.2628	1.2194	0.3098	DFR = 5
Asp. Ratio*Vf	0.0018	0.0013	1.4085	0.2537	SSR = 35.664
Aspect Ratio^2	0.0003	0.0008	0.3143	0.7739	F = 1.3501
Vf^2	-0.0068	0.0041	-1.6660	0.1943	P-val = 0.42821
	R ² = 0.6923	Adj.R ² = 0.1796			

Table 4.117: Empty Palm Bunch-Polyester Yield Strength ANOVA Table

Source	Sum Sq.	Df	Mean Sq.	F	Prob>F
Fiber Aspect Ratio (m/m)	7.4597	2	3.72987	0.57	0.6072
Fiber Volume Fraction (Vf) (%)	17.7236	2	8.86181	1.15	0.3572
Error	26.3302	4	6.58254		
Total	51.5135	8			

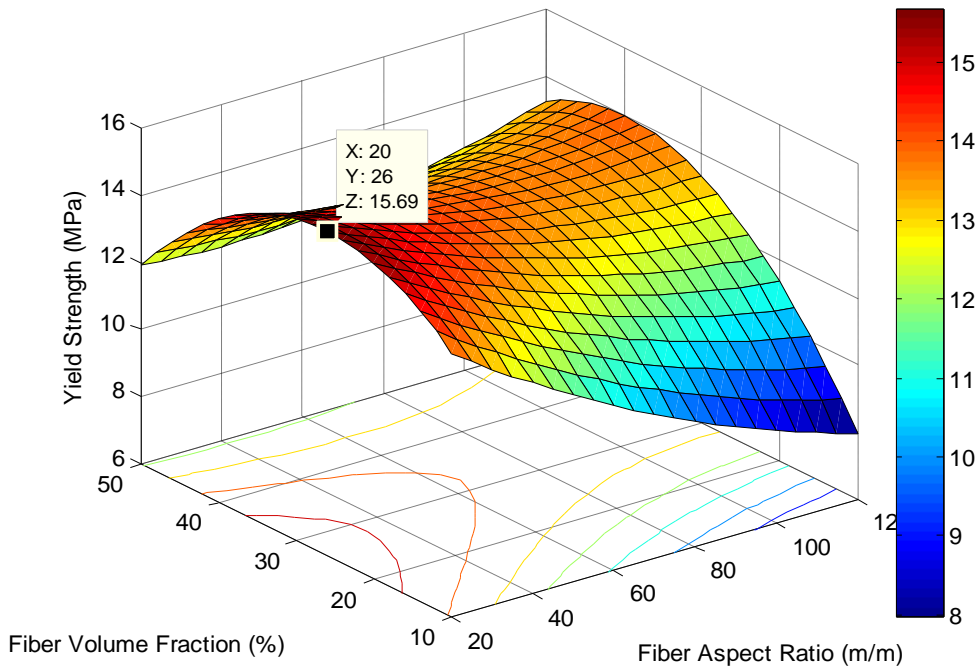


Figure 4.69: Surface plot for yield strength of empty palm bunch-polyester composite

4.11.4 Ultimate Elongation Analysis for Empty Palm Bunch-Polyester Composite

Ultimate elongation results from the traditional approach in Table 4.111 were modeled using response surface methodology and the results are presented in Table 4.118, Table 4.119 and Figure 4.70. The quadratic model ($y = a_1 + a_2x_1 + a_3x_2 + a_4x_1x_2 + a_5x_1^2 + a_6x_2^2$) gave the best fit, based on the Adjusted- R^2 and was therefore used. It can be observed from Table 4.118 that the response surface model for ultimate elongation of empty palm bunch-polyester composite explains 80% of the variability observed in the ultimate elongation of the composite. The t-statistics and its p-value show that no term is significant even at 90% confidence. The model is not adequate based on the f-statistics. It can be observed from the ANOVA table (Table 4.119) that none of the variables is significant. The surface plot (Figure 4.70) also reveals that

the elongation increases with increase in fiber aspect ratio and fiber volume fraction and with a good level of interaction.

Table 4.118: Empty Palm Bunch-Polyester Ultimate Elongation RSM Model Statistics

Variables	Coefficients	Std. Error	t-stat	P-value	F-stat
Constant	-0.6063	1.0292	-0.5891	0.5972	SSE =0.68576
Aspect Ratio (m/m)	0.0553	0.0246	2.2486	0.1101	DFE = 3
Fiber Vol. Frac.(%)	0.0088	0.0547	0.1619	0.8817	DFR = 5
Asp. Ratio*Vf	-0.0006	0.0003	-2.0917	0.1276	SSR = 2.7025
Aspect Ratio^2	-0.0003	0.0002	-1.4867	0.2338	F = 2.3625
Vf^2	0.0008	0.0008	0.9168	0.4268	P-val= 0.25493
	$R^2 = 0.7976$	$Adj.R^2 = 0.4603$			

Table 4.119: Empty Palm Bunch-Polyester Ultimate Elongation ANOVA Table

Source	Sum Sq.	Df	Mean Sq.	F	Prob>F
Fiber Aspect Ratio (m/m)	0.7465	2	0.37326	0.89	0.4804
Fiber Volume Fraction (Vf) (%)	0.9559	2	0.47795	1.13	0.4072
Error	1.68586	4	0.42146		
Total	3.38826	8			

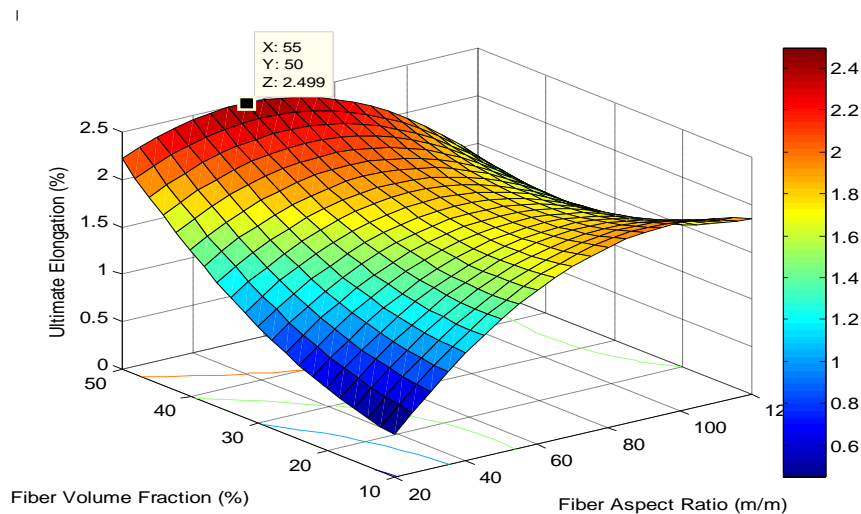


Figure 4.70: Surface plot of elongation of empty palm bunch-polyester composite

4.11.5 Toughness Analysis for Empty Palm Bunch-Polyester Composite

Results for toughness from the traditional approach in Table 4.111 were modeled using response surface methodology and the results are presented in Table 4.120, Table 4.121 and Figure 4.71. The quadratic model ($y = a_1 + a_2x_1 + a_3x_2 + a_4x_1x_2 + a_5x_1^2 + a_6x_2^2$) gave the best fit, based on the Adjusted- R^2 and was therefore used. It can be observed from Table 4.120 that the response surface model for toughness of empty palm bunch-polyester component explains 73% of the variability observed in the toughness of the composite. The t-statistics value and its p-value show that no term is significant. The model is not adequate based on the f-statistics. It can be observed from the ANOVA table (Table 4.121) that none of the variables is significant though fiber length has more effect. This corroborates observation from the surface plot (Figure 4.71). The surface plot also reveals that toughness increases with increase in fiber aspect ratio and fiber volume fraction.

Table 4.120: Empty Palm Bunch-Polyester Toughness RSM Model Statistics

Variables	Coefficients	Std. Error	t-stat	P-value	F-stat
Constant	-0.2068	0.2130	-0.9711	0.4031	SSE =0.029368
Aspect Ratio (m/m)	0.0103	0.0051	2.0217	0.1364	DFE = 3
Fiber Vol. Frac.(%)	0.0081	0.0113	0.7140	0.5268	DFR = 5
Asp. Ratio*Vf	-5.9916e-05	5.5655e-05	-1.0766	0.3605	SSR = 0.080709
Aspect Ratio^2	-6.1226e-05	3.5418e-05	-1.7287	0.1823	F = 1.6489
Vf^2	-1.0275e-06	0.0002	-0.0059	0.9957	P-val = 0.3611
	$R^2 = 0.7332$	$Adj.R^2 = 0.2885$			

Table 4.121: Empty Palm Bunch-Polyester Toughness ANOVA Table

Source	Sum Sq.	Df	Mean Sq.	F	Prob>F
Fiber Length (Fl) (mm)	0.03055	2	0.01528	1.5	0.3264
Fiber Volume Fraction (Vf) (%)	0.03881	2	0.01941	1.91	0.2621
Error	0.04071	4	0.01018		
Total	0.11008	8			

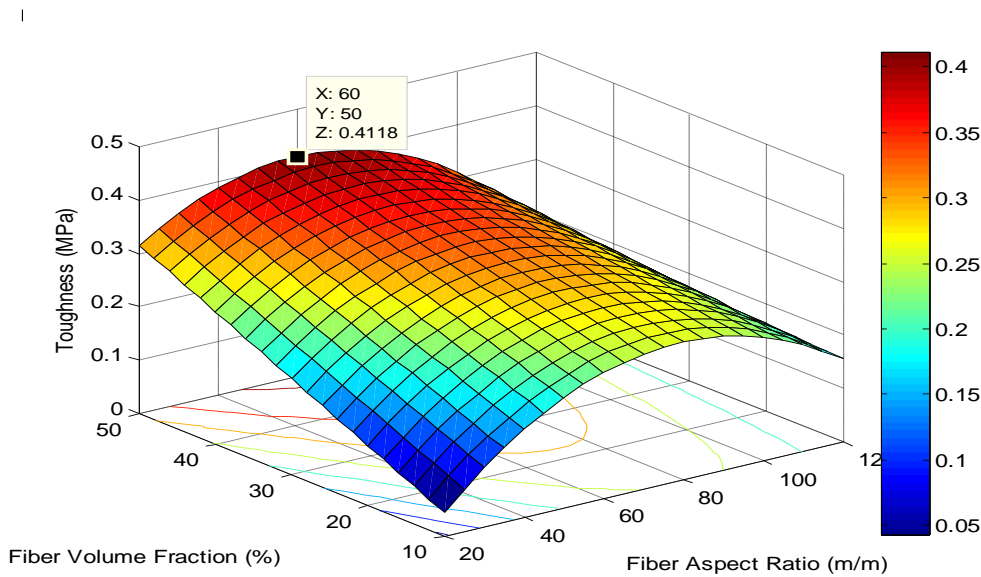


Figure 4.71: Surface plot for toughness of empty palm bunch-polyester composite

4.11.6 Empty Palm Bunch-Polyester Composite Tensile Properties Optimization

The RSM model coefficients from Table 4.112, Table 4.114, Table 4.116, Table 4.118 and Table 4.120 were used to run a MATLAB 7.9 optimization code and the optimal values for fiber length and fiber volume fraction are presented alongside predicted optimal values of mechanical properties and the experimental values for validation. It can be observed from Table 4.122 that the mechanical properties had their optimum at different fiber aspect ratios and fiber volume fractions. The optimum fiber aspect ratio and volume fraction varied between 70-80m/m and 28-34% for properties whose model fit was adequate. It can be observed from Table 4.123 that the

model predicted values for most mechanical properties are close to the experimentally validated values. Exceptions are due to the low fit of the RSM model for certain properties.

Table 4.122: Optimal Values for Mechanical Properties of Empty Palm Bunch-Polyester

Variables	Toughness	Tensile Strength	Young Modulus	Yield Strength	%El
Fiber Aspect Ratio (m/m)	60	70	80	20	55
Fiber Volume Fraction (%)	50	34	28	26	50

Table 4.123: Predicted versus Experimental Optimum for Empty Plantain Bunch-Epoxy

	Toughness (MPa)	Tensile Strength (MPa)	Young Modulus (GPa)	Yield Strength (MPa)	%El (%)
Model Predicted Values	0.4118	32.1100	4.6260	15.6900	2.4990
Experimental Values	0.3800	31.1211	4.0760	15.2403	2.5879

4.12 Mechanical Properties of Empty Palm Bunch Fiber-Epoxy Composite

The tensile test data for empty palm bunch-epoxy composite for fiber lengths of 10mm, 30mm and 50mm (fiber aspect ratios of 22.2222m/m, 66.6667m/m and 111.1111m/m) and fiber volume fractions of 10%, 30% and 50% were analyzed using the traditional approach for Young's modulus, tensile strength, yield strength, ultimate elongation and toughness, and the results are given in Table 4.124.

Table 4.124: Empty Palm Bunch-Epoxy Composite Tensile Test Analysis

Fiber Length (mm)	Fiber Aspect Ratio (m/m)	Volume Fraction (%)	Young Modulus (GPa)	Tensile Strength (MPa)	Yield Strength (MPa)	Ultimate Elongation (%)	Toughness (MPa)
10	22.2222	10	1.1572	5.4825	3.9411	3.5900	0.16003
10	22.2222	30	2.0740	10.1974	4.6027	2.2700	0.10821
10	22.2222	50	1.4303	5.4825	4.8465	3.4500	0.16653
30	66.6667	10	1.6508	7.1272	5.2061	2.4700	0.15023
30	66.6667	30	2.4607	10.7456	7.2104	2.9700	0.26012
30	66.6667	50	1.7133	8.5526	7.4425	2.9100	0.22009
50	111.1111	10	1.5134	5.2632	7.1638	2.3400	0.18865
50	111.1111	30	2.1628	10.3070	7.8887	2.9700	0.26228
50	111.1111	50	1.5882	8.9912	6.9596	3.1300	0.24157

4.12.1 Young’s Modulus Analysis for Empty Palm Bunch-Epoxy Composite

Young’s modulus results from the traditional approach in Table 4.124 were modeled using response surface methodology and the results are presented in Table 4.125, Table 4.126 and Figure 4.72. The quadratic model ($y = a_1 + a_2x_1 + a_3x_2 + a_4x_1x_2 + a_5x_1^2 + a_6x_2^2$) gave the best fit, based on the Adjusted-R² and was therefore used. It can be observed from Table 4.111 that the response surface model for Young’s modulus of empty palm bunch-epoxy composite explains 99% of the variability observed in the Young’s modulus of the composite. The t-statistics value and its p-value show that fiber aspect ratio, fiber volume fraction and their quadratic terms are significant at 95% confidence. The model is adequate at 95% confidence based on the f-statistics. It can be observed from the ANOVA table (Table 4.126) that both of the variables are significant, which corroborates observation from the surface plot. The surface plot also reveals a low level of interaction between the variables (Figure 4.72). Young’s modulus increases with increase in fiber aspect ratio and fiber volume fraction to a maximum before an observed decrease.

Table 4.125: Empty Palm Bunch-Epoxy Young's Modulus RSM Model Statistics

Variables	Coefficients	Std. Error	t-stat	P-value	F-stat
Constant	-0.2154	0.1601	-1.3451	0.2712	SSE =0.016603
Aspect Ratio (m/m)	0.0233	0.0038	6.0940	0.0089	DFE = 3
Fiber Vol. Frac.(%)	0.1157	0.0085	13.600	0.0009	DFR = 5
Aspect Ratio*Vf	-5.5772e-05	4.1846e-05	-1.3328	0.2748	SSR = 1.3108
Aspect Ratio^2	-0.0001	2.6631e-05	-5.4612	0.0121	F = 47.37
Vf^2	-0.0018	0.0001	-13.7562	0.0008	P-val = 0.00047
	$R^2 = 0.9875$	Adj. $R^2 = 0.9666$			

Table 4.126: Empty Palm Bunch-Epoxy Young's Modulus ANOVA Table

Source	Sum Sq.	Df	Mean Sq.	F	Prob>F
Fiber Length (Fl) (mm)	0.22564	2	0.11282	17.07	0.0110
Fiber Volume Fraction (Vf) (%)	1.07536	2	0.53768	81.36	0.0006
Error	0.02643	4	0.00661		
Total	1.32744	8			

1

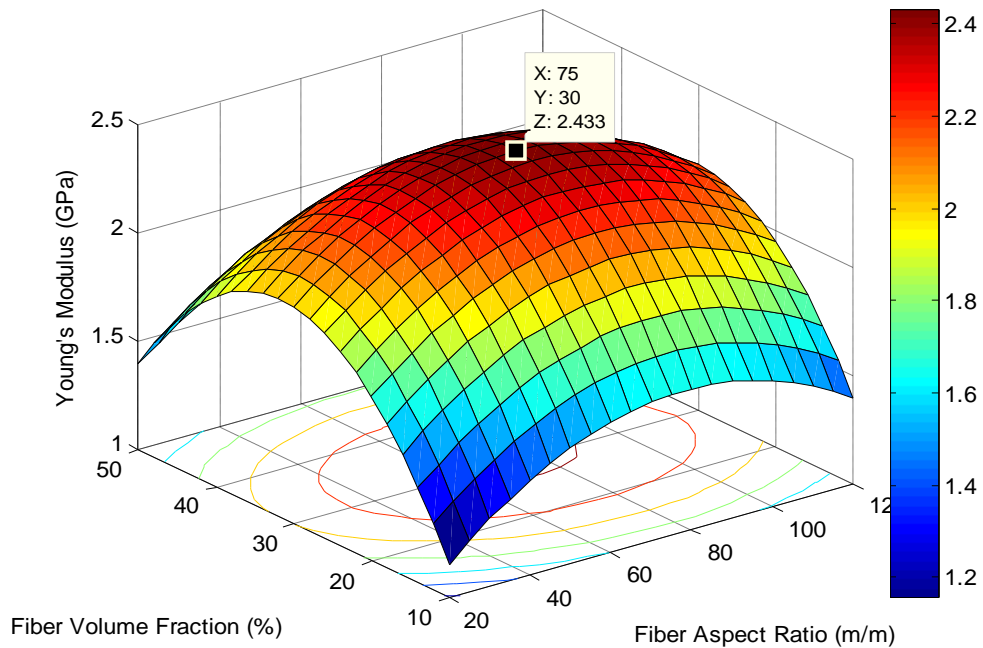


Figure 4.72: Surface plot of modulus of empty palm bunch-epoxy composite

4.12.2 Tensile Strength Analysis for Empty Palm Bunch-Epoxy Composite

Tensile strength results from the traditional approach in Table 4.124 were modeled using response surface methodology and the results are presented in Table 4.127, Table 4.128 and Figure 4.73. The quadratic model ($y = a_1 + a_2x_1 + a_3x_2 + a_4x_1x_2 + a_5x_1^2 + a_6x_2^2$) gave the best fit, based on the Adjusted-R² and was therefore used. It can be observed from Table 4.127 that the response surface model for tensile strength of empty palm bunch-epoxy composite explains 97% of the variability observed in the tensile strength of the composite. The t-statistics value and its p-value show that fiber volume fraction and its quadratic term are adequate at 95% confidence while the interaction term and quadratic term of fiber aspect ratio are significant at 90% confidence. The model is adequate based on the f-statistics. It can be observed from the ANOVA table (Table 4.128) that only fiber volume fraction is significant at 95% confidence. This corroborates observation from the surface plot (Figure 4.73) showing the significant change in tensile strength (as observed from the colour variation) along the fibervolume fraction axis. The contour lines of the surface plot also reveal the high level of interaction.

Table 4.127: Empty Palm Bunch-Epoxy Tensile Strength RSM Model Statistics

Variables	Coefficients	Std. Error	t-stat	P-value	F-stat
Constant	0.3945	1.4343	0.2751	0.8011	SSE = 1.3319
Aspect Ratio (m/m)	0.0615	0.0343	1.7931	0.1709	DFE = 3
Fiber Vol. Frac.(%)	0.5131	0.0762	6.7347	0.0067	DFR = 5
Aspect Ratio*Vf	0.0010	0.0004	2.7975	0.0680	SSR = 38.57
Aspect Ratio^2	-0.0006	0.0002	-2.5212	0.0861	F = 17.376
Vf^2	-0.0090	0.0012	-7.6412	0.0047	P-val = 0.020087
	R ² = 0.9666	Adj. R ² =0.9110			

Table 4.128: Empty Palm Bunch-Epoxy Tensile Strength ANOVA Table

Source	Sum Sq.	Df	Mean Sq.	F	Prob>F
Fiber Aspect ratio (m/m)	4.7474	2	2.3737	1.98	0.2531
Fiber Volume Fraction (Vf) (%)	30.3482	2	15.1741	12.63	0.0187
Error	4.8064	4	1.2016		
Total	39.902	8			

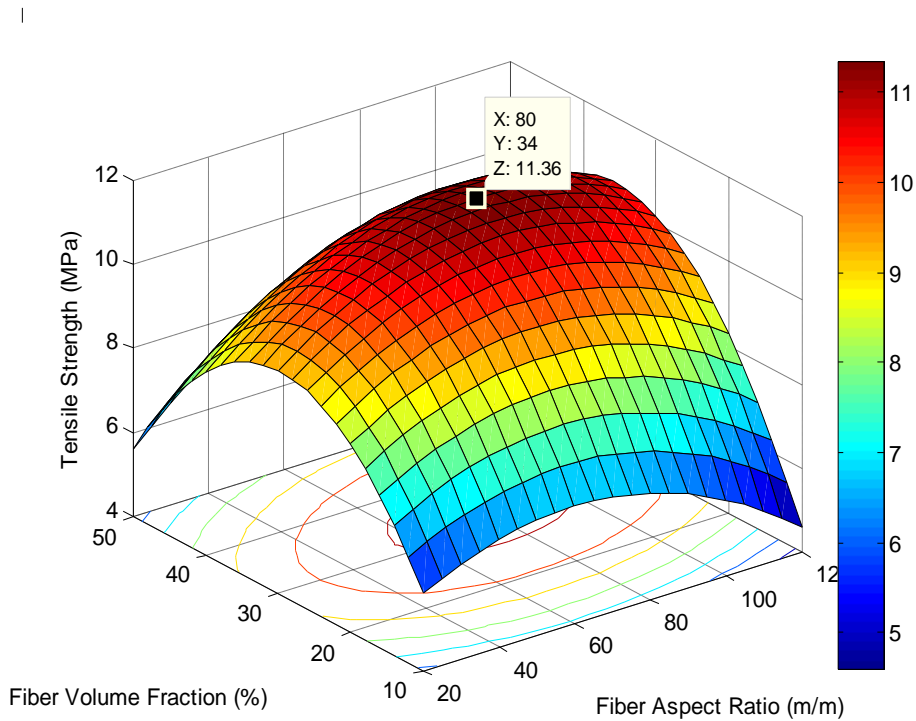


Figure 4.73: Surface plot for tensile strength of empty palm bunch-epoxy composite

4.12.3 Yield Strength Analysis for Empty Palm Bunch-Epoxy Composite

Yield strength results from the traditional approach in Table 4.124 were modeled using response surface methodology and the results are presented in Table 4.129, Table 4.130 and Figure 4.74.

The pure quadratic model ($y = a_1 + a_2x_1 + a_3x_2 + a_4x_1^2 + a_5x_2^2$) gave the best fit, based on the Adjusted-R² and was therefore used. It can be observed from Table 4.129 that the response

surface model for yield strength of empty palm bunch-epoxy composite explains 90% of the variability observed in the yield strength of the composite. The t-statistics value and its p-value show that only fiber aspect ratio is significant. The model is adequate based on the f-statistics. It can be observed from the ANOVA table (Table 4.130) that fiber aspect ratio is significant at 95% confidence. This corroborates observation from the surface plot (Figure 4.74). The surface plot also reveals that there is no significant aspect interaction and increase in the Yield Strength as fiber aspect ratio is increased.

Table 4.129: Empty Palm Bunch-Epoxy Yield Strength RSM Model Statistics

Variables	Coefficients	Std. Error	t-stat	P-value	F-stat
Constant	1.0971	1.1896	0.9222	0.4086	SSE = 1.6808
Aspect Ratio (m/m)	0.0809	0.0315	2.5671	0.0622	DFE = 4
Fiber Vol. Frac.(%)	0.1206	0.0700	1.7222	0.1601	DFR = 4
Aspect Ratio^2	-0.0004	0.0002	-1.5692	0.1917	SSR = 15.683
Vf^2	-0.0016	0.0011	-1.3977	0.2347	F = 9.3307
					P-val = 0.0263
	R ² = 0.9032	Adj. R ² = 0.8064			

Table 4.130: Empty Palm Bunch-Epoxy Yield Strength ANOVA Table

Source	Sum Sq.	Df	Mean Sq.	F	Prob>F
Fiber Aspect Ratio (m/m)	13.4239	2	6.71196	15.97	0.0124
Fiber Volume Fraction (Vf) (%)	2.2592	2	1.12958	2.69	0.1820
Error	1.6808	4	0.4202		
Total	17.3639	8			

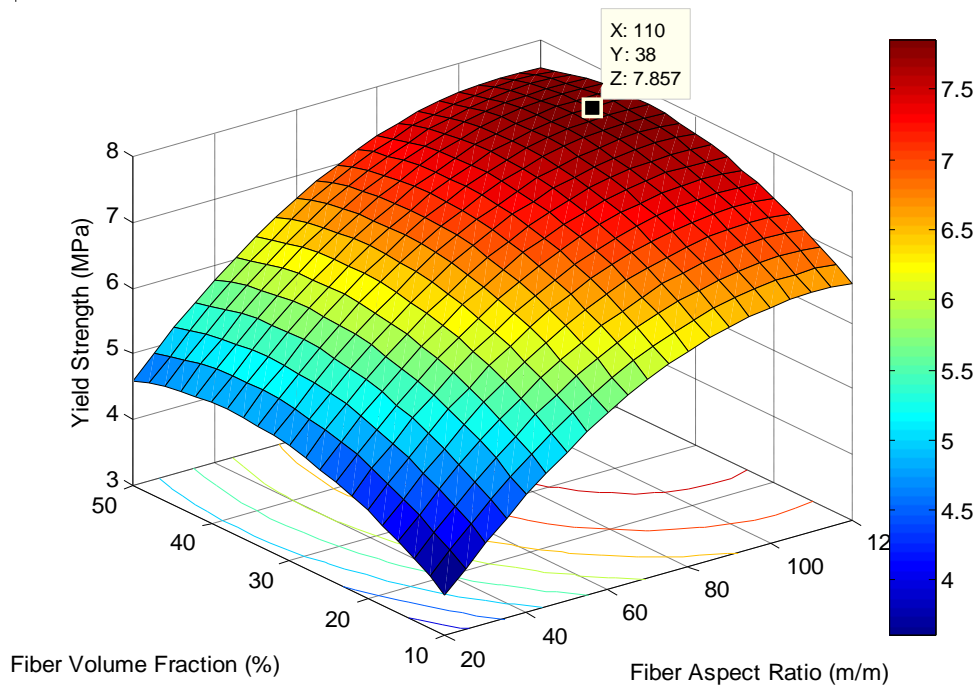


Figure 4.74: Surface plot for yield strength of empty palm bunch-epoxy composite

4.12.4 Ultimate Elongation Analysis for Empty Palm Bunch-Epoxy Composite

Ultimate elongation results from the traditional approach in Table 4.124 were modeled using response surface methodology and the results are presented in Table 4.131, Table 4.132 and Figure 4.75. The pure quadratic model ($y = a_1 + a_2x_1 + a_3x_2 + a_4x_1x_2 + a_5x_1^2 + a_6x_2^2$) gave the best fit, based on the Adjusted- R^2 and was therefore used. It can be observed from Table 4.131 that the response surface model for ultimate elongation of empty palm bunch-epoxy composite explains only 42% of the variability observed in the ultimate elongation of the composite. The t-statistics and its p-value show that only the constant term is significant. The model is not adequate based on the f-statistics. It can be observed from the ANOVA table (Table 4.132) that none of the variables is significant. This corroborates observation from the surface plot (Figure 4.75).

Table 4.131: Empty Palm Bunch-Epoxy Ultimate Elongation RSM Model Statistics

Variables	Coefficients	Std. Error	t-stat	P-value	F-stat
Constant	4.0331	1.2522	3.2209	0.0485	SSE = 1.0151
Aspect Ratio (m/m)	-0.0229	0.0299	-0.7659	0.4995	DFE = 3
Fiber Vol. Frac.(%)	-0.0451	0.0665	-0.6782	0.5463	DFR = 5
Aspect ratio*Vf	0.0003	0.0003	0.7994	0.4825	SSR = 0.72169
Aspect Ratio^2	8.8594e-05	0.0002	0.4255	0.6992	F = 0.42657
Vf^2	0.0006	0.0010	0.5956	0.5934	P-val= 0.81022
	$R^2 = 0.4155$	Adj. $R^2 = -0.5586$			

Table 4.132: Empty Palm Bunch-Epoxy Ultimate Elongation ANOVA Table

Source	Sum Sq.	Df	Mean Sq.	F	Prob>F
Fiber Aspect Ratio (m/m)	0.1874	2	0.0937	0.30	0.7533
Fiber Volume Fraction (Vf) (%)	0.31807	2	0.15903	0.52	0.6316
Error	1.23133	4	0.30783		
Total	1.7368	8			

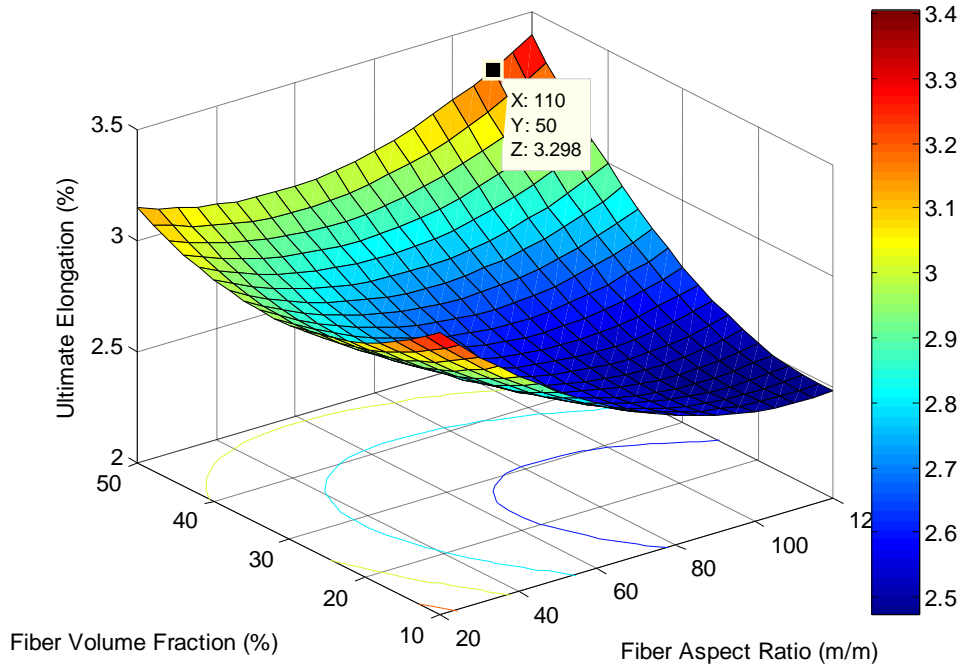


Figure 4.75: Surface plot for elongation of empty palm bunch-epoxy composite

4.12.5 Toughness Analysis for Empty Palm Bunch-Epoxy Composite

Results of toughness from the traditional approach in Table 4.124 were modeled using response surface methodology and the results are presented in Table 4.133, Table 4.134 and Figure 4.76. The linear model ($y = a_1 + a_2x_1 + a_3x_2$) gave the best fit, based on the Adjusted- R^2 and was therefore used. It can be observed from Table 4.133 that the response surface model for toughness of empty palm bunch-epoxy component explains about 60% of the variability observed in the toughness of the composite. The t-statistics value and its p-value show that the constant term and fiber aspect ratio are significant. The model is adequate based on the f-statistics. It can be observed from the ANOVA table (Table 4.134) that none of the variables is significant though fiber aspect ratio has more effect. This corroborates observation from the surface plot (Figure 4.76).

Table 4.133: Empty Palm Bunch-Epoxy Toughness RSM Model Statistics

Variables	Coefficients	Std. Error	t-stat	P-value	F-stat
Constant	0.0366	0.0366	2.6947	0.0358	SSE =0.00932
Aspect Ratio (m/m)	0.0004	0.0004	2.6698	0.0370	DFE = 6
Fiber Vol. Frac.(%)	0.0008	0.0008	1.3392	0.2290	DFR = 2
					SSR = 0.01386
					F = 4.4607
					P-val =0.065
	$R^2 = 0.5979$	$Adj.R^2 = 0.4639$			

Table 4.134: Empty Palm Bunch-Epoxy Toughness ANOVA Table

Source	Sum Sq.	Df	Mean Sq.	F	Prob>F
Fiber Aspect Ratio (m/m)	0.01206	2	0.00603	3.29	0.1428
Fiber Volume Fraction (Vf) (%)	0.00378	2	0.00189	1.03	0.4348
Error	0.00733	4	0.00183		
Total	0.02318	8			

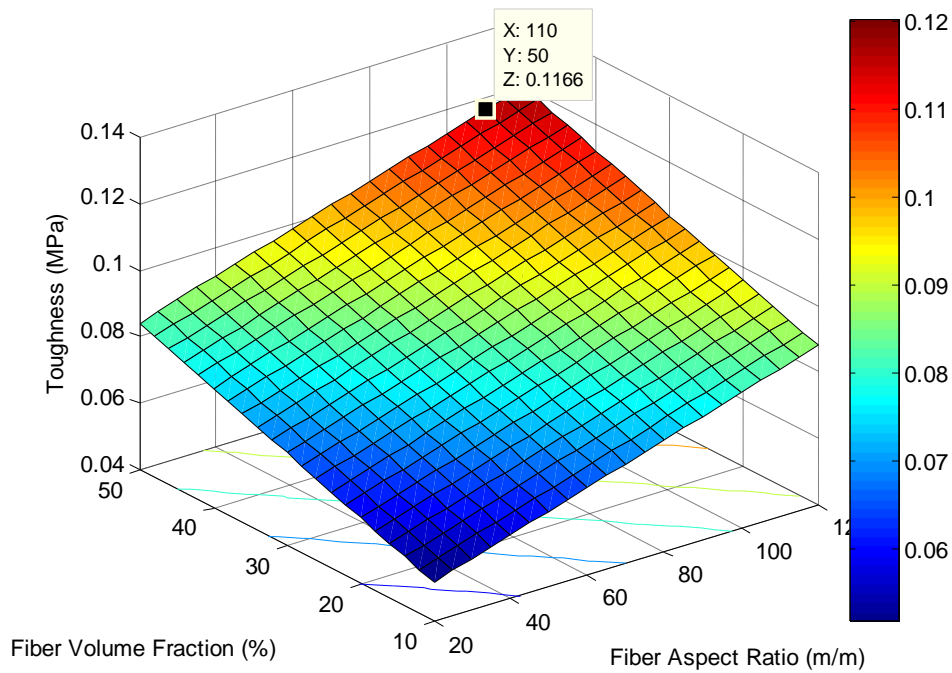


Figure 4.76: Surface plot for toughness of empty palm bunch-epoxy composite

4.12.6 Empty Palm Bunch-Epoxy Composite Tensile Properties Optimization

The RSM model coefficients from Table 4.125, Table 4.127, Table 4.129, Table 4.131 and Table 4.133 were used to run a MATLAB 7.9 optimization code and the optimal values for fiber length and fiber volume fraction are presented alongside predicted optimal values of mechanical properties and the experimental values for validation. It can be observed from Table 4.135 that the range for optimum volume fraction for the mechanical properties whose models are adequate is 30-38%. It can be observed from Table 4.136 that the model predicted values for most mechanical properties are close to the experimentally validated values. Exceptions are due to the low fit of the RSM model for certain properties.

Table 4.135: Optimal Values for Mechanical Properties of Empty Plantain Bunch-Epoxy

Variables	Toughness	Tensile Strength	Young Modulus	Yield Strength	%El
Fiber Aspect Ratio (m/m)	111.1	80	75	111.1	111.1
Fiber Volume Fraction (%)	50	34	30	38	50

Table 4.136: Predicted versus Experimental Optimum for Empty Plantain Bunch-Epoxy

	Toughness (MPa)	Tensile Strength (MPa)	Young Modulus (GPa)	Yield Strength (MPa)	%El (%)
Model Predicted Values	0.1210	11.3600	2.4330	7.8570	3.2980
Experimental Values	0.2417	10.3975	2.2849	7.5116	3.1300

4.13 Mechanical Properties of Rattan Palm Fiber-Polyester Composite

The tensile test data for rattan palm fiber-polyester composite for fiber lengths of 10mm, 30mm and 50mm (fiber aspect ratios of 8.1733m/m, 24.5198m/m and 40.8664m/m) and fiber volume fractions of 10%, 30% and 50% were analyzed using the traditional approach for Young's modulus, tensile strength, yield strength, ultimate elongation and toughness, and the results are given in Table 4.137.

Table 4.137: Rattan palmfiber-polyestercomposite tensile testanalysis

Fiber Length (mm)	Fiber Aspect Ratio (m/m)	Volume Fraction (%)	Young Modulus (GPa)	Tensile Strength (MPa)	Yield Strength (MPa)	Ultimate Elongation (%)	Toughness (MPa)
10	8.1733	10	1.4148	9.4298	9.1598	0.7800	0.0470
10	8.1733	30	2.8296	14.8026	8.5022	2.1600	0.1921
10	8.1733	50	2.1576	9.8684	9.6049	0.8300	0.0551
30	24.5198	10	1.2981	11.1842	11.1842	0.4700	0.0240
30	24.5198	30	3.0956	14.5833	9.5252	1.4100	0.1422
30	24.5198	50	2.8016	11.5132	11.4372	0.8100	0.0706
50	40.8664	10	1.9681	12.0614	8.8179	1.4100	0.1214
50	40.8664	30	3.2375	13.4868	10.2048	2.1900	0.2327
50	40.8664	50	2.3033	12.0614	8.8179	1.4100	0.1214

4.13.1 Young’s Modulus Analysis for Rattan Palm Fiber-Polyester Composite

Young’s modulus results from the traditional approach in Table 4.137 were modeled using response surface methodology and the results are presented in Table 4.138, Table 4.139 and Figure 4.77. The pure quadratic model ($y = a_1 + a_2x_1 + a_3x_2 + a_5x_1^2 + a_6x_2^2$) gave the best fit, based on the Adjusted-R² and was therefore used. It can be observed from Table 4.138 that the response surface model for Young’s modulus of rattan palm fiber-polyester composite explains 91% of the variability observed in the Young’s modulus of the composite. The t-statistics and its p-value reveal that fiber volume fraction and its quadratic term are the only significant terms. The model is also adequate based on the f-statistics. It can be observed from the ANOVA table (Table 4.139) that fiber volume fraction is significant. This corroborates observation from the surface plot (Figure 4.77). The surface plot also reveals increase in Young’s Modulus with increase in fiber volume fraction to a maximum before a decrease.

Table 4.138: Rattan palmfiber-polyester Young's modulus RSM model statistics

Variables	Coefficients	Std. Error	t-stat	P-value	F-stat
Constant	-0.3877	0.5453	-0.7110	0.5164	SSE = 0.35308
Aspect Ratio (m/m)	0.0260	0.0393	0.6611	0.5447	DFE = 4
Fiber Vol. Frac.(%)	0.1811	0.0321	5.6421	0.0049	DFR = 4
Aspect Ratio^2	-0.0003	0.0008	-0.3806	0.7229	SSR = 3.5904
Vf^2	-0.0027	0.0005	-5.0630	0.0072	F = 10.169
					P-val = 0.0226
	$R^2 = 0.9105$	Adj. $R^2 = 0.8209$			

Table 4.139: Rattan palm-polyester Young's modulus ANOVA table

Source	Sum Sq.	Df	Mean Sq.	F	Prob>F
Fiber Length (Fl) (mm)	0.21699	2	0.10849	1.23	0.3836
Fiber Volume Fraction (Vf) (%)	3.37339	2	1.6867	19.11	0.0090
Error	0.35308	4	0.08827		
Total	3.94346	8			

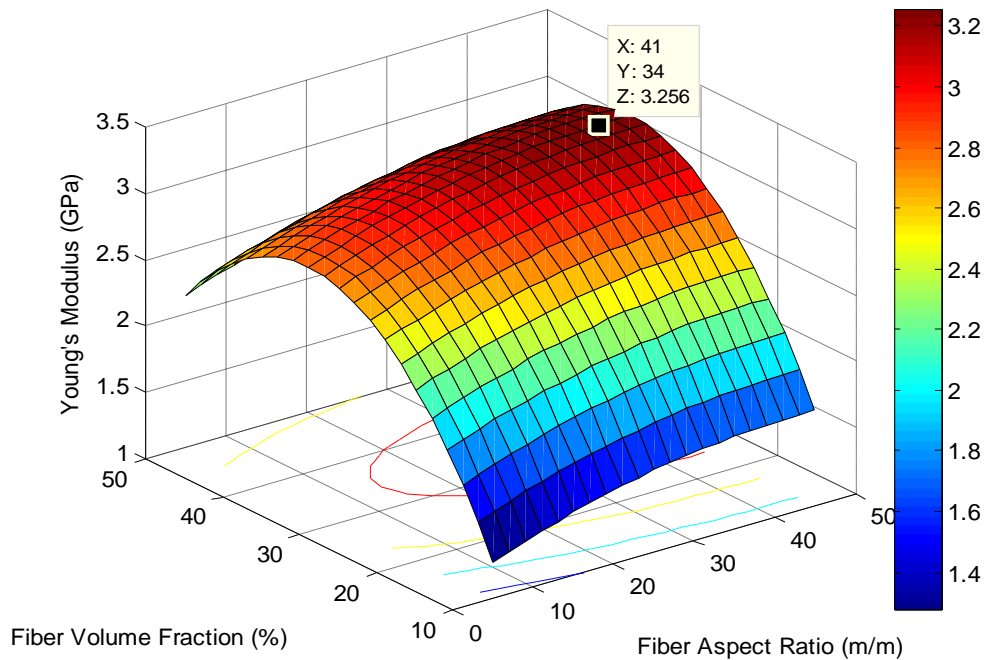


Figure 4.77: Surface plot for Young's modulus of rattan palm-polyester composite

4.13.2 Tensile Strength Analysis for Rattan Palm Fiber-Polyester Composite

Tensile strength results from the traditional approach in Table 4.137 were modeled using response surface methodology and the results are presented in Table 4.140, Table 4.141 and Figure 4.78. The pure quadratic model ($y = a_1 + a_2x_1 + a_3x_2 + a_4x_1^2 + a_5x_2^2$) gave the best fit, based on the Adjusted- R^2 and was therefore used. It can be observed from Table 4.140 that the response surface model for tensile strength of rattan palm fiber-polyester composite explains 84% of the variability observed in the tensile strength of the composite. The t-statistics value and its p-value show that the constant term, fiber volume fraction and its quadratic term are significant at 95% confidence interval. The model is adequate based on the f-statistics at 90% confidence. It can be observed from the ANOVA table (Table 4.141) that fiber volume fraction is significant. This corroborates observation from the surface plot (Figure 4.78) showing the significant change in tensile strength (as observed from the colour variation) along the fiber volume fraction axis. The surface plot also reveals that the tensile strength increases with increase in fiber volume fraction and fiber aspect ratio to an optimum before a decrease.

Table 4.140: Rattan palm fiber-polyester tensile strength RSM model statistics

Variables	Coefficients	Std. Error	t-stat	P-value	F-stat
Constant	5.1093	1.9865	2.5721	0.0618	SSE = 4.6864
Aspect Ratio (m/m)	0.1230	0.1430	0.8597	0.4384	DFE = 4
Fiber Vol. Frac.(%)	0.4971	0.1169	4.2517	0.0131	DFR = 4
Aspect Ratio ²	-0.0018	0.0029	-0.6208	0.5683	SSR = 24.003
Vf ²	-0.0082	0.0019	-4.2740	0.0129	F = 5.1218
					P-val= 0.071332
	$R^2 = 0.8367$	Adj. $R^2 = 0.6733$			

Table 4.141: Rattan palm-polyestertensilestrength ANOVA table

Source	Sum Sq.	Df	Mean Sq.	F	Prob>F
Fiber Length (Fl) (mm)	2.5035	2	1.2518	1.07	0.4248
Fiber Volume Fraction (Vf) (%)	21.4993	2	10.7496	9.18	0.0320
Error	4.6864	4	1.1716		
Total	28.6891	8			

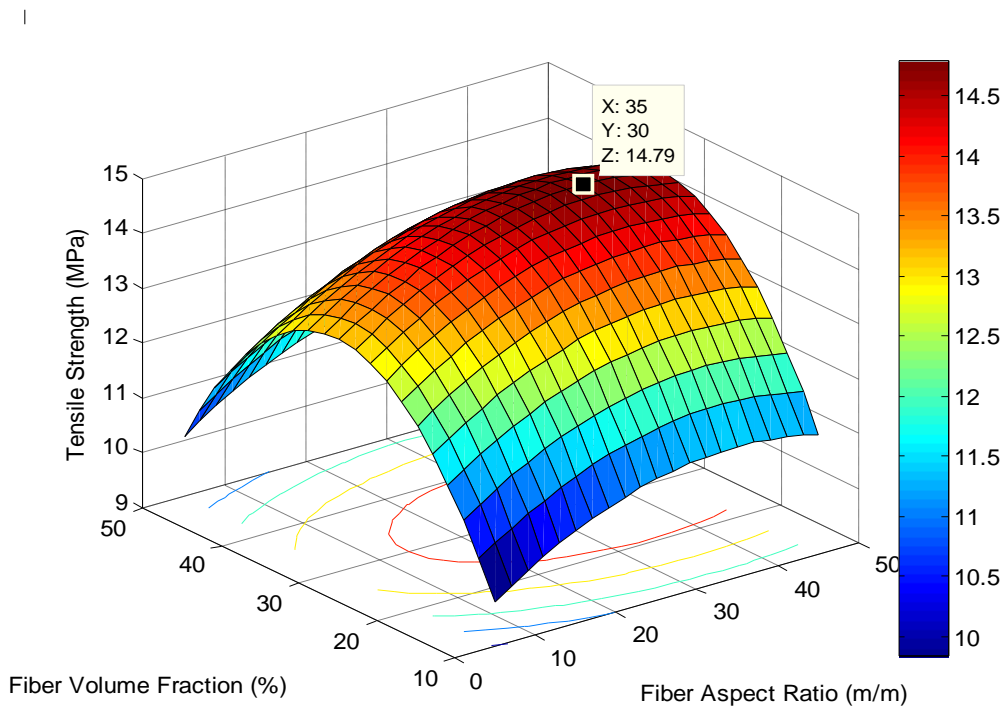


Figure 4.78: Surface plot for tensile strength of rattan palm-polyester composite

4.13.3 Yield Strength Analysis for Rattan Palm Fiber-Polyester Composite

Yield strength results from the traditional approach in Table 4.137 were modeled using response surface methodology and the results are presented in Table 4.142, Table 4.143 and Figure 4.79. The pure quadratic model ($y = a_1 + a_2x_1 + a_3x_2 + a_5x_1^2 + a_6x_2^2$) gave the best fit, based on the Adjusted-R² and was therefore used. It can be observed from Table 4.142 that the response surface model for yield strength of rattan palm fiber-polyester composite explains only

59% of the variability observed in the yield strength of the composite. The t-statistics value and its p-value show that the constant term is significant at 90% confidence while fiber aspect ratio and its quadratic term are significant at 90% confidence. This corroborates observation from the surface plot (Figure 4.79). The model is not adequate based on the f-statistics. It can be observed from the ANOVA table (Table 4.143) that none of the variables is significant. The surface plot also reveals increase in the yield strength followed by decrease as fiber aspect ratio is increased.

Table 4.142: Rattanpalmfiber-polyester yield strength RSM model statistics

Variables	Coefficients	Std. Error	t-stat	P-value	F-stat
Constant	7.6278	1.7436	4.3747	0.0119	SSE = 3.6106
Aspect Ratio (m/m)	0.2868	0.1256	2.2844	0.0844	DFE =4
Fiber Vol. Frac.(%)	-0.0581	0.1026	-0.5664	0.6014	DFR = 4
Aspect Ratio^2	-0.0057	0.0025	-2.2789	0.0849	SSR = 5.1871
Vf^2	0.0011	0.0017	0.6345	0.5602	F = 1.4366
					P-val= 0.3670
	$R^2 = 0.5896$	Adj. $R^2 =$			
		0.1792			

Table 4.143: Rattan palm-polyesteryield strength ANOVA table

Source	Sum Sq.	Df	Mean Sq.	F	Prob>F
Fiber Aspect Ratio (m/m)	4.74247	2	2.37124	2.63	0.1868
Fiber Volume Fraction (Vf) (%)	0.4446	2	0.2223	0.25	0.7927
Error	3.61057	4	0.90264		
Total	8.79764	8			

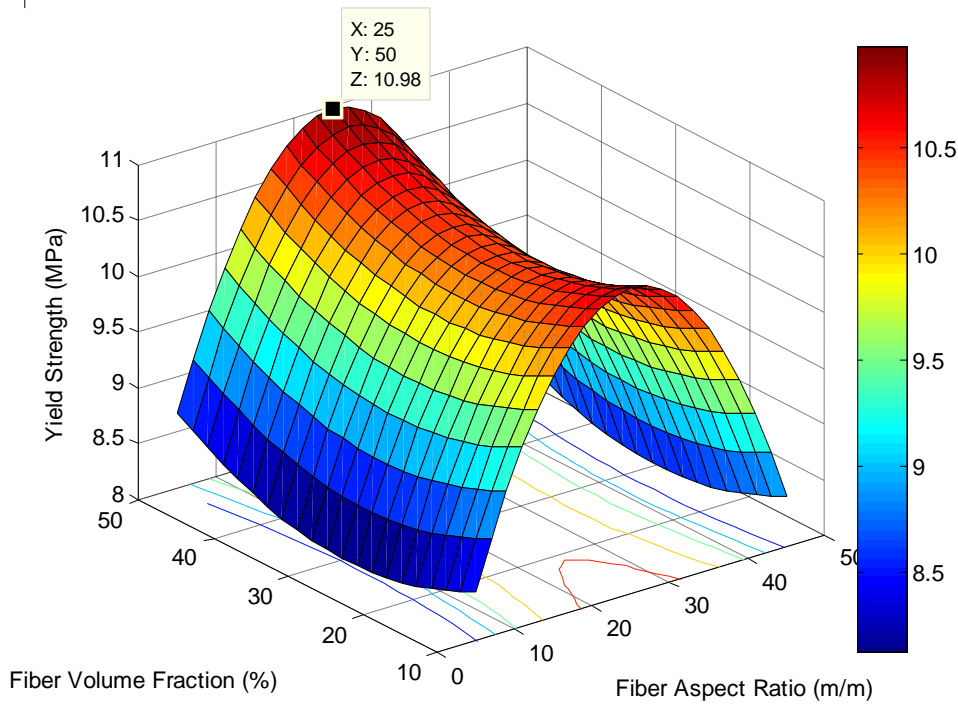


Figure 4.79: Surface plot for yield strength of rattan palm-polyester composite

4.13.4 Ultimate Elongation Analysis for Rattan Palm Fiber-Polyester Composite

Ultimate elongation results from the traditional approach in Table 4.137 were modeled using response surface methodology and the results are presented in Table 4.144, Table 4.145 and Figure 4.80. The pure quadratic model ($y = a_1 + a_2x_1 + a_3x_2 + a_5x_1^2 + a_6x_2^2$) gave the best fit, based on the Adjusted- R^2 and was therefore used. It can be observed from Table 4.144 that the response surface model for ultimate elongation of rattan palm fiber-polyester composite explains 94% of the variability observed in the ultimate elongation of the composite. The t-statistics and its p-value show that all terms are significant except the constant term. The model is adequate at 95% confidence based on the f-statistics. It can be observed from the ANOVA table (Table 4.145) that fiber aspect ratio and fiber volume fraction are significant at 95% confidence. This corroborates observation from the surface plot (Figure 4.80). The surface plot also reveals that

the elongation increases but subsequently dropped with increase in fibervolume fraction, but decreases with fiber aspect ratio initially before an observed increase.

Table 4.144: Rattan palm fiber-polyesterultimate elongation RSM model statistics

Variables	Coefficients	Std. Error	t-stat	P-value	F-stat
Constant	0.2310	0.3928	0.5880	0.5881	SSE = 0.18324
Aspect Ratio (m/m)	-0.0914	0.0283	-3.2297	0.0320	DFE = 4
Fiber Vol. Frac.(%)	0.1485	0.0231	6.4234	0.0030	DFR = 4
Aspect Ratio^2	0.0021	0.0006	3.7442	0.0200	SSR = 2.7992
Vf^2	-0.0024	0.0004	-6.3982	0.0031	F = 15.276
					P-val =0.01086
	$R^2 = 0.9386$	$Adj. R^2 = 0.8771$			

Table 4.145: Rattan palm-polyester ultimate elongation ANOVA table

Source	Sum Sq.	Df	Mean Sq.	F	Prob>F
Fiber Length (Fl) (mm)	0.89849	2	0.44924	9.81	0.0287
Fiber Volume Fraction (Vf) (%)	1.90069	2	0.95034	20.74	0.0077
Error	0.18324	4	0.04581		
Total	2.98242	8			

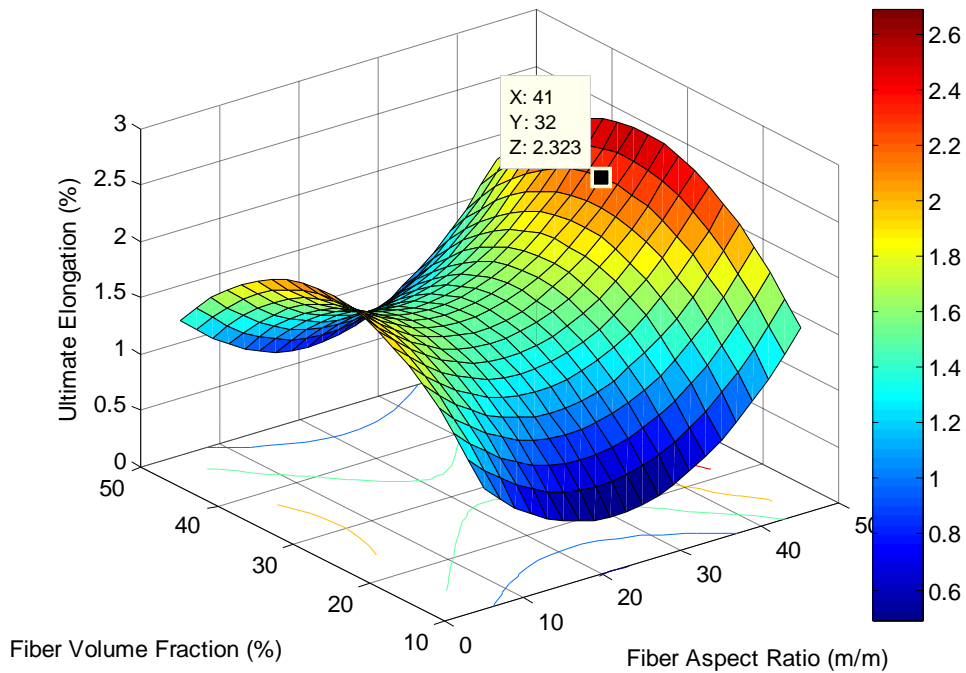


Figure 4.80: Surface plot forelongation of rattan palm-polyester composite

4.13.5 Toughness Analysis for Rattan Palm Fiber-Polyester Composite

Results for toughness from the traditional approach in Table 4.137 were modeled using response surface methodology and the results are presented in Table 4.146, Table 4.147 and Figure 4.81. The quadratic model ($y = a_1 + a_2x_1 + a_3x_2 + a_4x_1x_2 + a_5x_1^2 + a_6x_2^2$) gave the best fit, based on the Adjusted- R^2 and was therefore used. It can be observed from Table 4.146 that the response surface model for toughness of rattan palm fiber-polyester component explains 89% of the variability observed in the toughness of the composite. The t-statistics value and its p-value show fiber length and its quadratic term are significant. The model is adequate at 90% confidence based on the f-statistics. It can be observed from the ANOVA table (Table 4.147) that fiber length is significant. This corroborates observation from the surface plot (Figure 4.81). The

surface plot also reveals that the toughness increases but subsequently dropped with increase in fiber length, but decreases with fiber volume fraction.

Table 4.146:Rattan palm fiber-polyester toughness RSMmodel statistics

Variables	Coefficients	Std. Error	t-stat	P-value	F-stat
Constant	-0.0523	0.0337	-1.5514	0.1957	SSE = 0.00135
Aspect Ratio (m/m)	-0.0072	0.0024	-2.9695	0.0412	DFE = 4
Fiber Vol. Frac.(%)	0.0178	0.0020	8.9808	0.0009	DFR = 4
Aspect Ratio^2	0.0002	4.8609e-05	3.7995	0.0191	SSR = 0.037644
Vf^2	-0.0003	3.2472e-05	-8.9116	0.0009	F = 27.892
					P-val = 0.00351
	R ² =0. 9654	Adj. R ² = 0.9308			

Table 4.147: Rattanpalm-polyester toughness ANOVA table

Source	Sum Sq.	Df	Mean Sq.	F	Prob>F
Fiber Aspect Ratio (m/m)	0.01035	2	0.00517	15.34	0.0133
Fiber Volume Fraction (Vf) (%)	0.02729	2	0.01365	40.45	0.0022
Error	0.00135	4	0.00034		
Total	0.03899	8			

1

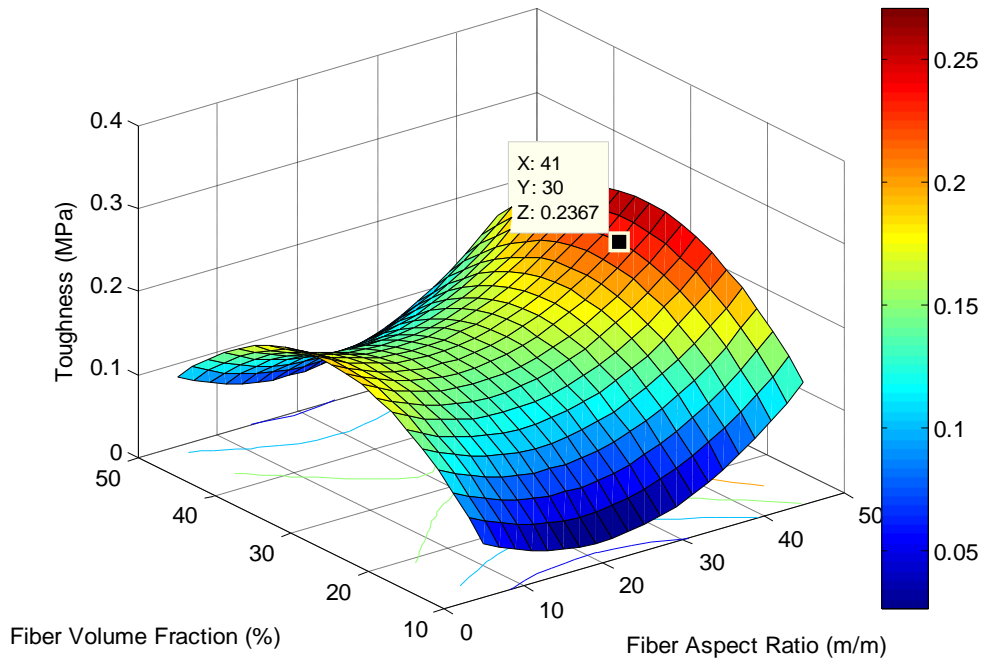


Figure 4.81: Surface plot for toughness of rattan palm-polyester composite

4.13.6 Rattan Palm Fiber-Polyester Composite Tensile Properties Optimization

The RSM model coefficients from Table 4.138, Table 4.140, Table 4.142, Table 4.144 and Table 4.146 were used to run a MATLAB 7.9 optimization code and the optimal values for fiber length and fiber volume fraction are presented alongside predicted optimal values of mechanical properties and the experimental values for validation. It can be observed from Table 4.148 that the optimal values occur at different points for the mechanical properties, but from the mechanical properties that their model fits were adequate optimum values will be a fiber aspect ratio of 35-41m/m and fiber volume fraction of 30-34%. It can also be observed from Table 4.149 that the model predicted values for most mechanical properties are close to the experimentally validated values. Exceptions are due to the low fit of the RSM model for certain properties.

Table 4.148: Optimal values for mechanical properties of rattan palm fiber-polyester

Variables	Toughness	Tensile Strength	Young Modulus	Yield Strength	%El
Fiber Aspect Ratio (m/m)	41	35	41	25	41
Fiber Volume Fraction (%)	30	30	34	50	32

Table 4.149: Predicted versus experimental optimum for rattan palm fiber-polyester

	Toughness (MPa)	Tensile Strength (MPa)	Young Modulus (GPa)	Yield Strength (MPa)	%El (%)
Model Predicted Values	0.2367	14.7900	3.2560	10.9800	2.3230
Experimental Values	0.2327	14.6207	2.9896	10.9688	2.1981

4.14 Mechanical Properties of Rattan Palm Fiber-Epoxy Composite

The tensile test data for rattan palm fiber-epoxy composite for fiber lengths of 10mm, 30mm and 50mm (fiber aspect ratios of 8.1733m/m, 24.5198m/m and 40.8664m/m) and fiber volume fractions of 10%, 30% and 50% were analyzed using the traditional approach for Young's modulus, tensile strength, yield strength, ultimate elongation and toughness, and the results are given in Table 4.150.

Table 4.150: Rattan Palm-Epoxy Composite Tensile Test Analysis

Fiber Length (mm)	Fiber Aspect Ratio (m/m)	Volume Fraction (%)	Young Modulus (GPa)	Tensile Strength (Mpa)	Yield Strength (MPa)	Ultimate Elongation (%)	Toughness (MPa)
10	8.1733	10	1.9649	8.9912	6.7145	2.8440	0.2198
10	8.1733	30	3.4090	12.0614	8.5622	3.5900	0.3748
10	8.1733	50	1.0260	10.0877	6.5069	4.0625	0.3358
30	24.5198	10	1.6321	10.7456	8.3939	2.9700	0.2646
30	24.5198	30	2.7131	12.0614	7.4590	1.4500	0.1227
30	24.5198	50	1.0182	10.0877	8.8959	2.6600	0.2057
50	40.8664	10	1.1422	9.9781	7.2879	4.5000	0.3853
50	40.8664	30	1.5762	12.0614	7.1882	2.7810	0.2375
50	40.8664	50	1.0315	8.7719	7.8808	2.8100	0.1996

4.14.1 Young’s Modulus Analysis for Rattan Palm Fiber-Epoxy Composite

Young’s modulus results from the traditional approach in Table 4.150 were modeled using response surface methodology and the results are presented in Table 4.151, Table 4.152 and Figure 4.82. The pure quadratic model ($y = a_1 + a_2x_1 + a_3x_2 + a_4x_1^2 + a_5x_2^2$) gave the best fit, based on the Adjusted-R² and was therefore used. It can be observed from Table 4.151 that the response surface model for Young’s modulus of rattan palm fiber-epoxy composite explains 85% of the variability observed in the Young’s modulus of the composite. The t-statistics value and its p-value show that fiber volume fraction and its quadratic term are significant at 95% confidence. The model is adequate based on the f-statistics at 90% confidence. It can be observed from the ANOVA table (Table 4.152) that fiber volume fraction is significant at 95% confidence. The surface plot (Figure 4.82) shows a reduction of Young’s Modulus with increase in fiber aspect ratio and a quadratic relationship (an increase to a maximum followed by a decrease) with increase in fiber volume fraction.

Table 4.151: Rattan palm-epoxy Young's modulus RSM model statistics

Variables	Coefficients	Std. Error	t-stat	P-value	F-stat
Constant	0.6491	0.8538	0.7602	0.4895	SSE = 0.8657
Aspect Ratio (m/m)	-0.0094	0.0615	-0.1524	0.8862	DFE = 4
Fiber Vol. Frac.(%)	0.1757	0.0502	3.4962	0.0250	DFR = 4
Asp. Ratio^2	-0.0004	0.0012	-0.2923	0.7846	SSR = 4.8436
Vf^2	-0.0032	0.0008	-3.8413	0.0184	F = 5.5950
	$R^2 = 0.8484$	Adj. $R^2 = 0.6967$			P-val = 0.062003

Table 4.152: Rattan palm-epoxy Young's modulus ANOVA table

Source	Sum Sq.	Df	Mean Sq.	F	Prob>F
Fiber Aspect Ratio (m/m)	1.18891	2	0.59446	2.75	0.1775
Fiber Volume Fraction (Vf) (%)	3.65466	2	1.82733	8.44	0.0367
Error	0.8657	4	0.21642		
Total	5.70927	8			

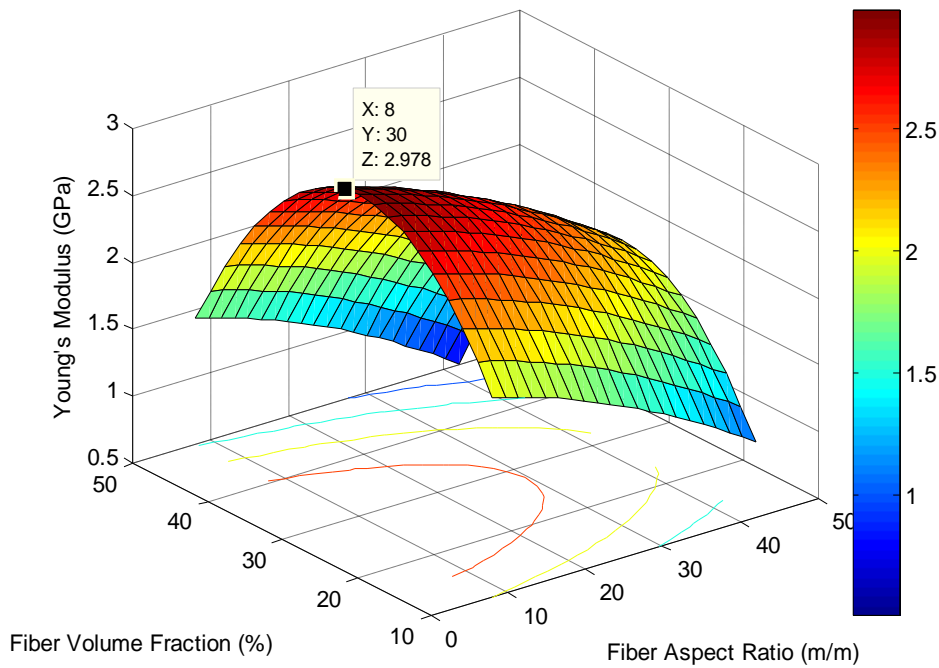


Figure 4.82: Surface plot for Young's modulus of rattan palm-epoxy composite

4.14.2 Tensile Strength Analysis for Rattan Palm Fiber-Epoxy Composite

Tensile strength results from the traditional approach in Table 4.150 were modeled using response surface methodology and the results are presented in Table 4.153, Table 4.154 and Figure 4.83. The quadratic model ($y = a_1 + a_2x_1 + a_3x_2 + a_4x_1x_2 + a_5x_1^2 + a_6x_2^2$) gave the best fit, based on the Adjusted- R^2 and was therefore used. It can be observed from Table 4.153 that the response surface model for tensile strength of rattan palm fiber-epoxy composite explains 96% of the variability observed in the tensile strength of the composite. The t-statistics value and its p-value show that all the terms are significant at 90% or 95% confidence interval except the quadratic term of fiber aspect ratio. The model is adequate based on the f-statistics. It can be observed from the ANOVA table (Table 1.154) that fiber volume fraction is significant. This corroborates observation from the surface plot (Figure 4.83) showing the significant change in tensile strength (as observed from the colour variation) along the fibervolume fraction axis. The surface plot also reveals that the Tensile Strength increases with increase in fiberaspect ratio but eventually decreases.

Table 4.153: Rattanpalm-epoxy tensile strength RSM model statistics

Variables	Coefficients	Std. Error	t-stat	P-value	F-stat
Constant	4.8877	0.9127	5.3551	0.0127	SSE =0.53935
Aspect ratio (m/m)	0.1669	0.0593	2.8131	0.0671	DFE = 3
Fiber Vol. Frac.(%)	0.3794	0.0485	7.8266	0.0043	DFR = 5
Asp. ratio*Vf	-0.0018	0.0006	-2.7154	0.0728	SSR = 12.697
Asp. ratio^2	-0.0024	0.0011	-2.1333	0.1226	F = 14.125
Vf^2	-0.0057	0.0007	-7.6192	0.0047	P-val =0.026912
	$R^2 = 0.9593$	Adj. $R^2 = 0.8913$			

Table 4.154: Rattan palm-epoxy tensile strength ANOVA table

Source	Sum Sq.	Df	Mean Sq.	F	Prob>F
Fiber Aspect Ratio (m/m)	0.8362	2	0.41812	0.90	0.4767
Fiber Volume Fraction (Vf) (%)	10.5349	2	5.26743	11.3	0.0226
Error	1.865	4	0.46624		
Total	13.2361	8			

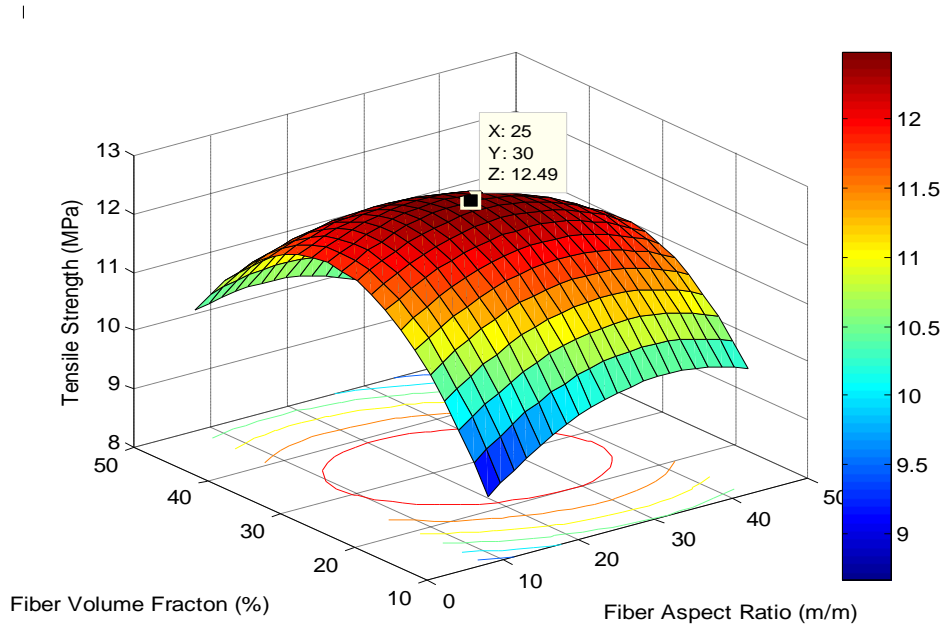


Figure 4.83: Surface plot for tensile strength of rattan palm-epoxy composite

4.14.3 Yield Strength Analysis for Rattan Palm Fiber-Epoxy Composite

Yield strength results from the traditional approach in Table 4.150 were modeled using response surface methodology and the results are presented in Table 4.154, Table 4.156 and Figure 4.84.

The quadratic model ($y = a_1 + a_2x_1 + a_3x_2 + a_4x_1x_2 + a_5x_1^2 + a_6x_2^2$) gave the best fit and was therefore used. It can be observed from Table 4.155 that the response surface model for yield strength of rattan palm fiber-epoxy composite explains only 35% of the variability observed in the yield strength of the composite. The t-statistics value and its p-value show that only the

constant term is significant. The model is not adequate based on the f-statistics. It can be observed from the ANOVA table (Table 4.156) that none of the variables is significant though fiber length has more effect. This corroborates observation from the surface plot (Figure 4.84).

Table 4.155: Rattan palm-epoxy yield strength RSM model statistics

Variables	Coefficients	Std. Error	t-stat	P-value	F-stat
Constant	6.1308	2.3524	2.6062	0.0799	SSE = 3.5827
Aspect Ratio (m/m)	0.1513	0.1529	0.9900	0.3952	DFE = 3
Fiber Vol. Frac.(%)	0.0109	0.1249	0.0869	0.9362	DFR = 5
Asp. Ratio*Vf	0.0006	0.0017	0.3663	0.7385	SSR = 1.9709
Asp. Ratio^2	-0.0033	0.0029	-1.1555	0.3316	F = 0.33007
Vf^2	-0.0003	0.0019	-0.1594	0.8835	P-val =0.8681
	$R^2 = 0.3549$	Adj. $R^2 = -0.7203$			

Table 4.156: Rattan palm-epoxy yield strength ANOVA table

Source	Sum Sq.	Df	Mean Sq.	F	Prob>F
Fiber Length (Fl) (mm)	1.64914	2	0.82457	0.88	0.4818
Fiber Volume Fraction (Vf) (%)	0.16155	2	0.08077	0.09	0.9190
Error	3.74286	4	0.93572		
Total	5.55355	8			

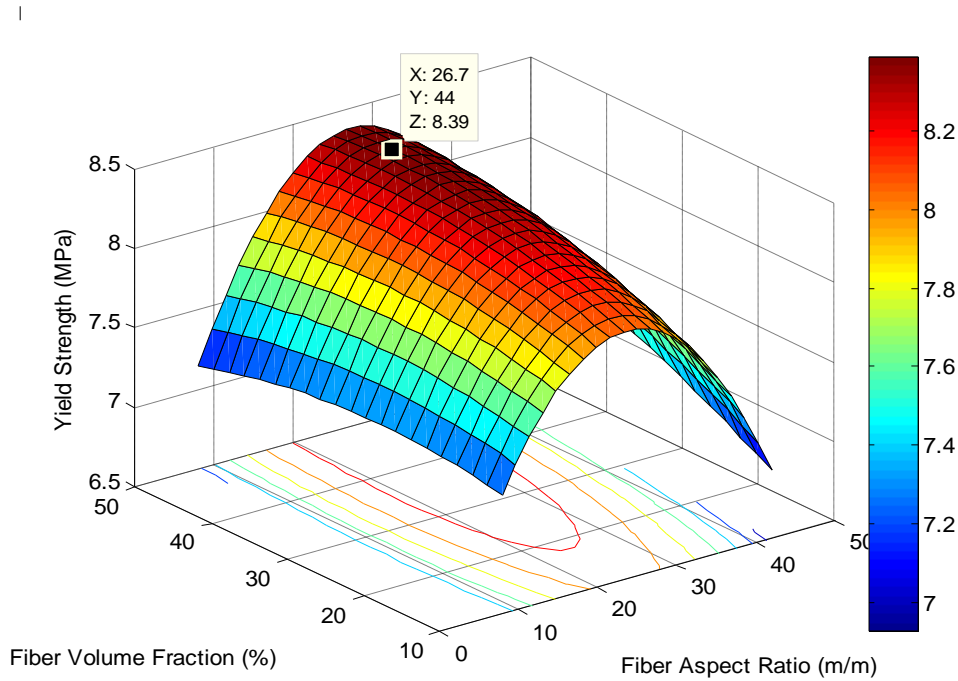


Figure 4.84: Surface plot for yield strength of rattan palm-epoxy composite

4.14.4 Ultimate Elongation Analysis for Rattan Palm Fiber-Epoxy Composite

Ultimate elongation results from the traditional approach in Table 4.150 were modeled using response surface methodology and the results are presented in Table 4.157, Table 4.158 and Figure 4.85. The quadratic model ($y = a_1 + a_2x_1 + a_3x_2 + a_4x_1x_2 + a_5x_1^2 + a_6x_2^2$) gave the best fit and was therefore used. It can be observed from Table 4.157 that the response surface model for ultimate elongation of rattan palm fiber-epoxy composite explains 88% of the variability observed in the ultimate elongation of the composite. The t-statistics value shows that the constant term is significant at 95% confidence interval while the interaction term and quadratic term of aspect ratio are significant at 90% confidence interval. The model is not adequate based on the f-statistics. It can be observed from the ANOVA table (Table 4.158) that none of the variables is significant though fiber aspect ratio has more effect. This corroborates

observation from the surface plot (Figure 4.85). The surface plot also reveals that the elongation initially drops but eventually increases with increase in fiber aspect ratio.

Table 4.157: Rattan palm-epoxy ultimate elongation RSM model statistics

Variables	Coefficients	Std. Error	t-stat	P-value	F-stat
Constant	4.5406	1.1001	4.1272	0.0258	SSE = 0.7836
Aspect Ratio (m/m)	-0.1340	0.0715	-1.8744	0.1576	DFE = 3
Fiber Vol. Frac.(%)	-0.0571	0.0584	-0.9770	0.4006	DFR = 5
Asp. Ratio*Vf	-0.0022	0.0008	-2.8455	0.0654	SSR = 5.5213
Asp. Ratio^2	0.0040	0.0014	2.9643	0.0593	F = 4.2276
Vf^2	0.0018	0.0009	1.9391	0.1478	P-val = 0.1325
	$R^2 = 0.8757$	Adj. $R^2 =$ 0.6686			

Table 4.158: Rattan palm-epoxy ultimate elongation ANOVA table

Source	Sum Sq.	Df	Mean Sq.	F	Prob>F
Fiber Length (Fl) (mm)	2.32256	2	1.16128	1.60	0.3082
Fiber Volume Fraction (Vf) (%)	1.08389	2	0.54195	0.75	0.5297
Error	2.89845	4	0.72461		
Total	6.3049	8			

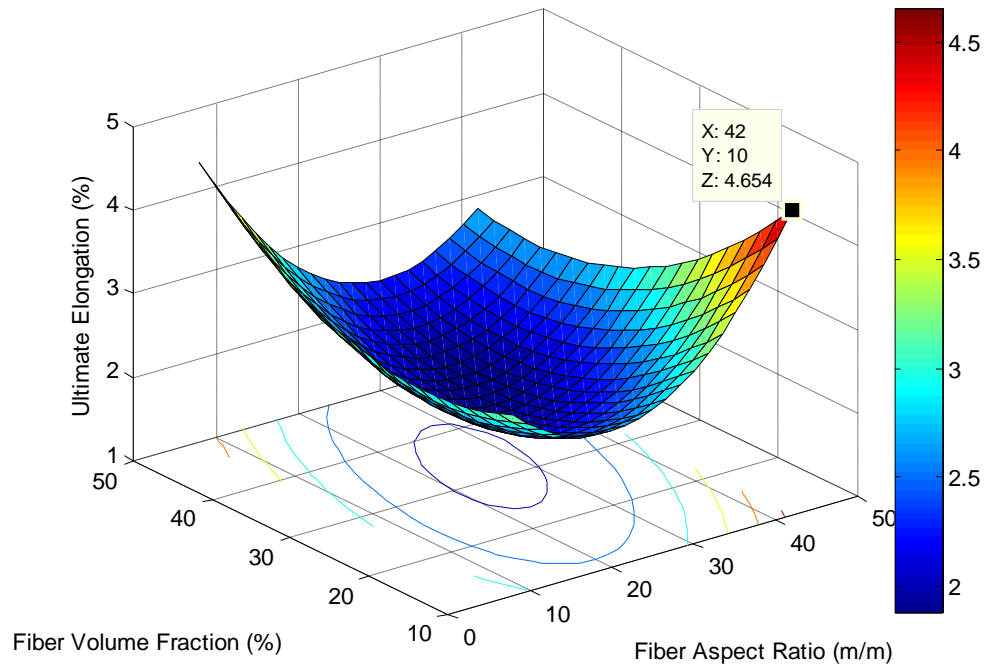


Figure 4.85: Surface plot for elongation of rattan palm fiber-epoxy composite

4.14.5 Toughness Analysis for Rattan Palm Fiber-Epoxy Composite

Results of toughness from the traditional approach in Table 4.150 were modeled using response surface methodology and the results are presented in Table 4.159, Table 4.160 and Figure 4.86. The quadratic model ($y = a_1 + a_2x_1 + a_3x_2 + a_4x_1x_2 + a_5x_1^2 + a_6x_2^2$) gave the best fit and was therefore used. It can be observed from Table 4.159 that the response surface model for toughness of rattan palm fiber-epoxy composite explains 48% of the variability observed in the toughness of the composite. The t-statistics value and its p-value show that none of the variables is significant. The model is not adequate based on the f-statistics. It can be observed from the ANOVA table (Table 4.160) that none of the variables is significant though fiber length has more effect. This corroborates observation from the surface plot (Figure 4.86). The surface plot also

reveals that the toughness decreases but subsequently increased with increase in fiber length, but the profile is the reverse for fiber volume fraction.

Table 4.159: Rattan palm fiber-epoxy toughness RSM model statistics

Variables	Coefficients	Std. Error	t-stat	P-value	F-stat
Constant	0.3368	0.1563	2.1556	0.1201	SSE = 0.015807
Aspect Ratio (m/m)	-0.0115	0.0102	-1.1342	0.3392	DFE = 3
Fiber Vol. Frac.(%)	0.0011	0.0083	0.1283	0.9060	DFR = 5
Asp. Ratio*Vf	-0.0002	0.0001	-2.0782	0.1292	SSR = 0.046405
Aspect Ratio^2	0.0004	0.0002	1.8405	0.1630	F = 1.7614
Vf^2	5.8667e-05	0.0001	0.4572	0.6786	P-val = 0.34009
	$R^2 = 0.7459$	Adj. $R^2 = 0.3224$			

Table 4.160: Rattan palm fiber-epoxy toughness ANOVA table

Source	Sum Sq.	Df	Mean Sq.	F	Prob>F
Fiber aspect Ratio (m/m)	0.019156	2	0.0095781	1.1708	0.39786
Fiber Volume Fraction (Vf) (%)	0.010332	2	0.0051661	0.63147	0.57765
Error	0.032724	4	0.008181		
Total	0.062212	8			

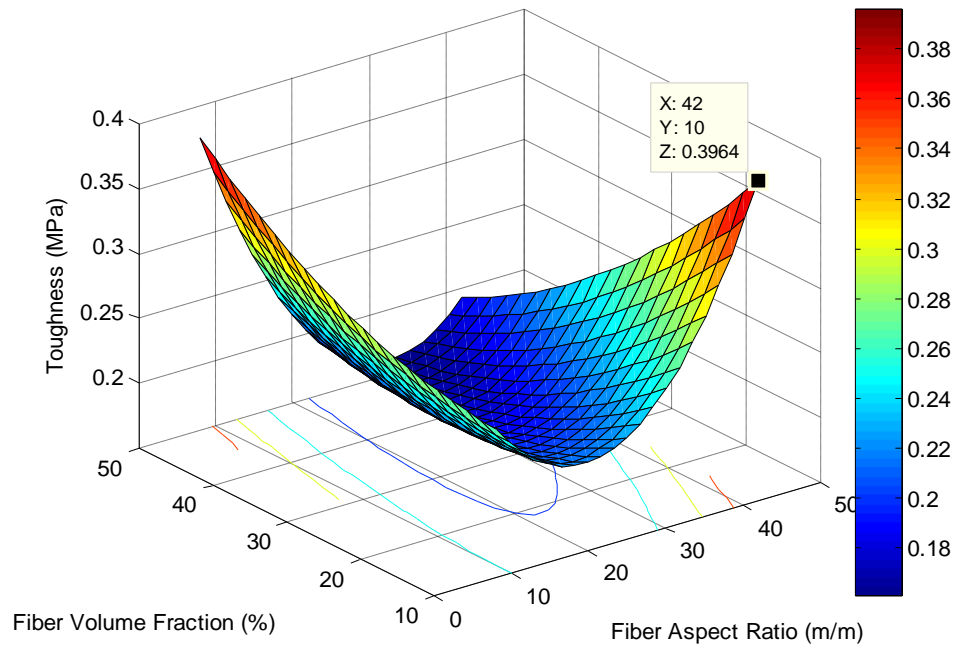


Figure 4.86: Surface plot for toughness of rattan palm-epoxy composite

4.14.6 Rattan Palm Fiber-Epoxy Composite Tensile Properties Optimization

The RSM model coefficients from Table 4.151, Table 4.153, Table 4.155, Table 4.157 and Table 4.159 were used to run a MATLAB 7.9 optimization code and the optimal values for fiber aspect ratio and fiber volume fraction are presented alongside predicted optimal values of mechanical properties and the experimental values for validation. It can be observed from Table 4.161 that the optimal values occur at different points for the mechanical properties, but from the two mechanical properties that their model fits were adequate optimum values will be a fiber aspect ratio of 8-25m/m and fiber volume fraction of 30%. It can also be observed from Table 4.162 that the model predicted values for most mechanical properties are close to the experimentally validated values. Exceptions are due to the low fit of the RSM model for certain properties.

Table 4.161: Optimal Values for Mechanical Properties of Rattan Palm Fiber-Epoxy

Variables	Toughness	Tensile Strength	Young Modulus	Yield Strength	%El
Fiber Aspect Ratio (m/m)	41	25	8	26.7	41
Fiber Volume Fraction (%)	10	30	30	44	10

Table 4.162: Predicted Versus Experimental Optimum for Rattan Palm Fiber-Polyester

	Toughness (MPa)	Tensile Strength (MPa)	Young Modulus (GPa)	Yield Strength (MPa)	%El (%)
Model Predicted Values	0.3964	12.4900	2.9780	8.3900	4.6540
Experimental Values	0.3853	12.2881	3.9430	8.9086	4.4442

4.15 Flexural Strength Analysis for All Composites

4.15.1 Empty Plantain Bunch-Polyester Composite Flexural Strength Analysis

Empty plantain bunch-polyester composites with fibers of length from 10-50mm (fiber aspect ratios of 23.6183m/m to 118.0916m/m) and volume fractions of 10-50% were subjected to flexural strength tests and the results are shown in Table 4.163. The data from Table 4.164 was modeled using response surface methodology and the results of the analysis are presented in Table 4.164, the analysis of variance results are presented in Table 4.165 and the surface plot is presented in Figure 4.87. It can be observed from Table 4.163 that the flexural strength of polyester-empty plantain bunch fiber composite varied from 14.57MPa to 54.65MPa as the fiber length and fiber volume fraction varied from 10-50mm (fiber aspect ratios of 23.6183m/m to 118.0916m/m) and 10-50% respectively. The R^2 value (Table 4.164) reveals that the model explains 93% of the variability observed in the experimental data. The model is adequate at 90% confidence based on the F-statistics p-value of 0.058. The significant variables based on the

value of the t-statistics are fiber aspect ratio squared, fiber volume fraction and the interaction between fiber aspect ratio and volume fraction, though only the last two are significant at 90% confidence based on the t-statistics p-value. It can be observed from the surface plot (Figure 4.87), especially by studying the colour variation along each axis, that fiber aspect ratio had more significant effect on the flexural strength than fiber volume fraction; this conclusion is easier to make, though, from the analysis of variance table (Table 4.165) which reveals that fiber aspect ratio is the significant of the two variables at 90% confidence. The natures of the surface plot contour lines also reveal a good level of interaction among the two variables. The optimum flexural strength was obtained using the response surface model and gave a maximum flexural strength at a fiber aspect ratio of 25m/m and volume fraction of 44%. The optimum flexural strength obtained is 51.6 MPa (54.65 MPa based on the experiment), which is higher than 40.16 MPa obtained by Lina Herrera-Estrado et al (2008) and 42.40MPa obtained by Ihueze and Okafor (2014) for empty plantain bunch fiber reinforced polyester composite. The observed improvement may be linked to use of fibers obtained by treatment at optimum conditions. The optimum volume fraction of 44% is also not far from 50% quoted by Chimekwene et al (2012) and Ihueze and Okafor (2014) for empty plantain bunch fiber reinforced epoxy composite, though the later authors did not use a random orientation.

Table 4.163: Emptyplantainbunch-polyester flexural strength data

Fiber Length (mm)	10	10	10	30	30	30	50	50	50
Aspect Ratio (m/m)	23.62	23.62	23.62	70.86	70.86	70.86	118.1	118.1	118.1
Volume Fraction(%)	10	30	50	10	30	50	10	30	50
Force (N)	15.75	18.70	23.63	15.75	21.66	15.75	9.84	10.83	6.30
Flexural Strength (MPa)	36.43	43.25	54.65	36.43	50.10	36.43	22.76	25.05	14.57

Table 4.164: Empty plantain bunch-polyester flexural strength RSM model results

Variables	Coefficients	Std. Error	t-stat	P-value	F-stat
Constant	13.7813	12.0177	1.1468	0.3347	SSE = 93.505
Aspect Ratio (m/m)	0.4767	0.2703	1.7638	0.1760	DFE = 3
Fiber Vol. Frac.(%)	1.4670	0.6383	2.2982	0.1052	DFR = 5
Aspect ratio*Vf	-0.0070	0.0030	-2.3653	0.0989	SSR = 1258.6
Aspect Ratio^2	-0.0037	0.0018	-2.0776	0.1293	F = 8.0762
Vf^2	-0.0148	0.0099	-1.5000	0.2306	P-val = 0.058
	$R^2 = 0.9308$	$Adj. R^2 = 0.8156$			

Table 4.165: Empty Plantain Bunch-Polyester Flexural Strength ANOVA Table

Source	Sum Sq.	Df	Mean Sq.	F	Prob>F
Fiber Aspect Ratio (m/m)	997.34	2	498.668	7.45	0.0448
Fiber Volume Fraction (Vf) (%)	86.9	2	43.45	0.65	0.5701
Error	267.88	4	66.969		
Total	1352.11	8			

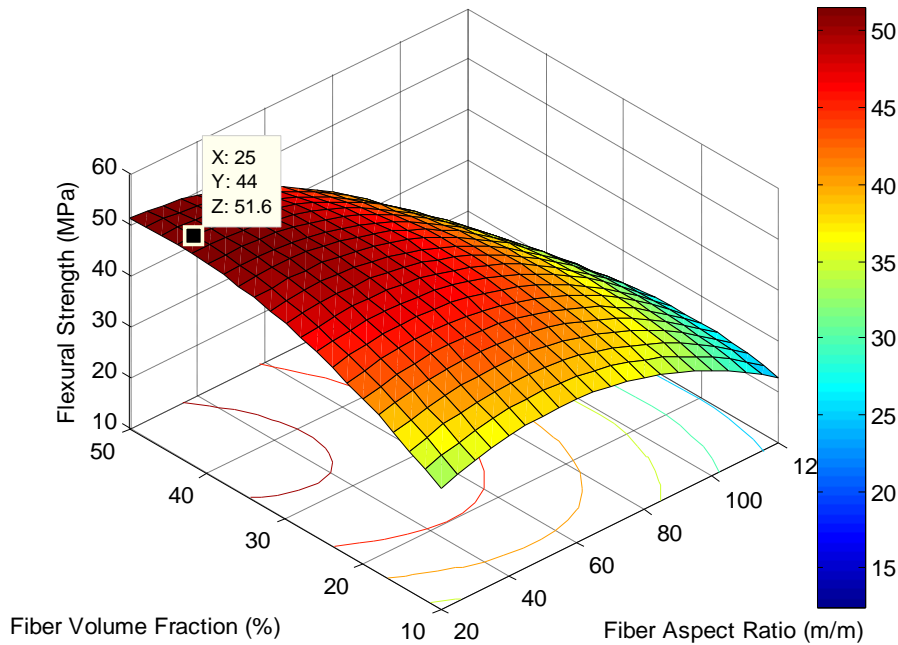


Figure 4.87: Surface plot for flexural strength of empty plantain bunch-polyester

4.15.2 Empty Plantain Bunch-Epoxy Composite Flexural Strength Analysis

Empty plantain bunch-epoxy composites with fibers of length from 10-50mm (fiber aspect ratios of 23.6183m/m to 118.0916m/m) and volume fractions of 10-50% were subjected to flexural strength tests and the results are shown in Table 4.166. The data from Table 4.166 was modeled using response surface methodology and the results of the analysis are presented in Table 4.167, the analysis of variance results are presented in Table 4.168 and the surface plot is presented in Figure 4.88. It can be observed from Table 4.167 that the Flexural strength of epoxy-empty plantain bunch fiber composite varies from 14.10MPa to 37.60MPa as the fiber length (aspect ratio) and fiber volume fraction varied from 10-50mm (fiber aspect ratios of 23.6183m/m to 118.0916m/m) and 10-50% respectively. The R^2 value (Table 4.167) reveals that the model explains 94% of the variability observed in the experimental data. The model is adequate at 95% confidence based on the F-statistics p-value of 0.0419. The only significant variables based on the value of the response surface model t-statistics is fiber aspect ratio, though none of the variables is significant based on the t-statistics p-value. It can be observed from the surface plot (Figure 4.88), especially by studying the colour variation along each axis, that fiber volume fraction had more significant effect on the flexural strength than fiber aspect ratio; this conclusion is easier to make, though, from the analysis of variance table (Table 4.168) which reveals that fiber volume fraction is the significant of the two variables at 95% confidence. The optimum flexural strength was obtained using the response surface model and this gave a maximum flexural strength at a fiber aspect ratio 90m/m and volume fraction of 50%.The optimum flexural strength obtained is 37.39 MPa (37.6 MPa based on experiment), which is higher than 34.99 MPa obtained by Chimekwene et al (2012) for empty plantain bunch fiber reinforced epoxy composite.The observed improvement may be linked to use of fibers obtained

by treatment at optimum conditions. They also obtained the optimum volume fraction of as 50% in agreement with this study.

Generally, empty plantain bunch fiber composite produced using polyester had maximum flexural strength higher than that from epoxy by about 45%.

Table 4.166: Empty Plantain Bunch-Epoxy Flexural Strength Data

Fiber Length (mm)	10	10	10	30	30	30	50	50	50
Aspect Ratio (m/m)	23.62	23.62	23.62	70.86	70.86	70.86	118.1	118.1	118.1
Volume Fraction (%)	10	30	50	10	30	50	10	30	50
Force (N)	6.10	10.16	12.19	9.15	12.19	15.24	7.11	9.15	16.26
Flexural Strength (MPa)	14.10	23.50	28.20	21.15	28.20	35.25	16.45	21.15	37.60

Table 4.167: Empty Plantain Bunch-Epoxy Flexural Strength RSM Model Data

Variables	Coefficients	Std. Error	t-stat	P-value	F-stat
Constant	8.7636	6.5848	1.3309	0.2753	SSE = 28.073
Aspect Ratio (m/m)	0.2757	0.1481	1.8617	0.1596	DFE = 3
Fiber Vol. Frac.(%)	0.1028	0.3498	0.2940	0.7880	DFR = 5
Aspect Ratio*Vf	0.0019	0.0016	1.1523	0.3327	SSR = 480
Aspect Ratio^2	-0.0021	0.0010	-2.1729	0.1181	F = 10.259
Vf^2	0.0029	0.0054	0.5432	0.6247	P-val = 0.0419
	$R^2 = 0.9447$	$Adj. R^2 = 0.8527$			

Table 4.168: Empty Plantain Bunch-Epoxy Flexural Strength ANOVA Table

Source	Sum Sq.	Df	Mean Sq.	F	Prob>F
Fiber Aspect Ratio (m/m)	58.907	2	29.453	2.91	0.166
Fiber Volume Fraction (Vf) (%)	408.665	2	204.333	20.18	0.0081
Error	40.498	4	10.125		
Total	508.07	8			

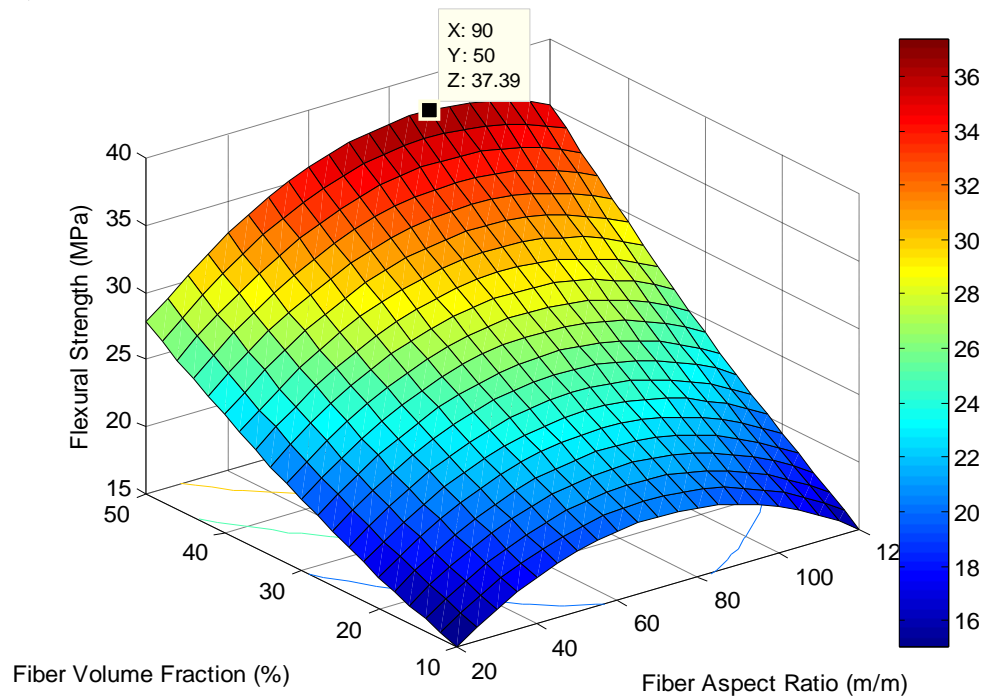


Figure 4.88: Surface plot for flexural strength of empty plantain bunch-epoxy

4.15.3 Empty Palm Bunch-Polyester Composite Flexural Strength Analysis

Empty palm bunch-polyester composites with fibers of length from 10-50mm (fiber aspect ratios of 22.2222m/m to 111.1111m/m) and volume fractions of 10-50% were subjected to flexural strength tests and the results are shown in Table 4.169. The data from Table 4.169 was modeled using response surface methodology and the results of the analysis are presented in Table 4.170, the analysis of variance results are presented in Table 4.171 and the surface plot is presented in Figure 4.89. It can be observed from Table 4.169 that the flexural strength of polyester-empty palm bunch fiber composite was observed to vary from 23.52MPa to 50.72MPa as the fiber length (aspect ratio) and fiber volume fraction varied from 10-50mm (fiber aspect ratios of 22.2222m/m to 111.1111m/m) and 10-50% respectively. The R^2 value (Table 4.170) reveals that the model explains 98% of the variability observed in the experimental data. The model is

adequate at 95% confidence interval based on the F-statistics p-value of 0.008. The constant term, fiber volume fraction and its quadratic term are significant at 95% confidence interval while the interaction variable is significant at 90% confidence interval based on the t-statistics p-value. It can be observed from the surface plot (Figure 4.89), especially by studying the colour variation along each axis, that fiber volume fraction had more significant effect on the flexural strength than fiber aspect ratio; this conclusion is easier to make, though, from the analysis of variance table (Table 4.171) which reveals that fiber volume fraction is the significant of the two variables at 95% confidence interval, though fiber length is also significant at 90% confidence interval. The nature of the surface plot contour lines also reveals that there is good interaction among the two variables. The optimum flexural strength was obtained at a fiber aspect ratio of 111.11m/m and volume fraction of 50%. This result agrees with the 40-70% volume fraction given by Myrtha et al (2008) and their observation of better flexural strength for long fibers. The optimum flexural strength is 50.72MPa, which is higher than 36.8MPa reported by the earlier mentioned authors for long fibers because their result was at a lower volume fraction of 18%.

Table 4.169: Empty Palm Bunch-Polyester Composite Flexural StrengthData

Fiber Length (mm)	10	10	10	30	30	30	50	50	50
Aspect Ratio (m/m)	22.22	22.22	22.22	66.67	66.67	66.67	111.1	111.1	111.1
Volume Fraction (%)	10	30	50	10	30	50	10	30	50
Force (N)	11.96	10.17	17.94	10.97	11.96	18.14	11.96	14.35	21.93
Flexural Strength (MPa)	27.66	23.52	41.49	25.37	27.66	41.96	27.66	33.19	50.72

Table 4.170: Empty Palm Bunch-Polyester Composite Flexural StrengthRSM Data

Variables	Coefficients	Std. Error	t-stat	P-value	F-stat
Constant	36.2783	4.3927	8.2588	0.0037	SSE = 12.493
Aspect Ratio (m/m)	-0.1674	0.1050	-1.5946	0.2091	DFE = 3
Fiber Vol. Frac.(%)	-0.8804	0.2333	-3.7733	0.0326	DFR = 5
Aspect Ratio*Vf	0.0026	0.0011	2.2615	0.1088	SSR = 686.99
Aspect Ratio^2	0.0012	0.0007	1.6471	0.1981	F = 32.995
Vf^2	0.0192	0.0036	5.3270	0.0129	P-val = 0.008
	$R^2=0.9821$	$Adj.R^2=0.9524$			

Table 4.171: Empty Palm Bunch-Polyester Composite Flexural StrengthANOVA Table

Source	Sum Sq.	Df	Mean Sq.	F	Prob>F
Fiber Aspect Ratio (m/m)	70.832	2	35.416	4.19	0.1043
Fiber Volume Fraction (Vf) (%)	594.855	2	297.427	35.21	0.0029
Error	33.791	4	8.448		
Total	699.478	8			

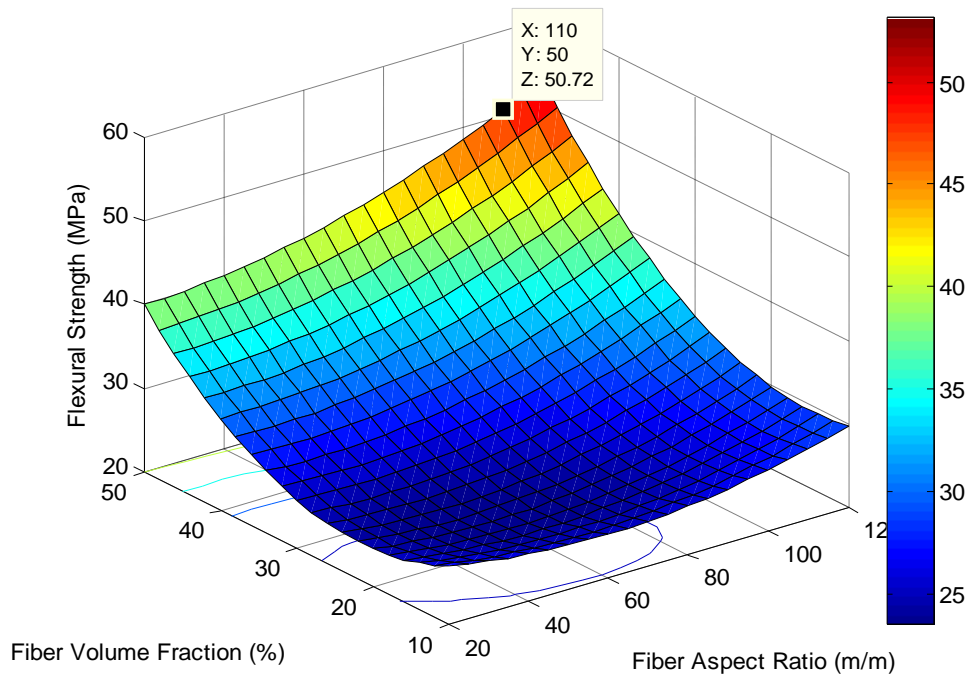


Figure 4.89: Surface plot for flexural strength of empty palm bunch-polyester

4.15.4 Empty Palm Bunch-Epoxy Composite Flexural Strength Analysis

Empty palm bunch-epoxy composites with fibers of length from 10-50mm (fiber aspect ratios of 22.2222m/m to 111.1111m/m) and volume fractions of 10-50% were subjected to flexural strength tests and the results are shown in Table 4.172. The data from Table 4.172 was modeled using response surface methodology and the results of the analysis are presented in Table 4.173, the analysis of variance results are presented in Table 4.174 and the surface plot is presented in Figure 4.90. It can be observed from Table 4.172 that the Flexural strength of epoxy-empty palm bunch fiber composite varied from 9.22MPa to 28.13MPa as the fiber length (aspect ratio) and fiber volume fraction varied from 10-50mm (fiber aspect ratios of 22.2222m/m to 111.1111m/m) and 10-50% respectively. The R^2 value (Table 4.174) reveals that the model explains about 80% of the variability observed in the experimental data. The model is not adequate even at 90% confidence interval, based on the F-statistics p-value. The only significant variable based on the value of the response surface model t-statistics is fiber length, though none of the variables is significant based on the t-statistics p-value, even at 90% confidence interval. It can be observed from the surface plot (Figure 4.90), especially by studying the colour variation along each axis, that fiber volume fraction had more significant effect on the flexural strength than fiber aspect ratio; this conclusion is easier to make, though, from the analysis of variance table (Table 4.174) which reveals that fiber volume fraction is the more significant of the two variables, though none is significant even at 90% confidence interval. The nature of the surface plot contour lines (Figure 4.90) also reveals that the interaction among the two variables is not significant. The optimum flexural strength was obtained using the response surface model and this gave a maximum flexural strength of 25.45MPa at a fiber aspect ratio of 55m/m and volume fraction of 44%.

Generally, empty palm bunch fibre composite produced using polyester had its maximum flexural strength higher than that from epoxy by about 80%. Composites from empty palm bunch fibre had lower flexural strength than those of empty plantain bunch fibre.

Table 4.172: Empty Palm Bunch-Epoxy Flexural Strength Data

Fiber Length (mm)	10	10	10	30	30	30	50	50	50
Aspect Ratio (m/m)	22.22	22.22	22.22	66.67	66.67	66.67	111.1	111.1	111.1
Volume Fraction (%)	10	30	50	10	30	50	10	30	50
Force (N)	3.99	6.58	9.97	6.18	9.97	12.16	6.98	9.97	4.98
Flexural Strength (MPa)	9.22	15.22	23.06	14.29	23.06	28.13	16.14	23.06	11.53

Table 4.173: Empty Palm Bunch-Epoxy Flexural StrengthRSM Data

Variables	Coefficients	Std. Error	t-stat	P-value	F-stat
Constant	-12.7598	10.0221	-1.2732	0.2927	SSE = 65.03
Aspect Ratio (m/m)	0.5360	0.2395	2.2375	0.1112	DFE = 3
Fiber Vol. Frac.(%)	1.0459	0.5323	1.9648	0.1442	DFR = 5
Aspect Ratio*Vf	-0.0052	0.0026	-1.9815	0.1419	SSR = 257.97
Aspect Ratio^2	-0.0028	0.0017	-1.6570	0.1961	F = 2.3802
Vf^2	-0.0085	0.0082	-1.0282	0.3795	P-val = 0.2532
	$R^2 = 0.7987$	$Adj. R^2 = 0.4631$			

Table 4.174: Empty Palm Bunch-Epoxy Flexural StrengthANOVA Table

Source	Sum Sq.	Df	Mean Sq.	F	Prob>F
Fiber Aspect Ratio (mm)	61.253	2	30.6264	0.82	0.5044
Fiber Volume Fraction (Vf) (%)	111.621	2	55.8103	1.49	0.329
Error	150.131	4	37.5327		
Total	322.004	8			

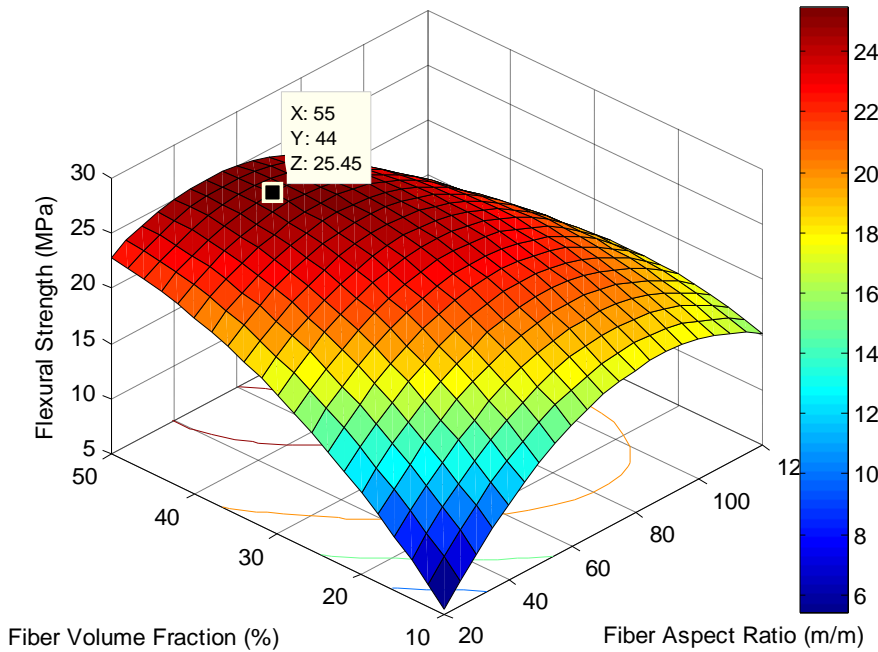


Figure 4.90: Surface plot for flexural strength of empty palm bunch-epoxy

4.15.5 Rattan Palm Fiber-Polyester Composite Flexural Strength Analysis

Rattan palm fiber-polyester composites with fibers of length from 10-50mm (fiber aspect ratios of 8.1733m/m to 40.8664m/m) and volume fractions of 10-50% were subjected to flexural strength tests and the results are shown in Table 4.175. The data from Table 4.175 was modeled using response surface methodology, a pure-quadratic model was used because it gave the best fit based on the adjusted- R^2 , and the results of the analysis are presented in Table 4.176, the analysis of variance results are presented in Table 4.177 and the surface plot is presented in Figure 4.91. It can be observed from Table 4.175 that the Flexural strength of polyester-rattan palm fiber composite varies from 20.29MPa to 37.35MPa as the fiber length (aspect ratio) and fiber volume fraction varied from 10-50mm(fiber aspect ratios of 8.1733m/m to 40.8664m/m)and 10-50% respectively. The R^2 value (Table 4.176) reveals that the model

explains 89% of the variability observed in the experimental data. The model is adequate at 95% confidence interval, based on the F-statistics p-value. All the variables (constant term, fiber aspect ratio and volume fraction with their quadratic terms) are significant at 95% confidence interval based on the value of the response surface model t-statistics and its p-value. It can be observed from the surface plot (Figure 4.91), especially by studying the colour variation along each axis, that fiber volume fraction had more significant effect on the flexural strength than fiber aspect ratio; this conclusion is easier to make, though, from the analysis of variance table (Table 4.177) which reveals that fiber volume fraction is the more significant of the two variables, being significant at 95% confidence interval, while fiber aspect ratio is significant at 90% confidence interval. The optimum flexural strength was obtained using the response surface model and this gave a maximum flexural strength of 35.41MPa (37.35MPa from experiment) at a fiber aspect ratio of 41mm and volume fraction of 26%.

Table 4.175: Rattan Palm Fiber-Polyester Flexural Strength Data

Fiber Length (mm)	10	10	10	30	30	30	50	50	50
Aspect Ratio (m/m)	8.173	8.173	8.173	24.52	24.52	24.52	40.87	40.87	40.87
Volume Fraction (%)	10	30	50	10	30	50	10	30	50
Force (N)	12.96	16.15	9.97	9.97	10.57	8.77	12.56	15.95	9.97
Flexural Strength (MPa)	29.97	37.35	23.06	23.06	24.44	20.29	29.05	36.89	23.06

Table 4.176: Rattan Palm Fiber-Polyester Flexural Strength RSMDData

Variables	Coefficients	Std. Error	t-stat	P-value	F-stat
Constant	30.3880	5.3245	5.7071	0.0047	SSE =33.67
Aspect Ratio (m/m)	-1.3538	0.3834	-3.5309	0.0242	DFE = 4
Fiber Vol. Frac.(%)	1.0912	0.3134	3.4820	0.0253	DFR = 4
Aspect Ratio^2	0.0273	0.0077	3.5583	0.0236	SSR = 280.5
Vf^2	-0.0204	0.0051	-3.9702	0.0165	F = 8.331
	$R^2 = 0.8928$	$Adj. R^2 = 0.7857$			P-val= 0.032

Table 4.177: Rattan Palm Fiber-Polyester Flexural Strength ANOVA Table

Source	Sum Sq.	Df	Mean Sq.	F	Prob>F
Fiber Aspect Ratio (m/m)	106.897	2	53.4487	6.35	0.0574
Fiber Volume Fraction (Vf) (%)	173.607	2	86.8034	10.31	0.0264
Error	33.67	4	8.4175		
Total	314.174	8			

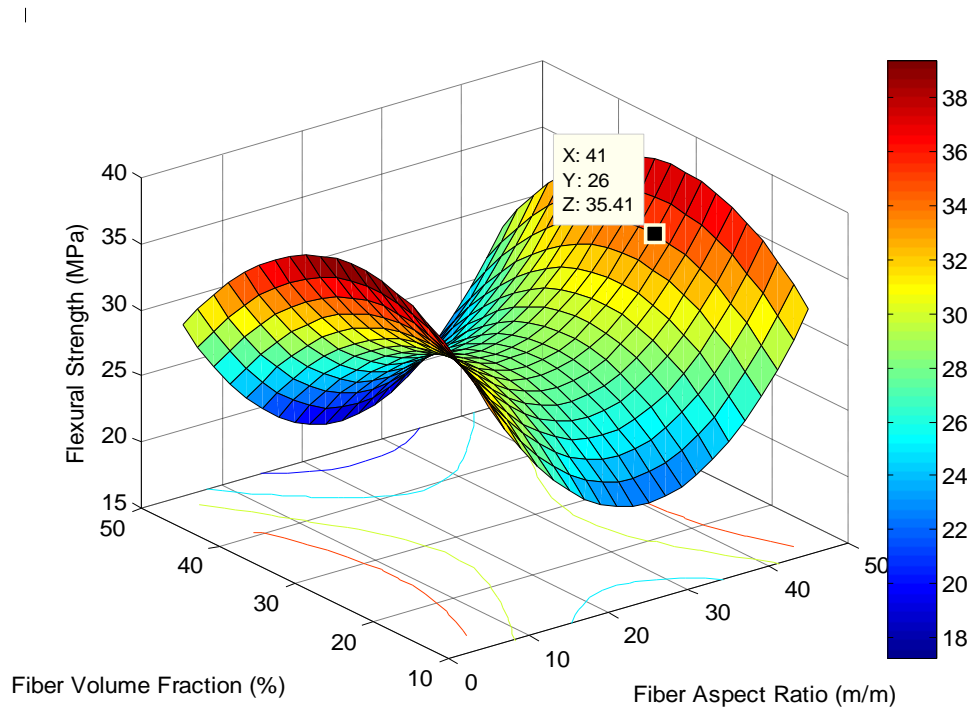


Figure 4.91: Surface plot for flexural strength of rattan palm-polyester composite

4.15.6 Rattan Palm Fiber-Epoxy Composite Flexural Strength Analysis

Rattan palm fiber-epoxy composites with fibers of length from 10-50mm (fiber aspect ratios of 8.1733m/m to 40.8664m/m) and volume fractions of 10-50% were subjected to flexural strength tests and the results are shown in Table 4.178. The data from Table 4.178 was modeled using response surface methodology, the pure-quadratic model was used because it gave the best fit based on the adjusted- R^2 , and the results of the analysis are presented in Table 4.179. The

analysis of variance results are presented in Table 4.180 and the surface plot is presented in Figure 4.92. It can be observed from Table 4.178 that the Flexural strength of epoxy-rattan palm bunch fiber composite varied from 7.84MPa to 31.36MPa as the fiber length (aspect ratio) and fiber volume fraction varied from 10-50mm (fiber aspect ratios of 8.1733m/m to 40.8664m/m) and 10-50% respectively. The R^2 value (Table 4.179) reveals that the model explains 85% of the variability observed in the experimental data. The model is adequate at 90% confidence interval, based on the F-statistics p-value. The significant variables based on the value of the response surface model t-statistics and its p-value are fiber volume fraction at 95% confidence and fiber aspect ratio, its quadratic term and the quadratic term of fiber volume fraction at 90% confidence interval. It can be observed from the surface plot (Figure 4.92), especially by studying the colour variation along each axis, that fiber volume fraction had more significant effect on the flexural strength than fiber aspect ratio; this conclusion is easier to make, though, from the analysis of variance table (Table 4.180) which reveals that fiber volume fraction is the more significant of the two variables, being significant at 95% confidence interval. The optimum flexural strength was obtained by using the response surface model and this gave a maximum flexural strength of 28.98MPa (31.36MPa from experiment) at a fiber aspect ratio of 41m/m and volume fraction of 38%.

Generally, rattan palm fibre composite produced using polyester had its maximum flexural strength higher than that from epoxy by about 16%. Composites from rattan palm fibre had lower flexural strength than those of empty plantain bunch fibre.

Table 4.178: Rattan Palm Fiber-Epoxy Composite Flexural Strength Data

Fiber Length (mm)	10	10	10	30	30	30	50	50	50
Aspect Ratio (m/m)	8.173	8.173	8.173	24.52	24.52	24.52	40.87	40.87	40.87
Volume Fraction (%)	10	30	50	10	30	50	10	30	50
Force (N)	6.48	11.56	9.57	3.39	7.18	9.97	6.58	13.56	9.97
Flexural Strength (MPa)	14.99	26.74	22.13	7.84	16.60	23.06	15.22	31.36	23.06

Table 4.179: Rattan Palm Fiber-Epoxy Composite Flexural Strength RSM Data

Variables	Coefficients	Std. Error	t-stat	P-value	F-stat
Constant	9.9022	7.2184	1.3718	0.2420	SSE = 61.882
Aspect Ratio (m/m)	-1.1187	0.5198	-2.1522	0.0977	DFE = 4
Fiber Vol. Frac.(%)	1.3292	0.4248	3.1286	0.0352	DFR = 4
Aspect Ratio ²	0.0240	0.0104	2.3071	0.0823	SSR = 343.12
Vf ²	-0.0180	0.0070	-2.5828	0.0611	F = 5.5448
	R ² = 0.8472	Adj. R ² = 0.6944			P-val = 0.0629

Table 4.180: Rattan Palm Fiber-Epoxy Composite Flexural Strength ANOVA Table

Source	Sum Sq.	Df	Mean Sq.	F	Prob>F
Fiber Aspect Ratio (m/m)	87.915	2	43.958	2.84	0.1707
Fiber Volume Fraction (Vf) (%)	255.207	2	127.604	8.25	0.0381
Error	61.882	4	15.47		
Total	405.004	8			

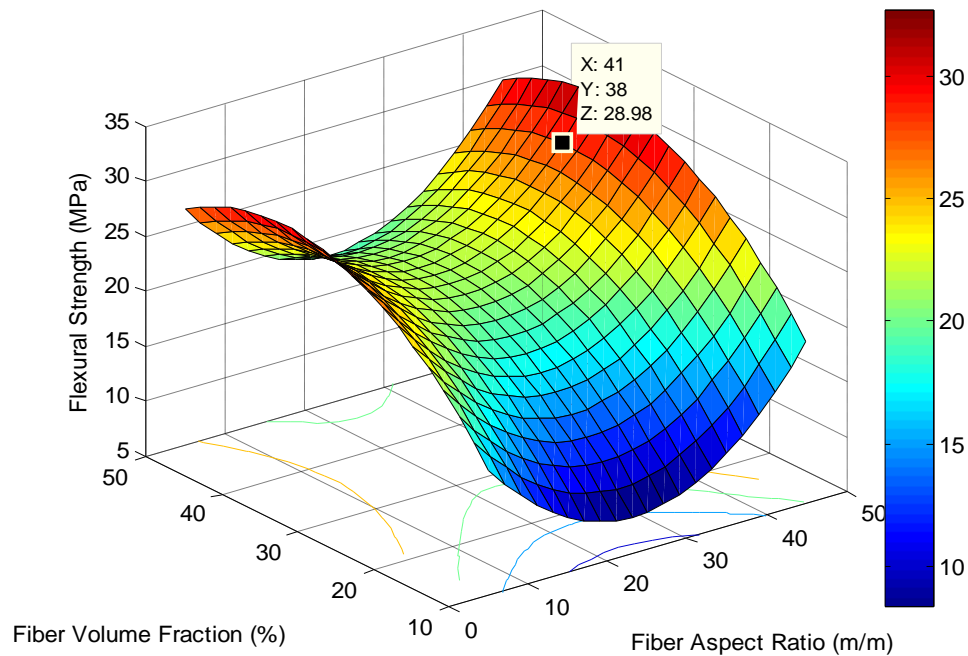


Figure 4.92: Surface plot for flexural strength of rattan palm-epoxy composite

4.16 Impact Strength Analysis for All Composites

4.16.1 Empty Plantain Bunch-Polyester Composite Impact Strength Analysis

Empty plantain bunch-polyester composites with fibers of length from 10-50mm (fiber aspect ratios of 23.6183m/m to 118.0916m/m) and volume fractions of 10-50% were subjected to Impact strength tests and the results are shown in Table 4.181. The data from Table 4.181 was modeled using response surface methodology (a pure-quadratic model was used because it gave the best fit based on the adjusted- R^2) and the results of the analysis are presented in Table 4.182, the analysis of variance results are presented in Table 4.183 and the surface plot is presented in Figure 4.93. The ANOVA table (Table 4.183) reveals that fiber volume fraction has significant effect (at 90% confidence interval) on the impact strength of polyester-empty plantain bunch

fiber composite since its p-value is less than 0.1. This result is in agreement with the p-values from the t-statistics of the coefficients in the response surface model (Table 4.182), which shows that the constant term, fiber volume fraction and its quadratic term are significant. Impact strength remains relatively constant though for empty plantain bunch fiber-polyester composite, for all fiber aspect ratios and volume fractions studied. The model explains about 80% of observed variability in data and is barely adequate at 90% confidence interval. The surface plots (Figure 4.93) corroborate the significance of fiber volume fraction and the low level of interaction between the two factors as revealed in the nature of the surface plot contour lines, which are parallel to each other. The maximum Impact Strength occurred for fiber aspect ratio of 95m/m and fiber volume fraction of 30%, but this maximum value of 10.58Kgfm/cm²(1037.5 KJ/m²) is not far from the surface response model constant term (10.2185Kgfm/cm²).

Table 4.181: Empty Plantain Bunch-Polyester Impact Strength Data

Fiber Length (mm)	10	10	10	30	30	30	50	50	50
Aspect Ratio (m/m)	23.62	23.62	23.62	70.855	70.855	70.855	118.1	118.1	118.1
Volume Fraction (%)	10	30	50	10	30	50	10	30	50
Impact Strength (kgfm/cm ²)	10.42	10.45	10.45	10.46	10.60	10.46	10.46	10.60	10.46

Table 4.182: Empty Plantain Bunch-Polyester Impact Strength RSM Model Statistics

Variables	Coefficients	Std. Error	t-stat	P-value	F-stat
Constant	10.2185	0.0781	130.835	2.0469e-08	SSE = 0.00724
Aspect Ratio (m/m)	0.0028	0.0019	1.4503	0.2206	DFE = 4
Fiber Vol. Frac.(%)	0.0150	0.0046	3.2632	0.0310	DFR = 4
Aspect Ratio ²	-1.4939	1.3487e-05	-1.1077	0.3301	SSR = 0.028378
Vf ²	-0.0002	7.5231e-05	-3.2677	0.0309	F = 3.9172
	R ² =0.7966	Adj. R ² = 0.4745			P-val = 0.10725

Table 4.183: Empty Plantain Bunch-Polyester Impact Strength ANOVA Table

Source	Sum Sq.	Df	Mean Sq.	F	Prob>F
Fiber Aspect Ratio (m/m)	0.00889	2	0.00444	2.45	0.2016
Fiber Volume Fraction (Vf) (%)	0.01949	2	0.00974	5.38	0.0734
Error	0.00724	4	0.00181		
Total	0.03562	8			

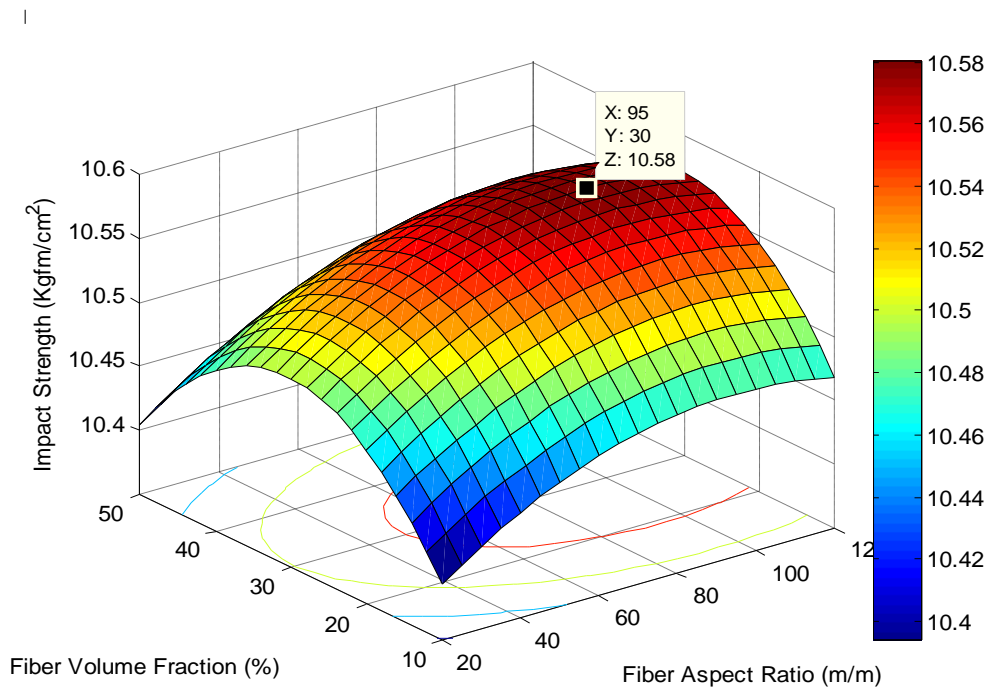


Figure 4.93: Surface plot for impact strength of empty plantain bunch-polyester composite

4.16.2 Empty Plantain Bunch-Epoxy Composite Impact Strength Analysis

Empty plantain bunch-epoxy composites with fibers of length from 10-50mm (fiber aspect ratios of 23.6183m/m to 118.0916m/m) and volume fractions of 10-50% were subjected to impact strength tests and the results are shown in Table 4.184. The data from Table 4.184 was modeled using response surface methodology and the results of the analysis are presented in Table 4.185, the analysis of variance results are presented in Table 4.186 and the surface plot is presented in

Figure 4.94. The ANOVA table (Table 4.186) reveals that both fiber aspect ratio and fiber volume fraction had significant effect on the impact strength of epoxy-empty plantain bunch fiber composite, since the p-value for both variables is much less than 0.05, with fiber volume fraction playing the more significant role. This result is in agreement with the surface plot (Figure 4.94) which shows greater change in impact strength along the fiber volume fraction axis and also reveals a low level of interaction between the two factors as seen in the parallel nature of the contour lines. The p-values from the t-statistics of the coefficients in the response surface model (Table 4.185) show that all terms are significant, except the interaction term, in agreement with surface plot. The interaction term can therefore be deleted from the model without any significant negative effect on model fit and accuracy. The coefficient of determination (R^2) indicates that the response surface model explains 100% of the variations observed in experimental data and is adequate, based on the p-value of the f-statistics table. Fiber volume fraction and its quadratic term are most significant, followed by the constant term. The maximum Impact Strength occurred for fiber aspect ratio of 85m/m and fiber volume fraction of 40% with a value of 21.37Kgf/cm² (2095.7KJ/m²). This value is about twice the maximum impact strength obtained using polyester as matrix.

Table 4.184: Empty Plantain Bunch-Epoxy Impact Strength Data

Fiber Length (mm)	10	10	10	30	30	30	50	50	50
Aspect Ratio (m/m)	23.62	23.62	23.62	70.855	70.855	70.855	118.1	118.1	118.1
Volume Fraction (%)	10	30	50	10	30	50	10	30	50
Impact Strength (kgfm/cm ²)	10.80	20.10	20.00	10.90	20.20	20.20	10.90	20.20	20.10

Table 4.185: Empty Plantain Bunch-Epoxy Impact Strength RSM Model Statistics

Variables	Coefficients	Std. Error	t-stat	P-value	F-stat
Constant	2.4972	0.0829	30.1402	8.023e-05	SSE = 0.00444
AspectRatio (m/m)	0.0064	0.0019	3.4085	0.0422	DFE = 3
Fiber Vol. Frac.(%)	0.9333	0.0044	212.0813	2.3117e-07	DFR = 5
Aspect Ratio*Vf	1.8674e-11	2.0371e-05	9.167e-07	1.0000	SSR = 171.78
Aspect Ratio^2	-3.7347e-05	1.2198e-05	-3.0619	0.0549	F = 23190
Vf^2	-0.0117	6.8041e-05	-172.0767	4.3276e-07	P-val = 4.47e-7
	$R^2 = 1.0$	Adj. $R^2 = 0.9999$			

Table 4.186: Empty Plantain Bunch-Epoxy Impact Strength ANOVA Table

Source	Sum Sq.	Df	Mean Sq.	F	Prob>F
Fiber Length (Fl) (mm)	0.029	2	0.0144	13	0.0178
Fiber Volume Fraction (Vf) (%)	171.749	2	85.8744	77287	0
Error	0.004	4	0.0011		
Total	171.782	8			

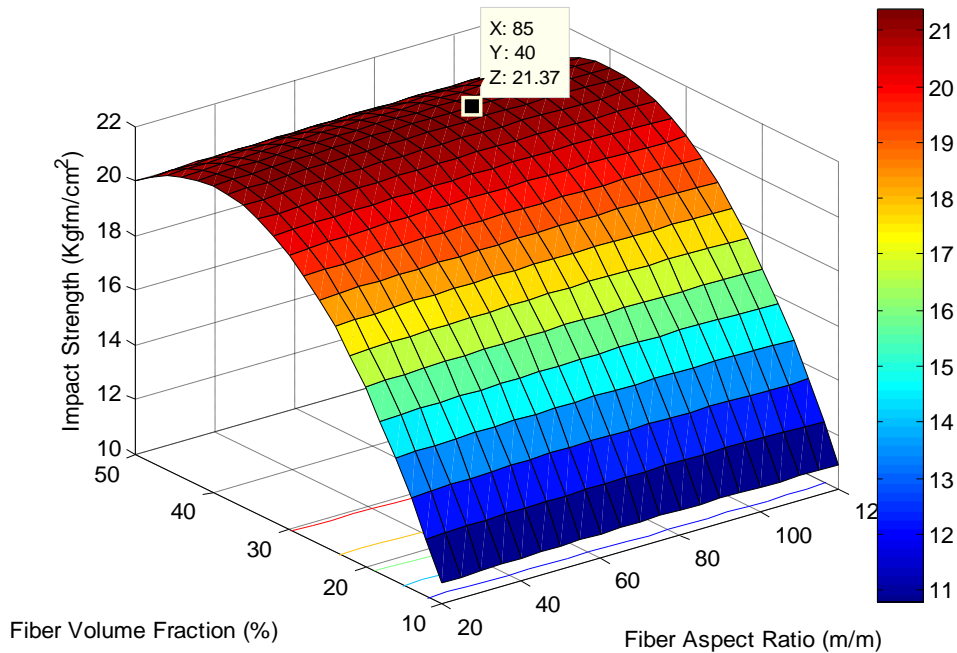


Figure 4.94: Surface plot for impact strength of empty plantain bunch-epoxy composite

4.16.3 Empty Palm Bunch-Polyester Composite Impact Strength Analysis

Empty palm bunch-polyester composites with fibers of length from 10-50mm (fiber aspect ratios of 22.2222m/m to 111.1111m/m) and volume fractions of 10-50% were subjected to impact strength tests and the results are shown in Table 4.187. The data from Table 4.187 was modeled using response surface methodology and the results of the analysis are presented in Table 4.188, the analysis of variance results are presented in Table 4.189 and the surface plot is presented in Figure 4.95. The ANOVA table (Table 4.189) reveals that fiber aspect ratio had a significant effect on the impact strength. This result is in agreement with the p-values from the t-statistics of the coefficients in the response surface model (Table 4.188), which shows that only the constant term and the linear term of the fiber aspect ratio are significant, though the model is not adequate based on f-statistics though it explains 86% of variability in data. Thus impact strength for polyester-empty palm bunch fiber can be modeled as a linear function of the two variables (fiber aspect ratio and fiber volume fraction). The significant effect of fiber aspect ratio can also be observed from the surface plots (Figure 4.95), there is also some degree of interaction between the two factors as revealed in the nature of the surface plot contour lines. The maximum Impact Strength occurred for fiber aspect ratio of 95m/m and fiber volume fraction of 30% with a maximum value of 10.67Kgf/cm²(1046.4KJ/m²) which is not far from the surface response model constant term (10.3281Kgf/cm²).

Table 4.187: Empty Palm Bunch-Polyester Impact Strength Data

Fiber Length (mm)	10	10	10	30	30	30	50	50	50
Aspect Ratio (m/m)	22.22	22.22	22.22	66.67	66.67	66.67	111.1	111.1	111.1
Volume Fraction (%)	10	30	50	10	30	50	10	30	50
Impact Strength (kgfm/cm ²)	10.49	10.49	10.60	10.63	10.68	10.62	10.65	10.68	10.65

Table 4.188: Empty Palm Bunch-Polyester Impact Strength Data RSM Model Statistics

Variables	Coefficients	Std. Error	t-stat	P-value	F-stat
Constant	10.3281	0.0950	108.7304	1.715e-06	SSE = 0.0058417
Aspect Ratio (m/m)	0.0058	0.0023	2.5560	0.0835	DFE = 3
Fiber Vol. Frac.(%)	0.0044	0.0050	0.8713	0.4477	DFR = 5
Aspect Ratio*Vf	-3.0938e-05	2.4822e-05	-1.2464	0.3011	SSR = 0.036558
Aspect Ratio^2	-2.5312e-05	1.5796e-05	-1.6024	0.2074	F = 3.7549
Vf^2	-2.5e-05	7.8007e-05	-0.3205	0.7696	P-val = 0.15264
	R ² = 0.8622	Adj. R ² = 0.6326			

Table 4.189: Empty Palm Bunch-Polyester Impact Strength ANOVA Table

Source	Sum Sq.	Df	Mean Sq.	F	Prob>F
Fiber Length (Fl) (mm)	0.03167	2	0.01583	7.14	0.0479
Fiber Volume Fraction (Vf) (%)	0.00187	2	0.00093	0.42	0.6824
Error	0.00887	4	0.00222		
Total	0.0424	8			

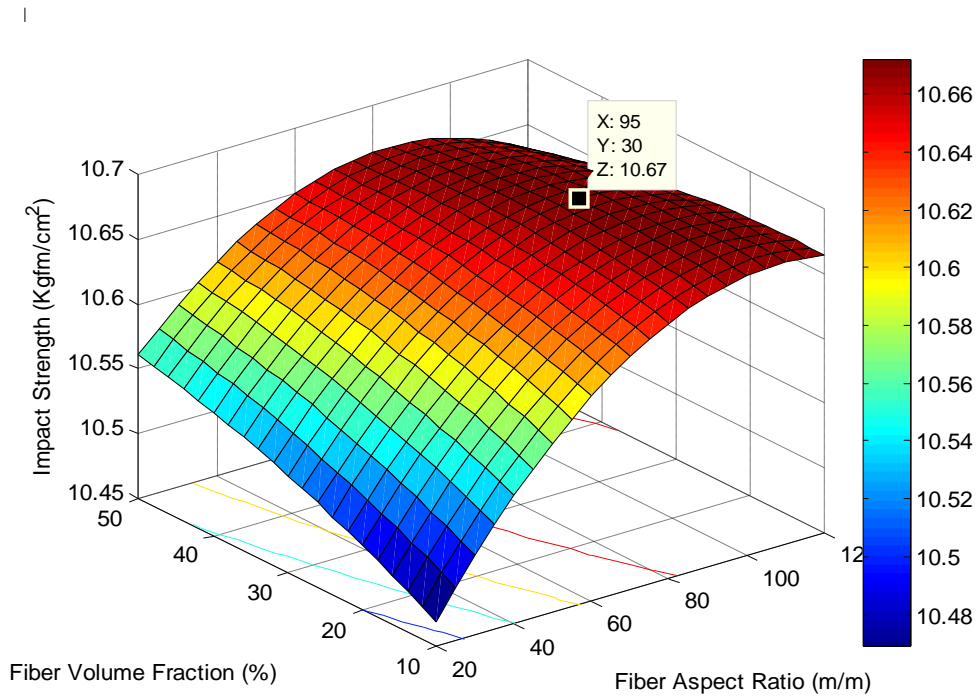


Figure 4.95: Surface plot for impact strength of empty palm bunch-polyester

4.16.4 Empty Palm Bunch-Epoxy Composite Impact Strength Analysis

Empty palm bunch-epoxy composites with fibers of length from 10-50mm (fiber aspect ratios of 22.2222m/m to 111.1111m/m) and volume fractions of 10-50% were subjected to impact strength tests and the results are shown in Table 4.190. The data from Table 4.190 was modeled using response surface methodology (the pure-quadratic model was used because it gave the best fit based on the adjusted- R^2) and the results of the analysis are presented in Table 4.191, the analysis of variance results are presented in Table 4.192 and the surface plot is presented in Figure 4.96. The ANOVA table (Table 4.192) reveals only fiber aspect ratio had significant effect on the Impact Strength of Epoxy-Empty Palm Bunch Fiber composite, since the p-value is less than 0.05. This result is in agreement with the surface plot (Figure 4.96) which shows greater change in Impact Strength along the fiber aspect ratio axis and also reveals a very low level of interaction between the two factors as seen in the parallel nature of the contour lines, though they are circular due to the quadratic nature of the model. The p-values from the t-statistics of the coefficients in the response surface model (Table 4.191) show that only the linear and quadratic terms of fiber aspect ratio are significant 95% confidence bound, in agreement with the quadratic nature of the surface plot. The model is adequate at 90% confidence based on the f-statistics and explains about 81% of the observed variability in the experimental data. The maximum Impact Strength occurred for fiber aspect ratio of 70m/m and fiber volume fraction of 30% with a value of 22.6Kgf/cm² (2216.3KJ/m²). This value is more than twice the Impact Strength obtained using polyester as matrix. This value is about twice the maximum impact strength obtained using polyester as matrix.

Table 4.190: Empty Palm Bunch-Epoxy Impact Strength Data

Fiber Length (mm)	10	10	10	30	30	30	50	50	50
Aspect Ratio (m/m)	22.22	22.22	22.22	66.67	66.67	66.67	111.1	111.1	111.1
Volume Fraction (%)	10	30	50	10	30	50	10	30	50
Impact Strength (kgfm/cm ²)	10.80	10.85	10.81	20.22	20.60	20.21	10.85	20.21	10.82

Table 4.191: Empty Palm Bunch-Epoxy Impact Strength RSM Model Statistics

Variables	Coefficients	Std. Error	t-stat	P-value	F-stat
Constant	-5.0740	5.6065	-0.9050	0.4166	SSE = 37.33
Aspect Ratio (m/m)	0.5722	0.1485	3.8534	0.0182	DFE = 4
Fiber Vol. Frac.(%)	0.4900	0.3300	1.4850	0.2117	DFR = 4
Aspect Ratio ²	-0.0040	0.0011	-3.6818	0.0212	SSR = 162.66
Vf ²	-0.0082	0.0054	-1.5130	0.2048	F = 4.3574
	R ² = 0.8133	Adj. R ² = 0.6267			P-val = 0.0915

Table 4.192: Empty Palm Bunch Fiber-Epoxy Impact Strength ANOVA Table

Source	Sum Sq.	Df	Mean Sq.	F	Prob>F
Fiber Length (Fl) (mm)	141.3	2	70.6502	7.57	0.0437
Fiber Volume Fraction (Vf) (%)	21.364	2	10.6821	1.14	0.4045
Error	37.33	4	9.3326		
Total	199.995	8			

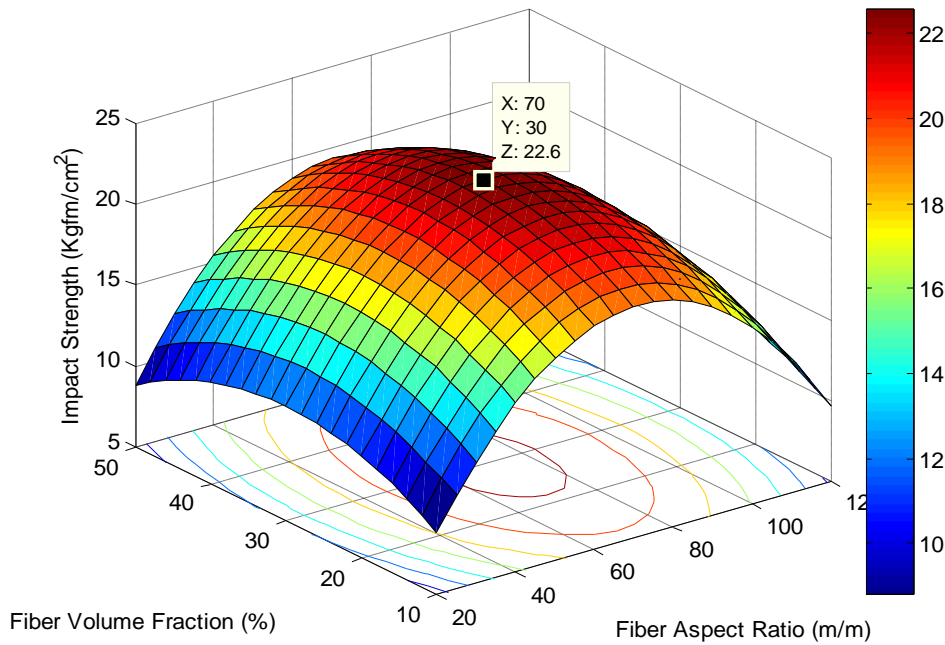


Figure 4.96: Surface plot for impact strength of empty palm bunch-epoxy

4.16.5 Rattan Palm Fiber-Polyester Composite Impact Strength Analysis

Rattan palm fiber-polyester composites with fibers of length from 10-50mm (fiber aspect ratios of 8.1733m/m to 40.8664m/m) and volume fractions of 10-50% were subjected to impact strength tests and the results are shown in Table 4.193. The data from Table 4.193 was modeled using response surface methodology and the results of the analysis are presented in Table 4.194, the analysis of variance results are presented in Table 4.195 and the surface plot is presented in Figure 4.97. The ANOVA table (Table 4.195) shows that none of the factors has significant effect on the impact strength of polyester-rattan palm fiber composite, since the p-value for both variables is much higher than 0.05. This result of the p-values from the t-statistics of the coefficients in the response surface model (Table 4.194) show, though, that the constant term is significant at 95% confidence. Thus impact strength remains relatively constant for polyester-

rattan palm bunch fiber, for all fiber aspect ratios and volume fractions studied. The quadratic and linear terms of fiber aspect ratio are barely significant at 90% interval in agreement with the surface plot(Figure 4.97). The model is not adequate based on the f-statistics though it explains about 69% of the observed variability in Impact Strength. The maximum Impact Strength occurred for fiber aspect ratio of 24m/m and fiber volume fraction of 30%, but this maximum value of 20.16Kgf/cm² (1977KJ/m²) is not far from the surface response model constant term (19.8681Kgf/cm²).

Table 4.193: Rattan Palm Fiber-Polyester Impact Strength Data

Fiber Length (mm)	10	10	10	30	30	30	50	50	50
Aspect Ratio (m/m)	8.173	8.173	8.173	24.52	24.52	24.52	40.87	40.87	40.87
Volume Fraction (%)	10	30	50	10	30	50	10	30	50
Impact Strength (kgf/cm ²)	20.00	20.10	20.10	20.10	20.10	20.20	20.00	20.10	20.00

Table 4.194: Rattan Palm Fiber-Polyester Impact Strength RSM Model Statistics

Variables	Coefficients	Std. Error	t-stat	P-value	F-stat
Constant	19.8681	0.0967	205.4075	3.3699e-09	SSE = 0.01111
Aspect Ratio (m/m)	0.0143	0.0070	2.0494	0.1098	DFE = 4
Fiber Vol. Frac.(%)	0.0067	0.0057	1.1711	0.3066	DFR = 4
Aspect Ratio^2	-0.0003	0.0001	-2.2361	0.0890	SSR = 0.02444
Vf^2	-8.3333e-05	9.3169e-05	-0.8944	0.4216	F = 2.2
	R ² = 0.6875	Adj.R ² = 0.3750			P-val = 0.23199

Table 4.195: Rattan Palm Fiber-Polyester Impact Strength ANOVA Table

Source	Sum Sq.	Df	Mean Sq.	F	Prob>F
Fiber Length (Fl) (mm)	0.01556	2	0.00778	2.8	0.1736
Fiber Volume Fraction (Vf) (%)	0.00889	2	0.00444	1.6	0.3086
Error	0.01111	4	0.00278		
Total	0.03556	8			

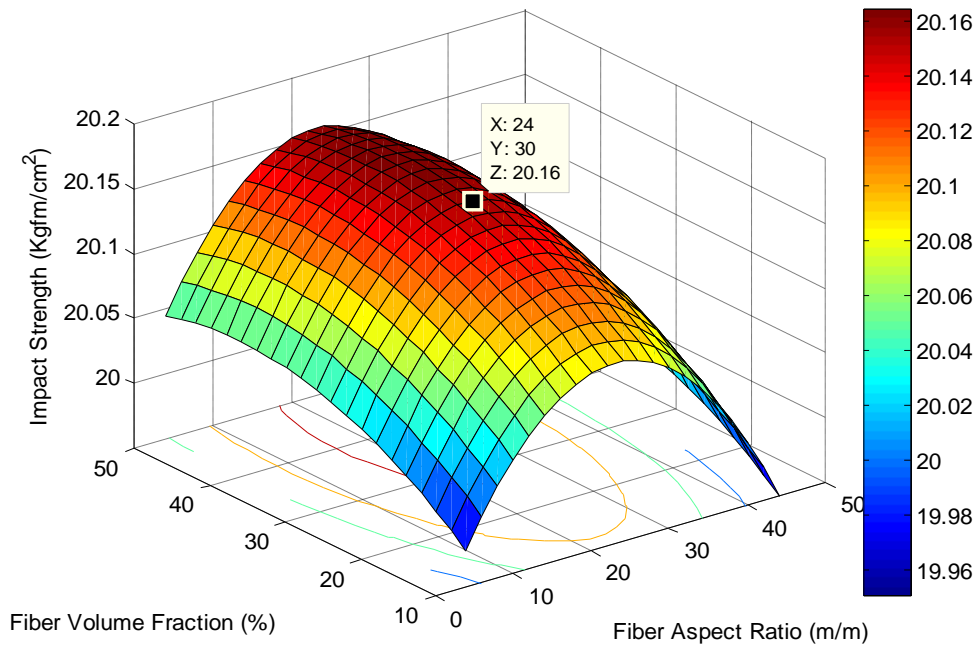


Figure 4.97: Surface plot for impact strength of rattan palm-polyester

4.16.6 Rattan Palm Fiber-Epoxy Composite Impact Strength Analysis

Rattan palm fiber-epoxy composites with fibers of length from 10-50mm (fiber aspect ratios of 8.1733m/m to 40.8664m/m) and volume fractions of 10-50% were subjected to impact strength tests and the results are shown in Table 4.196. The data from Table 4.196 was modeled using response surface methodology (the interaction model gave the best fit based on the adjusted-R² and was therefore used) and the results of the analysis are presented in Table 4.197, the analysis of variance results are presented in Table 4.198 and the surface plot is presented in Figure 4.98. The ANOVA table (Table 4.198) reveals that only fiber aspect ratio had significant effect on the impact strength of epoxy-rattan palm fiber composite at 90% confidence bound. This result is in agreement with the surface plot (Figure 4.98) which shows greater change in impact strength along the fiber aspect ratio axis and also reveals a good level of interaction between the two

factors as seen in the nature of the contour line. The p-values from the t-statistics of the coefficients in the response surface model (Table 4.197) show that only the constant term is significant. Therefore, the impact strength of epoxy-rattan palm fiber composite remains relatively constant with variation in fiber aspect ratio and fiber volume fraction. The model explains 83% of the observed variability in the data and is adequate based on the p-value of the f-statistics table. The maximum impact strength occurred for fiber aspect ratio of 40.87m/m and fiber volume fraction of 50% with a value of 20.78Kgf/cm² (2037.8KJ/m²). This value of impact strength is comparable to that obtained using polyester as matrix and is not too far from the constant term of the response surface model with a value of 20.1740Kgf/cm²

The impact strength analysis shows generally, that, epoxy is a better matrix than polyester for applications where impact strength is of uttermost concern and automobile applications are one of such. This is evident from the observed impact strength for most of the fibers using epoxy, which is usually, double that of polyester. The only exception to the above is rattan palm fiber, which gives good impact strength, the choice of matrix notwithstanding. In addition, varying fiber aspect ratio and fiber volume fraction has little effect on the impact strength of polyester based composites; while epoxy based composites vary significantly with fiber aspect ratio, and less with fiber volume fraction, except for rattan palm fiber.

Table 4.196: Rattan Palm Fiber-Epoxy Impact Strength Data

Fiber Length (mm)	10	10	10	30	30	30	50	50	50
Aspect Ratio (m/m)	8.173	8.173	8.173	24.52	24.52	24.52	40.87	40.87	40.87
Volume Fraction (%)	10	30	50	10	30	50	10	30	50
Impact Strength (kgf/cm ²)	20.00	20.00	20.24	20.20	20.20	20.20	20.21	20.60	20.90

Table 4.197: Rattan Palm Fiber-Epoxy Impact StrengthRSM Model Statistics

Variables	Coefficients	Std. Error	t-stat	P-value	F-stat
Constant	19.9365	0.2205	90.4277	3.1349e-09	SSE = 0.11427
Aspect Ratio (m/m)	0.0047	0.0079	0.5907	0.5804	DFE = 5
Fiber Vol. Frac.(%)	-0.0007	0.0065	-0.1065	0.9193	DFR = 3
Aspect Ratio*Vf	0.0003	0.0002	1.4883	0.1968	SSR = 0.55493
					F = 8.0935
	$R^2 = 0.8292$	Adj. $R^2 = 0.7268$			P-val = 0.023

Table 4.198: Rattan Palm Fiber-Epoxy Impact StrengthANOVA Table

Source	Sum Sq.	Df	Mean Sq.	F	Prob>F
Fiber Length (Fl) (mm)	0.3914	2	0.1957	5.91	0.0639
Fiber Volume Fraction (Vf) (%)	0.1454	2	0.0727	2.2	0.2271
Error	0.1324	4	0.0331		
Total	0.6692	8			

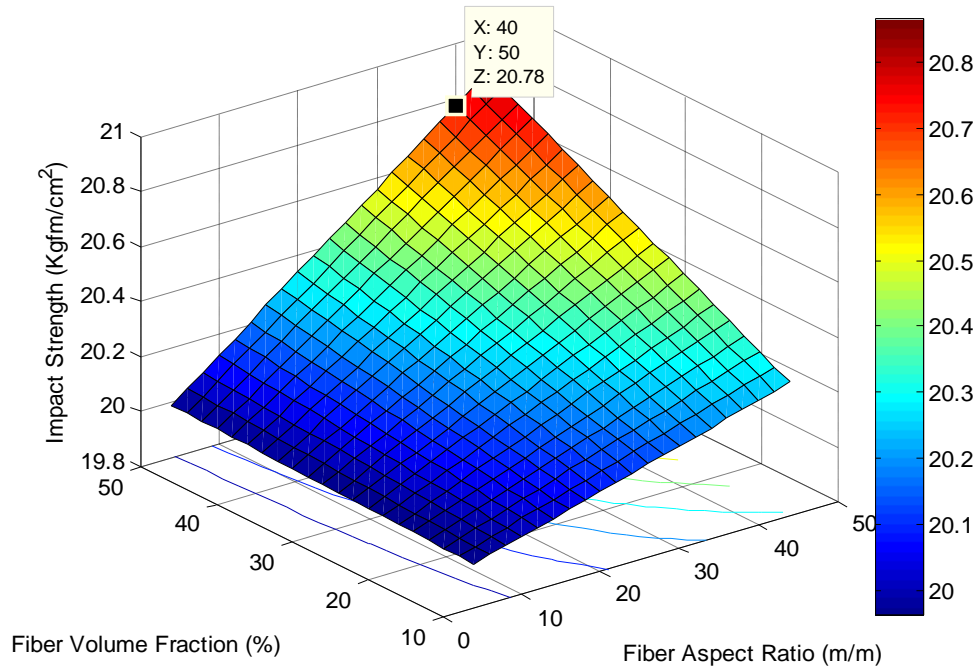


Figure 4.98: Surface plot for impact strength of rattan palm-epoxy

4.15.7 Optimum Conditions for Impact Strength of All Composites

The RSM model coefficients from Table 4.182, Table 4.185, Table 4.188, Table 4.191, Table 4.194 and Table 4.197 were used to run a MATLAB 7.9 optimization code and the optimal values for fiber length and fiber volume fraction are presented in Table 4.199 alongside predicted optimal values of impact strength and the experimental values for validation. It can be observed from Table 4.199 that for most of the composites, the optimum impact strength occurs at fiber volume fraction between 30 and 40%. The optimum impact strength for most of the samples is a global optimum that cannot be improved by changes in fiber aspect ratio or volume fraction, except for rattan palm fiber-epoxy composites that have indication of possible improvement on observed impact strength as indicated in Table 4.199.

Table 4.199: Optimum Values of Fiber Length and Volume Fraction for Impact Strength

Composite (Matrix /Fiber)	Fiber Aspect Ratio (m/m)	Fiber Volume Fraction (%)	Impact Strength (Model) (Kgf/cm ²)	Impact Strength (Experiment) (Kgf/cm ²)	Nature of Optimal	Remarks (How to Improve Optimal)
Polyester /Plantain	95	30	10.58	10.60	Global	Cannot be improved
Epoxy /Plantain	85	40	21.37	20.20	Global	Cannot be improved
Polyester /Palm Bunch	95	30	10.67	10.70	Global	Cannot be improved
Epoxy /Palm Bunch	70	30	22.60	21.10	Global	Cannot be improved
Polyester /Rattan Palm	24	30	20.16	20.10	Global	Cannot be improved
Epoxy /Rattan Palm	40.87	50	20.78	20.90	Local	Increase fiber aspect ratio and/or volume fraction

4.17 Micromechanics Modelling of Composite Properties

The general equation for micromechanics modeling of composite modulus is given in equation (2.13). Four equations are presented [equations (2.15), (2.18), (2.19) and (2.20)] for computation of the shear lag parameter which is applied in equation 2.14 to obtain the fiber length distribution factor and then equation (2.13) can be used to estimate the composite modulus, based on the modulus and volume fractions of the fiber and matrix.

For this work, equation (2.19) was used to compute the shear lag parameter. This is because equation (2.15) requires inter-fiber spacing, which is not available for our random fiber orientation, while equation (2.18) requires packing factor, for which values are not available for a random arrangement. Equations (2.25) to (2.27) could not be used because of challenges in obtaining or measuring the critical fiber length and mean shear stress at fiber-matrix interface. Short MATLAB 7.9 programs(Appendix 7.8) were used to compute the shear lag parameter, the corresponding Cox shear-lag model fiber distribution parameter and composite modulus. Two multiaxial models, the Bintrup equation (equation 2.12) and the modified Halpin-tsai equation (equations 2.7, 2.8 and 2.11) for different constant reinforcing efficiencies in the transverse direction, were also used and compared to equation 2.13 to know the model that best fits the data.

In this study, it was observed that composite mechanical properties increased with increase in fiber volume fraction to a maximum before a decline. A simple model which is a modification of Halpin-tsai equation is presented below based on the above observation.

$$E = \sin^2\left(\frac{3\pi}{2} V_f^\alpha\right) \left(\frac{3}{8} E_1 + \frac{5}{8} E_2\right) \quad (4.1)$$

Where α is a model constant and V_f is fiber volume fraction. E_1 and E_2 are composite modulus in lateral and transverse directions based on Halpin-tsai equation using $\xi = 2$ for the transverse direction. Equation 4.1 was used to simulate composite modulus for $\alpha=11/16$ and the simulated results are presented in Table 4.200 to Table 4.205 alongside other micromechanics models.

4.17.1 Micromechanics Study for Empty Plantain Bunch-Polyester Reinforced Composite

It can be observed from Table 4.200 that the experimental modulus increases to a maximum, with increase in volume fraction, after which it declines. The micromechanics models do not follow this trend, instead their predicted modulus increase continually with increase in fiber volume fraction, except the modified model proposed in this work. The model predicted modulus in each case was compared to the experimental modulus using an R^2 value obtained by regression of the experimental modulus against the model predicted modulus, for each model. The most accurate model would be one with the highest R^2 value. All model predicted modulus values were significantly different from the experimental, though the modified model proposed in this work was the closest to the experimental modulus with R^2 of 0.4712. The shear-lag model is the least accurate model for empty plantain bunch-polyester composite with an R^2 value of 0.1155 and this can be explained based on the fact that the model is a uniaxial model and thus is likely to be less accurate. The Bintrup model is the least accurate of the multiaxial models.

Table 4.200: Comparison of Predicted Modulus for Empty Plantain Bunch-Polyester

Fiber Aspect Ratio (m/m)	Volume Fraction (%)	Modulus Expt. (GPa)	Shear-lag model	Halpin-Tsai ($\xi=2$)	Halpin-Tsai ($\xi=0.5$)	Bintrup model	Osoka-Onukwuli model
23.6183	10	4.4744	4.9559	2.0400	2.1339	3.8737	1.7575
23.6183	30	5.6100	13.8464	4.5323	4.8844	6.7356	4.3126
23.6183	50	3.7312	23.1306	7.8186	8.6000	10.6260	1.8393
70.8550	10	3.9542	5.4607	2.4628	2.5567	4.2965	2.1056
70.8550	30	4.6690	14.7097	5.6925	6.0445	7.8958	5.3370
70.8550	50	3.5700	24.0899	9.4701	10.2514	12.2774	2.1925
118.0916	10	3.6803	5.5616	2.6000	2.6938	4.4336	2.2186
118.0916	30	4.7661	14.8823	6.0415	6.3935	8.2448	5.6451
118.0916	50	3.1617	24.2817	9.9251	10.7064	12.7324	2.2898
R-squared			0.1155	0.1852	0.1859	0.1857	0.4712

4.17.2 Micromechanics Study for Empty Plantain Bunch-Epoxy Reinforced Composite

It can be observed from Table 4.201 that the experimental modulus increases to a maximum, with increase in volume fraction, after which it declines. The micromechanics models do not follow this trend, instead their predicted modulus increase continually with increase in fiber volume fraction, except the modified model proposed in this work. The model predicted modulus in each case was compared to the experimental modulus using an R^2 value obtained by regression of the experimental modulus against the model predicted modulus, for each model. The most accurate model would be one with the highest R^2 value. All model predicted modulus values were significantly different from the experimental, though the modified model proposed in this work was the closest to the experimental modulus with R^2 value of 0.8479.

Table 4.201: Comparison of Predicted Modulus for Empty Plantain Bunch-Epoxy

Fiber Aspect Ratio (m/m)	Volume Fraction (%)	Modulus Expt. (GPa)	Shear-lag model	Halpin-Tsai ($\xi=2$)	Halpin-Tsai ($\xi=0.5$)	Bintrup model	Osoka-Onukwuli model
23.6183	10	1.1027	5.1994	2.7035	2.5794	4.9708	2.2266
23.6183	30	2.2720	13.9007	5.8711	5.4106	8.2515	5.1839
23.6183	50	1.7210	23.0768	10.0399	9.0350	12.5860	2.1472
70.8550	10	1.6760	5.7651	3.0756	2.9515	5.3429	2.5330
70.8550	30	2.9710	14.9014	6.8604	6.3999	9.2408	6.0574
70.8550	50	1.7710	24.1959	11.3964	10.3915	13.9425	2.4373
118.0916	10	1.6320	5.8782	3.1852	3.0612	5.4526	2.6233
118.0916	30	2.5850	15.1015	7.1338	6.6733	9.5141	6.2987
118.0916	50	1.6430	24.4198	11.7448	10.7399	14.2909	2.5119
R-squared			0.0362	0.0246	0.0283	0.0239	0.8479

4.17.3 Micromechanics Study for Empty Palm Bunch-Polyester Reinforced Composite

It can be observed from Table 4.202 that the experimental modulus increases to a maximum, with increase in volume fraction, after which it declines. The micromechanics models do not follow this trend, instead their predicted modulus increase continually with increase in fiber volume fraction, except the modified model proposed in this work. The model predicted modulus in each case was compared to the experimental modulus using an R^2 value obtained by regression of the experimental modulus against the model predicted modulus, for each model. The most accurate model would be one with the highest R^2 value. All model predicted modulus values were significantly different from the experimental, though the modified model proposed in this work was the closest to the experimental modulus with an R^2 value of 0.8477. The shear-

lag model is the least accurate model for empty palm bunch-polyester composite with an R^2 value of 0.0836 and this can be explained based on the fact that the model is a uniaxial model.

Table 4.202: Comparison of Predicted Modulus for Empty Palm Bunch-Polyester

Fiber Aspect Ratio (m/m)	Volume Fraction (%)	Modulus Expt. (GPa)	Shear-lag model	Halpin-Tsai ($\xi=2$)	Halpin-Tsai ($\xi=0.5$)	Bintrup model	Osoka-Onukwuli model
22.2222	10	2.9470	2.4075	1.6152	1.5378	3.3370	1.3303
22.2222	30	4.4500	5.3889	3.0363	2.7599	4.8087	2.6809
22.2222	50	2.4989	8.4551	4.8340	4.2679	6.6501	1.0338
66.6667	10	3.6756	2.5026	1.6972	1.6198	3.4190	1.3978
66.6667	30	4.4643	5.5645	3.2425	2.9661	5.0149	2.8629
66.6667	50	3.1069	8.6547	5.0995	4.5338	6.9156	1.0906
111.1111	10	3.5699	2.5216	1.7177	1.6404	3.4396	1.4147
111.1111	30	4.3021	5.5996	3.2921	3.0157	5.0645	2.9067
111.1111	50	3.1357	8.6946	5.1606	4.5945	6.9767	1.1037
R-squared			0.0836	0.1049	0.0980	0.1037	0.8477

4.17.4 Micromechanics Study for Empty Palm Bunch-Epoxy Reinforced Composite

It can be observed from Table 4.203 that the experimental modulus increases to a maximum, with increase in volume fraction, after which it declines. The micromechanics models do not follow this trend, instead their predicted modulus increase continually with increase in fiber volume fraction, except the modified model proposed in this work. The model predicted modulus in each case was compared to the experimental modulus using an R^2 value obtained by regression of the experimental modulus against the model predicted modulus, for each model. The most accurate model would be one with the highest R^2 value. There is significant difference between the experimental modulus and predicted for most models with the modified model

proposed in this work having the best fit with R^2 value 0.7076. All other micromechanics models gave very poor fit to the experimental modulus for empty palm bunch-epoxy composite.

Table 4.203: Comparison of Predicted Modulus for Empty Palm Bunch-Epoxy

Fiber Aspect Ratio (m/m)	Volume Fraction (%)	Modulus Expt. (GPa)	Shear-lag model	Halpin-Tsai ($\xi=2$)	Halpin-Tsai ($\xi=0.5$)	Bintrup model	Osoka-Onukwuli model
22.2222	10	1.1572	2.7292	2.0562	1.9609	4.2930	1.6935
22.2222	30	2.0740	5.6116	3.6202	3.2879	5.8714	3.1964
22.2222	50	1.4303	8.5935	5.5677	4.9128	7.7899	1.1908
66.6667	10	1.6508	2.8330	2.1190	2.0237	4.3557	1.7452
66.6667	30	2.4607	5.8123	3.7751	3.4428	6.0263	3.3332
66.6667	50	1.7133	8.8248	5.7631	5.1082	7.9853	1.2325
111.1111	10	1.5134	2.8538	2.1339	2.0386	4.3706	1.7575
111.1111	30	2.1628	5.8525	3.8108	3.4785	6.0619	3.3647
111.1111	50	1.5882	8.8711	5.8066	5.1518	8.0289	1.2419
R-squared			0.0232	0.0121	0.0139	0.0134	0.7076

4.17.5 Micromechanics Study for Rattan Palm Fiber-Polyester Reinforced Composite

It can be observed from Table 4.204 that the experimental modulus increases to a maximum, with increase in volume fraction, after which it declines. The micromechanics models do not follow this trend, instead their predicted modulus increase continually with increase in fiber volume fraction, except the modified model proposed in this work. The model predicted modulus in each case was compared to the experimental modulus using an R^2 value obtained by regression of the experimental modulus against the model predicted modulus, for each model. The most accurate model would be one with the highest R^2 value. All the micromechanics models presented failed to effectively predict the experimental modulus for rattan palm fiber-

polyester composite, with the shear lag model having the highest R^2 value of 0.2880. This is a deviation from previous observations.

Table 4.204: Comparison of Predicted Modulus for Rattan Palm Fiber-Polyester

Fiber Aspect Ratio (m/m)	Volume Fraction (%)	Modulus Expt. (GPa)	Shear-lag model	Halpin-Tsai ($\xi=2$)	Halpin-Tsai ($\xi=0.5$)	Bintrup model	Osoka-Onukwuli model
8.1733	10	1.4148	1.2157	1.1668	1.1409	2.7569	0.9610
8.1733	30	2.8296	1.6668	1.5335	1.4589	2.8837	1.3558
8.1733	50	2.1576	2.1354	1.9593	1.8395	3.0205	0.4190
24.5198	10	1.2981	1.2320	1.1731	1.1473	2.7632	0.9662
24.5198	30	3.0956	1.7040	1.5508	1.4741	2.8989	1.3692
24.5198	50	2.8016	2.1818	1.9781	1.8582	3.0393	0.4230
40.8664	10	1.9681	1.2353	1.1746	1.1487	2.7646	0.9673
40.8664	30	3.2375	1.7114	1.5542	1.4776	2.9023	1.3723
40.8664	50	2.3033	2.1911	1.9822	1.8624	3.0435	0.4239
R-squared			0.2880	0.2571	0.2496	0.2859	0.1018

4.17.6 Micromechanics Study for Rattan PalmFiber-Epoxy Reinforced Composite

It can be observed from Table 4.205 that the experimental modulus increases to a maximum, with increase in volume fraction, after which it declines. The micromechanics models do not follow this trend, instead their predicted modulus increase continually with increase in fiber volume fraction, except the modified model proposed in this work. The model predicted modulus in each case was compared to the experimental modulus using an R^2 value obtained by regression of the experimental modulus against the model predicted modulus, for each model. The most accurate model would be one with the highest R^2 value. The modified model proposed

in this work predicted the modulus more accurately than other micromechanics models with an R^2 value of 0.562 while the Bintrup model is the least accurate of all models studied for rattan palm fiber-epoxy composite modulus prediction.

Table 4.205: Comparison of Predicted Modulus for Rattan Palm Fiber-Epoxy

Fiber Aspect Ratio (m/m)	Volume Fraction (%)	Modulus Expt. (GPa)	Shear-lag model	Halpin-Tsai ($\xi=2$)	Halpin-Tsai ($\xi=0.5$)	Bintrup model	Osoka-Onukwuli model
8.1733	10	1.9649	1.5496	1.5302	1.5094	3.5345	1.2602
8.1733	30	3.4090	1.9222	1.8714	1.8132	3.4484	1.6524
8.1733	50	1.0260	2.3127	2.2486	2.1639	3.4008	0.4809
24.5198	10	1.6321	1.5665	1.5337	1.5129	3.5380	1.2631
24.5198	30	2.7131	1.9627	1.8797	1.8216	3.4567	1.6597
24.5198	50	1.0182	2.3649	2.2587	2.1740	3.4109	0.4831
40.8664	10	1.1422	1.5699	1.5344	1.5136	3.5388	1.2637
40.8664	30	1.5762	1.9708	1.8816	1.8234	3.4585	1.6613
40.8664	50	1.0315	2.3753	2.2609	2.1762	3.4131	0.4835
R-squared			0.0963	0.0956	0.1015	0.0176	0.5621

The modification of the Halpin-tsai equation as proposed in this work improved its effectiveness in modeling composites from natural (plant) fibers as opposed to synthetic fibers. The new modified model gave modulus predictions that followed the profile of the experimental modulus for all samples and closest to the experimental based on the R^2 value.

4.18 Neural Network Model of Composite Properties

Several authors have modeled data from design of experiment using neural network, therefore it has been included in this section.

The Neural Network Toolbox of MATLAB 7.9 which uses 60% of the data fed to train the neural network, 20% for network validation and another 20% for testing network performance was used and the codes are presented in the appendices (A 7.10).

4.18.1 Neural Network Training of Empty Plantain Bunch-Polyester Composite Modulus

Neural network simulation of the modulus of empty plantain bunch-polyester composite is presented in Table 4.206 and Fig. 4.99. Sixty percent of the data points were used for the neural network training, twenty percent for validation and twenty percent for testing, as is the acceptable practice and MATLAB default. The simulation was done using thirty hidden neurons before a regression coefficient of 1.000 (Fig. 4.99a) was obtained for the training data. The overall regression coefficient obtained was 0.8207 (Fig. 4.99b) due to the poor fit of the neural network model to validation and testing data. It can be observed from Table 4.206 and Fig. 4.99 that the neural network model fit well to data used for training but failed for data used for validation and testing, which reduced the overall regression coefficient of the model.

Table 4.206: Empty Plantain Bunch-Polyester Reinforced Composite Neural Network Data

Aspect Ratio(m/m)	23.618	23.618	23.618	70.855	70.855	70.855	118.09	118.09	118.09
Volume Fraction (%)	10	30	50	10	30	50	10	30	50
Modulus (Expmt)	4.4744	5.61	3.7312	3.9542	4.669	3.57	3.6803	4.7661	3.1617
Modulus (Predicted)	4.4744	5.6100	3.3004	3.9542	4.6690	7.5917	2.5404	4.7661	3.1617

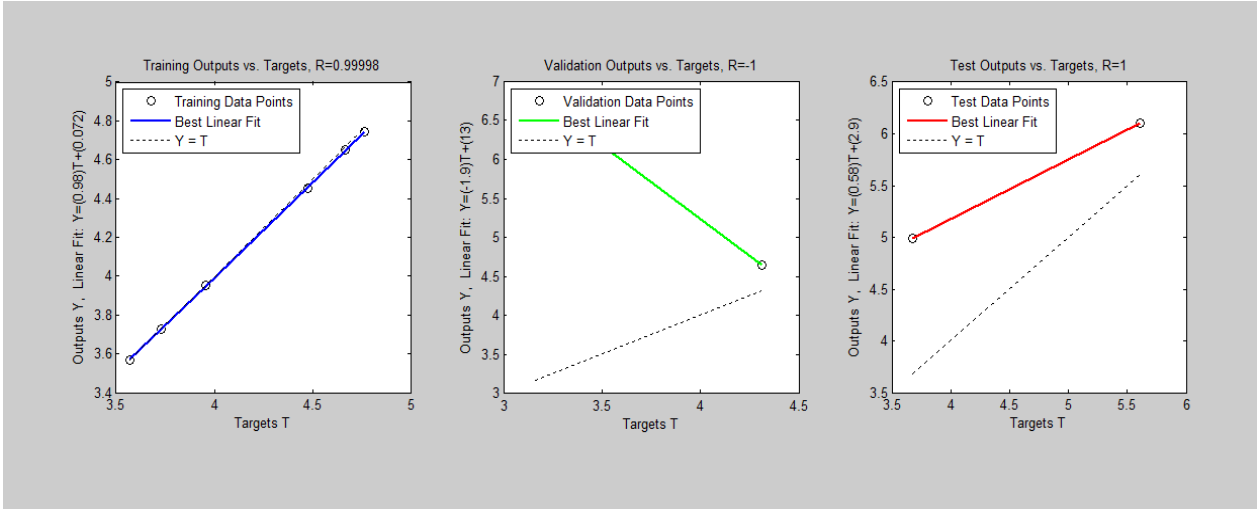


Figure 4.99a: Experimental vs. model results for modulus of empty plantain bunch-polyester

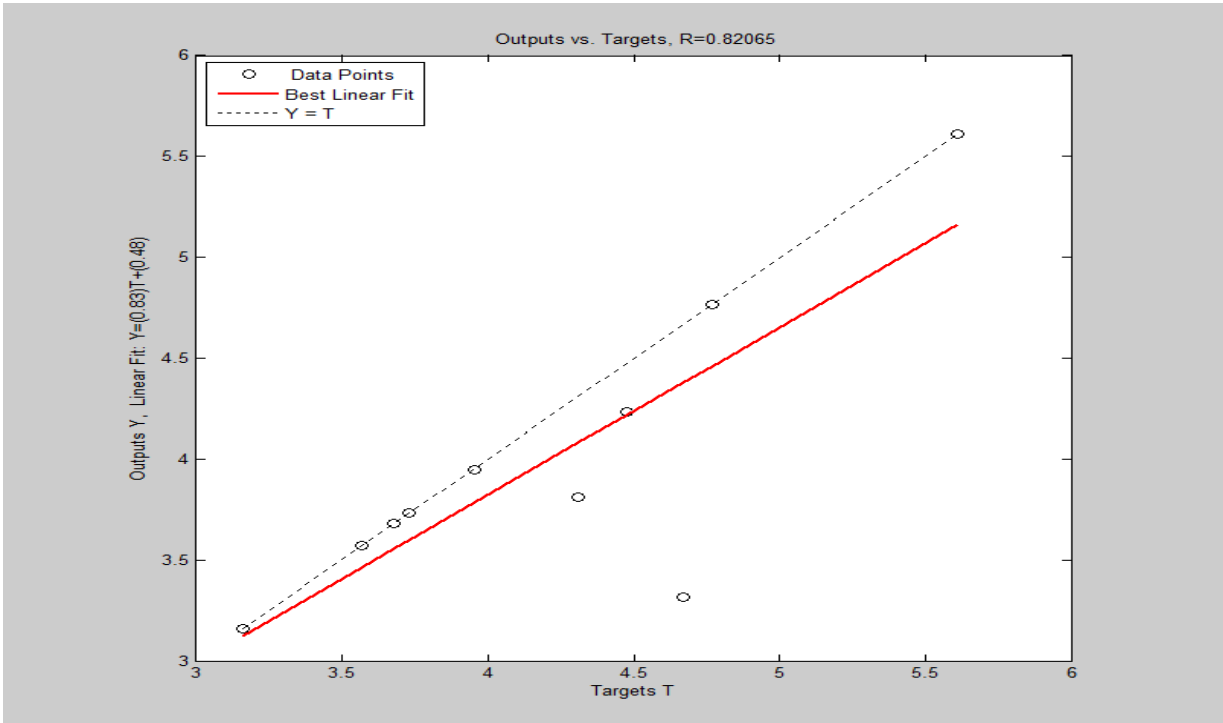


Figure 4.99b: Experimental vs. model results for modulus of empty plantain bunch-polyester

4.18.2 Neural Network Training of Empty Plantain Bunch-Epoxy Composite Modulus

Neural network simulation of the modulus of empty plantain bunch-epoxy composite is presented in Table 4.207 and Fig. 4.100. Sixty percent of the data points were used for the neural network training, twenty percent for validation and twenty percent for testing, as is the acceptable practice and MATLAB default. The simulation was done using thirty hidden neurons before a regression coefficient of 1.000 (Fig. 4.100a) was obtained for the training data. The overall regression coefficient obtained was 0.4059 (Fig. 4.100b) due to the poor fit of the neural network model to validation and testing data. It can be observed from Table 4.207 and Fig. 4.100 that the neural network model fit well to data used for training but failed for data used for validation and testing, which reduced the overall regression coefficient of the model.

Table 4.207: Empty Plantain Bunch-Epoxy Reinforced Composite Neural Network Data

Aspect Ratio(m/m)	23.618	23.618	23.618	70.855	70.855	70.855	118.09	118.09	118.09
Volume Fraction (%)	10	30	50	10	30	50	10	30	50
Modulus (Expmt)	1.1027	2.2720	1.7210	1.6760	2.9710	1.7710	1.6320	2.5850	1.6430
Modulus (Predicted)	1.1027	2.2720	1.7210	0.9071	2.9710	1.7710	3.3746	2.5850	1.4070

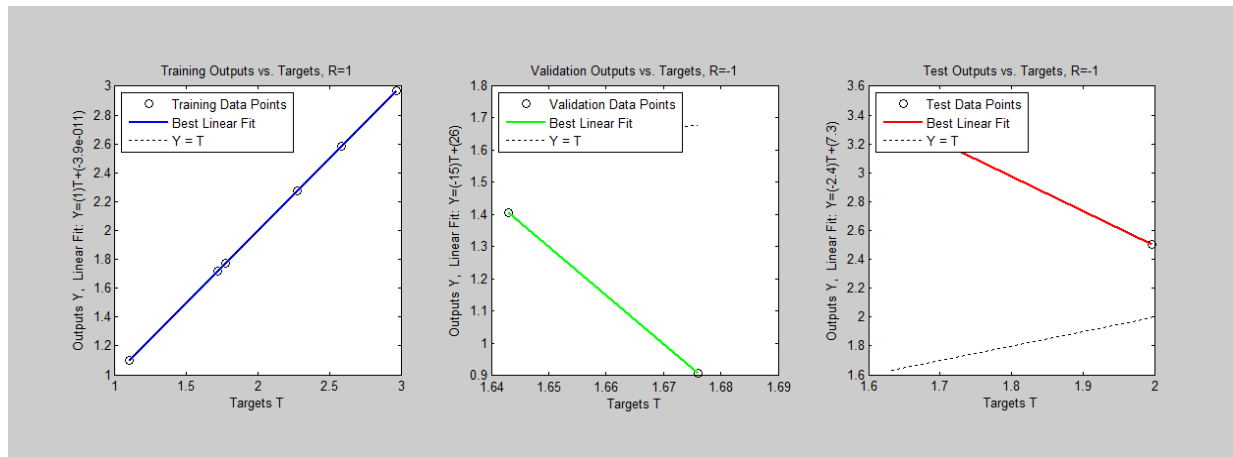


Figure 4.100a: Experimental vs. neural model results for modulus of empty plantain bunch-epoxy

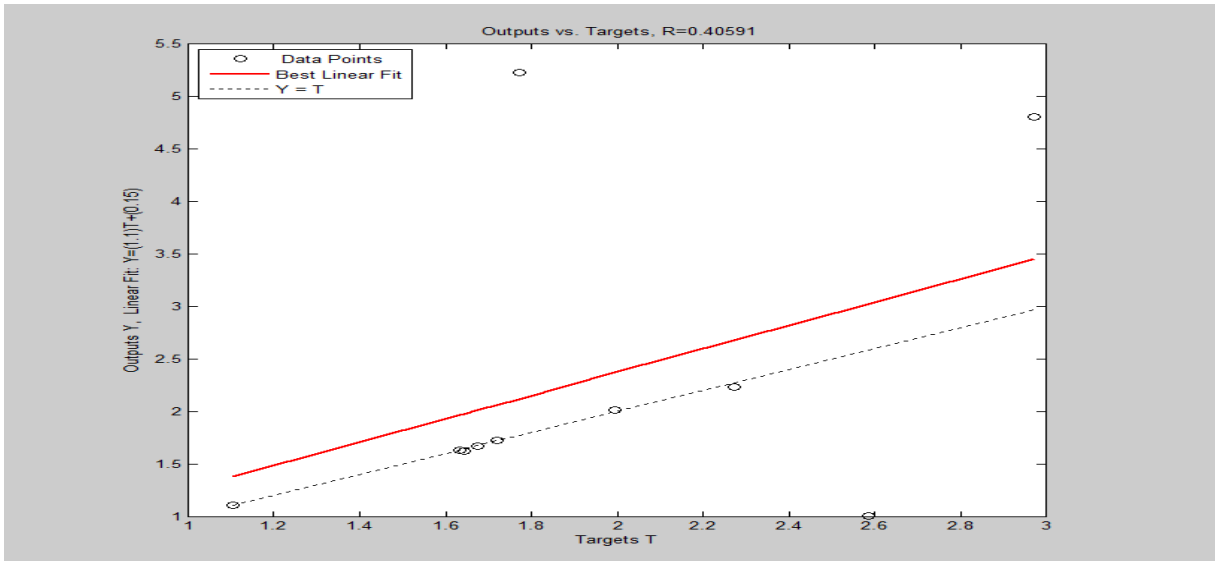


Figure 4.100b: Experimental vs. neural model results for modulus of empty plantain bunch-epoxy

4.18.3 Neural Network Training of Empty Palm Bunch-Polyester Composite Modulus

Neural network simulation of the modulus of empty palm bunch-polyester composite is presented in Table 4.208 and Fig. 4.101. Sixty percent of the data points were used for the neural network training, twenty percent for validation and twenty percent for testing, as is the acceptable practice. The simulation was done using thirty hidden neurons before a regression coefficient of 0.9999 (Fig. 4.101a) was obtained for the training data. The overall regression coefficient obtained was 0.5390 (Fig. 4.101b) due to the poor fit of the neural network model to validation and testing data. It can be observed from Table 4.208 and Fig. 4.101 that the neural network model fit well to data used for training but failed for data used for validation and testing, which reduced the overall regression coefficient of the model.

Table 4.208: Empty Palm Bunch-Polyester Reinforced Composite Neural Network Data

Aspect Ratio(m/m)	22.222	22.222	22.222	66.667	66.667	66.667	111.11	111.11	111.11
Volume Fraction (%)	10	30	50	10	30	50	10	30	50
Modulus (Expmt)	2.9470	4.4500	2.4989	3.6756	4.4643	3.1069	3.5699	4.3021	3.1357
Modulus (Predicted)	3.9788	4.4314	2.4734	0.0515	4.4641	2.3099	3.5769	4.3055	1.7351

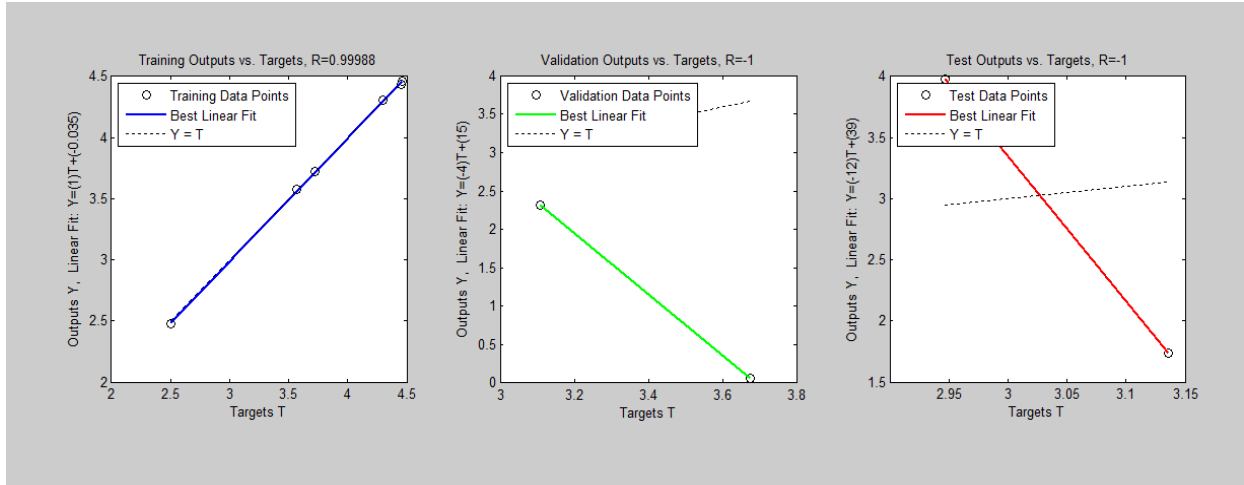


Figure 4.101a: Experimental vs. neural model results for modulus of empty palm bunch-polyester

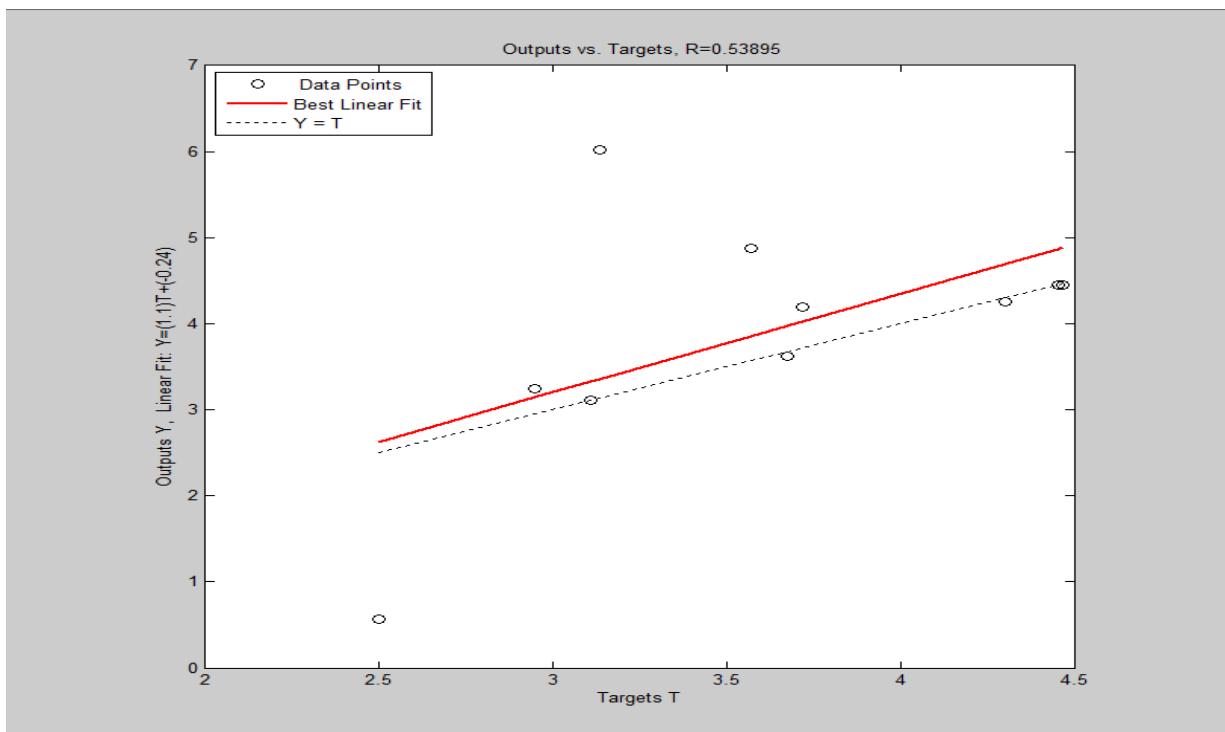


Figure 4.101b: Experimental vs. neural model results for modulus of empty palm bunch-polyester

4.18.4 Neural Network Training of Empty Palm Bunch-Epoxy Composite Modulus

Neural network simulation of the modulus of empty palm bunch-epoxy composite is presented in Table 4.209 and Fig. 4.102. Sixty percent of the data points were used for the neural network training, twenty percent for validation and twenty percent for testing, as is the acceptable practice. The simulation was done using thirty hidden neurons before a regression coefficient of 0.9999 (Fig. 4.102a) was obtained for the training data. The overall regression coefficient obtained was 0.4581 (Fig. 4.102b) due to the poor fit of the neural network model to validation and testing data. It can be observed from Table 4.209 and Fig. 4.102 that the neural network model fit well to data used for training but failed for data used for validation and testing, which reduced the overall regression coefficient of the model.

Table 4.209: Empty Palm Bunch-Epoxy Reinforced Composite Neural Network Data

Aspect Ratio(m/m)	22.222	22.222	22.222	66.667	66.667	66.667	111.11	111.11	111.11
Volume Fraction (%)	10	30	50	10	30	50	10	30	50
Modulus (Expmt)	1.1572	2.0740	1.4303	1.6508	2.4607	1.7133	1.5134	2.1628	1.5882
Modulus (Predicted)	1.1573	2.0767	2.1770	1.6524	1.8863	1.7198	1.5208	1.5535	1.5883

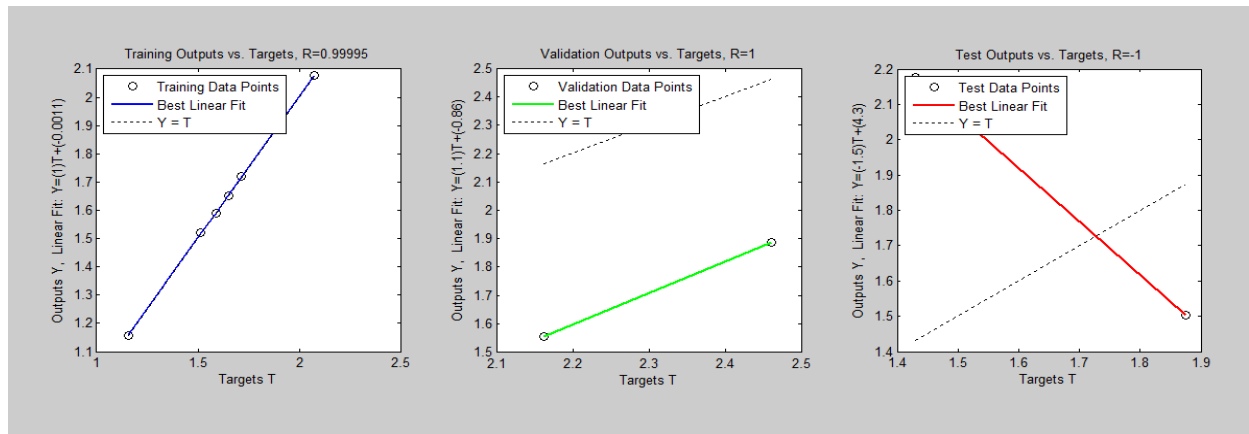


Figure 4.102a: Experimental vs. neural model results for modulus of empty palm bunch-epoxy

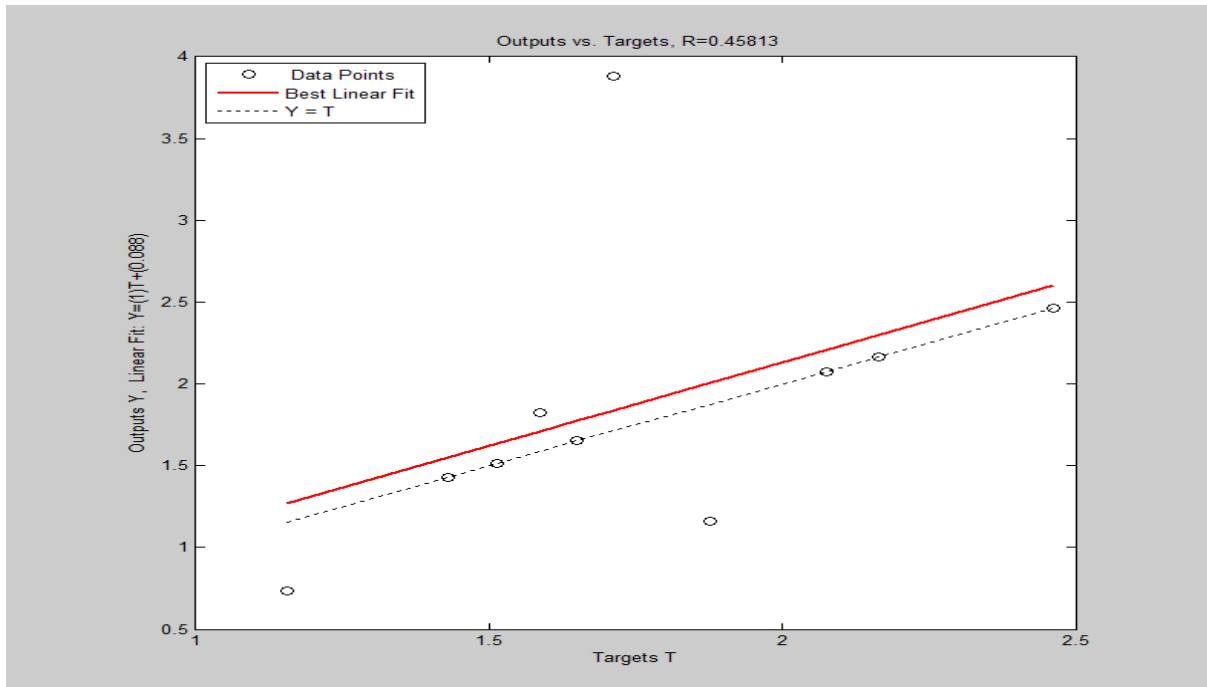


Figure 4.102b: Experimental vs. neural model results for modulus of empty palm bunch-epoxy

4.18.5 Neural Network Training of Rattan Palm Fiber-Polyester Composite Modulus

Neural network simulation of the modulus of rattan palm fiber-polyester composite is presented in Table 4.210 and Fig. 4.103. Sixty percent of the data points were used for the neural network training, twenty percent for validation and twenty percent for testing, as is the acceptable practice. The simulation was done using thirty hidden neurons before a regression coefficient of 0.8724 (Fig. 4.103a) was obtained for the training data. The overall regression coefficient obtained was 0.5805 (Fig. 4.103b) due to the poor fit of the neural network model to validation and testing data. It can be observed from Table 4.210 and Fig. 4.103 that the neural network model fit well to data used for training but failed for data used for validation and testing, which reduced the overall regression coefficient of the model.

Table 4.210: Rattan PalmFiber-Polyester Reinforced Composite Neural Network Data

Aspect	Ratio	8.1733	8.1733	8.1733	24.5198	24.5198	24.5198	40.8664	40.8664	40.8664
--------	-------	--------	--------	--------	---------	---------	---------	---------	---------	---------

(m/m)									
Vol. Frac. (%)	10	30	50	10	30	50	10	30	50
Modulus (Expt)	1.4148	2.8296	2.1576	1.2981	3.0956	2.8016	1.9681	3.2375	2.3033
Modulus (Predicted)	1.4148	1.4297	2.1576	1.2981	3.0956	2.8016	1.6451	2.1584	2.3033

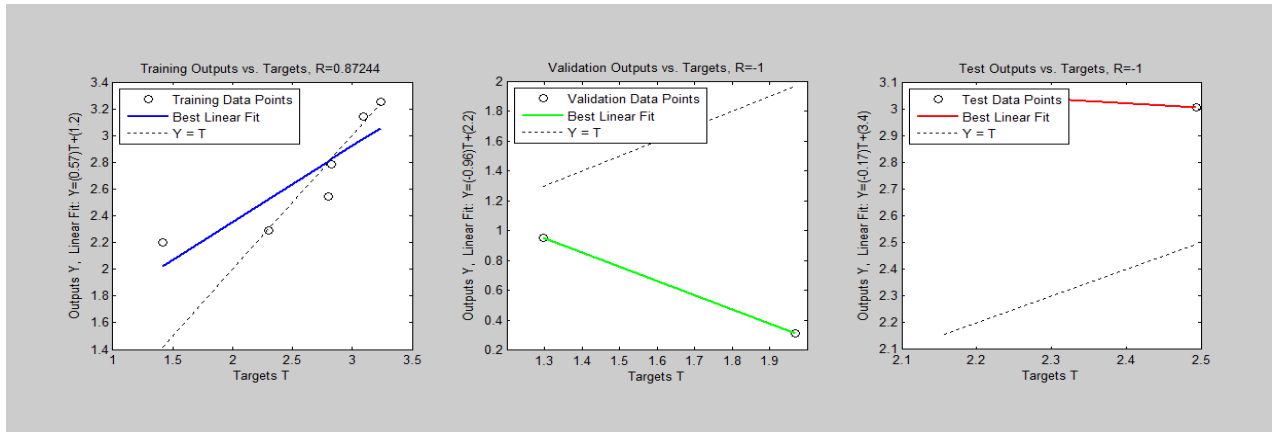


Figure 4.103a: Experimental vs. neural model results for modulus of rattan palm-polyester

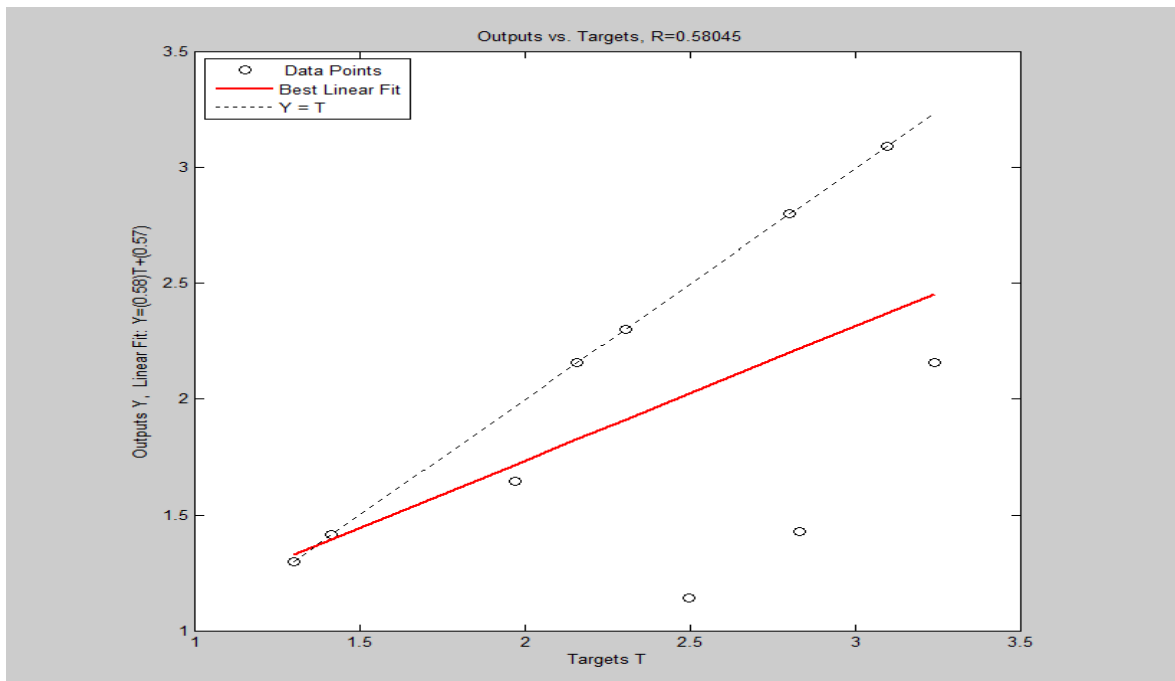


Figure 4.103b: Experimental vs. neural model results for modulus of rattan palm-polyester

4.18.6 Neural Network Training of Rattan Palm Fiber-Epoxy Composite Modulus

Neural network simulation of the modulus of rattan palm fiber-epoxy composite is presented in Table 4.211 and Fig. 4.104. Sixty percent of the data points were used for the neural network training, twenty percent for validation and twenty percent for testing, as is the acceptable practice. The simulation was done using thirty hidden neurons before a regression coefficient of 0.997 (Fig. 4.104a) was obtained for the training data. The overall regression coefficient obtained was 0.7671(Fig. 4.104b) due to the poor fit of the neural network model to validation and testing data. It can be observed from Table 4.211 and Fig. 4.104 that the neural network model fit well to data used for training but failed for data used for validation and testing, which reduced the overall regression coefficient of the model.

Table 4.211: Rattan PalmFiber-Epoxy Reinforced Composite Neural Network Data

Aspect Ratio (m/m)	8.1733	8.1733	8.1733	24.5198	24.5198	24.5198	40.8664	40.8664	40.8664
Vol. Frac. (%)	10	30	50	10	30	50	10	30	50
Modulus (Expmt)	1.9649	3.4090	1.0260	1.6321	2.7131	1.0182	1.1422	1.5762	1.0315
Modulus (Predicted)	1.9649	3.4094	1.0260	1.6323	1.2592	-0.3896	1.1422	1.7290	1.0259

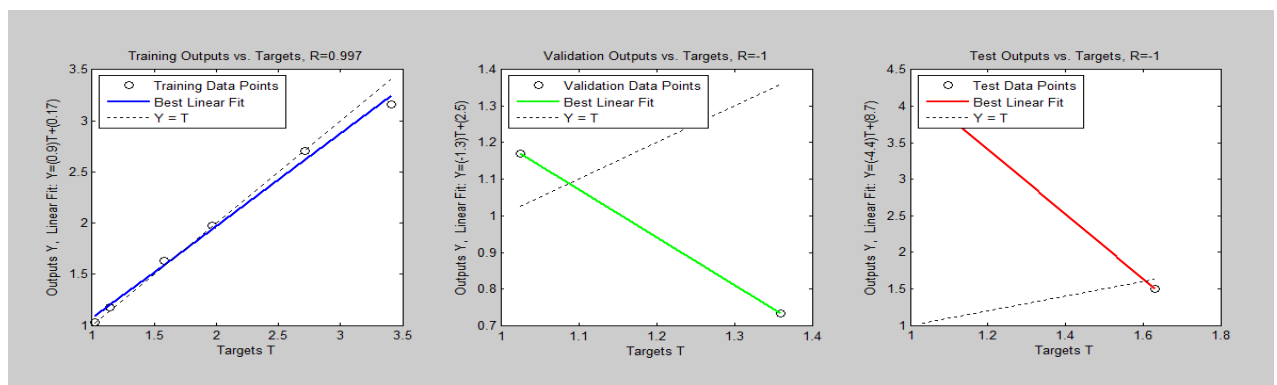


Figure 4.104a: Experimental vs. neural model results for modulus of rattan palm-epoxy

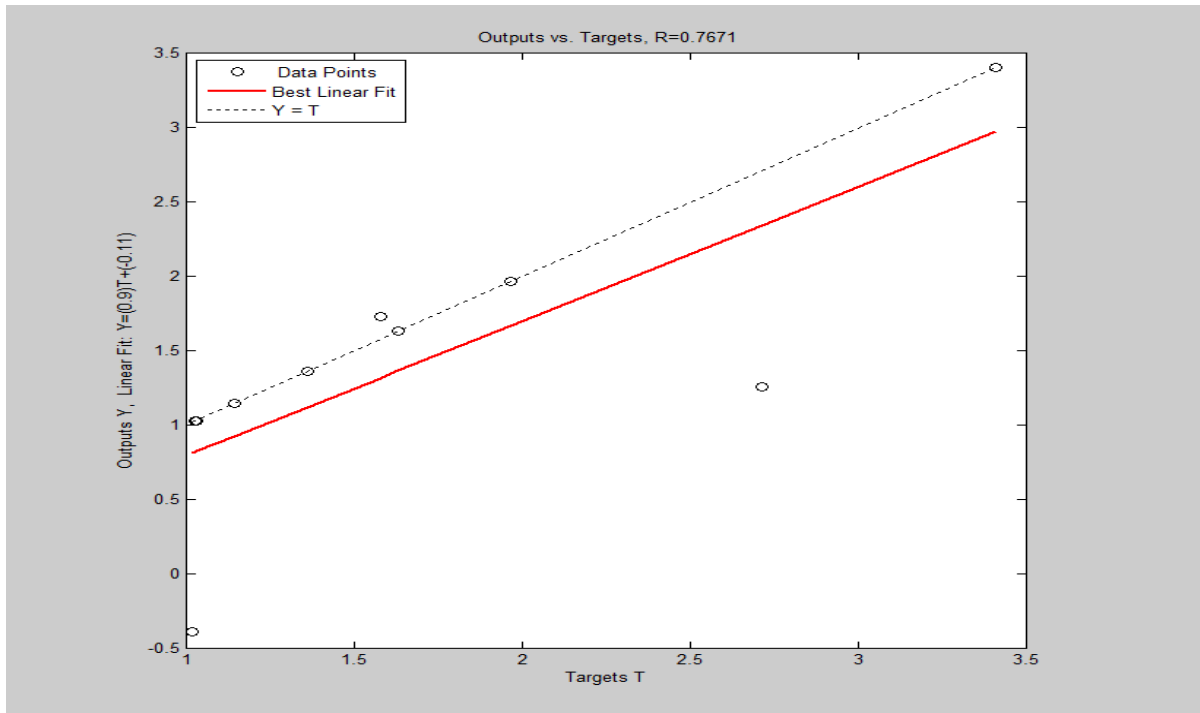


Figure 4.104b: Experimental vs. neural model results for modulus of rattan palm-epoxy

Most of the limitation observed in neural network is inherent in its nature as a classification technique (Abu-Mostafa, 2014). Improvement may be possible if many more experimental data points are used in the neural network training.

It can be observed from the Table 4.212 below that the response surface model gave the best fit for the modulus of all composites modeled. The micromechanics model, especially the modified model proposed in this work, is barely ahead of the neural network model in accuracy, with a mean R^2 value of 0.6208 as against a mean R^2 of 0.5952 for the neural network model.

Table 4.212: Comparison of the three Modeling techniques based on the R-squared values

Model	Composite	Plantain-Polyester	Plantain-Epoxy	Palm-Polyester	Palm-Epoxy	Rattan-Polyester	Rattan-Epoxy
Response Surface Model		0.9651	0.9728	0.9413	0.9875	0.9105	0.8484
Best Micromechanics Model		0.4712	0.8479	0.8477	0.7076	0.2880	0.5621
Neural Network model		0.8207	0.4059	0.5390	0.4581	0.5805	0.7671

4.19 Automobile Application of Composites

The automotive industry began its adventure with composites in 1953 to provide weight savings, reduced fuel consumption and CO₂ emission and due to challenges of high weight to volume ratio and corrosion with steel. Presently up to 15% of the weight of cars is made of composites and the automobile body accounts for about 30% of this weight.

In consideration of material strength in automobile application, the most useful term is specific strength, which is the ratio of force per unit area at failure to density of the material. It is also known as strength to weight ratio. While replacing existing materials used for auto body parts with new materials, the main aspect to be considered is its crashworthiness. Crashworthiness is the ability of vehicle components to protect an occupant from serious injuries at a time of accident. Selecting materials with high energy absorption capability is the base of crashworthiness design. The amount of energy or impact absorbed (Energy Absorption (EA)) by a material is the area under the load versus displacement curve. While comparing the performance of materials, the useful property considered is the specific energy absorption (SEA) which is the energy absorbed per unit mass of crushed structure expressed in J/g. This ability to absorb rapidly applied energy is impact resistance measured by impact tests like Izod, Charpy impact tests among others (Wagmare and Deshmukh, 2014).

The properties of steel used for auto body parts is compared below with glass fiber reinforced polyester (GFRP), carbon fiber reinforced polyester (CFRP), plantain bunch fiber reinforced polyester (PBFRRP), plantain bunch fiber reinforced epoxy (PBFRE), oil palm bunch fiber reinforced polyester (OPBRP), oil palm bunch fiber reinforced epoxy (OPBRE), rattan palm fiber reinforced polyester (RPFRRP) and rattan palm fiber reinforced epoxy (RPFRE).

It can be observed from Table 4.213 and Fig. 4.105 that the tensile strength of steel is more than ten times that of PBFRRP, which has the highest tensile strength of the six composites studied. It also has higher yield strength, modulus and flexural strength, but PBFRRP has impact strength more than four times that of steel, while all the composites of rattan palm or epoxy matrix have impact strength about nine times that of steel. This is close to the observation of Henry Ford, that his hemp based composite was ten times stronger than steel. Impact strength, is about the most important single parameter in choice of materials for auto body parts and in consideration of crashworthiness.

Table 4.213: Comparison of the properties of steel with fiber reinforced composites

Material Property	Steel	GFRP	CFRP	PBFRRP	PBFRE	OPBRP	OPBRE	RPFRP	RPFRE
Tensile strength (MPa)	440	1490	110	34.87	8.43	30.15	10.75	14.80	12.06
Yield Strength (MPa)	180	-	-	31.71	6.79	18.10	7.89	11.44	8.90
Tensile Modulus (GPa)	210	35	37.5	5.61	2.97	4.46	2.46	3.24	3.41
Flexural Strength (MPa)	450	1150	250	54.65	37.60	50.72	28.13	37.35	31.36
Impact Strength (J/cm ²)	21.36	46.36	0.55	103.95	198.1	104.74	202.02	198.1	204.97
Density (g/cm ³)	7.85	2.50	1.325	1.315	1.245	1.248	1.178	1.360	1.290

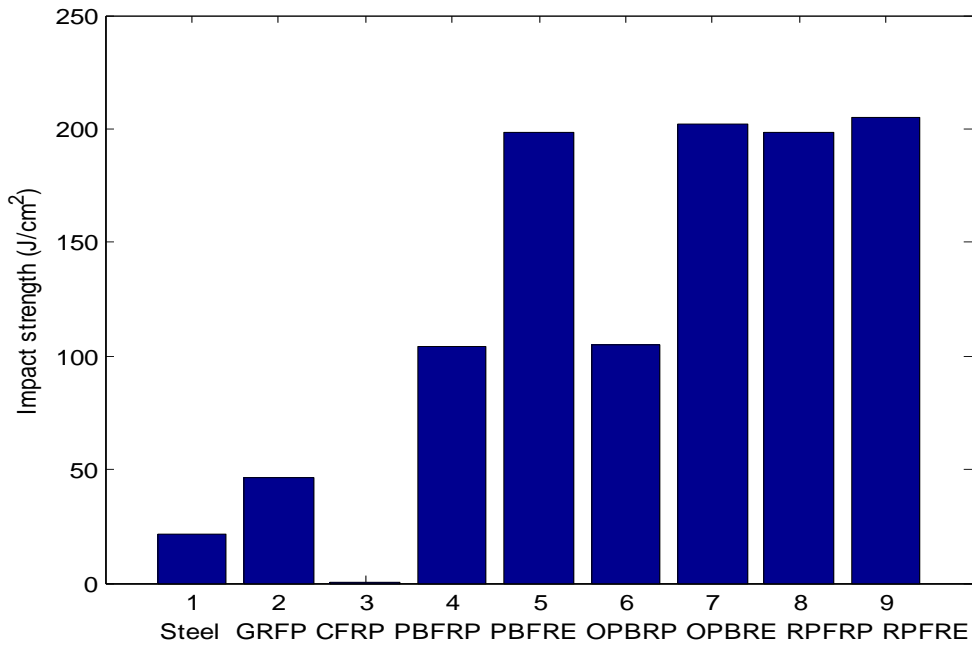


Figure 4.105: Comparison of Impact strength of steel with all composites

Table 4.214 and Fig. 4.106 show specific strength and energy absorption of steel and all composites. It can be observed that specific strength of steel is less than twice that of PBFPR while the specific energy absorption of the composites studied are from 29-50 times that of steel.

Table 4.214: Comparison of the specific properties of steel with fiber reinforced composites

Material Property	Steel	GFRP	CFRP	PBFPR	PBFRE	OPBRP	OPBRE	RPFPR	RPFRE
Specific Strength (KNm/kg)	50	587.5	75	26.5171	6.7711	24.1587	9.1256	10.8824	9.3488
Specific Energy Absorption (J/g)	2.72	18.54	0.42	79.05	159.12	83.93	171.49	145.66	158.89

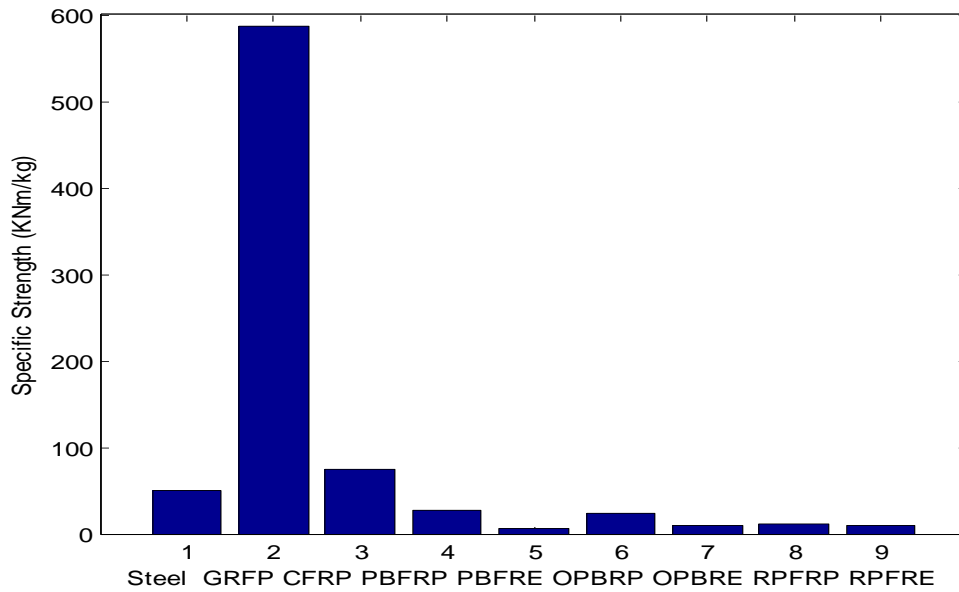


Figure 4.106: Comparison of Specific strength of steel with all composites

CHAPTER FIVE

CONCLUSIONS AND RECOMMENDATIONS

5.1 Conclusions

The mechanical properties of Composites formed from three selected natural fiber sources (Empty Plantain Bunch Fiber, Empty Palm Bunch Fiber and Rattan Palm Fiber), mercerized at optimum conditions, with two selected thermosetting resins (Polyester and Epoxy resins) have been studied. Analytical techniques and algebraic relations that can extend the use of traditional tensile test data for computation of Poisson ratio, thus fully characterizing the sample linear elastic properties, was presented and validated based on its limiting value. A new approach for analysis of tensile test data using linear-quadratic rational models was also proposed. Though

this technique needs further validation from experiment, it was observed that it prevents erroneous results that may produce a Composite Modulus with a value below the Modulus of the fiber and matrix.

Optimum conditions for mercerization of Empty Plantain Bunch fiber, Empty Palm Bunch fiber and Rattan Palm fiber are 4wt% NaOH for 120mins, 6wt% NaOH for 90mins and 4wt% NaOH for 120mins respectively. Empty Plantain Bunch fiber responds the most to mercerization and the process is controlled by NaOH concentration. The Modulus of Empty Plantain Bunch fiber increases 50 times to 70GPa, while the Tensile Strength increases 15 times to 860MPa after mercerization at optimum conditions. Water absorption of the fibers reduced by about one-third with treated at optimum conditions. Composites formed from the fibers and matrices show that Empty Plantain Bunch fiber is quite compatible with Polyester resin, increasing its modulus 5 times, while Rattan Palm fiber produces the best properties with Epoxy resin, increasing its modulus 3 times. Composites from Polyester resin have the best flexural properties (54.65MPa for Empty Plantain Bunch-Polyester) but have the least Impact strength, about half of that obtained when Epoxy resin is used as matrix. The only exception is for Composites from Rattan Palm fibers which have relatively equal impact strength, the matrix of choice notwithstanding. Flexural strength is significantly volume fraction controlled, while impact strength is mostly affected by fiber length.

All Composites formed from Epoxy resin or rattan palm fiber have impact strength greater than 20kgfm/cm²(approximately 200J/cm²), which is nine times the impact strength for mild steel used in auto body parts. Rattan palm fiber reinforced polyester can replace steel in auto body parts with its high impact strength and considering lower cost of polyester resin in comparison to epoxy.

The Response Surface model is the most appropriate model for this study.

5.2 Recommendations

Empty Plantain Bunch fiber, Empty Palm Bunch fiber and Rattan Palm fiber should be mercerized with 4wt% NaOH for 120mins, 6wt% NaOH for 90mins and 4wt% NaOH for 120mins respectively prior to use in composite manufacture.

Rattan palm fiber reinforced polyester should be considered as a replacement for steel in auto body parts. It is recommended that such replacements may start from the roof of the car.

The modified Halpin-tsai model presented in this work should be used to model natural fiber based composites and attempts made to improve its accuracy by obtaining more suitable values for the constant parameters in the model.

5.3 Contributions to Knowledge

* Optimum mercerization conditions for empty plantain bunch fiber, empty palm bunch fiber and rattan palm fiber were determined.

* New relations for determination of percentage reduction in area and poisson ratio from the ultimate elongation value (for different sample configurations) were obtained.

* A new technique for analysis of tensile test data, which could reduce errors due to contribution to strain from material creep and deflection of test machine, was presented.

* Water absorption kinetics and mechanism for untreated and treated empty plantain bunch fiber, empty palm bunch fiber and rattan palm fiber were determined.

- * Optimum fiber aspect ratio and volume fractions for forming composites from empty plantain bunch fiber, empty palm bunch fiber and rattan palm fiber using polyester and epoxy resin were determined.
- * A modified micromechanics model for the composite modulus was proposed.
- * Three techniques for modeling mechanical properties of natural fiber composite samples were studied and the best method presented.

6.0 REFERENCES

- Abu-Mostafa, Y.S. (2014). Machine Learning Lectures. California Institute of Tech. USA.
- Addo, A., Bart-Plange, A. (2009). Kinetics of water sorption by egusi melon (*cucumeropsis edulis*) seeds. *ARPN Journal of Agricultural and Biological Science* 4(6): 14-18.
- Akova, I.E.(2013). Development of natural fiber reinforced composites. *Transfer Inovacii* 25:3-5
- Amar, K.M., Manjusriand, M., Lawrence, T.D.(2005). Natural Fibers, Biopolymers, and Bio-composites. CRC Press, Tailor & Francis.
- Anyakora, A.N., Abubakre, O.L. (2011). Effect of Silane Treatment on the Impact Strength Properties of Oil Palm Empty Fruit Bunch Fiber-Reinforced Polyester Composites. *World Journal of Engineering and Pure and Applied Sciences* 1(2):40-45.
- Ashby M.F. and D. Cebon.(2011). Young's modulus, shear modulus, bulk modulus and Poisson ratio. Granta Design CES EduPack. Cambridge UK (www.grantadesign.com/education/datasheet).

- Ball, R., Tissot, P. (2006). Demonstration of artificial neural network in MATLAB. Division of Nearshore Research, Texas A&M University, Corpus Christi.
- Bataille, P., Richard, L., Sapieha, S. (1989). Effects of cellulose fibers In Polypropylene composites. *Polymer Composites* 10(2):103-108.
- Becker, H.A. (1960). On the absorption of liquid water by the wheat kernel. *Cereal Chemistry*. 37(3): 309-323.
- Bhatnagar, M.S. (1996). *The Polymeric materials encyclopedia: Epoxy resins (overview)*. CRC Press Inc.
- Bledzki, A.K., Gassan, J. (1999). Composites reinforced with cellulose based fibers. *Progress in polymer science* 24:221-274.
- Bledzki, A.K., Speber, V.E., Frank, O. (2002). Natural and wood fiber reinforcement in polymers. *Rapra Review Report* 13(8). Report 152. Rapra publishing.
- Bodros, E., Baley, C. (2008). Study of the tensile properties of stinging nettle fibers (*Urticadioica*). *Materials Letters* 62(14):2143-2145.
- Box, G.E.P., Draper, N.R. (1987). *Empirical Model-Building and Response Surfaces*, Wiley, New York. ISBN 0-471-81033-9.
- Bower, A.F. (2011). *Applied Mechanics of solids: Constitutive models-relations between stress and strain*. Chapter 3. CRC Press Ltd.
- Bradley, N. (2007). *The Response Surface Methodology*. An MSc Thesis submitted to the Department of Mathematical Sciences, Indiana University of South Bend, Indiana.
- Ceccarini, L., Angelini, L.G. (2010). *Spartiumjunceum L. A new crop for natural fiber for automotive industry*. A paper presented to the Department of Agronomy, University of Pisa, Italy
- Chimekwene, C.P., Fagbemi, E.A., Ayeke, P.O. (2012). Mechanical properties of plantain empty fruit bunch fiber reinforced epoxy composite. *International Journal of Research in Engineering, IT and Social Sciences* 2(6):86-94.
- Coutinho, F.M.B., Costa, T.H.S., Carvalho, D.L. (1997). Polypropylene-wood fiber composites: effect of treatment and mixing conditions on mechanical properties. *Journal of Applied Polymer Science* 65(6):1227-1235.
- Cox, H.L. (1952). The elasticity and strength of paper and other fibrous materials. *British Journal of Applied Physics* 3(3):72-79.
- Culler, S.R., Ishida, H., Koenig, J.L. (1986). The silane interphase of composites: effects of process conditions on γ -aminopropyltriethoxysilane. *Polymer Composites* 7(4):231-238.

Daniel, I.M., Ishai, O. (2005). Engineering mechanics of composite materials. Oxford University Press. ISBN 019515097X

Dhakal, H.N., Zhang, Z.Y., Richardson, M.O.W. (2006). Effect of water absorption on the mechanical properties of hemp fiber reinforced unsaturated polyester composites. *Composites Science and Technology*. 67(7): 1674-1683.

Ebrahimzadeh, P.R. (1997). Dynamic Mechanical Studies of Wood, Paper and Some Polymers Subjected to Humidity Changes, Ph.D. Thesis, Chalmers University of Technology, Goteborg.

Edeerozey A.M.M. et al. (2007). Chemical modification of kenaf fibers. *Materials Letters* 61:2023-2025.

Facca, A.G., Kortschot, M.T., Yan, N. (2006). Predicting the elastic modulus of natural fiber reinforced thermoplastics. *Composites: Part A* 37: 1660-1671.

Facca, A.G., Kortschot, M.T., Yan, N. (2007). Predicting the tensile strength of natural fiber reinforced thermoplastics. *Composites Science and Technology* 67: 2454-2466.

Folkes, M.J. (1982). Short fiber reinforced thermoplastics. *Research studies Press*. Pp 51-55.

Gassan, J., Bledzki, A.K. (1999). Alkali treatment of jute fibers: relationship between structure and mechanical properties. *Journal of Applied Polymer Science* 71(4):623-629.

George, J., Sreekala, M.S., Thomas, S. (2001). A review on interface modification and characterization of natural fiber reinforced plastic composites. *Polymer Engineering and Science* 41(9):1471-1485.

Ghatge, N.D., Khisti, R.S. (1989). Performance of new silane coupling agents along with phenolic no-bake binder for sand core. *Journal of Polymer Materials* 6:145-149.

González, L., Rodríguez, A., de Benito, J.L., Marcos-Fernández, A. (1997). Applications of an azidesulfonylsilane as elastomer crosslinking and coupling agent. *Journal of Applied Polymer Science* 63(10):1353-1359.

Goring, D. (1976). Plasma-Induced Adhesion in Cellulose and Synthetic Polymers. In *The Fundamental Properties of Paper Related to its Uses*, F. Bolam, Ed., Ernest Benn Limited, London, 172.

Greaves, G.N., Greer, A.L., Lakes, R.S., Rouxel, T. (2011). Poisson's ratio and modern materials. *Nature Materials* 10:823-837.

Gu, H. (2009). Tensile behaviors of the coir fiber and related composites after NaOH treatment. *Materials and Design* 30:3931-3934.

Hai, N.M., Kim, B.S., Lee, S. (2009).Effect of NaOH Treatments on jute and coir fibers PP composites.Advanced Composite Materials 18(3):197-208.

Halpin, J.C., Tsai, S.W. (1969). Effect of environment factors on composite materials.AFML-TR-67-423.

Hamdaoui, M., Achour, N.S., Nasrallah, S.B. (2014).The influence of woven fabric structure on kinetics of water sorption.Journal of Engineered Fibers and Fabrics. 9(1): 101-106.

Hashim, M.Y., Roslan, M.N., Amin, A.M., Zaidi, A.M.A., Ariffin, S. (2012). Mercerization treatment parameters effect on natural fiber reinforced polymer matrix composite: A Brief Review. World Academy of Science, Engineering and Technology 68:1638-1644.

Hull, D., Clyne, T.W. (1996). An introduction to composite materials.Cambridge University Press,Cambridge

Hyer, M.W., Waas, A.M. (2000). Micromechanics of linear elastic continuous fiber composites In Kelly, A. and C. Zweben, Volume 1: Fiber reinforcements and general theory of composites. Elsevier Science. Chapter 12:345-375.

Ichhaporia, P.K. (2008). Composites from Natural Fibres.PhD Thesis, North Carolina University, USA.

Ihueze, C.C., Okafor, E.C. (2014a). Response Surface Optimization of the Impact Strength of Plantain Fiber Reinforced Polyester for Application in Auto Body Works. Journal of Innovative Research in Engr. and Sci. 4(4):505-520.

Ihueze, C.C., Okafor, E.C. (2014b). Optimal Design of Flexural Strengthof Plantain Fibers Reinforced Polyester Matrix. Journal of Innovative Research in Engr. and Sci. 4(4):520-537.

Ihueze, C.C., Okafor, E.C., Nwigbo, S.C. (2013). Optimization of Hardness Strength Response of Plantain Fibres Reinforced Polyester Matrix Composites (PFRP) Applying Taguchi Robust Design. Int. J. Sci. Emerging Tech. 5(1):217-227.

Ihueze, C.C., Okafor, E.C., Ujam, A.J. (2012). Optimization of Tensile Strength Response of Plantain Fibres Reinforced Polyester Composite (PFRP) Applying Taguchi Robust Design. Innovative Systems Designs & Engr. 3(7): 62-76.

Ishida, H. (1990). Introduction to Polymer Composite Manufacturing.NSF Center for Molecular and Microstructure of Composites (CMMC), Department of Macromolecular Science. Case Western Reserve University,Cleveland, Ohio.

Jones, R.M. (1998). Mechanics of composite materials.CRC Press. ISBN 156032712X

Joseph, K., Mattoso, L.H.C., Toledo, R.D., Thomas, S., de Carvalho, L.H., Pothen, L., Kala, S., James, B. (2000). Natural fiber reinforced thermoplastic composites. In *Natural Polymers and Agrofibers Composites*, ed. E. Frollini, A.L. Leão and L.H.C. Mattoso, 159-201. São Carlos, Brazil: Embrapa, USP-IQSC, UNESP.

Kalia, S., Kaith, B.S., Kaur, I. (2009). Pretreatments of natural fibers and their application as reinforcing material in polymer composites – A Review. *Polymer Engineering and Science* 47(7): 1253-1275.

Kalpakjian, S., Schmid, S.R. (2001). *Manufacturing, Engineering and Technology*. International Edition. 4th Edition. Prentice Hall Inc. pp. 5.

Katchy, E.M. (2008a). *Introduction to Polymer Technology*. Second edition. EL 'DEMAK Publishers. Enugu. Nigeria.

Katchy, E.M. (2008b). *Principles of polymer science*. Second edition. EL 'DEMAK Publishers. Enugu. Nigeria.

Kelly, A., Tyson, W.R. (1965). Tensile properties of fiber reinforced metals: Copper/Tungsten and Copper/Molybdenum. *Journal of the Mechanics and Physics of Solids*. 13:329-350.

Khuri, A.I., Mukhopadhyay, S. (2010). *Response Surface Methodology: Advanced Review*. WIREs Computational Statistics, John Wiley and Sons 2:128-149.

Krenchel, H. (1964). *Fiber reinforcement*. Akademisk Forlag. Copenhagen. Pp 27.

Ku, H., Wang, H., Pattarachaiyakop, H., Trada, M. (2011). A review on the tensile properties of natural fiber reinforced polymer composites. *Composites: Part B: Engineering* 42(4):856- 873.

Lamy, B., Baley, C. (2000). Stiffness prediction of flax fibers-epoxy composite materials. *Journal of Materials Science Letters*. 19(11): 979-980.

Li, X., Panigrahiand, S., Tabil, L. (2009). A study of flax fiber-reinforced polyethylene biocomposites. *Applied Engineering in Agriculture* 25: 525-531.

McIntyre, K. (2012). Nonwovens offer win-win solutions for car makers. *Nonwovens-Industry*. Rodman Media. Available at: www.nonwovens-industry.com. Accessed: 25-05-2014.

Milauskas, M.K. (2013). *Composites by design*. Available at : nptel.iitm.ac.in/courses/....Glossory.pdf. Accessed: 25-05-2014.

Mishra, S., Misra, M., Tripathy, S.S., Nayak, S.K., Mohanty, A.K. (2001). Potentiality of pineapple leaf fiber as reinforcement in PALF-Polyester composite: surface modification and mechanical performance. *Journal of Reinforced Plastics and Composites* 20(4):321-334.

- Mishra, S., Tripathy, S.S., Misra, M., Mohanty, A.K., Nayak, S.K.(2002). Novel ecofriendly biocomposite: biofiber reinforced biodegradable polyester amide composite – fabrication and property evaluation. *Journal of Reinforced Plastics and Composites*21:55-70.
- Mishra, S. et al. (2003). Studies on mechanical performance of biofiber/glass reinforced polyester hybrid composites. *Composites Science and Technology* 63:1377-1385.
- Mohanty, A.K.,Khan, M.A., Hinrichsen, G. (2000). Influence of Chemical Surface Modification on The Properties of Biodegradable Jute Fabrics-Polyester Amide Composites. *Composites Part A: Applied Science and Manufacturing* 31(2):143-150.
- Montgomery, D. C. (2005).*Design and Analysis of Experiments: Responsesurface method and designs*. New Jersey: John Wiley and Sons, Inc.
- Mueller, D.H. (2004). Improving the Impact Strength of natural fiber reinforced composites by specifically designed material and process parameters. *International Nonwovens Journal*.Winter.31-38.
- Murray, J.E. (1998). Acetylated Natural Fibers and Composite Reinforcement.In 21st International BPF Composites Congress. British Plastics Federation, London. Publication Number 293/12.
- Mwaikambo, L., Ansell, M. (2002).Chemical modification of hemp, sisal, jute and kapok fibers by alkalization.*Journal of applied Polymer Sciences* 84:2222 – 2234.
- Myrtha, K., Holia, O., Dawan, A. A. H., Anung, S. (2008). Effect of Oil Palm Empty Fruit Bunch Fiber on the Physical and Mechanical Properties of fiber glass reinforced polyester resin. *Journal of Biological Sciences* 8(1):101-106.
- Okafor, E.C., Godwin, H. C. (2014). Evaluation of compressive and energy adsorption characteristics of plantain fiber reinforced composites.*World Journal of Engr. and Phy. Sci.* 2(3):36-48.
- Panigrahi, S., Li, X., Tabil, L. (2008).Injection moulding processing of flax fiber-reinforced polyethylene biocomposites.*International Conference on Flax and other Bast Plants*: 399-407.
- Paul, S.A., Boudenne, A., Ibos, L., Candau, Y., Joseph, K., Thomas, S. (2008). Effect of fiber loading and chemical treatment on thermophysical properties of banana fiber/polypropylene comingled composite material. *Composites: Part A* 39:1582-1588.
- Peleg, M. (1988). An empirical model for the description of moisture sorption curves. *Journal of Food Science*. 53: 1216-1217.
- Piggot, M.R. (1980). Load bearing fiber composites. Pergamon Press. Oxford. Chapter 5.
- Potter, R.T. (1994). Strength of composite.In Kelly, A. *Concise Encyclopedia of composite materials*.Pergamon.ISBN 0080423000.

- Ray, D., Sarkar, B.K., Rana, A.K., Bose, N.R. (2001). Effect of alkali treated jute fibers on composite properties. *Bulletin of Materials Science* 24(2):129-135.
- Rowell, R.M. (1991). Natural Composites; Fiber Modification. In *International Encyclopedia of Composites*. S.M. Lee, Ed., VHC. New York: 4.
- Rowell, R.M. (1998). Property Enhanced Natural Fiber Composite Material based on Chemical Modification. In *Science and Technology of Polymers and Advanced Materials*, P.N. Prasad, J.E. Mark, S.H. Kendil, and Z.H. Kafafi, Eds., Plenum Press, New York. 717.
- Rowell, R.M., Ham, M., Rowe, J.S. (2000). Characterization and factors affecting fiber properties. *Natural Polymer and Agrofiber Composites*. San Carlos, Brazil: 115-134.
- Sapieha, S., Allard, P., Zang, Y.H. (1990). Dicumyl peroxide-modified cellulose/LLDPE composites. *Journal of Applied Polymer Science* 41:2039-2048.
- Scandola, M., Frisoni, G., Baiardo, M. (2000). Chemically Modified Cellulosic Reinforcements. In *Book of Abstracts 219th ACS National Meeting*, Washington, D.C., American Chemical Society, 26.
- Sharifah, H.A., Martin, P.A., Simon, T.C., Simon, R.P. (2005). Modified polyester resins for natural fiber composites. *Compos. Sci. Technol.* 65:525-535.
- Singla, M., Chawla, V. (2010). Mechanical properties of epoxy resin-fly ash composite. *Journal of Minerals and Materials Characterization and engineering* 9(3): 199-210.
- Singh, B.P.N., Kulshrestha, S.P. (1986). Kinetics of water sorption by soybean and pigeonpea grains. *Journal of Food Science*. 52(6): 1538-1544.
- Sinha, R. (2000). *Outlines of Polymer Technology*. Prentice-Hall by India private Ltd. New Delhi -10001
- Skramstad, J.D. (1999). Evaluation of hand-layup and Resin Transfer Molding in Composite Wind Turbine Blade Manufacturing, M. Sc. Thesis, Montana State University, Bozeman, Montana, USA.
- Sreekala, M.S., Kumaran, M.G., Joseph, S., Jacob, M., Thomas, S. (2000). Oil palm fiber reinforced phenol formaldehyde composites: influence of fiber surface modifications on the mechanical performance. *Applied Composite Materials* 7:295-329.
- Srubar, W.V., Frank, C.W., Billington, S.L. (2012). Modeling the kinetics of water transport and hydroexpansion in lignocelluloses-reinforced bacterial copolyester. *Polymer* 53: 2152-2161.
- Suddell, B. (2009). Industrial Fibers: Recent and Current Developments. In *Proceedings of the Symposium on Natural Fibers*: 71-82. <ftp://ftp.fao.org/docrep/fao/011/i0709e/i0709e10.pdf>

- Summerscales, J., Dissanayake, N., Hall, W., Virk, A.S. (2010). A review of bast fibers and their composites. Part 2: Composites. *Composites Part A: Applied Science and Manufacturing*. 41(10): 1336-1344.
- Suraya, N.L., Abdul Khalil, H.P.S. (2011). Anhydride modification of cultivated kenaf Bast fibers: Morphological, Spectroscopic and Thermal Studies. *BioResources* 6(2): 1122-1135.
- Taj, S., Munawar, M.A., Khan, S. (2007). Natural fiber-reinforced polymer composites. *Proceedings of Academic Science* 44(2):129-144.
- Timmins, N., Almaguer, R., Clark, A., Odea, N. (2011). Opportunities in natural fiber composites. *Creating the equation for growth*. Lucintel Texas USA.
- Turhan, M., Sayar, S., Gunasekaran, S. (2002). Application of Peleg model to study water absorption in chickenpea during soaking. *Journal of Food Engineering*. 53: 153-159.
- Velumani S., Navaneethakrishnan, P. (2012). Optimization of Mechanical Properties of Non-woven Short Sisal Fiber Reinforced Vinyl Ester Composite Using Factorial Design and GA Design. *Bulletin of Material Science* 36(4), pp.575-583.
- Virk, A.S. (2010). Numerical models for natural fiber composites with stochastic properties. Thesis submitted to School of Marine and Science and Engineering, University of Plymouth, England.
- Wagmare, S.A., Deshmukh, P.D. (2014). Strategic selection of alternative material for automotive roof to improve crashworthiness in rollover accident. *Intl. Journal of Emerging Tech. and Advance Engr.* 4(6):132-138.
- Wambua, P., Ivensand, U., Verpoest, I. (2003). Natural fibers: can they replace glass in fiber-reinforced plastics? *Compos. Sci. Technol.* 63:1259-1264.
- Wang, B. (2004). Pre-treatment of Flax Fibers for Use in Rotationally Molded Biocomposites. M.Sc. Thesis, University of Saskatchewan.
- Williams, G.I., Wool, R. (2000). Composites from natural fibers and soy oil resins. *Applied Composite Materials* 7:421-432.
- Wlodek, A.B., Koziol, M., Myalski, J. (2012). Influence of surface treatment on the wetting process of jute fibers with thermosetting polyester resin. *Polish Journal of Chemical Technology* 14(1):21-27.
- Young, R. (1992). Activation and Characterization of Fiber Surfaces for Composites. In *Emerging Technologies for Materials and Chemicals from Biomass*, R. Rowell, T.P. Shulz, and R. Narayan, Eds., American Chemical Society, Washington D.C., 115.

Yang, X., Huang, L., Cheng, L., Yu, J. (2012).Studies of moisture absorption and release behavior of Akund fiber.Advances in Mechanical Engineering. Hindawi Publishing Corporation. Vol. 2012: 1-4.

7.0 APPENDICES

A 7.1: TENSILE TEST RESULT ANALYSIS FOR EMPTY PLANTAIN BUNCH FIBER

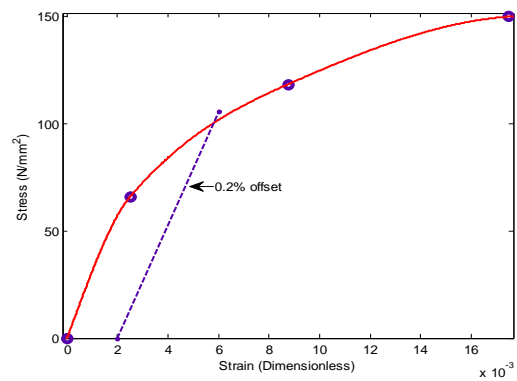
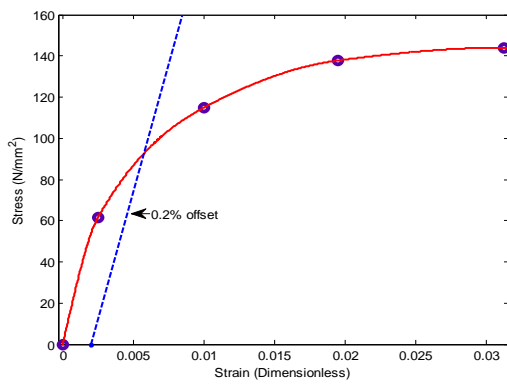


Fig. 7.1:Mercerization with 2wt% NaOH for 30mins Fig 7.2: Mercerization with 2wt% NaOH for 60mins

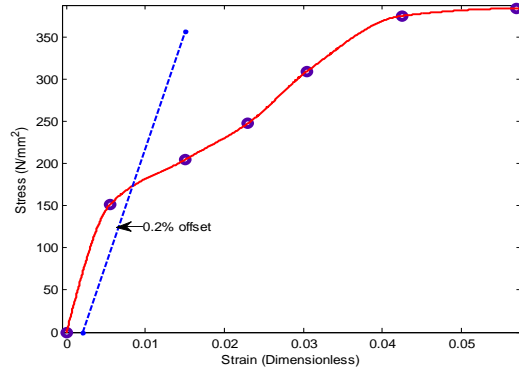
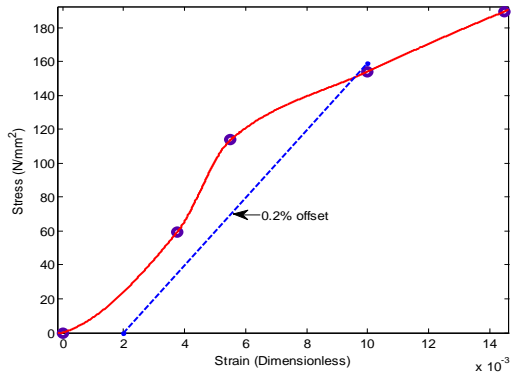


Fig. 7.3:Mercerization with 2wt% NaOH for 90mins Fig 7.4: Mercerization with 2wt% NaOH for 120mins

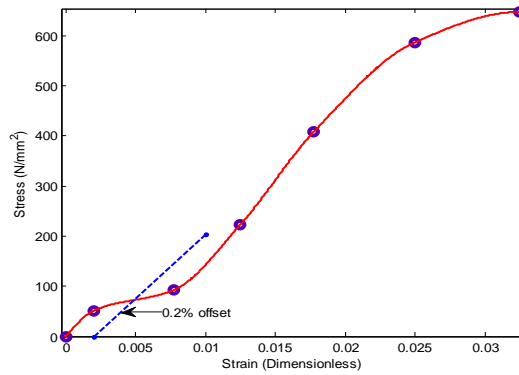


Fig. 7.5: Mercerization with 2wt% NaOH for 150mins

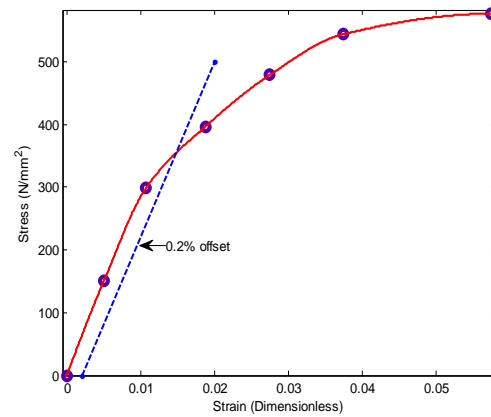
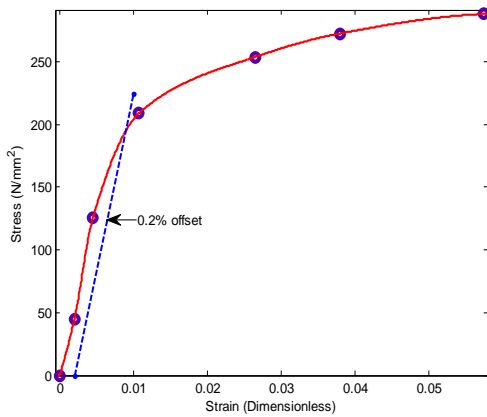


Fig. 7.6:Mercerization with 4wt% NaOH for 30mins Fig 7.7: Mercerization with 4wt% NaOH for 60mins

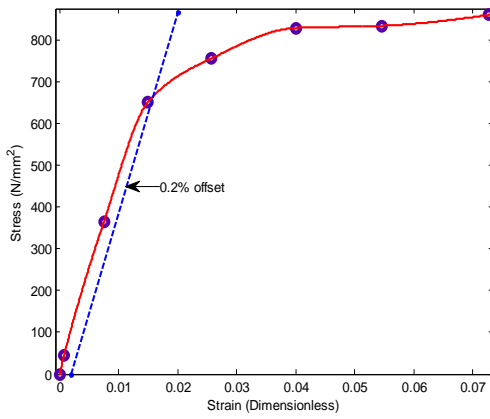
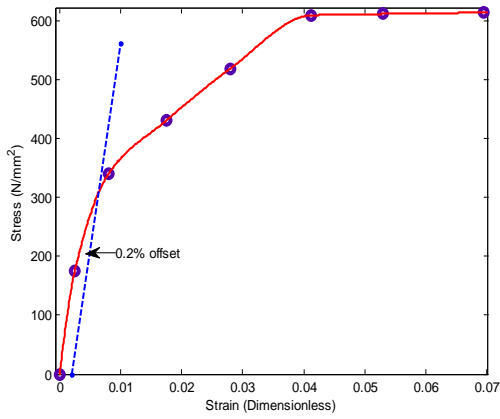


Fig. 7.8:Mercerization with 4wt% NaOH for 90mins Fig 7.9: Mercerization with 4wt% NaOH for 120mins

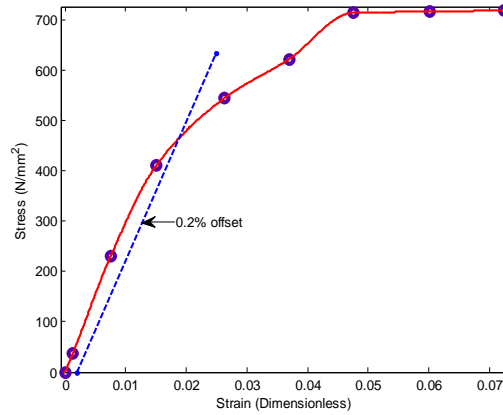


Fig 7.10: Mercerization with 4wt% NaOH for 150mins

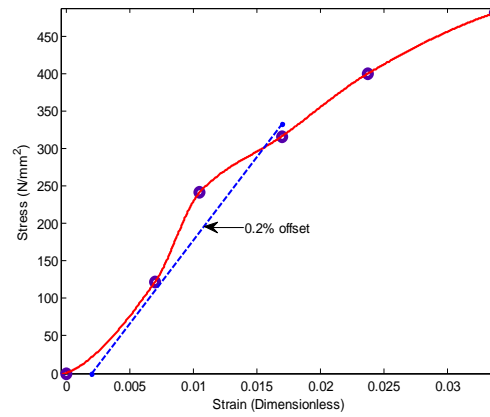
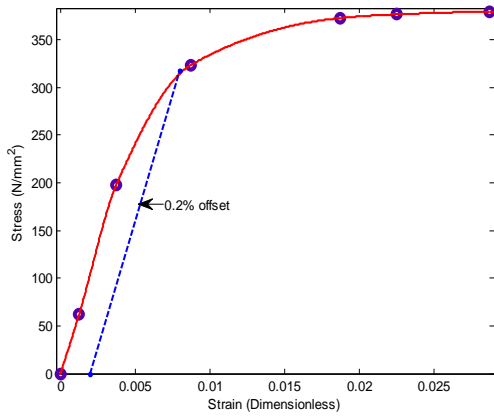


Fig. 7.11:Mercerization with 6wt% NaOH for 30mins Fig 7.12: Mercerization with 6wt% NaOH for 60mins

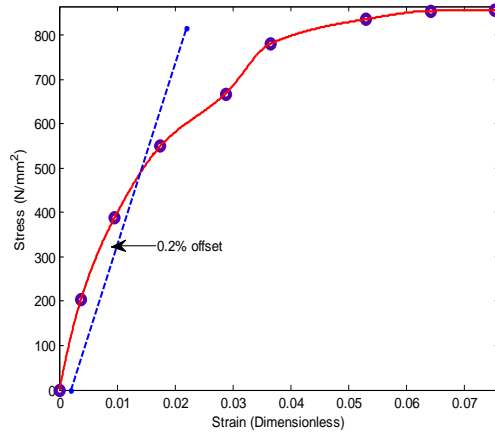
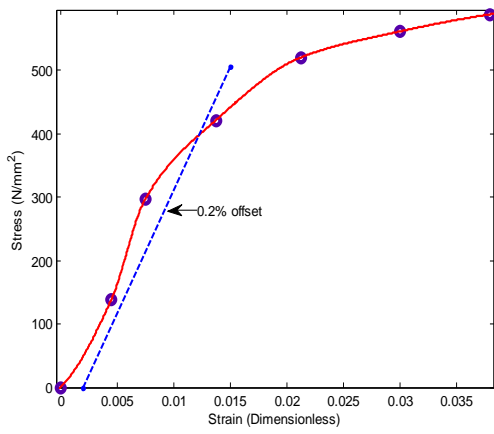


Fig. 7.13:Mercerization with 6wt% NaOH for 90mins Fig 7.14: Mercerization with 6wt% NaOH for 120mins

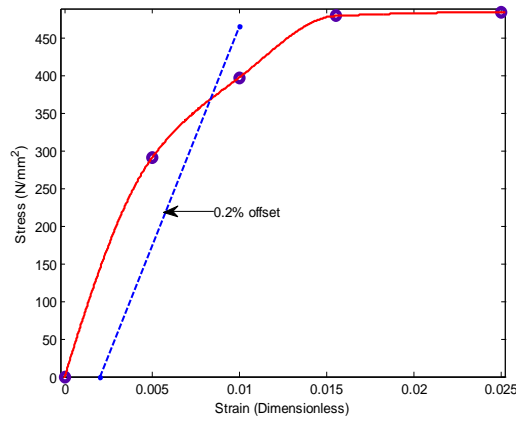


Fig 7.15: Mercerization with 6wt% NaOH for 150mins

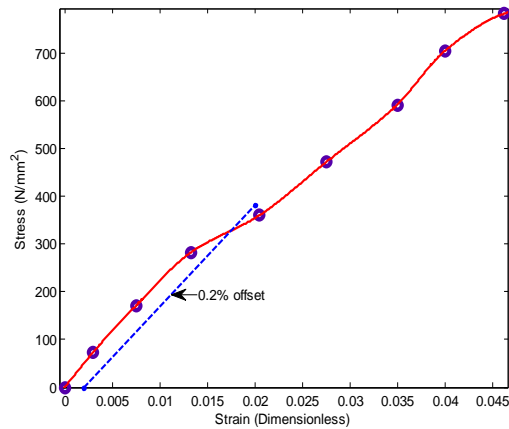
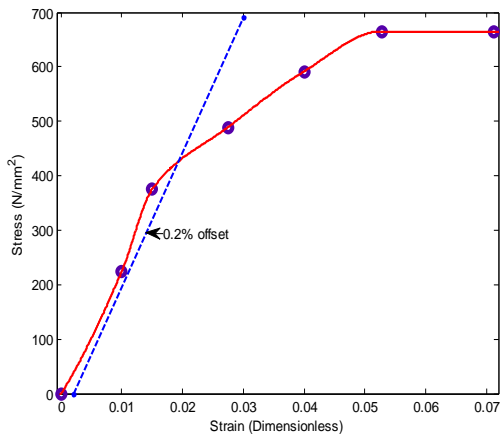


Fig. 7.16: Mercerization with 8wt% NaOH for 30mins Fig 7.17: Mercerization with 8wt% NaOH for 60mins

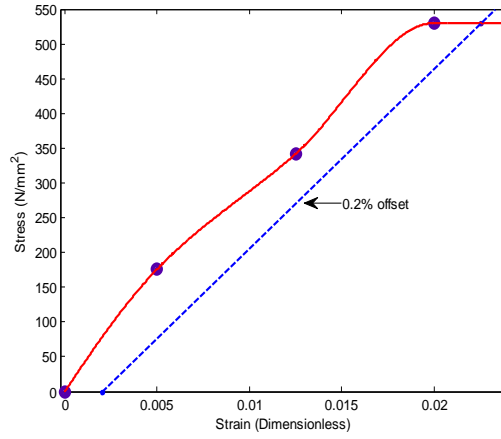
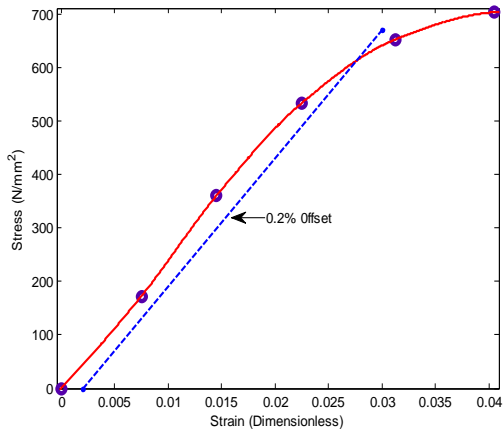


Fig. 7.18: Mercerization with 8wt% NaOH for 90mins Fig 7.19: Mercerization with 8wt% NaOH for 120mins

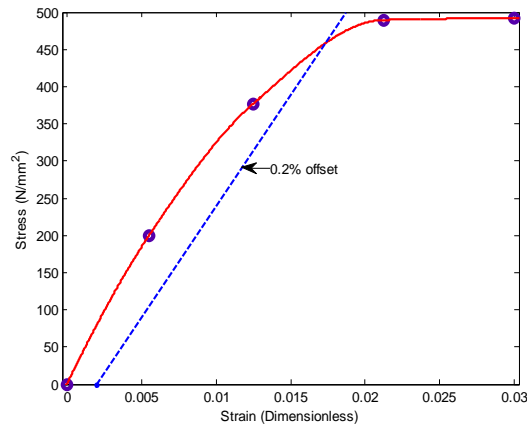


Fig 7.20: Mercerization with 8wt% NaOH for 150mins

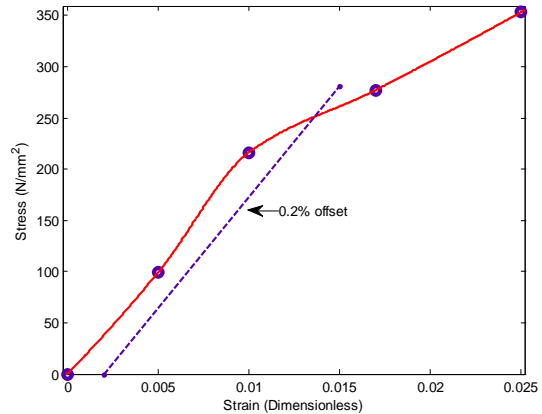
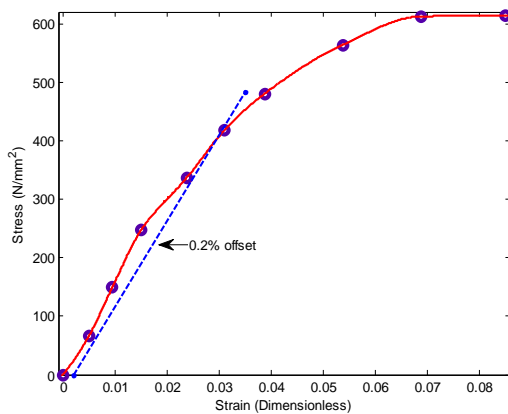


Fig. 7.21: Mercerization with 10wt% NaOH for 30mins Fig 7.22: Mercerization with 10wt% NaOH for 60mins

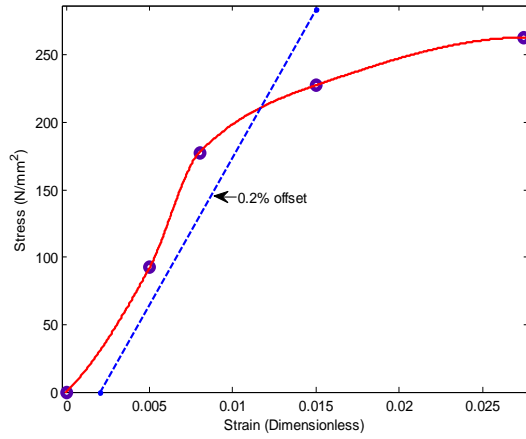
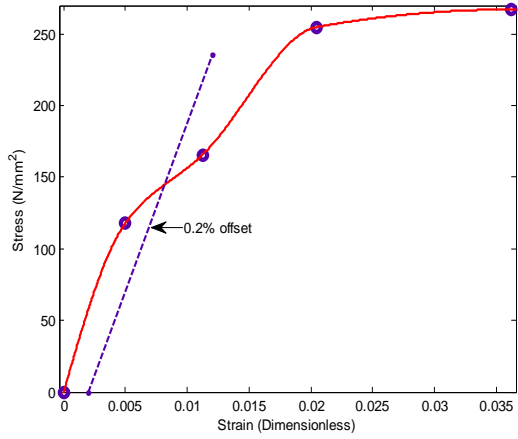


Fig. 7.23: Mercerization with 10wt% NaOH for 90mins Fig 7.24: Mercerization with 10wt% NaOH for 120mins

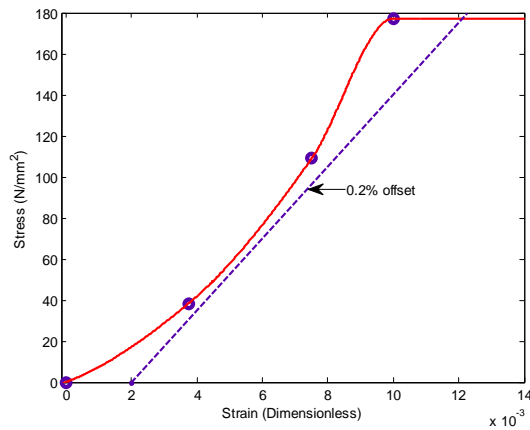


Fig 7.25: Mercerization with 10wt% NaOH for 150mins

A 7.2: TENSILE TEST RESULTS ANALYSIS FOREMPTY PALM BUNCH FIBER

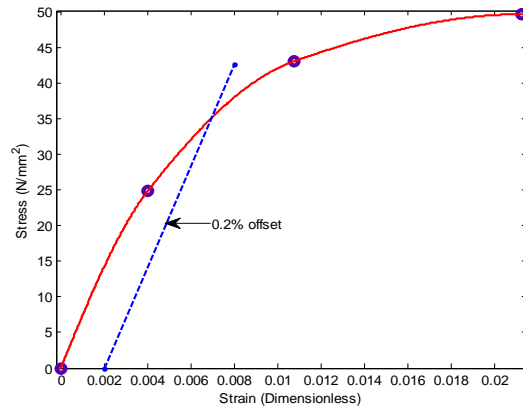
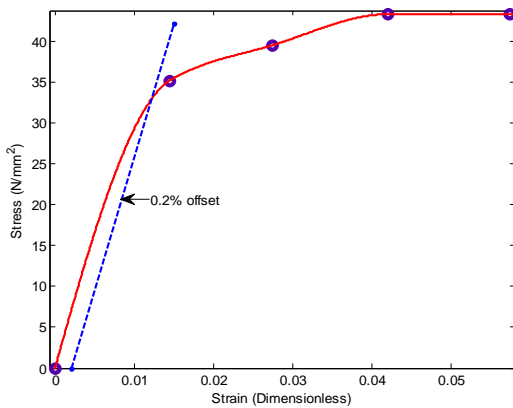


Fig. 7.26: Mercerization with 2wt% NaOH for 30mins Fig 7.27: Mercerization with 2wt% NaOH for 60mins

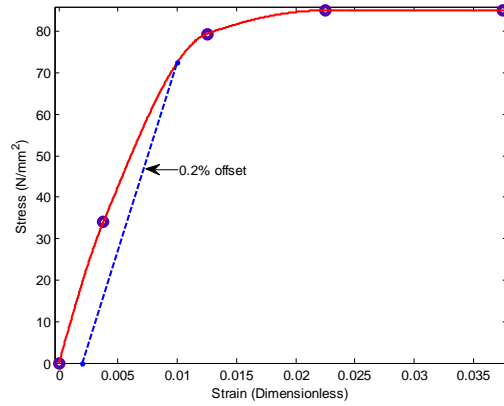
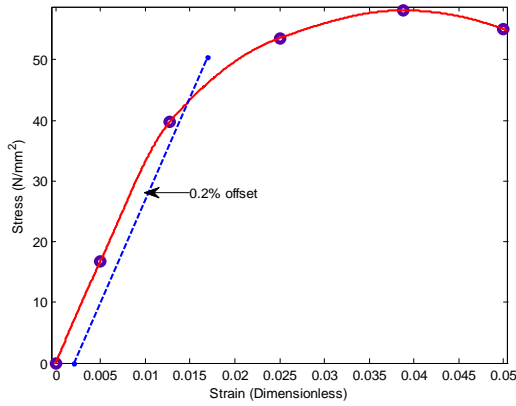


Fig. 7.28: Mercerization with 2wt% NaOH for 90mins Fig 7.29: Mercerization with 2wt% NaOH for 120mins

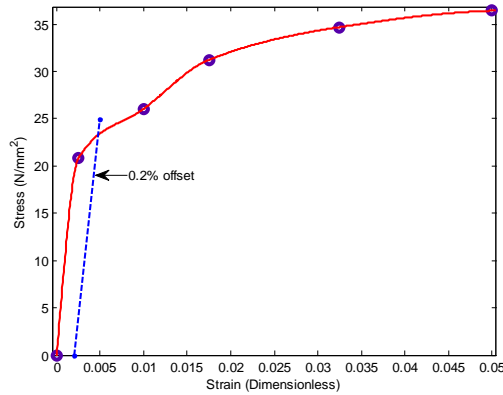


Fig 7.30: Mercerization with 2wt% NaOH for 150mins

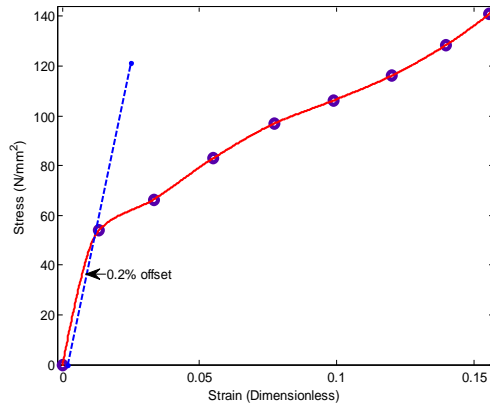
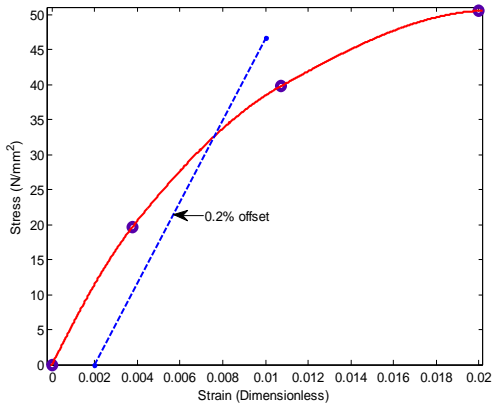


Fig. 7.31: Mercerization with 4wt% NaOH for 30mins Fig 7.32: Mercerization with 4wt% NaOH for 60mins

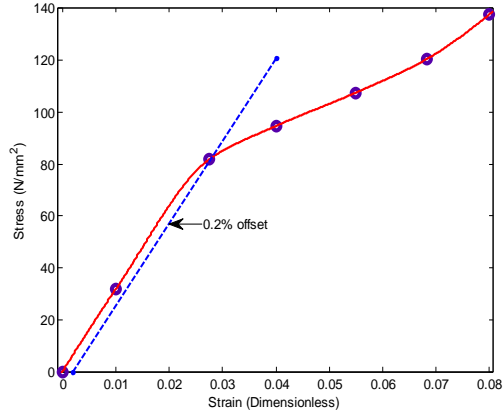
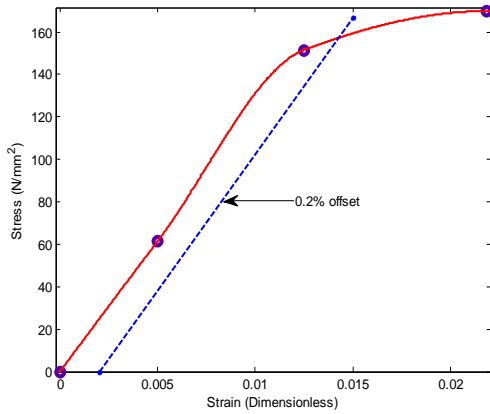


Fig. 7.33: Mercerization with 4wt% NaOH for 90mins Fig 7.34: Mercerization with 4wt% NaOH for 120mins

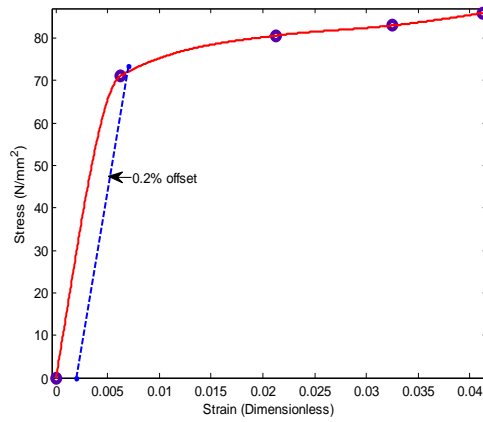


Fig 7.35: Mercerization with 4wt% NaOH for 150mins

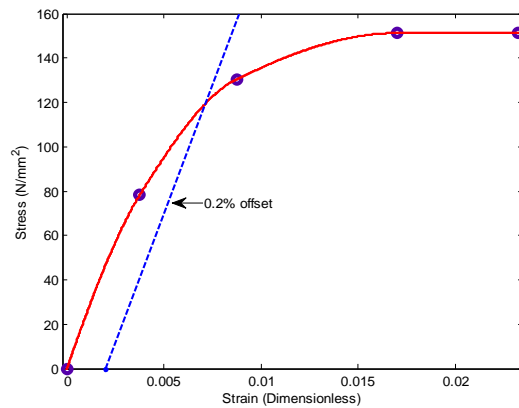
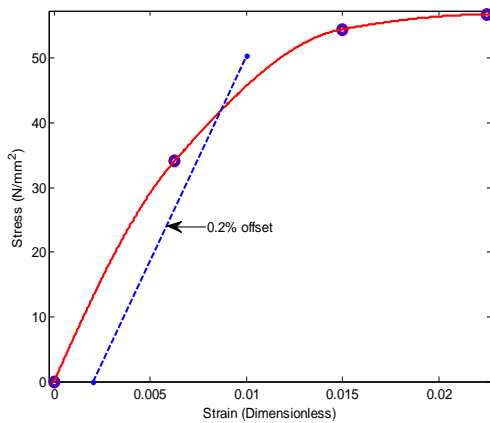


Fig. 7.36: Mercerization with 6wt% NaOH for 30mins Fig 7.37: Mercerization with 6wt% NaOH for 60mins

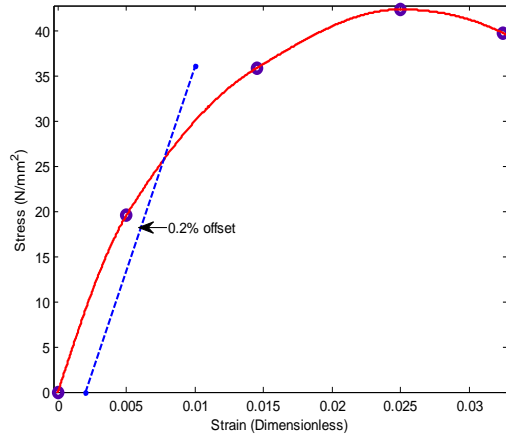
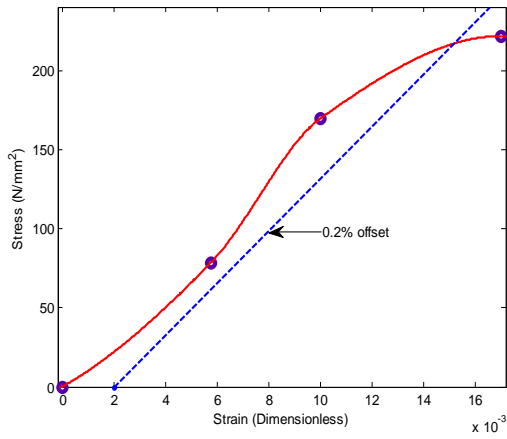


Fig. 7.38: Mercerization with 6wt% NaOH for 90mins Fig 7.39: Mercerization with 6wt% NaOH for 120mins

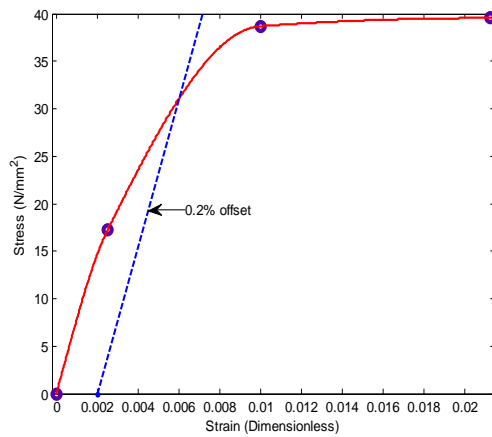


Fig 7.40: Mercerization with 6wt% NaOH for 150mins

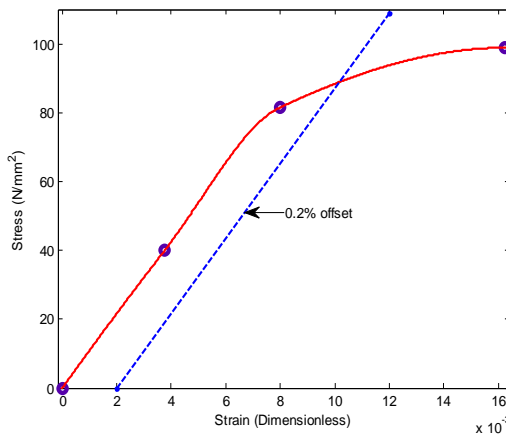
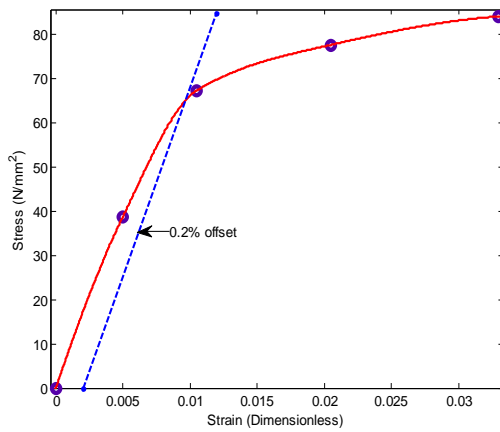


Fig. 7.41: Mercerization with 8wt% NaOH for 30mins Fig 7.42: Mercerization with 8wt% NaOH for 60mins

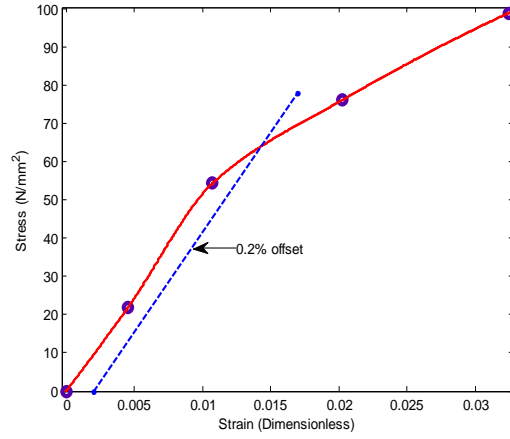
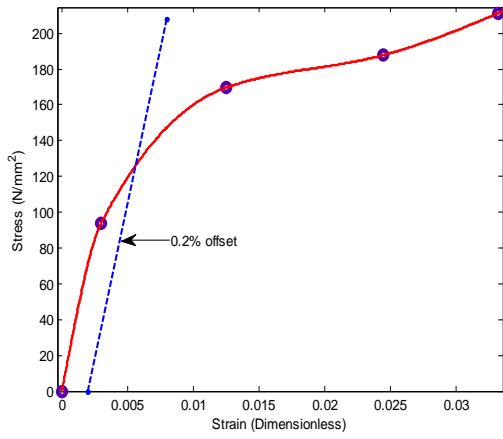


Fig. 7.43: Mercerization with 8wt% NaOH for 90mins Fig 7.44: Mercerization with 8wt% NaOH for 120mins

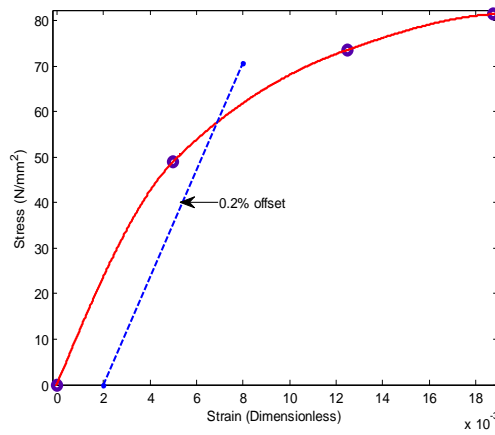


Fig 7.45: Mercerization with 8wt% NaOH for 150mins

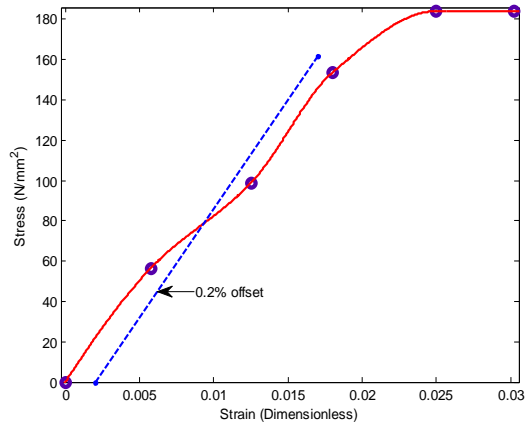
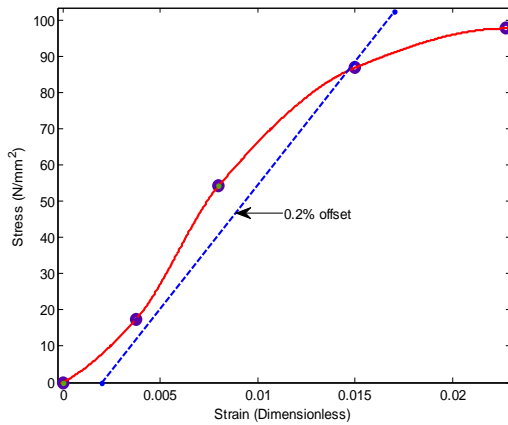


Fig. 7.46:Mercerization with 10wt% NaOH for 30mins Fig 7.47: Mercerization with 10wt% NaOH for 60mins

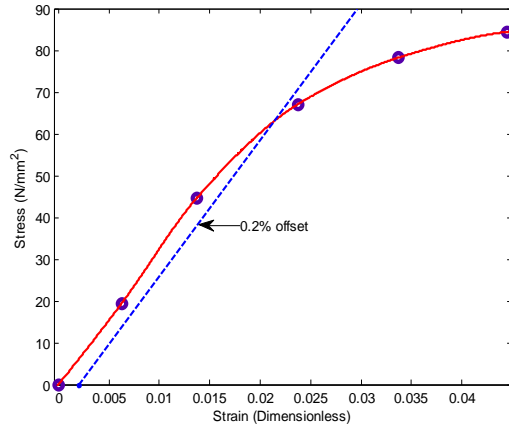
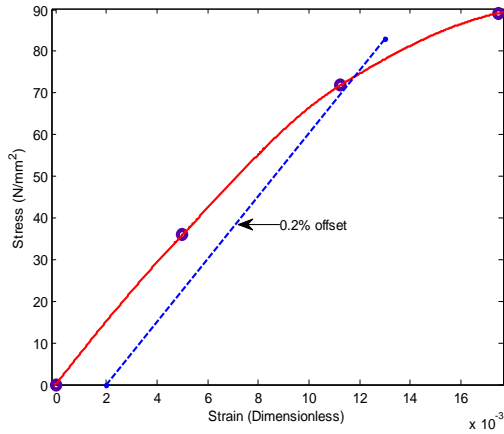


Fig. 7.48:Mercerization with 10wt% NaOH for 90mins Fig 7.49: Mercerization with 10wt% NaOH for 120mins

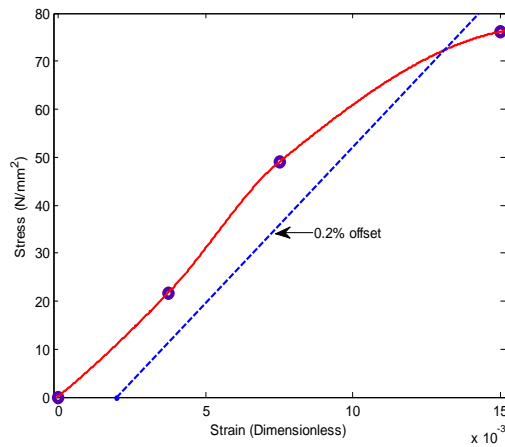


Fig 7.50: Mercerization with 10wt% NaOH for 150mins

A 7.3: TENSILE TEST RESULTS ANALYSIS FOR RATTAN PALM FIBER

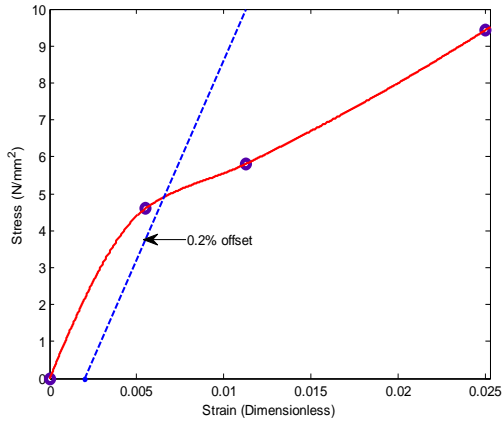


Fig. 7.51:Mercerization with 2wt% NaOH for 30mins

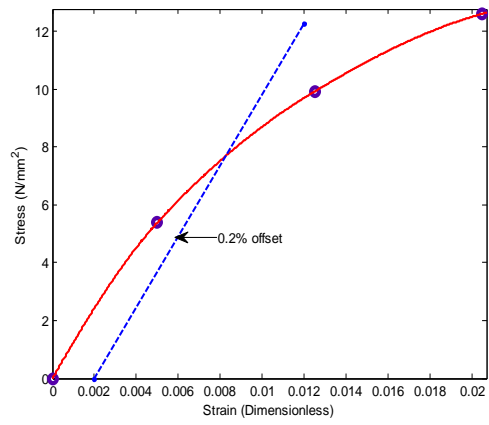


Fig 7.52: Mercerization with 2wt% NaOH for 60mins

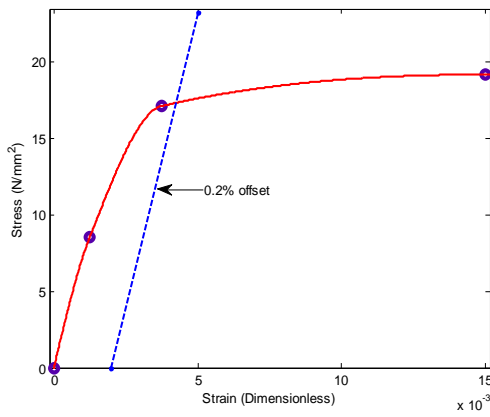


Fig. 7.53:Mercerization with 2wt% NaOH for 90mins

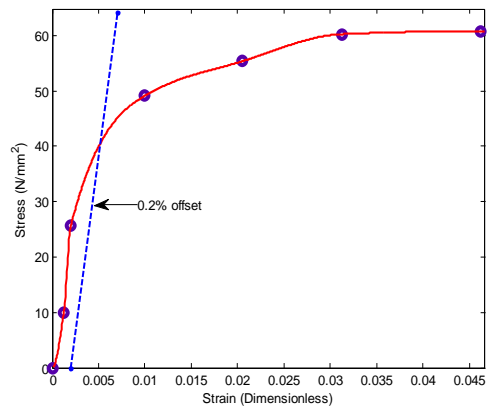


Fig 7.54: Mercerization with 2wt% NaOH for 120mins

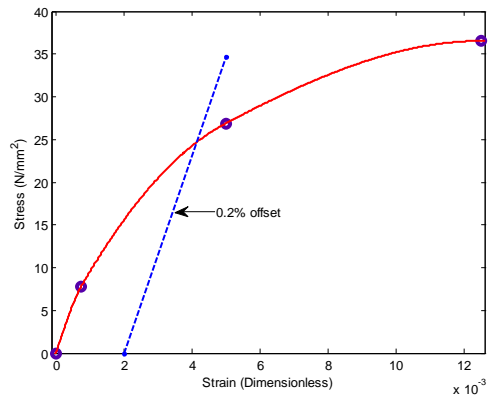


Fig. 7.55:Mercerization with 2wt% NaOH for 150mins

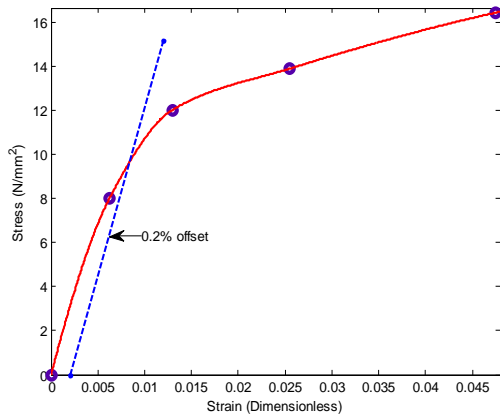


Fig. 7.56:Mercerization with 4wt% NaOH for 30mins

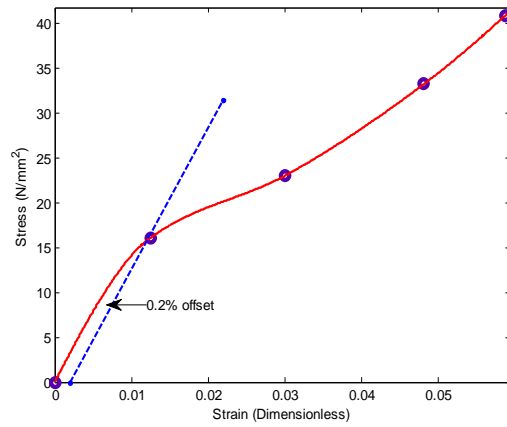


Fig 7.57: Mercerization with 4wt% NaOH for 60mins

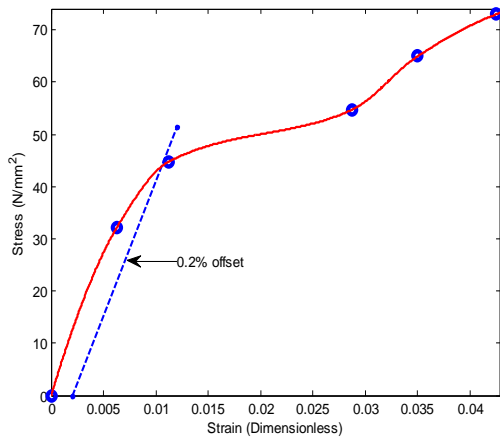


Fig. 7.58:Mercerization with 4wt% NaOH for 90mins

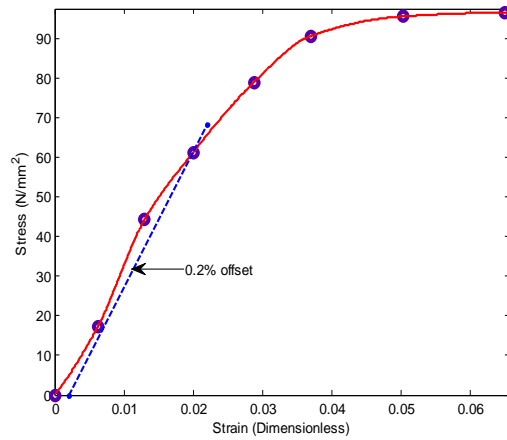


Fig 7.59: Mercerization with 4wt% NaOH for 120mins

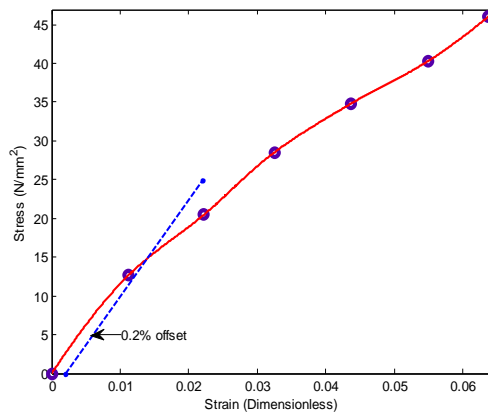


Fig 7.60: Mercerization with 4wt% NaOH for 150mins

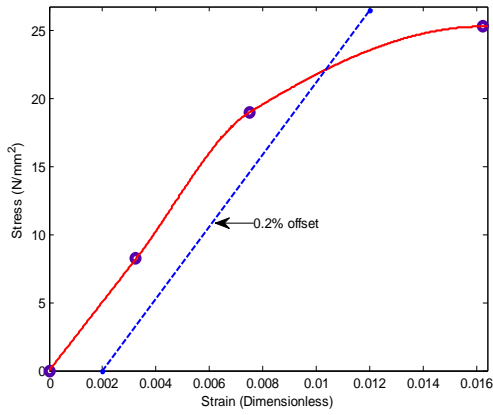


Fig. 7.61:Mercerization with 6wt% NaOH for 30mins

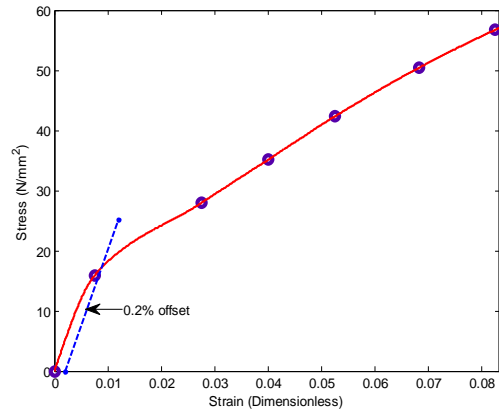


Fig. 7.62: Mercerization with 6wt% NaOH for 60mins

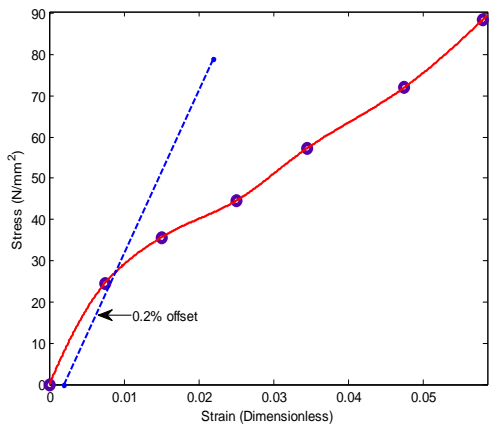


Fig. 7.63:Mercerization with 6wt% NaOH for 90mins

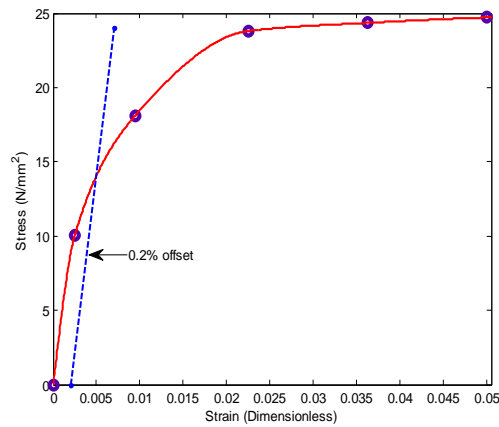


Fig 7.64: Mercerization with 6wt% NaOH for 120mins

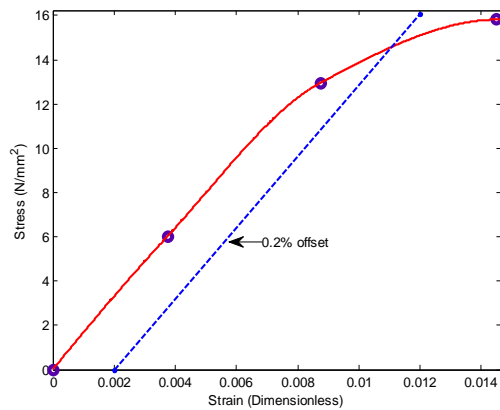


Fig 7.65: Mercerization with 6wt% NaOH for 150mins

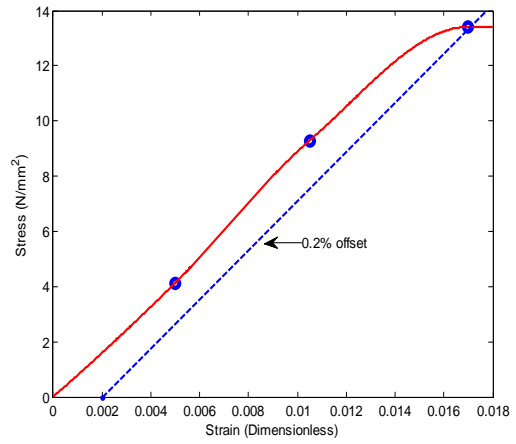
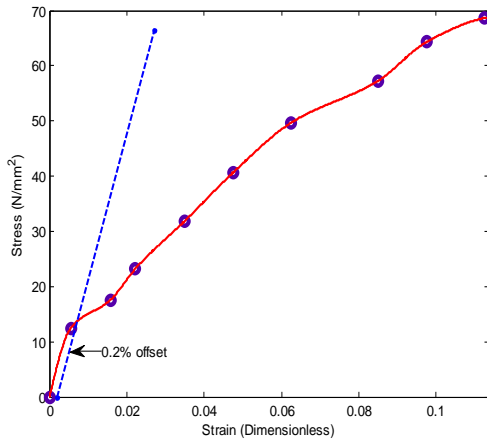


Fig. 7.66:Mercerization with 8wt% NaOH for 30mins Fig 7.67: Mercerization with 8wt% NaOH for 60mins

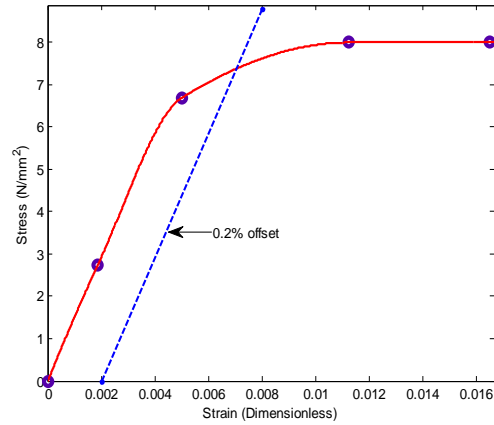
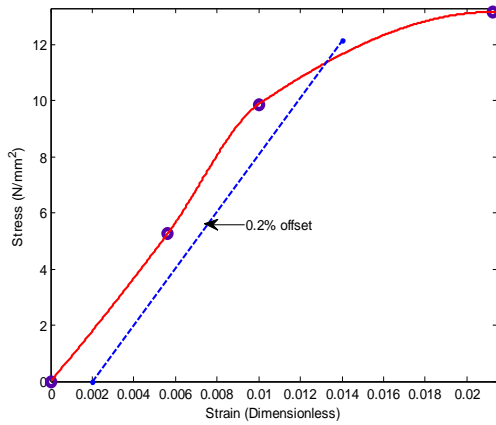


Fig. 7.68:Mercerization with 8wt% NaOH for 90mins Fig 7.69: Mercerization with 8wt% NaOH for 120mins

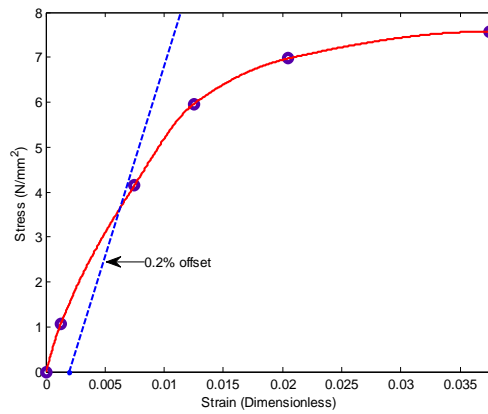


Fig 7.70: Mercerization with 8wt% NaOH for 150mins

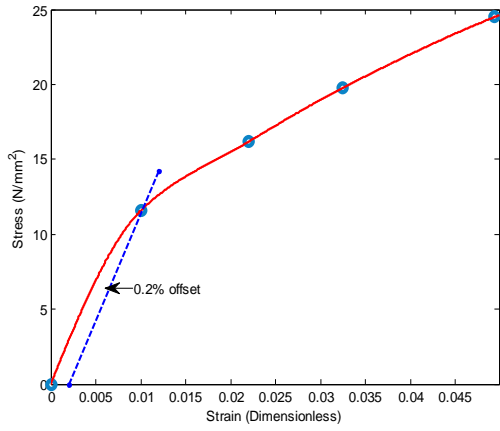


Fig. 7.71: Mercerization with 10wt% NaOH for 30mins

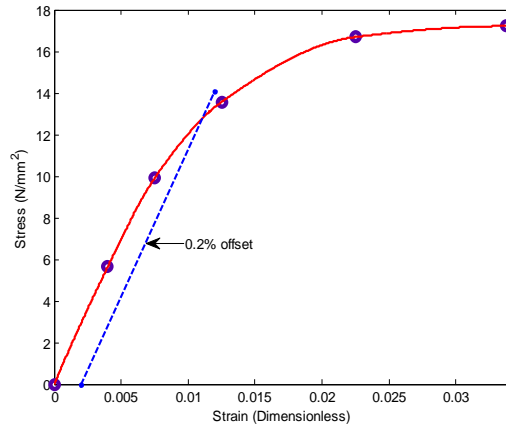


Fig. 7.72: Mercerization with 10wt% NaOH for 60mins

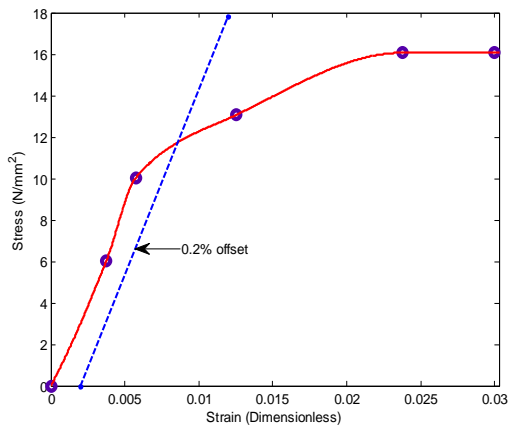


Fig. 7.73: Mercerization with 10wt% NaOH for 90mins

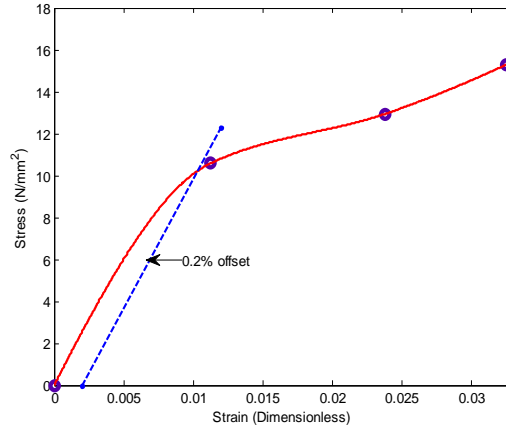


Fig. 7.74: Mercerization with 10wt% NaOH for 120mins

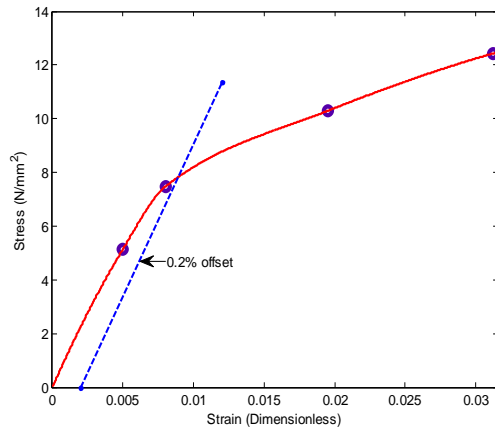


Fig. 7.75: Mercerization with 10wt% NaOH for 150mins

A 7.4 NEW APPROACH FOR TENSILE DATA ANALYSIS OF EMPTY PLANTAIN BUNCH FIBER

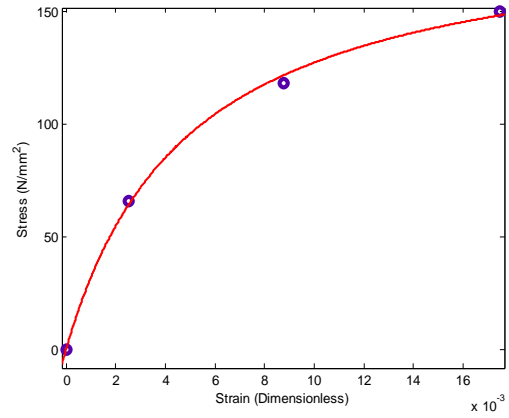
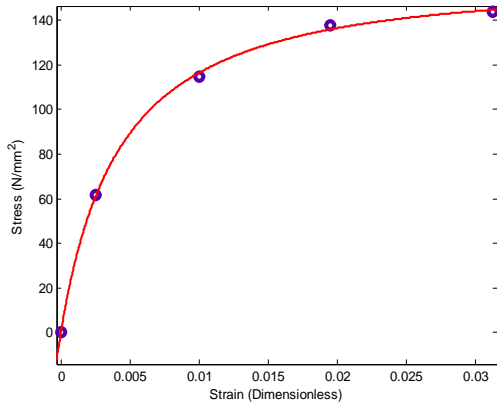


Fig. 7.76: Mercerization with 2wt% NaOH for 30mins Fig 7.77: Mercerization with 2wt% NaOH for 60mins

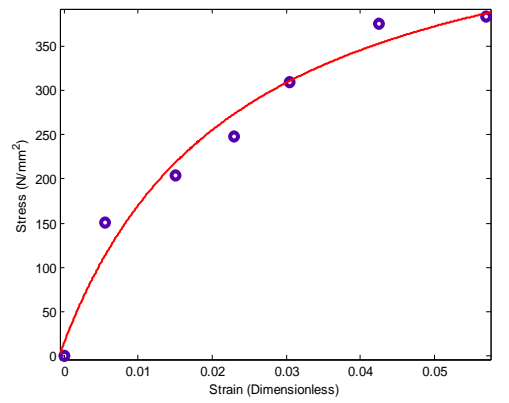
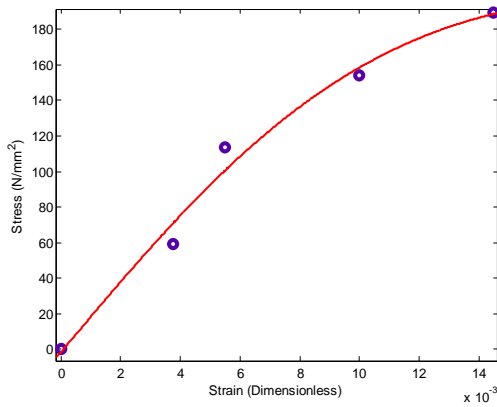


Fig. 7.78: Mercerization with 2wt% NaOH for 90mins Fig 7.79: Mercerization with 2wt% NaOH for 120mins

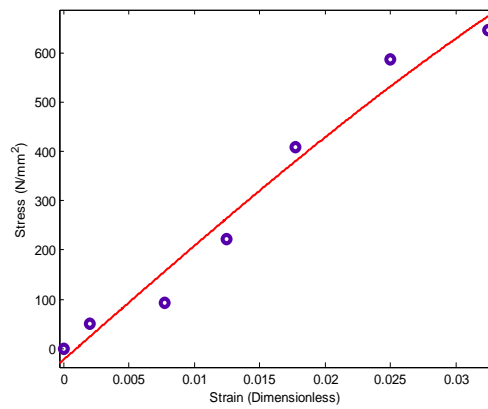


Fig 7.80: Mercerization with 2wt% NaOH for 150mins

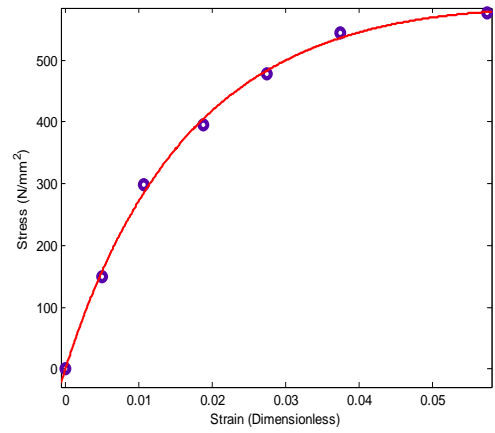
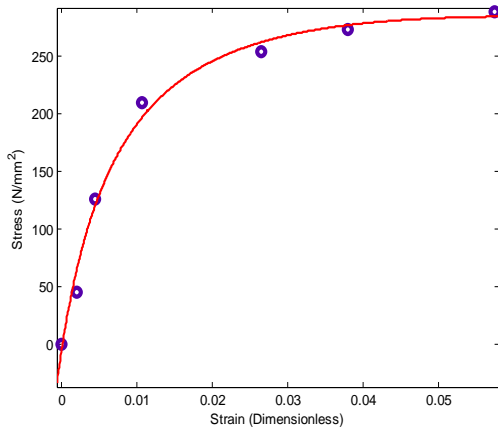


Fig. 7.81:Mercerization with 4wt% NaOH for 30mins Fig 7.82: Mercerization with 4wt% NaOH for 60mins

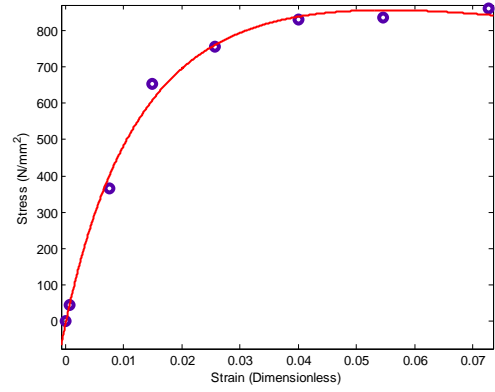
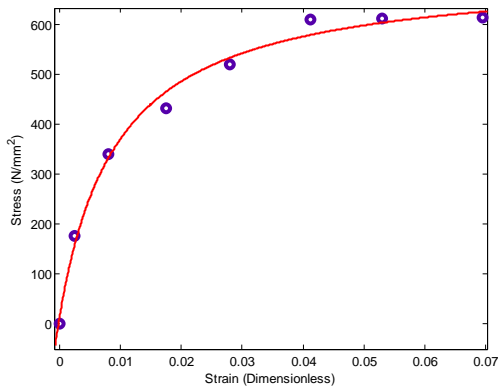


Fig. 7.83:Mercerization with 4wt% NaOH for 90mins Fig 7.84: Mercerization with 4wt% NaOH for 120mins

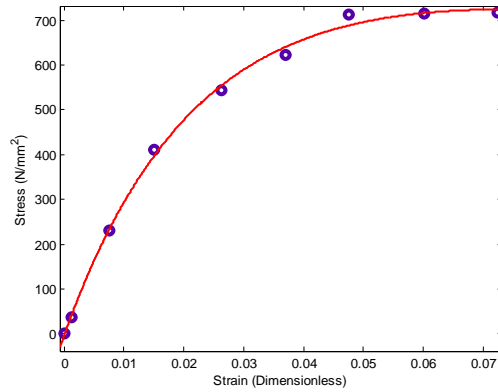


Fig 7.85: Mercerization with 4wt% NaOH for 150mins

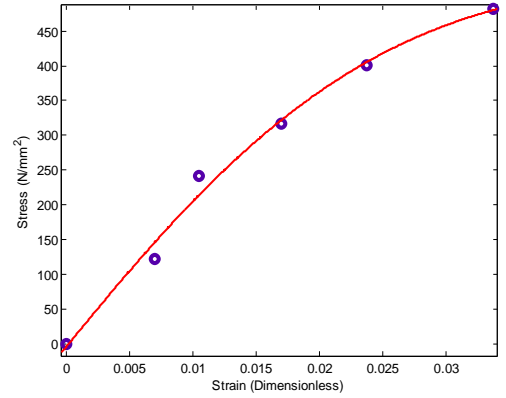
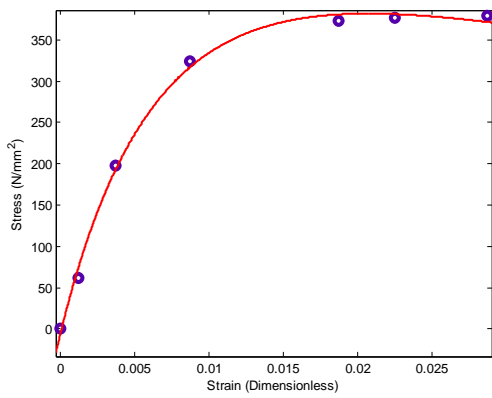


Fig. 7.86: Mercerization with 6wt% NaOH for 30mins Fig 7.87: Mercerization with 6wt% NaOH for 60mins

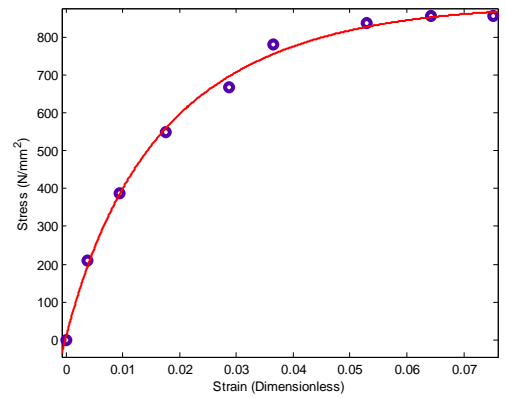
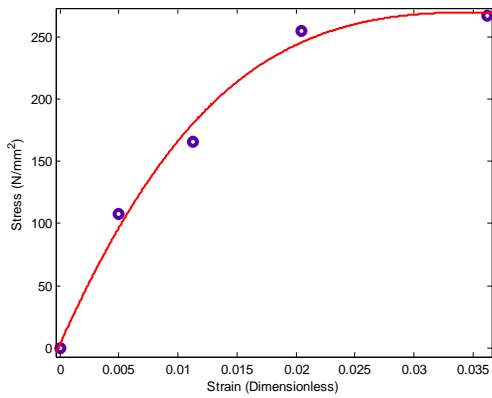


Fig. 7.88: Mercerization with 6wt% NaOH for 90mins Fig 7.89: Mercerization with 6wt% NaOH for 120mins

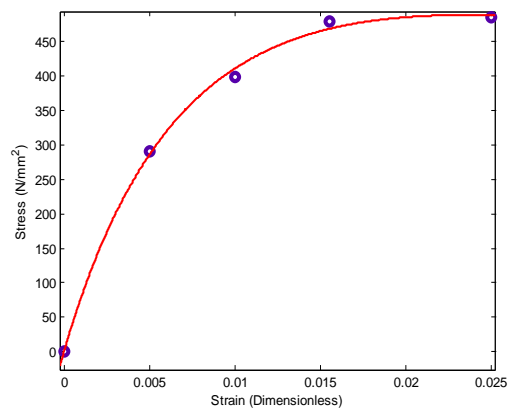


Fig. 7.90: Mercerization with 6wt% NaOH for 150mins

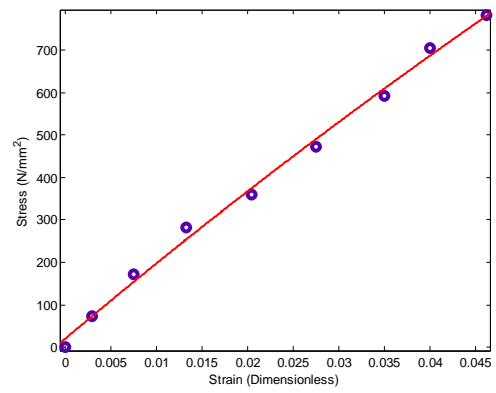
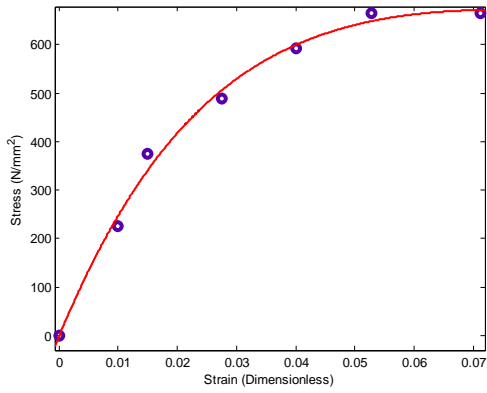


Fig. 7.91:Mercerization with 8wt% NaOH for 30mins Fig 7.92: Mercerization with 8wt% NaOH for 60mins

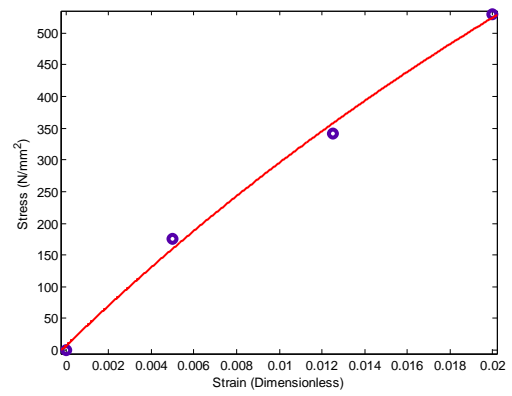
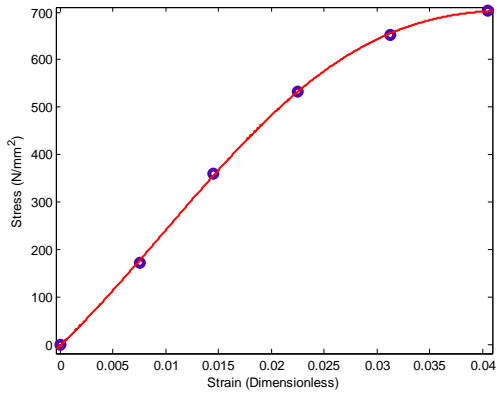


Fig. 7.93:Mercerization with 8wt% NaOH for 90mins Fig 7.94: Mercerization with 8wt% NaOH for 120mins

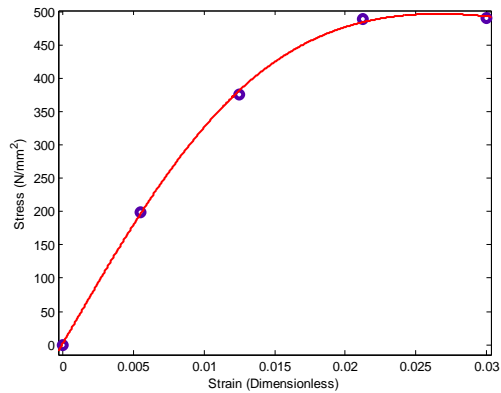


Fig. 7.95:Mercerization with 8wt% NaOH for 150mins

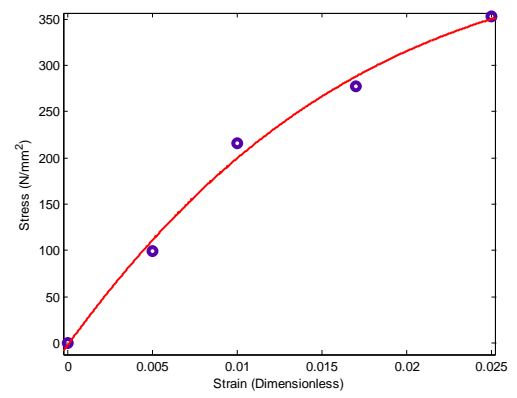
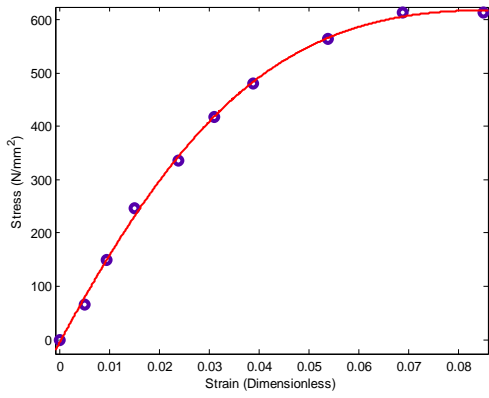


Fig. 7.96: Mercerization with 10wt% NaOH for 30mins Fig 7.97: Mercerization with 10wt% NaOH for 60mins

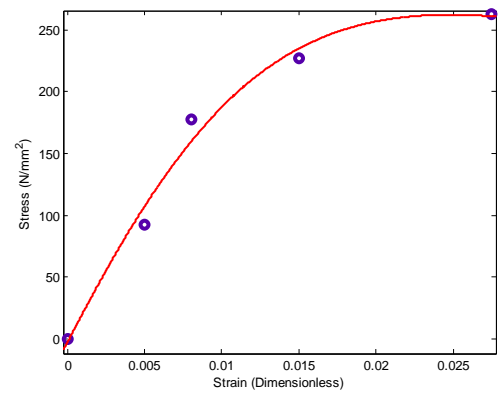
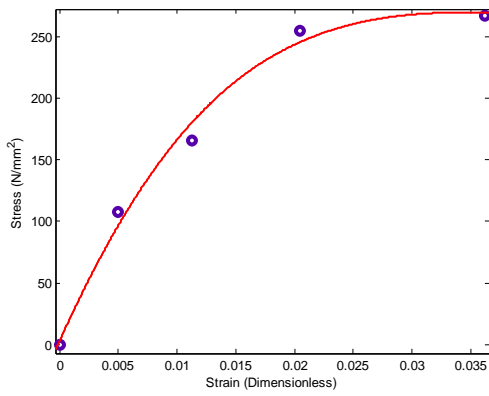


Fig. 7.98: Mercerization with 10wt% NaOH for 90mins Fig 7.99: Mercerization with 10wt% NaOH for 120mins

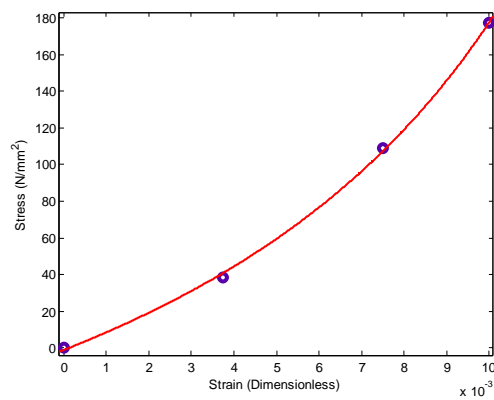


Fig. 7.100: Mercerization with 10wt% NaOH for 150mins

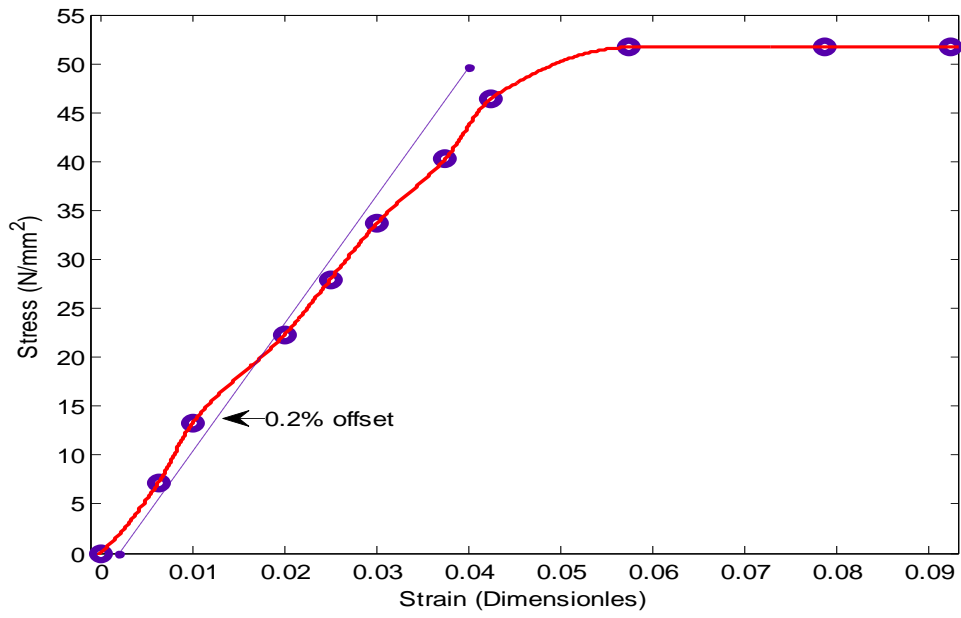


Fig. 7.101: Stress versus Strain Plot for Untreated Empty Plantain bunch Fiber

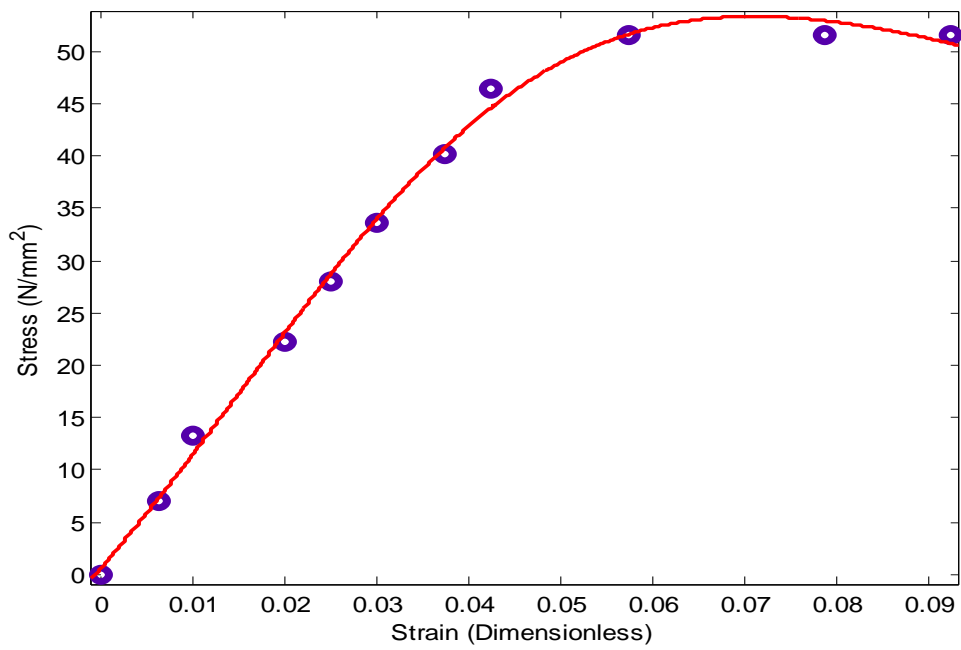


Fig. 7.102: Stress versus Strain Plot for Untreated Empty Plantain bunch Fiber (New Approach)

A 7.5 ANALYSIS FOR SILANE TREATED EMPTY PLANTAIN BUNCH FIBRE

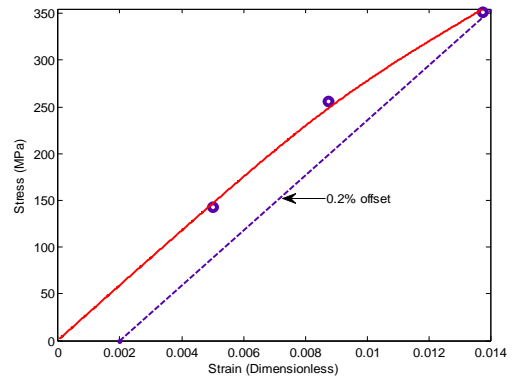
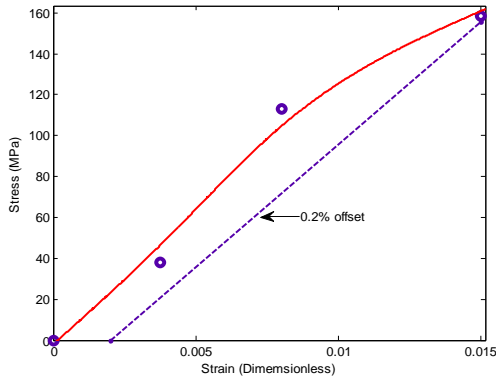


Fig. 7.103: Treatment with 0.25wt% Silane for 20mins Fig. 7.104: Treatment with 0.25wt% Silane for 60mins

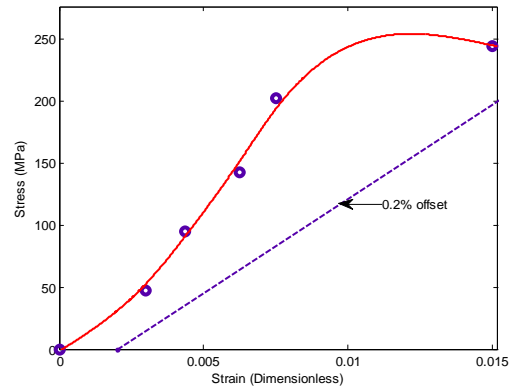
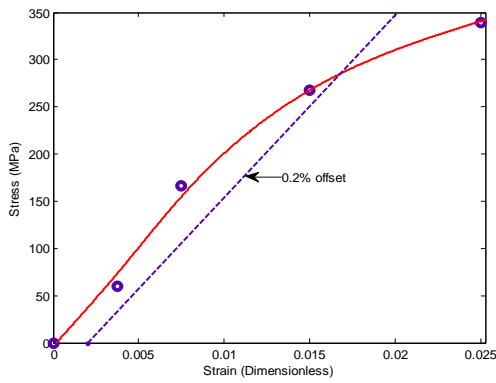


Fig. 7.105: Treatment with 0.25wt% Silane for 100mins Fig. 7.106: Treatment with 0.75wt% Silane for 20mins

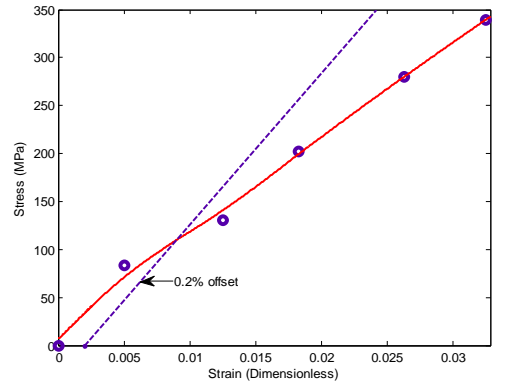
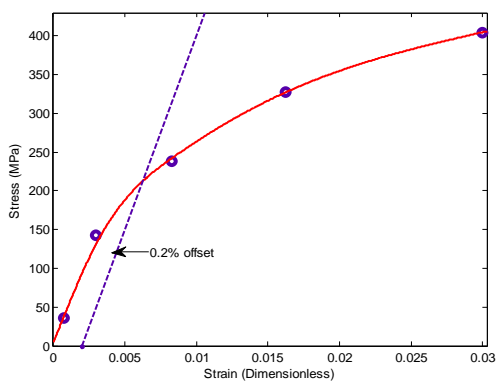


Fig. 7.107: Treatment with 0.75wt% Silane for 60mins Fig. 7.108: Treatment with 0.75wt% Silane for 100mins

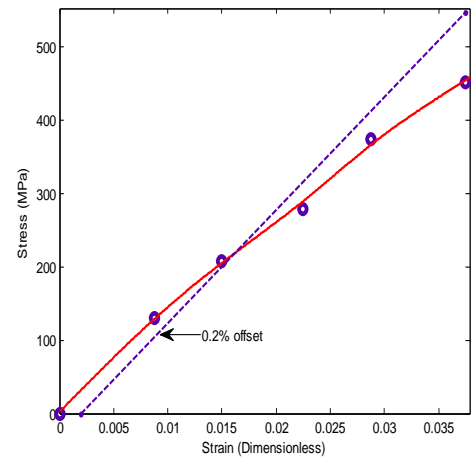
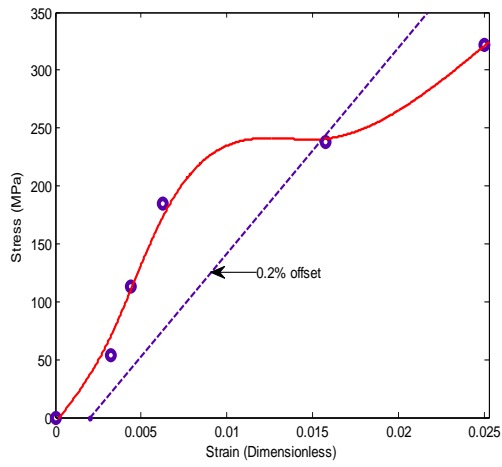


Fig. 7.109: Treatment with 1.25wt% Silane for 20mins Fig. 7.110: Treatment with 1.25wt% Silane for 60mins

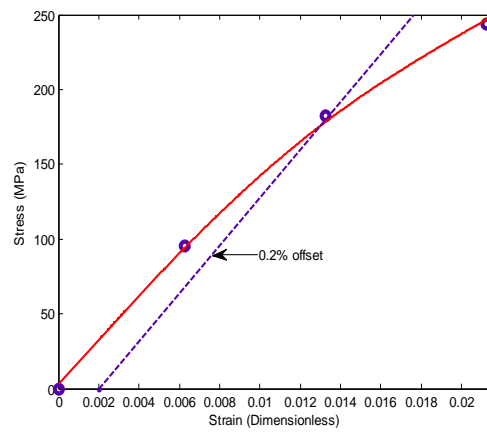


Fig. 7.111: Treatment with 1.25wt% Silane for 100mins

A 7.6 RESULTS FOR WATER ABSORPTION CAPACITY OF FIBERS

Table 7.1: Percentage Moisture Absorption for Untreated Empty Plantain Bunch Fiber

T(^o C) Time (mins)	30	40	50	60	70
5	192	247	167	198	229
10	263	339	229	296	319
15	348	471	307	407	419
20	388	538	344	481	469
25	422	657	387	558	502

Table 7.2: Percentage Moisture Absorption for Untreated Empty Palm Bunch Fiber

T(^o C) Time (mins)	30	40	50	60	70
5	112	95	100	101	103
10	176	160	140	127	148
15	249	231	183	175	199
20	302	290	205	191	228
25	362	354	218	241	256

Table 7.3: Percentage Moisture Absorption for Untreated Rattan Palm Fiber

T(^o C) Time (mins)	30	40	50	60	70
5	21	39	59	56	64
10	42	75	89	89	100
15	63	108	91	99	109
20	83	129	102	119	125
25	101	137	122	149	148

Table 7.4: Percentage Moisture Absorption for Treated Empty Plantain Bunch Fiber

T(^o C) Time (mins)	30	40	50	60	70
10	19	97	97	107	74
20	85	134	111	134	114
30	123	173	148	173	149
40	187	192	170	182	175
50	193	197	183	197	179

Table 7.5: Percentage Moisture Absorption for Treated Empty Palm Bunch Fiber

T(^o C) Time (mins)	30	40	50	60	70
10	6	62	64	53	47
20	43	87	85	70	65
30	66	114	113	91	94
40	104	128	124	99	110
50	112	137	138	102	145

Table 7.6: Percentage Moisture Absorption for Treated Rattan Palm Fiber

T(^o C) Time (mins)	30	40	50	60	70
10	5	27	12	36	19
20	18	43	36	50	41
30	35	58	53	66	62
40	54	69	76	73	85
50	85	73	85	79	108

A 7.7 NUMERICAL FIT FOR NEW APPROACH FOR TENSILE TEST DATA ANALYSIS

Table 7.7: Linear-Quadratic Model fit results for Plantain Fiber treated with 2wt% NaOH

Time (mins)	p1	p2	q1	q2	R ²	Adj.R ²	RMSE	SSE
30	205.3	0.0008142	1.215	0.005388	0.9995	0.9981	2.645	6.998
60	9.425e5	12.6	4964	24.58	0.9987	-	-	16.81
90	7.995	-0.000667	1.187e-6	0.0004006	0.9855	0.9711	12.82	328.6
120	1.202e7	8098	2.207e4	532.8	0.9727	0.9455	31.71	3017
150	283.9	-0.2837	1.352e-9	0.01219	0.9718	0.9578	53.97	1.165e4

Table 7.8: Linear-Quadratic Model fit results for Plantain Fiber treated with 4wt% NaOH

Time (mins)	p1	p2	q1	q2	R ²	Adj. R ²	RMSE	SSE
30	159.4	-0.02818	0.437	0.00376	0.9919	0.9838	14.67	645.7
60	178.2	-0.006159	0.1676	0.00476	0.9986	0.9972	11.24	378.7
90	1.189e7	1678	1.677e4	158.1	0.9917	0.9854	27.5	3024
120	230.2	-0.02353	0.1585	0.003027	0.9957	0.9925	31.1	3869
150	205.3	-0.01965	0.1351	0.005465	0.9980	0.9968	16.48	1358

Table 7.9: Linear-Quadratic Model fit results for Plantain Fiber treated with 6wt% NaOH

Time (mins)	p1	p2	q1	q2	R ²	Adj. R ²	RMSE	SSE
30	31.13	-0.003048	0.03998	0.0004236	0.9971	0.9943	12.08	437.9
60	54.65	-0.009447	0.006924	0.002451	0.9912	0.9781	26.4	1394
90	25.03	0.003746	0.02435	0.001183	0.9911	0.9645	20.82	433.3
120	557.1	0.08777	0.4419	0.00961	0.9973	0.9956	20.6	2123
150	47.61	0.000354	0.0503	0.0005568	0.9979	0.9915	18.49	341.7

Table 7.10: Linear-Quadratic Model fit results for Plantain Fiber treated with 8wt% NaOH

Time (mins)	p1	p2	q1	q2	R ²	Adj.R ²	RMSE	SSE
30	163.1	-0.009897	0.09429	0.005502	0.9937	0.9875	27.81	2320
60	5.116e7	5.383e4	6184	2814	0.9956	0.9929	23.3	2714
90	39.27	-0.003314	-0.02925	0.001805	0.9999	0.9997	5.186	53.78
120	2.591e7	5142	1.027e4	792.8	0.9962	-	-	584.1
150	26.21	0.0007511	-0.0005839	0.0007113	0.9996	0.9986	8.032	64.51

Table 7.11: Linear-Quadratic Model fit results for Plantain Fiber treated with 10wt% NaOH

Time (mins)	p1	p2	q1	q2	R ²	Adj. R ²	RMSE	SSE
30	124	-0.038	0.0303	0.007195	0.9988	0.9982	9.617	554.9
60	57.76	-0.006045	0.04762	0.002291	0.9931	0.9724	23.37	546.1
90	25.03	0.003747	0.02434	0.001183	0.9911	0.9645	20.82	433.3
120	14.66	-0.001575	0.00615	0.0006125	0.9863	0.9452	24.91	620.6
150	3.477e6	-435.8	-1.844e4	377.7	0.9994	-	-	11.14

Table 7.12: Linear-Quadratic Model fit results for Untreated Plantain Fiber

p1	p2	q1	q2	R ²	Adj. R ²	RMSE	SSE
5.167	0.002886	-0.04538	0.00511	0.9969	0.9956	1.255	11.02

A 7.8 TENSILE TEST DATA FOR EMPTY PLANTAIN BUNCH-EPOXY

Table 7.13: 10mm Fiber and 10% Vol. frac.

Load (N)	Extension (mm)	Stress (MPa)	Strain (Dimensionless)
0	0	0	0
275	0.650	4.5211	0.0041
357.5	2.250	5.8826	0.0141
374.15	4.125	6.1541	0.0258
374.15	6.000	6.1541	0.0375

Table 7.14: 10mm Fiber and 30% Vol. frac.

Load (N)	Extension (mm)	Stress (MPa)	Strain (Dimensionless)
0	0	0	0
262.5	0.300	4.3168	0.0019
350	0.625	5.7565	0.0039
403.85	1.650	6.6421	0.0103
410.55	3.625	6.7528	0.0227
417.30	5.800	6.8637	0.0362
437.5	7.550	7.1957	0.0472

fract. Table 7.15: 10mm Fiber and 50% Vol. frac.

Load (N)	Extension (mm)	Stress (MPa)	Strain (Dimensionless)
0	0	0	0
282.5	0.4375	4.6467	0.0027
365.60	2.250	6.0136	0.0141
406.25	4.050	6.6817	0.0253
406.25	4.750	6.6817	0.0297

Table 7.16: 30mm Fiber and 10% Vol.

Load (N)	Extension (mm)	Stress (MPa)	Strain (Dimensionless)
0	0	0	0
250	0.500	4.1118	0.0031
343.75	1.625	5.6538	0.0102
375	2.850	6.1678	0.0178
425	4.950	6.9901	0.0309
437.5	6.950	7.1957	0.0434
456.25	8.250	7.5041	0.0516

Table 7.17: 30mm Fiber and 30% Vol. frac.

Load (N)	Extension (mm)	Stress (MPa)	Strain (Dimensionless)
0	0	0	0
375	0.4375	6.1678	0.0027
456.25	1.3125	7.5041	0.0082
500	3.125	8.2237	0.0195
512.5	4.3750	8.4293	0.0273

Table 7.18: 30mm Fiber and 50% Vol. frac.

Load (N)	Extension (mm)	Stress (MPa)	Strain (Dimensionless)
0	0	0	0
333.75	0.500	5.4901	0.0031
360.5	1.400	5.9324	0.0087
385.5	2.800	6.3415	0.0175
435.5	5.150	7.1597	0.0322
435.5	6.750	7.1597	0.0422

Table 7.19: 50mm Fiber and 10% Vol. frac.

Table 7.20: 50mm Fiber and 30% Vol. frac.

Load (N)	Extension (mm)	Stress (MPa)	Strain (Dimensionless)
0	0	0	0
268	0.4375	4.4064	0.0027
378.5	1.3125	6.2232	0.0082
414.5	3.125	6.8196	0.0195
425	4.3750	6.9901	0.0273

Load (N)	Extension (mm)	Stress (MPa)	Strain (Dimensionless)
0	0	0	0
281.25	0.125	2.0163	0.00078
337.5	1.925	5.5510	0.0120
416.25	3.250	6.8462	0.0203
412.5	4.750	8.0344	0.0297
412.5	6.000	8.0344	0.0375
406.25	7.125	7.9127	0.0445

Table 7.21: 50mm Fiber and 50% Vol. frac.

Load (N)	Extension (mm)	Stress (MPa)	Strain (Dimensionless)
0	0	0	0
300	0.200	2.0538	0.00125
375	1.975	6.9623	0.0123
381.25	3.875	7.0783	0.0242
393.75	6.225	7.3104	0.0389
393.75	7.250	7.3104	0.0453

Table 7.22: Linear-Quadratic Model Numerical fit results for Plantain Fiber-Epoxy Composite

Fl (mm)	Vf (%)	p1	p2	q1	q2	R ²	Adj. R ²	RMSE	SSE
10	10	3.609	1.238e-7	0.5180	1.133e-3	1.000	1.000	0.01834	0.00034
10	30	17.66	-3.143e-5	2.401	2.959e-3	0.9966	0.9931	0.2116	0.1343
10	50	5.089e5	0.3448	7.398e4	98.95	0.9966	0.9865	0.3264	0.1065
30	10	2.385e5	4.405	3.118e4	96.38	0.9920	0.9840	0.3329	0.3324
30	30	7118	0.002622	818.1	0.9343	0.9995	0.9978	0.1632	0.02664
30	50	3.325e4	0.04676	4683	5.054	0.9875	0.9687	0.4782	0.4573
50	10	3.944	-1.147e-6	0.5007	0.001051	0.9999	0.9995	0.06711	0.0045
50	30	1.228e5	51.39	1.302e4	100.4	0.9817	0.9634	0.6197	1.152
50	50	3.784e4	-1.58	4733	13.76	0.9922	0.9805	0.4522	0.409

*Fl (Fiber length), Vf (Fiber Volume fraction)

GRAPHICAL FIT RESULTS FOR TRADITIONAL AND NEW APPROACH

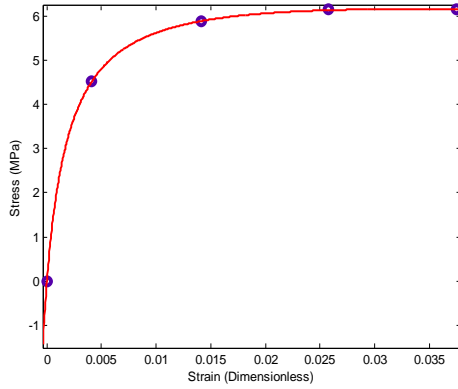


Fig. 7.112: New Approach(10mm and 10%)

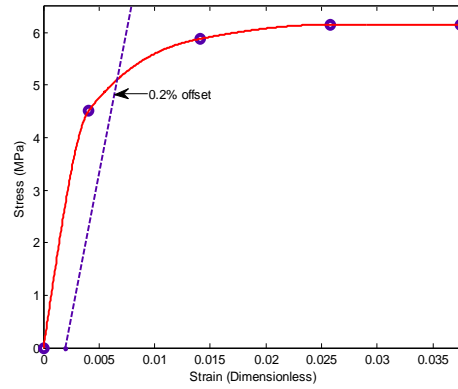


Fig. 7.113: Traditional approach (10mm and 10%)

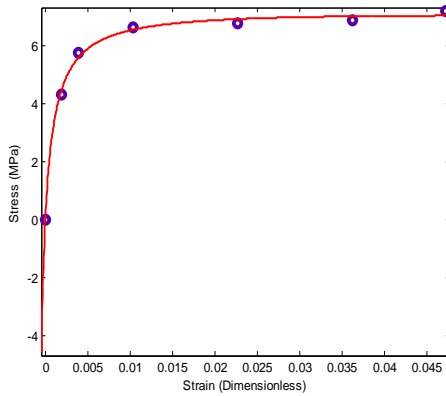


Fig. 7.114: New Approach (10mm and 30%)

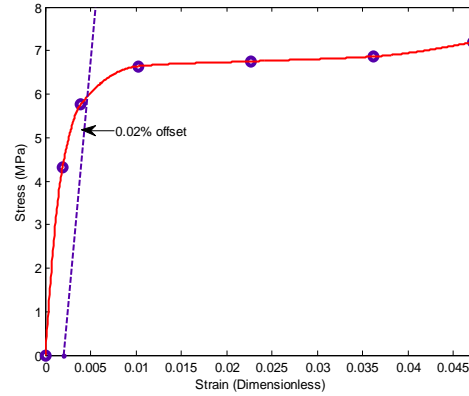


Fig. 7.115: Traditional approach (10mm and 30%)

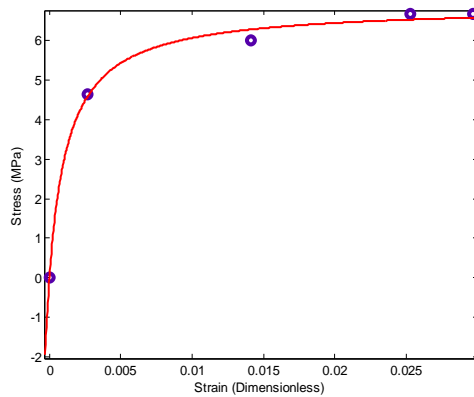


Fig. 7.116: New Approach (10mm and 50%)

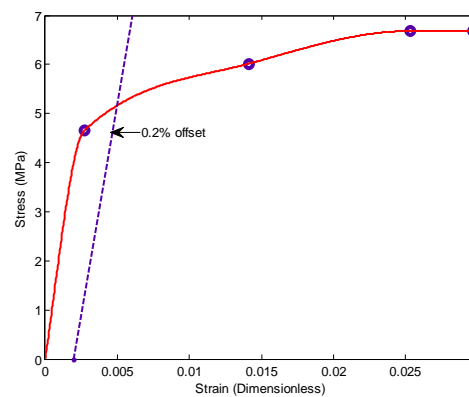


Fig. 7.117: Traditional approach (10mm and 50%)

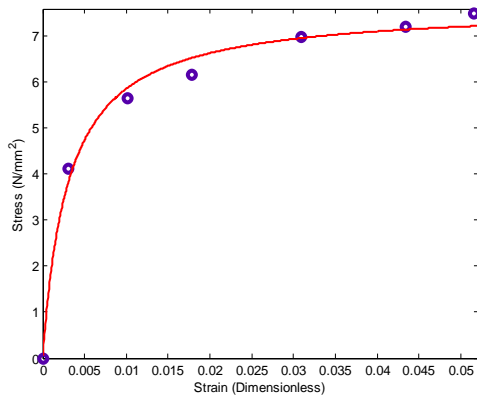


Fig. 7.118: New Approach (30mm and 10%)

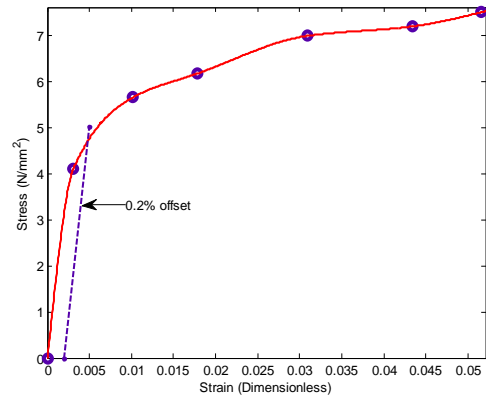


Fig. 7.119: Traditional approach (30mm and 10%)

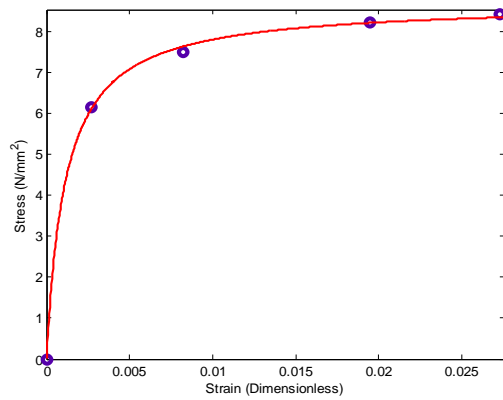


Fig. 7.201: New Approach (30mm and 30%)

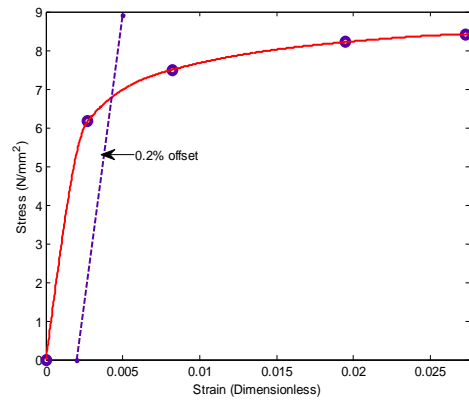


Fig. 7.121: Traditional approach (30mm and 30%)

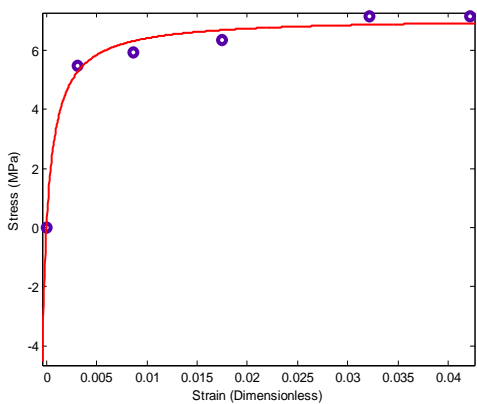


Fig. 7.122: New Approach (30mm and 50%)

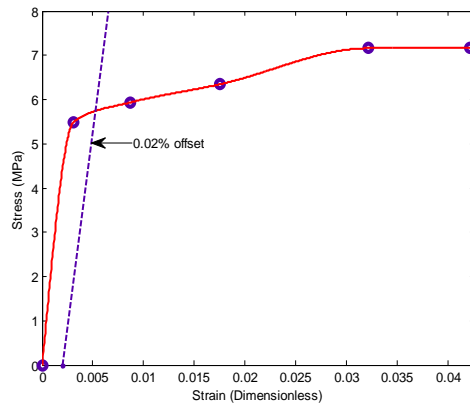


Fig. 7.123: Traditional approach (30mm and 50%)

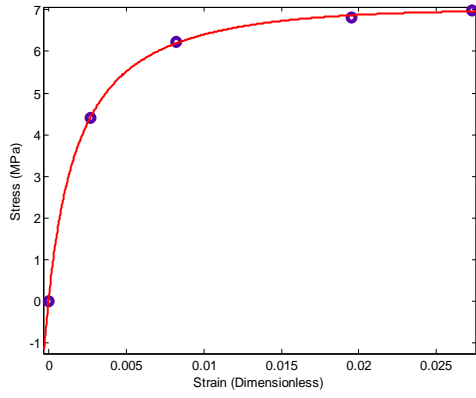


Fig. 7.124: New Approach (50mm and 10%)

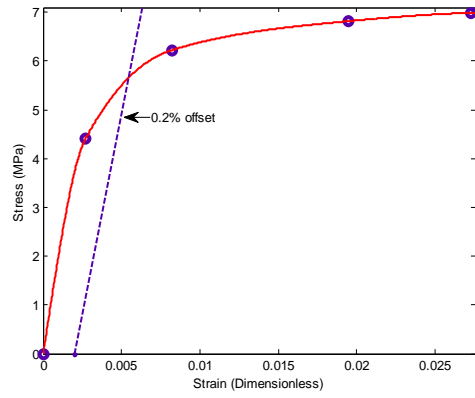


Fig. 7.125: Traditional approach (50mm and 10%)

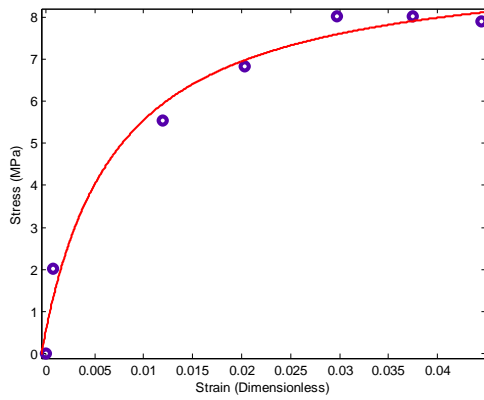


Fig. 7.126: New Approach (50mm and 30%)

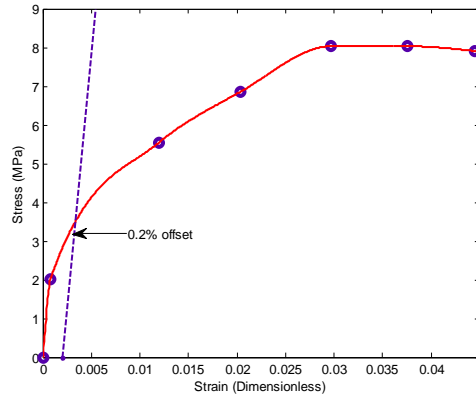


Fig. 7.127: Traditional approach (50mm and 30%)

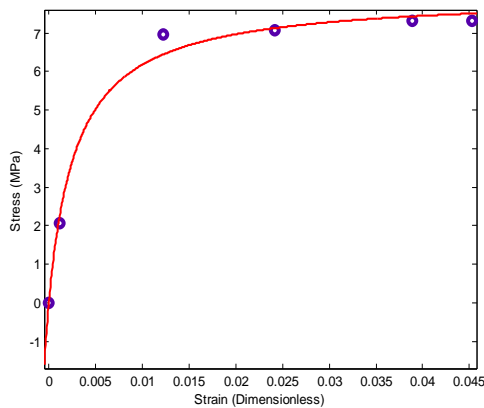


Fig. 7.128: New Approach (50mm and 50%)

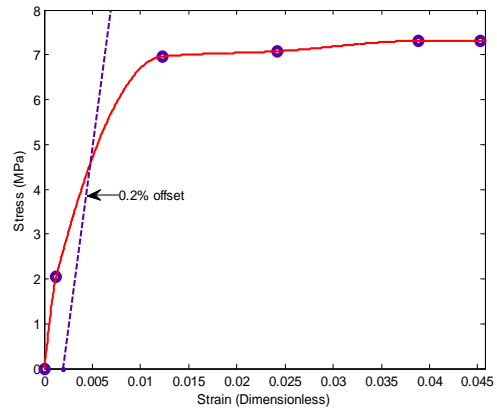


Fig. 7.129: Traditional approach (50mm and 50%)

A 7.9 TENSILE TEST DATA FOR EMPTY PLANTAIN BUNCH-POLYESTER COMPOSITE

Table 7.23: 10mm Fiber and 10% Vol. frac.

Load (N)	Extension (mm)	Stress (MPa)	Strain (Dimensionless)
0	0	0	0
340.1	0.200	5.5930	0.00125
851.5	0.500	14.0049	0.00313
1416.1	1.075	23.2913	0.00672
1480.5	2.000	24.3509	0.01250
1519.2	2.975	24.9876	0.01859

Table 7.24: 10mm Fiber and 50% Vol frac.

Load (N)	Extension (mm)	Stress (MPa)	Strain (Dimensionless)
0	0	0	0
354.6	0.25	5.8319	0.001563
1240.9	0.875	20.4097	0.00547
1525.3	1.50	25.0870	0.009375
1594.7	2.50	26.2285	0.01563
1636.5	3.30	26.9155	0.02063

Table 7.25: 10mm Fiber and 30% Vol. frac.

Load (N)	Extension (mm)	Stress (MPa)	Strain (Dimensionless)
0	0	0	0
354.8	0.125	5.837	0.00078
594.6	0.625	9.780	0.00391
891.9	1.450	14.670	0.00906
1167.8	2.550	19.208	0.01594
1460.1	3.500	24.014	0.02188
1778.2	4.000	29.247	0.0250

Table 7.26: 30mm Fiber and 10% Vol frac

Load (N)	Extension (mm)	Stress (MPa)	Strain (Dimensionless)
0	0	0	0
315.2	0.125	5.1834	0.00078
692.3	0.250	11.3872	0.00156
1349.6	1.125	22.1976	0.00703
1912.0	2.125	31.4467	0.01328

Table 7.27: 30mm Fiber and 30% Vol. frac.

Load (N)	Extension (mm)	Stress (MPa)	Strain (Dimensionless)
0	0	0	0
532.3	0.300	8.7544	0.001875
1330.9	0.750	21.889	0.004688
1923.6	1.950	31.6389	0.012188
2076.7	3.050	34.1561	0.019060
2120.3	4.000	34.8739	0.025000

Table 7.28: 30mm Fiber and 50% Vol. frac.

Load (N)	Extension (mm)	Stress (MPa)	Strain (Dimensionless)
0	0	0	0
101.8	0.075	1.6743	0.000469
607.8	0.450	9.9968	0.002800
1878.1	1.500	30.8895	0.009375
2020.2	2.625	33.2262	0.016400
2020.2	3.450	33.2262	0.021560

Table 7.29: 50mm Fiber and 10% Vol.frac.

Load (N)	Extension (mm)	Stress (MPa)	Strain (Dimensionless)
0	0	0	0
	0.4500	10.3048	0.00280
	1.1250	23.190	0.00703
	2.1250	27.179	0.01330
	3.3250	28.0112	0.02080
	4.2500	28.0112	0.02266

Table 7.30: 50mm Fiber and 30% Vol. frac.

Load (N)	Extension (mm)	Stress (MPa)	Strain (Dimensionless)
0	0	0	0
379.75	0.200	6.2458	0.0013
664.56	1.375	10.930	0.0086
949.37	2.250	15.615	0.0141
1297.5	3.250	21.340	0.0203
1645.6	4.325	27.065	0.0270
1962.0	4.825	32.270	0.0302

Tabl

e 7.31: 50mm Fiber and 50% Vol. frac.

Load (N)	Extension (mm)	Stress (MPa)	Strain (Dimensionless)
0	0	0	0
595.9	0.500	9.8012	0.0031
1051.5	0.875	17.2944	0.00547
1481.0	1.875	24.3588	0.0117
1759.2	2.750	28.9349	0.0172
1803.3	3.625	29.6589	0.0266

Table 7.32: Linear-Quadratic Model Numerical fit results for Plantain Fiber-Polyester Composite

Fl (mm)	Vf (%)	p1	p2	q1	q2	R ²	Adj. R ²	RMSE	SSE
10	10	0.9126	-6.283e-5	0.01035	0.000157	0.9936	0.9841	1.3470	3.629
10	30	4.19e5	672.4	6098	254.9	0.9666	0.9332	2.6640	21.29
10	50	1.123	-1.143e-4	0.01147	2.173e-4	0.9943	0.9858	1.3840	3.830
30	10	6.005e4	3.8200	1383	7.971	0.9876	0.9505	2.841	8.074
30	30	3.098	-2.203e-4	0.04624	4.585e-4	0.9956	0.9891	1.525	4.650
30	50	0.9025	-5.891e-5	-4.792e-3	2.367e-4	0.9972	0.9931	3.567	1.335
50	10	1.612	-1.036e-4	0.01981	3.255e-4	0.9940	0.9849	4.123	1.436
50	30	2.131e4	58.24	-28.07	23.26	0.9809	0.9618	15.14	2.246
50	50	2.683	-7.397e-5	0.03895	6.531e-4	0.9965	0.9914	2.373	1.089

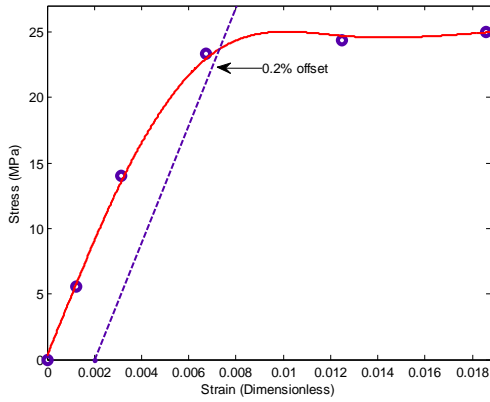


Fig. 7.130: Traditional Approach (10mm and 10%)

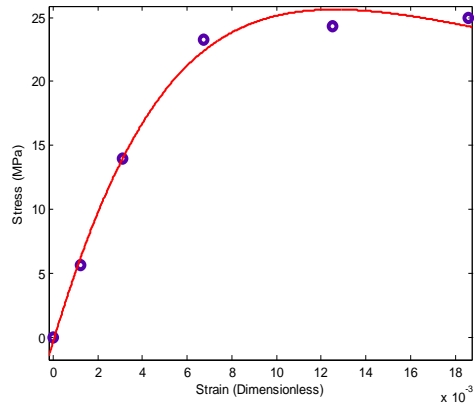


Fig. 7.131: New Approach (10mm and 10%)

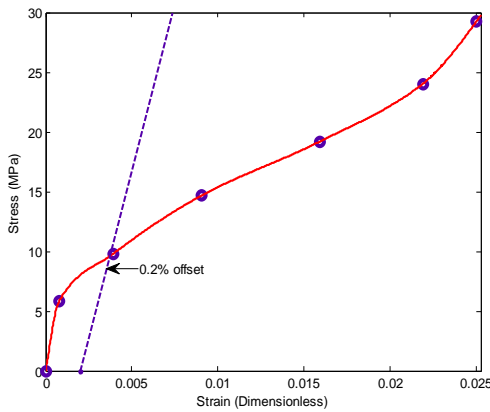


Fig. 7.132: Traditional Approach (10mm and 30%)

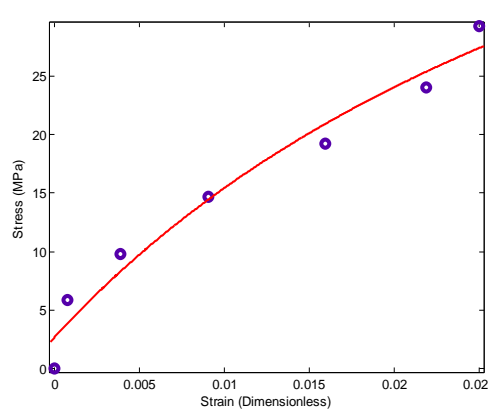


Fig. 7.133: New Approach (10mm and 30%)

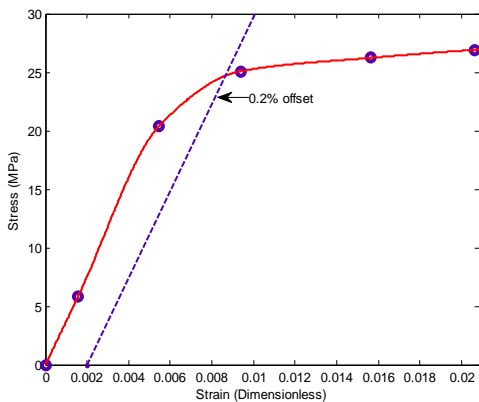


Fig. 7.134: Traditional Approach (10mm and 50%)

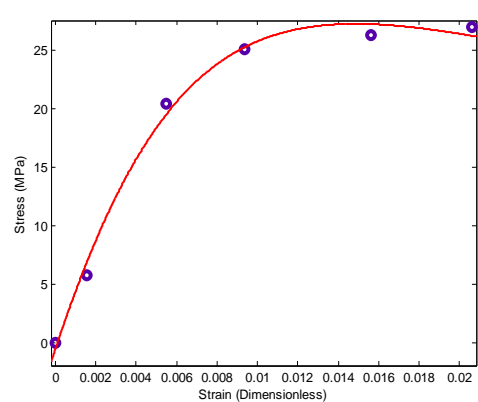


Fig. 7.135: New Approach (10mm and 50%)

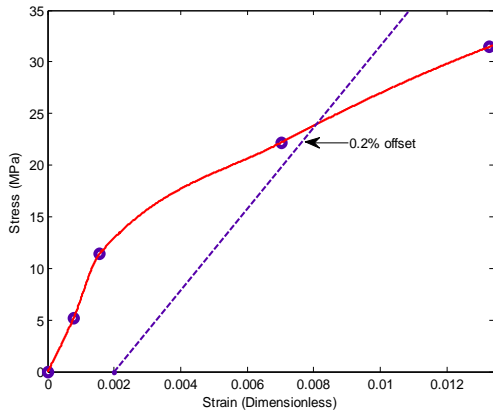


Fig. 7.136: Traditional Approach (30mm and 10%)

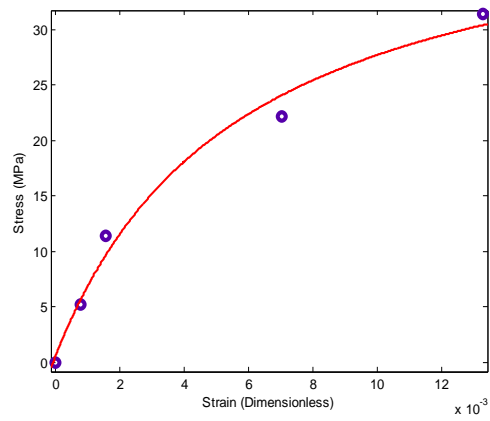


Fig. 7.137: New Approach (30mm and 10%)

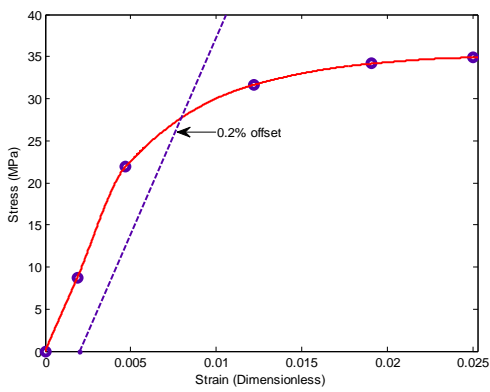


Fig. 7.138: Traditional Approach (30mm and 30%)

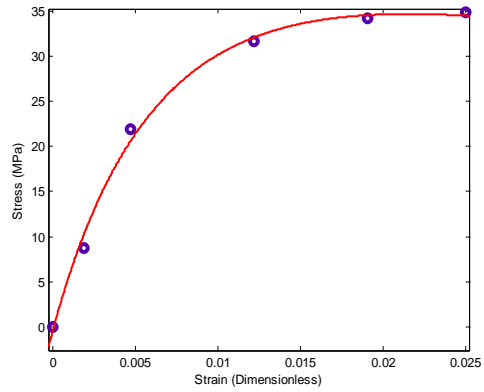


Fig. 7.139: New Approach (30mm and 30%)

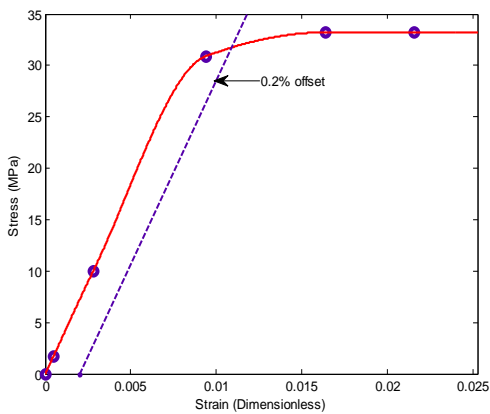


Fig. 7.140: Traditional Approach (30mm and 50%)

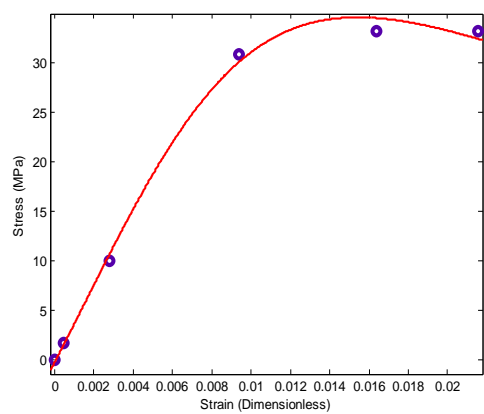


Fig. 7.141: New Approach (30mm and 50%)

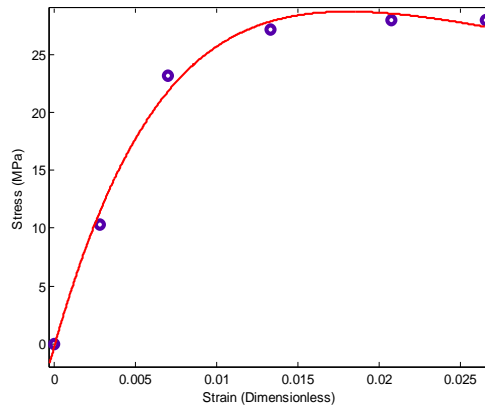
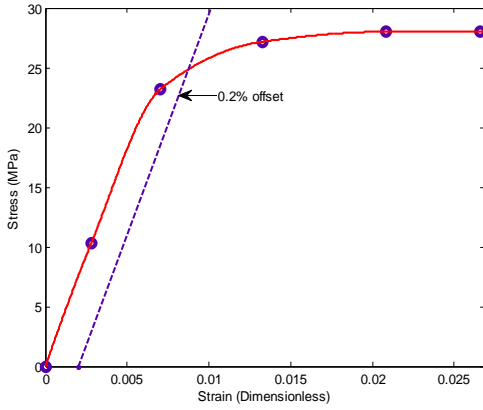


Fig. 7.142: Traditional Approach (50mm and 10%) Fig. 7.143: New Approach (50mm and 10%)

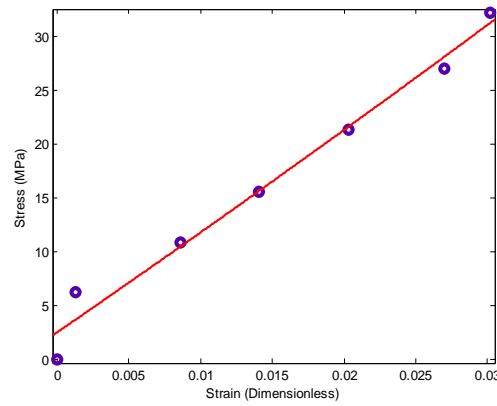
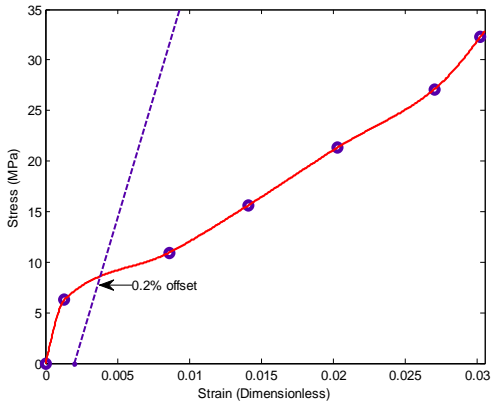


Fig. 7.144: Traditional Approach (50mm and 30%) Fig. 7.145: New Approach (50mm and 30%)

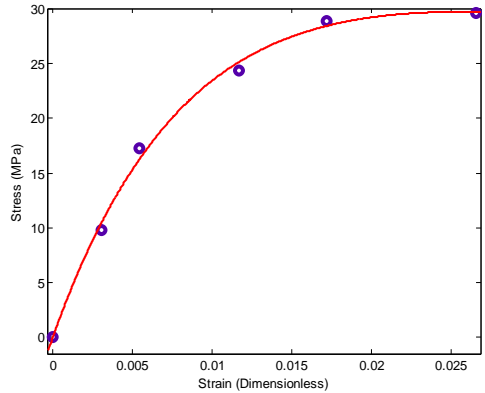
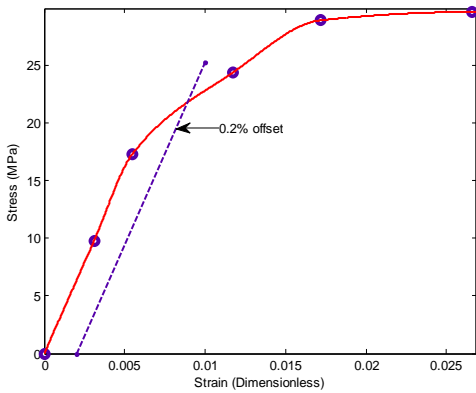


Fig. 7.146: Traditional Approach (50mm and 50%) Fig. 7.147: New Approach (50mm and 50%)

Table 7.33: TENSILE PROPERTIES COMPUTATION (NEW APPROACH)

```

p1=.7325;p2=-4.822e-6;q1=.05076;q2=.0006646;sm=.0375;%Enter values of constants in linear-
quadratic model and maximum strain

E=(p1*q2-p2*q1)/q2^2 %Compute the Modulus of Elasticity

ts=p1^2/(2*sqrt(p2^2+p1*(p1*q2-p2*q1))+p1*q1-2*p2)%Compute tensile strength

x=roots([E E*(q1-0.002) E*q2-0.002*E*q1-p1 -0.002*E*q2-p2])%Solve equation for yield
strength intersection

x=x(x>0)%Choose the positive value

Sy=E*(x-0.002)%Compute the yield strength

if 4*q2>q1^2

Tough=(p1/2)*log((sm^2+q1*sm+q2)/q2)+((2*p2-p1*q1)/sqrt(4*q2-
q1^2))*(atan((2*sm+q1/2)/sqrt(4*q2-q1^2))-atan(q1/sqrt(4*q2-q1^2)))% Compute the toughness

elseif 4*q2<q1^2

Tough=(p1*(q1+sqrt(q1^2-4*q2))-2*p2)/(2*sqrt(q1^2-4*q2))*log((2*sm+q1+sqrt(q1^2-
4*q2))/(q1+sqrt(q1^2-4*q2)))+(2*p2-p1*(q1-sqrt(q1^2-4*q2)))/(2*sqrt(q1^2-
4*q2))*log((2*sm+q1-sqrt(q1^2-4*q2))/(q1-sqrt(q1^2-4*q2)))

else Tough=p1*log((2*sm+q1)/q1)+(sm*(2*p2-p1*q1))/(q1*(sm+q1))

end

```

Table 7.34: COMPUTING MODULUS USING THE SHEAR LAG PARAMETER

```
r=0.0002117;ef=48.14;em=0.999;gf=16.3267;gm=0.3372;beta=[];  
  
for vf=0.1:0.2:0.5  
  
vm=1-vf  
  
betacox=sqrt((2/(r^2*ef*em))*((ef*vf+em*vm)/(vm/4*gf)+(1/2*gm)*((1/vm)*log(1/vf)-1-  
vm/2)));  
  
beta=[beta betacox];  
  
end  
  
betavalue=[beta beta beta];  
  
l=[.01 .01 .01 .03 .03 .03 .05 .05 .05];  
  
nl=1-(tanh(betavalue.*l/2)./(betavalue.*l/2))  
  
volf=[.1 .3 .5 .1 .3 .5 .1 .3 .5];  
  
ec=(nl.*volf.*ef)+(em*(1-volf))
```

Table 7.35: COMPUTING MODULUS USING HALPIN-TSAI MODEL

```
em=0.999;ef=3.411;vf=0.1;

while vf<0.55

asp=8.1733;

nl=((ef/em)-1)/((ef/em)+2*asp);

a=2;nt=((ef/em)-1)/((ef/em)+a);

el=em*(1+2*asp*nl*vf)/(1-nl*vf);

et=em*(1+a*nt*vf)/(1-nt*vf);

ec=(3/8)*el+(5/8)*et

vf=vf+0.2;

end
```

Table 7.36: COMPUTING MODULUS USING THE BINTRUP MODEL

```
em=1.371;ef=3.411;vf=0.1;poissonm=0.4726;

while vf<0.55

asp=8.1733;

nl=((ef/em)-1)/((ef/em)+2*asp);

el=em*(1+2*asp*nl*vf)/(1-nl*vf);

emp=em/((1-poissonm)^2);

et=(emp*ef)/(ef*(1-vf)+vf*emp);

ec=(3/8)*el+(5/8)*et

vf=vf+0.2;

end
```

Table 7.37: COMPUTING MODULUS USING THE MODIFIED MODEL

```

em=1.371;ef=3.411;vf=0.1;

while vf<0.55

asp=8.1733;

nl=((ef/em)-1)/((ef/em)+2*asp);

a=2;nt=((ef/em)-1)/((ef/em)+a);

el=em*(1+2*asp*nl*vf)/(1-nl*vf);

et=em*(1+a*nt*vf)/(1-nt*vf);

ec=(sin(3*vf^(11/16)*pi/2))*((3/8)*el+(5/8)*et)

vf=vf+0.2;

end

```

Table 7.38: Properties of Matrix and Fiber used for Micromechanics Modeling of Composite

Material	Polyester	Epoxy	Plantain bunch Fiber	Palm Bunch Fiber	Rattan Palm Fiber
Young's Modulus (GPa)	0.999	1.371	48.18	16.5100	3.4110
Poisson Ratio	0.4815	0.4726	0.4743	0.4937	0.4769
Shear Modulus (GPa)	0.3372	0.4655	16.3267	5.5265	1.1548
Mean Radius (m)	-	-	0.0002117	0.000225	0.0006117

Table 7.39: NEURAL NETWORK TRAINING USING MATLAB 7.9

```
>>x=[23.6183 23.6183 23.6183 70.855 70.855 70.855 70.855 118.0916 118.0916 118.0916;10  
30 50 10 20 30 50 10 30 50];
```

```
>> y=[4.4744 5.61 3.7312 3.9542 4.3116 4.669 3.57 3.6803 4.7661 3.1617];
```

```
>>net=newff(x,y,20)
```

```
>>net=train(net,x,y)
```

```
>> Y=sim(net,x)
```

```
>> [m,b,r]=postreg(Y,y)
```



Fig. 7.148: Carbolite electric oven
(Serial number 4/95/1113, max. temp 300⁰c)



Fig. 7.149: Arthur Thomas Laboratory mill
(model number Ed-5 USA)



Fig. 7.150: Santorion digital weighing balance
Model number BL3002 (Max = 300g)



Fig. 7.151: Water Heating bath